IntechOpen

Gasification for Low-grade Feedstock

Edited by Yongseung Yun

GASIFICATION FOR LOW-GRADE FEEDSTOCK

Edited by **Yongseung Yun**

Gasification for Low-grade Feedstock
http://dx.doi.org/10.5772/intechopen.69788
Edited by Yongseung Yun

Contributors

Edris Madadian, Jayaraman Kandasamy, Iskender GôKALP, Muhammad Aziz, Lukman Adi Prananto, Xiang Luo, Tao Wu, Kaiqi Shi, Mingxuan Song, Chan Seung Park, Partho Roy, Suhyun Kim, Said Samih, Sherif Farag, Jamal Chaouki, Mariusz Siudak, Dariusz Wiśniewski, Janusz Piechocki, Yong-Chil Seo, Md Tanvir Alam, Won-Seok Yang, Annarita Salladini, Gaetano Iaquaniello, Maria Cristina Annesini, Alessia Borgogna, Emanuela Agostini, Luca Spadacini, Victor Zhovtyansky, Vitas Valinčius, Lola Domnina Pestaño, Wilfredo Jose, Abdul-Sattar Nizami, Mohammad Rehan, Muhammad Saghir, Rosa Rodriguez

Notice

Statements and opinions expressed in the chapters are these of the individual contributors and not necessarily those of the editors or publisher. No responsibility is accepted for the accuracy of information contained in the published chapters. The publisher assumes no responsibility for any damage or injury to persons or property arising out of the use of any materials, instructions, methods or ideas contained in the book.

First published in London, United Kingdom, 2018 by IntechOpen
eBook (PDF) Published by IntechOpen, 2019
IntechOpen is the global imprint of INTECHOPEN LIMITED, registered in England and Wales, registration number: 11086078, The Shard, 25th floor, 32 London Bridge Street
London, SE19SG – United Kingdom
Printed in Croatia

British Library Cataloguing-in-Publication Data
A catalogue record for this book is available from the British Library

Additional hard and PDF copies can be obtained from orders@intechopen.com

Gasification for Low-grade Feedstock
Edited by Yongseung Yun

p. cm.

Print ISBN 978-1-78923-288-2

Online ISBN 978-1-78923-289-9

eBook (PDF) ISBN 978-1-83881-421-2

Meet the editor

Dr. Yongseung Yun majored in chemical engineering and received his PhD degree from the University of Utah in 1990; MS degree from KAIST, Korea, in 1981; and BS degree from Yonsei University, Korea, in 1979. He currently works as the director at Plant Engineering Division, IAE, in Korea. At KIST from 1981 to 1984, he researched on the oil agglomeration and FBC. For his PhD degree, he worked on the low-temperature air oxidation of coal. At Brown University from 1991 to 1992, he researched on the pretreatment methods for coal liquefaction. He has concentrated on coal gasification for IGCC from 1993 until now. From 2000, he expanded gasification research to wastes. From 2013, he has been working as the president in Korea Association of Waste to Energy (KAWET) and as vice president of KSWM, Korea DME Association, and KSIEC.

Contents

Preface

Society has evolved to use energy in gas and electricity in a more user-friendly form. The most coveted energy forms nowadays are gas in nature and electricity due to their environmental cleanness and convenience. Even with plentiful shale gas available in some countries, many areas around the globe still lack a gas source and a sustainable supply of electricity.

Gas energy that contains a heating value even one-tenth of natural gas is a more attractive option instead of using solid feedstock directly in combustion or pyrolysis mode. Combustion produces a gas of mainly CO2, which does not possess any heating value. In contrast, gasification converts solid feedstock into gas, which possesses energy content and can be cleaned in easier way than in liquid or in solid shape.

Recently, gasification market trend has started to switch to low-grade feedstock such as biomass and wastes, which are inherently low grade in terms of heating value and homogeneity. In this sense, the most promising area of development in gasification field lies in low-grade feedstock that should be converted into more user-friendly gas or electricity form in utilization.

Gasification technology has been around more than a century, and it has reached a commercial scale of 3,000 ton/day in coal gasification cases. With cheaper natural gas available by shale gas revolution, adopting coal in gasification in large scale has dropped to a minimal level in most countries. Low-grade feedstock such as biomass and wastes becomes more interesting for gasification at much smaller capacity of few dozens to few hundreds of tons per day.

Most key nations that require gasification technology for low-grade feedstock must be those in active development and in short of clean and easy-to-use energy, especially electricity. Developing countries can bypass the centralized energy distribution system through a proper localized distributed energy system that can save a heavy infrastructure expenditure.

Typical examples of low-grade feedstock are biomass, wastes, low-grade coals, and petroleum residues (petroleum coke and asphalt). They contain higher pollution-incurring components like sulfur and nitrogen and in a heterogeneous state with many contaminants as in wastes, in addition to the inherent nature of low heating value.

Biomass is regarded as carbon neutral, which should be a good feedstock in climate-conscious society. Since biomass feedstock can be obtained in local areas especially in tropical and subtropical countries, most pragmatic route in securing electricity and clean gas for household or industries can come from gasification of biomass. Biomass that suits in gasification encompasses from wood chips, straw, rice husk, miscanthus, and leftover from oil extraction of palm trees.

Municipal and industrial wastes are attractive feedstock for gasification. Wastes in principle should be treated for disposal through an environmentally clean process, which means tipping fee can supplement the economics of waste gasification. The most common way to treat wastes is through incineration, which is more viable with large-scale facility. Most countries prohibit using small-scale incinerators because of involved higher risk of producing dioxin than larger facilities. When wastes need to be disposed in small scale (about 30–150 ton/day), gasification can be a profitable choice than incineration.

Low-grade coals are available in large quantity in India, Turkey, South Asian countries, and Eastern Europe countries. Low-grade coals that typically contain high ash, high volatile matter, and moisture make exporting and long transportation difficult due to their low energy quality and their propensity for self-heating that might lead to fire during transportation. The low-grade coal is best to be utilized at local mine area, which makes gasification a good technology choice for extracting energy value in gas form. Due to the ever more stringent environmental regulations, these coals should be utilized through clean technology, and gasification can also be a tool that suits to this purpose.

Examples of distinctive target market that applies gasification for low-grade feedstock are localized distributed electricity and clean gas that can replace expensive natural gas/naphtha/heavy oil. Further, high-purity carbon monoxide gas separated from syngas that is produced from industrial/municipal wastes can be a cheaper raw material for acetic acid/acetic anhydride compared to the case manufactured from heavy oil or naphtha.

The book has complied the contributed 13 chapters by individual authors from 13 countries who have different level of background and expertise. In one sense, it might appear to be too general and diverse in topics. But, the book tried to shed light on the works on gasification from many parts of the world and thus can feel the technology status and the areas of interest regarding gasification for low-grade feedstock.

The book comprises four sections that allocate each section on low-grade feedstock. The first section containing five chapters examines biomass gasification that has attracted practical interests as a way to provide energy in the form of gas, solid fuel, and electricity. Definitely biomass gasification is the technology that exhibits most attention from many research groups and companies during the last several years for immediate commercialization. The second section looks into waste gasification with five chapters to examine the recent trend and diverse applicable cases, including one chapter on plasma gasification. The third section of two chapters deals with gasification for low-grade coals, one for the Indian and Turkish coals, and one for the development of fluidized-bed TGA to identify the fundamental kinetic data. The last section deals with the process integration and utilization with one chapter, concentrating on the possible routes of syngas utilization.

It took 9 months in finishing the editing process, which was actually much harder than my experience in earlier two books with IntechOpen. In fact, initial diverse topics and a wide range of author expertise only convinced me the necessity for filling up the information gap between the in-depth gasification information on coal and natural gas and the recently occurring practical need on gasification for low-grade feedstock that should be in a more compact plant scale. I hope this book can act as catalyst in fulfilling virtuous circle of information on gasification for low-grade feedstock and eventual practical applications for localized distributed energy in a less-privileged region.

I would like to thank all the authors for contributing each chapter and who went through together a lengthy revising process, sometimes four times. I also like to express my sincere thanks to Ms. Kristina Kardum who provided support during the long 9-month process. With cooperation from all participants, I am glad to see the final product as the book *Gasification for Low-Grade Feedstock*.

Dr. Yongseung Yun
Institute for Advanced Engineering
Yongin, Republic of Korea

Section 1

Biomass Gasification

Chapter 1

Biomass Gasification: An Overview of Technological Barriers and Socio-Environmental Impact

Xiang Luo, Tao Wu, Kaiqi Shi, Mingxuan Song and Yusen Rao

Additional information is available at the end of the chapter

http://dx.doi.org/10.5772/intechopen.74191

Abstract

Biomass gasification has been regarded as a promising technology to utilize bioenergy sustainably. However, further exploitation of biomass gasification still needs to overcome a significant number of technological and logistic challenges. In this chapter, the current development status of biomass gasification, especially for the activities in China, has been presented. The biomass characters and the challenges associated with biomass collection and transportation are covered and it is believed that biomass gasification coupled with distributed power generation will be more competitive in some small communities with large amount of local biomass materials. The technical part of biomass gasification is detailed by introducing different types of gasifiers as well as investigating the minimization methods of tar, which have become more and more important. In fact, applying biomass gasification also needs to deal with other socio-environmental barriers, such as health concerns, environmental issues and public fears. However, an objective financial return can actually accelerate the commercialization of biomass gasification for power and heat generation, and in the meantime, it will also contribute to other technical breakthroughs.

Keywords: biomass gasification, gasifiers, tar removal, socio-environmental impact

1. Introduction

Fossil fuel is on the verge of depletion in this century. Scientists and governments around world are looking for new energy resources which could be used safely and efficiently with enough amount for deployment and security. Bioenergy is a renewable energy, which

is stored in the organic form in the chemical state and supports human beings' daily life since our ancestor apes knew how to use fire to cook. In these millions of years, bioenergy was mostly used in small scale like household cooking. Now, people have realized that efficient exploitation of biomass resource can actually reduce their dependency over fossil fuel. Biomass gasification has been regarded as an effective pathway to utilization of bioresource. It takes biomass as raw materials and employs pyrolysis or thermal cracking under anoxic conditions. This is an energy conversion process including a group of complex chemical reactions that large organic molecules degrade into carbon monoxide, methane and hydrogen and other flammable gases in accordance with chemical bonding theory. Biomass feedstock with the gasification agent is heated inside an integrated gasifier. With temperature increase, biomass goes through dehydration, volatilization and decomposition. Eventually, the produced gases are used for central gas supply and power generation. This technology has already been developed over several decades and progressively achieved commercialization all over the world, especially in Sweden, Germany, Canada, the United States, India and China. In the early stage, downdraft gasifier had been implemented at a large scale in China and India due to its relatively low tar production. Recently, the development of circulating fluidized bed (CFB) gasifier makes it adaptable for both biomass quality and the raw particle size. Besides, CFB is also easy for scale-up and ash cleaning.

China, as a large agricultural country, produces a large number of crop straw, poultry manure, agricultural by-products and other plant biomass every year. Thus, research and development on key technologies and integrated peripherals of biomass gasification become very necessary. China has already developed various gasifiers, the size of which range from 400 KW to 10 MW. However, compared with fossil fuel, biomass has lower bulk density and energy density, which make it uneconomic for collection and transportation. Therefore, biomass gasification coupled with distributed power generation in small communities with abundant biomass resource would be the way out in future [1].

In recent years in China, the yield of domestic waste has increased every year and exceeds 400 million tonnes per year. Chinese government's 13th five-year plan proposed that the proportion of waste harmless treatment should be no less than 70% by 2020. But waste landfill is still the primary method used to deal with waste in rural areas. Compared with landfill, gasification has advantages of lower environmental impacts and does not consume land resource. When contrasting gasification with incineration, the gasification technology has better quality of gaseous emissions with much lower capital input, which makes gasification more suitable for distributed deployment in rural area. Therefore, there will be a great demand for deployment of waste gasification treatment plants in Chinese rural areas, and more and more people are now focusing on the development of more efficient small-scale gasifiers with capacity under 300 tonne/day. The relevant equipment has also been deployed in Iran, Thailand, Burma and Laos. However, several technical barriers are still there such as effective removal of tar with low cost, environmental influence, accuracy control of gasifier inner temperature, solidification of fly ash and so on.

Therefore, this chapter introduces both technological and logistics challenges of biomass gasification via introducing biomass characters and gasifier technologies. The details of tar minimization and socio-environmental impacts of biomass gasification are also presented as main contents to help understand the primary barriers for the deployment of biomass gasification.

2. Biomass characteristics and general conversion

2.1. Composition of biomass and its common characteristics

Biomass includes all the living or recently living organisms, like land plants, grasses, water-based vegetation and manures [2], and these organisms consist of a number of major elements such as C, H, O, N, P and S. The classification of biomass into different categories is based on their properties. One feasible way is based on the appearances and the growth environment of biomass: woody plants, herbaceous plants/grasses, aquatic plants, manures and wastes [2]. Biomass could also be divided into two types: low moisture content and high moisture content. The low moisture content biomass can be used in thermo-chemical processes (i.e., gasification, combustion and pyrolysis), while the high moisture content plants are more suitable to be used in some wet processing technologies (i.e., fermentation and anaerobic digestion) [3]. Such high moisture contents would consume a large amount of energy for the drying process if employed as resources for thermo-chemical processing.

Biomass is derived from solar energy via photosynthesis. Under a good illumination condition, carbon dioxide in the atmosphere can be converted into organic materials or, in another way, the solar energy is stored as chemical energy, which existed as chemical bonds in the organisms [4]. The said chemical energy is released when these bonds are broken either via thermo-chemical or wet processing. This is an ongoing energy transfer from the sun and hence the sustainability of biomass resource could be ensured. As we have known, the total energy captured annually in biomass is more than that of the annual energy consumption globally [5]. On the other hand, biomass is clean as it is carbon neutral. On the view of carbon network, the net emission of carbon dioxide into the environment during the harvesting of energy from biomass is zero. The final products of conversion of biomass (CO_2 and H_2O) are originally absorbed into the plants from the atmosphere during photosynthesis. The conversion of biomass also has less harmful releases such as NO_x and SO_x compared with fossil fuels [6].

However, the characters of biomass also create many barriers during its actual application. On the aspect of species diversity, biomass usually does not behave as steady as fossil fuels, which causes a lot of difficulty during project planning stage including gasifier type, plant size and the way of energy output. On the other hand, the varieties of biomass resource also lead to different heating values and moisture contents. Compared with other energy carriers, biomass has much lower heating values. Taking wood and wheat straw as examples, their lower heating values are only 18.6 and 17.3 MJ/kg, respectively, while the lower heating value of coal is as high as 23–28 MJ/kg [2, 7]. The reason for this disparity is that the oxygen content of biomass carbohydrates is very high while the combustible elements such as C and H are low. In addition, the intrinsic moisture content in biomass is also very high, which requires more energy for drying before further processes take place [3]. Hence, use of biomass requires the complexity in material handling, pre-treatment and the design of processing facilities [3]. For the purpose of transportation and collection, biomass is unlike any other renewable resources (solar, wind, hydropower) where it is able to be stored directly and transported somewhere else. However, biomass is highly dispersed in regional distribution and the low volumetric of biomass makes it a bit more difficult for the collection and transportation. Therefore, small-scale gasification unit operated in small communities with abundant biomass resource or domestic waste would be the way out in future.

2.2. General conversion technologies of biomass except gasification

For the utilization purpose, the conversion technologies of biomass could be classified in three categories: mechanical extraction; thermo-chemical conversion; and biological conversion, as illustrated in **Figure 1** [3, 8]. Among them, direct combustion, gasification and pyrolysis are considered as the thermo-chemical processes; fermentation and anaerobic digestion are regarded as biological conversion.

2.2.1. Direct combustion

The direct combustion of biomass is widely applied in small-scale cooking and domestic heating by converting chemical energy stored in biomass into heat [9]. In modern industrial technology, combustion is also employed in large-scale applications to produce mechanical power and electricity with the aid of boilers, steam turbines and turbo-generators. The temperature range of biomass combustion is within 800–1000 °C. Materials with the moisture content higher than 50 wt% are not suitable for combustion processes [3]. The net efficiency of electricity generation from biomass combustion varies between 20 and 40% [8]. The efficiency could be improved either by scaling up the system to over 100 MWe or co-firing with coal (<10 wt% by weight) [10].

2.2.2. Pyrolysis

Pyrolysis is a thermo-chemical process, in which biomass decomposes into fuel gas, bio-oil and solid char in the absence of oxygen. The selectivity leading to different types of products could be controlled by manipulating the operating conditions (temperature and residence time). Low temperatures (<500 °C) and long residence time favor the production of solid char

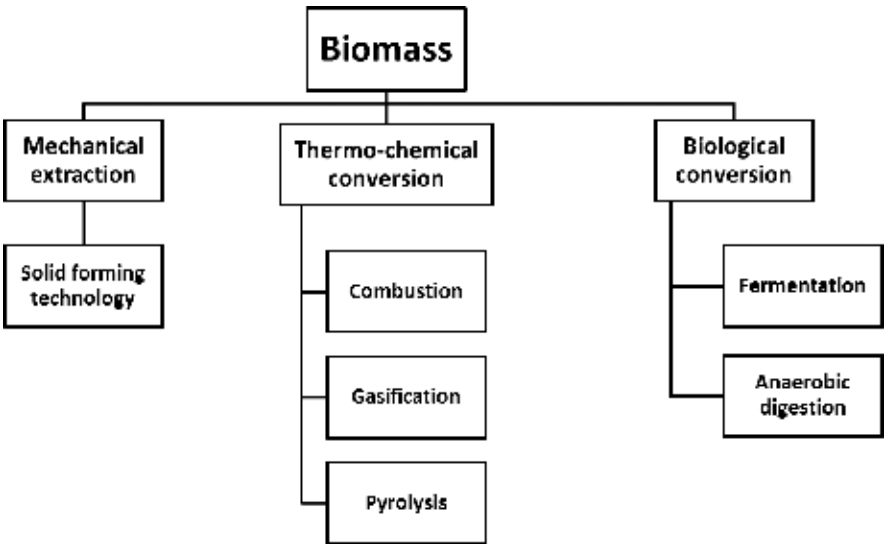

Figure 1. The main processes for the biomass conversion technologies [3].

(up to 35 wt% yield), while high temperatures (700–1100°C) and short reaction time favor the production of gases (up to 80 wt% yield) [11]. Bio-oil production is normally favored at 500°C, with very short retention time (<1 s) [12].

2.2.3. Fermentation

Fermentation is a bio-chemical process which is used for the production of about 80% of the world's ethanol [13]. The main process of fermentation involves using microorganisms to convert sugars into ethanol under a warm and wet environment. The sugar is typically obtained from the mechanical handling (crushing and mixing with water) of sugar-rich crops, such as sugar cane and sugar beet. However, the high cost of sugar-rich crops has diminished its proportion of utilization in fermentation. The starch-based biomass is also commonly used for ethanol production. However, it requires an extra step to convert starch into sugar by enzymatic reactions.

2.2.4. Anaerobic digestion

Anaerobic digestion involves using anaerobic microorganisms to convert biomass into biogas (CH_4 and CO_2 as the main gaseous products) by means of decomposition. Under the anaerobic environment, the organic material in biomass is decomposed into usable-sized molecules, such as sugar, as the first step. The sugar molecules is then converted into organic acids and further decomposed to CH_4 gas. This process has been proven as a commercially feasible technology and is widely applied in the rural areas of China.

3. Technologies of biomass gasification

Gasification process converts biomass, a low-energy density material, into a gaseous product (LHV at 4–11 MJ/N/m^3), which is a mixture of CO, H_2, CH_4 and CO_2 [10]. Gasification is a partial oxidation process and it is commonly operated at 800–900°C for biomass gasification [2]. In some cases, steam is also used as the gasification agents. The gaseous products from the gasifier can be utilized in gas engines or gas turbines for the generation of electricity. In terms of economics, it has also been proven that the performance of a biomass gasification plant with a combined cycle gas turbine (CCGT) is comparable to that of a conventional coal power plant [7], if not better.

3.1. Types of gasifiers

The gasifier, as the principle component of a gasification plant, actually provides a space for biomass and gasification agent being mixed to a certain extent, in some cases with catalysts or additives [14]. The different selection of gasifiers is actually responsible for keeping steady the production of syngas regarding the variations of biomass. Literature shows that gasifiers could be categorized into three main types: fixed bed gasifiers, fluidized gasifiers and the entrained flow gasifiers [15].

3.1.1. Fixed bed gasifier

Fixed bed gasifiers is the traditional approach applied for biomass gasification and generally operated around 1000°C. An alternative name for the fixed bed gasifier is "moving bed reactor". This is due to the movement of the biomass material in the main flow direction with very slow flowrate. The fixed bed gasifiers could be principally classified as updraft (countercurrent) and downdraft (co-current) due to the different airflow direction [14].

In an updraft gasifier (shown in **Figure 2**), the biomass material is fed from the top of the reactor, while the gasification agent enters from the bottom. The gasification agent flows through the bed of ash and biomass. The gas generated is exhausted through the top. For the reaction, the gasification agent meets the bottom char at first and achieves a complete combustion and raises temperature to c.a. 1000°C with production of H_2O and CO_2. This hot gas dries the incoming biomass near the top of the vessel and provides heat for pyrolysis of the descending biomass as well as percolates through the unreacted char bed to produce H_2 and CO [15]. In this gasification system, the product gas is withdrawn from the low temperature zone; thus, the product would be contaminated with significant amount of tars. If the product is used for further downstream applications like fuel in combustion engine electricity generator, a set of cleaning processes for tar removal is essential. However, the cleaning processes require intensive operation and establishment; therefore, the application of updraft gasification is not suitable for internal combustion engines [1].

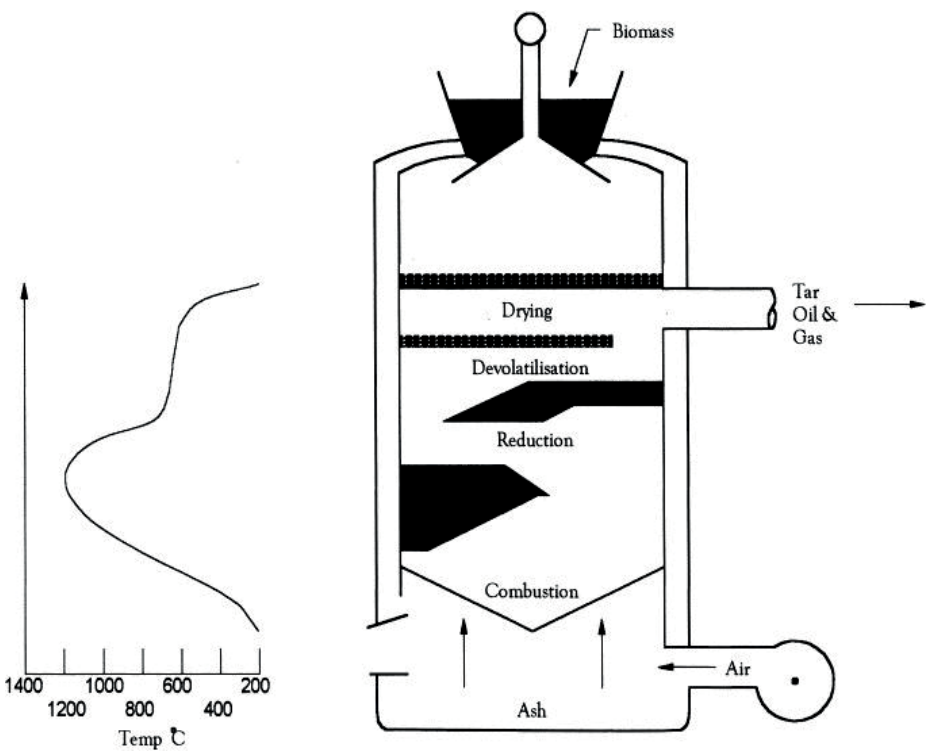

Figure 2. Schematic of updraft gasifier [16].

For the downdraft gasifier (shown in **Figure 3**), both biomass and gasification agent flow into the vessel from the top. At the "throated" area, where air or O_2 is fed into system with homogeneously distribution. The temperature could rise to around 1200–1400°C, which leads to both combustion and pyrolysis of the fuel. The produced hot gases will then be reduced to H_2 and CO as the main components after passing the hot char bed and will leave the gasifier unit at temperatures of about 900–1000°C. The tar content of the product gas is lower than that of the updraft gasifier, but the particulate content of the gas is higher [16]. Hence, the downdraft gasifier is suitable for downstream applications like internal combustion engines electricity generator. However, the product is withdrawn at a relatively high temperature; it needs to be cooled to acceptable range before further usage.

3.1.2. Fluidized gasifier

In the fluidized gasifier, the gasification agent enters the bed at a relatively fast rate from the bottom of the vessel and exits from the top. This kind of gasification features uniform temperature distribution in the bed zone. The consistency of temperature is obtained by the application of air-fluidized bed material, which ensured the intimate mixing of fuel, hot combustion gas and bed material. Currently, three main types of fluidized gasifiers are widely used [15], bubbling fluidized bed (BFB), circulating fluidized bed (CFB) and dual fluidized bed (DFB).

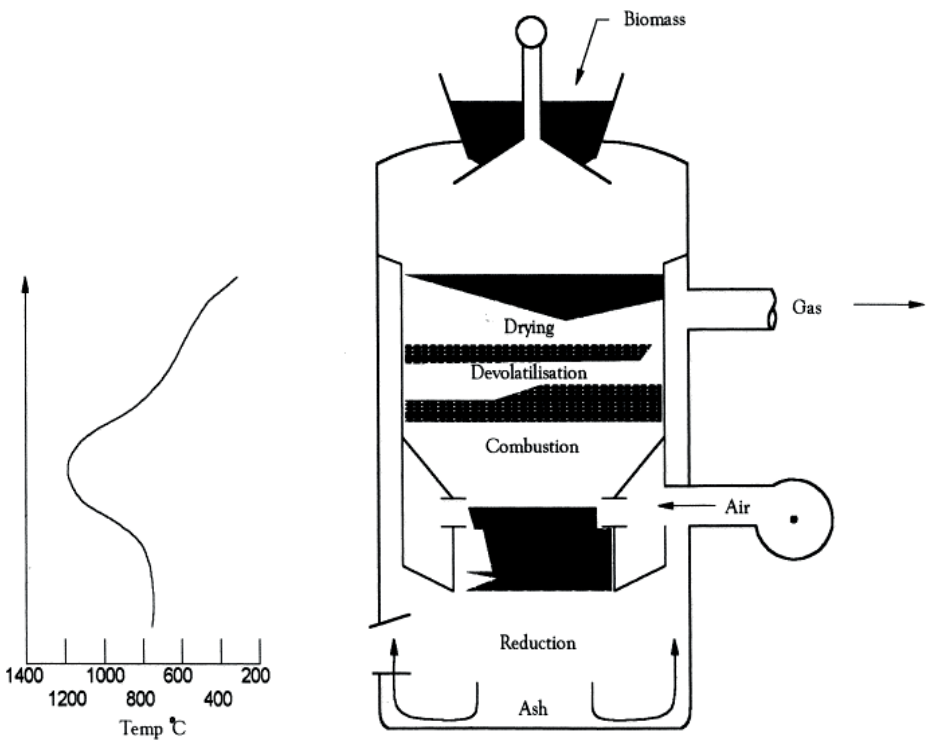

Figure 3. Schematic of downdraft gasifier [16].

BFB gasifier applies inlet from the bottom and moves the bed of fine-grained materials. The bed temperature is maintained at 700–900°C by manipulating the ratio of fed biomass and gasification agent [16]. The flowrate of gasification agent is set to be slightly greater than the minimum velocity of fluidization of the bed material. The biomass is decomposed into char and gas products with a low tar percentage.

The CFB gasifier consists of two principle units: the gasifier unit and the circulation unit, as shown in **Figure 4**. The bed material and char in this type of gasifier is circulated between the reaction chamber and the cyclone separator, where ash and hot gas could be separated. The bed material is fully fluidized and leaves from the first unit, and then it is sent back by the second unit. The solids are moving in the solid circulation loop in greater extent of fluidization with higher residence time. Moreover, its operation pressure is also relatively higher.

Dual fluidized bed (DFB) gasifiers consist of two separated fluidized beds which are used for pyrolysis process and combustion process [14]. The first bed is operated as a pyrolysis reactor and it is heated by the second reactor with hot circulated bed material. The second reactor provides heat by burning char provided from the first reactor. The bed material plays an important role as a heat transfer medium, which prevents the dilution of the hot gas product.

3.1.3. Entrained flow gasifier

Entrained flow gasifiers are generally classified into two types: top-fed gasifier and side-fed gasifier (shown in **Figure 5**), which is according to how and where the fuel and gasification agent is fed. This type of gasifier is suitable for integrated gasification combined cycle (IGCC) plants. It is extensively applied in large-scale gasification and is widely employed for coal, biomass and refinery residues. The gasification temperature of this kind of gasifier could reach 1400°C with a pressure range of 20–70 bar [14]. This high temperature could accelerate tar cracking and mitigate severe tar issue of biomass gasification. However, this kind of high

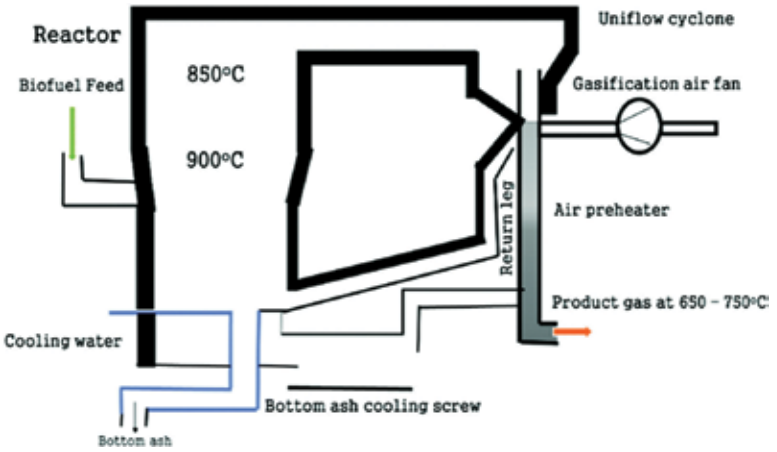

Figure 4. Schematic diagram of circulating fluidized bed gasifier (CFB) [17].

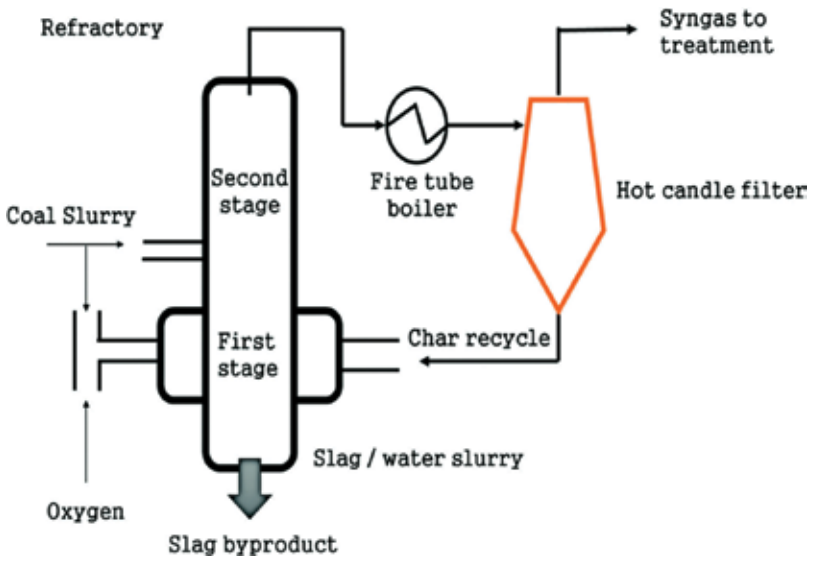

Figure 5. Schematic diagram of an entrained flow gasifier (side-fed) [17].

temperature gasification requires a finely fed biomass material (<0.1–0.4 mm), which makes this process unsuitable for most biomass materials (such as wood). Therefore, this process is not considered in detail.

3.2. Tar removal

Tar is a major inherent problem in biomass gasification; it can cause a lot of issues such as equipment blockages, lower system efficiency, poor quality gas output and increased maintenance. Tar consists of a group of very complicated mixtures with more than 200 components. Several key components include benzene, toluene, single-ring aromatic hydrocarbon, naphthalene and so on. The formation of tar was due to lower temperature of gasification. It was confirmed that increased temperature of gasification could reduce the content of tar in the outflow and it was believed that higher temperature can promote the cracking of tar [18]. Currently, there are a lot of methods that could be employed for tar minimization, and they can be divided into two categories depending on where the removal technology is applied.

Firstly, tar could be removed inside the gasifier by choosing an appropriate operation parameter or using a catalyst. Previous research indicates that both particle size and surface area-volume ratio of loading feedstock have a significant effect on tar yields [19, 20]. It showed that the gasification of pine saw dust only produced 0.4 wt% of tar at 700°C when the particle size was smaller than 75 micron. While if particle size increased to the range of 600–1000 micron, the tar yield would be higher than 10 wt% even at 900°C. From the view of thermal kinetics, the gasification of larger size of particles needs to overcome greater resistance of thermal conductivity; in other words, it needs more time to complete heat transfer and the devolatilization of biomass materials. On the other hand, small particle size also can contribute to a fast diffusion of the gasification agent and shorten time duration of the whole process. However,

the small size of feedstock particle required much more energy input during the biomass pre-preparation process. In addition, it is also effective by applying an optimal design of gasification reactor. A collaborative project between Switzerland and India demonstrated that an open-top fixed bed would produce much less tar and particulates than a closed-top fixed bed [15]. The reason behind this is that the open-top fixed bed could introduce dual air from the top and nozzles actually increase the residence time for degrading tar.

Secondly, in many processes, tar is removed as a downstream step after gasification, including mechanical method, thermal cracking and catalysis. The details of some common technologies have been listed in **Table 1**. Wet gas cleaning method has been accepted at an early stage. Its equipment investment is relatively low and the operation is also easy to handle. But this technology would also create a lot of waste water and bring serious environmental issues. Therefore, dry gas cleaning method becomes more widespread via various types of filters, rotating particle separators and dry cyclones. Although the dry method avoids waste water issues, its efficiency of tar removal is not good enough if compared with wet method. On the other hand, the replacement, renewal or disposal of filter materials reduces the financial effectiveness of the entire gasification system. This similar situation could also be applied to thermal cracking method and higher operation temperature requires much more energy input.

In the recent two decades, catalytic cracking has attracted more and more attention and has already become the central branch of research. Catalytic cracking is more like a downstream catalytic reforming unit and could easily degrade comparative stable tar to a significant extent. The previous research indicated that the catalytic cracking unit could promote gas yield by 10: 20 vol% and increase the heating value by c.a. 15% [23]. Ni-based catalyst is applied most widely and especially preferred for hydrogen or syngas production. Nickel has a very good catalytic activity and a preferable price advantage. While the application of Ni catalysts needs to avoid extremely high heavy-tar content flue gas, which will form a serious carbon deposition over the catalyst surface and lead to a quick deactivation. The other transition metal-based catalysts, such as co, Fe and cu, also have similar issues. Thus, some applications used the two-stage catalytic reforming process: the first stage used dolomite to

Method	Technique used	Details/examples
Wet gas cleaning [21]	Usage of mechanical device or equipment	Electrostatic precipitator, wet cyclone, wet scrubber
Dry gas cleaning [21]	Usage of mechanical device or equipment	Cyclone, rotary partial separator, fabric filter, ceramic filter, activated carbon adsorber, sand filter
Thermal cracking [21, 22]	Application of high temperature with long residence time	Maximum tar destruction was found at 1250 $^{\circ}$C and 0.5 s
Catalytic cracking [21]	Usage of appropriate catalyst	Tar cracking catalysts are divided into five major groups, namely Ni-based, non-Ni-based, alkali metal-based, acid catalysts, basic catalysts and activated carbon-based catalysts

Table 1. Post-gasification tar removal methods [15].

reduce the concentration of tar to a certain level and then the second stage employed transition metal-based catalysts bed for near-completed removal of tar. But this kind of two-stage reforming process would increase operational cost clearly. In the research scale, some people applied noble metal catalysts and achieved highly catalytic activity as well as better carbon-resistant ability. However, high cost and low accessibility still restrain the wide utilization of noble metal-based catalysts before the technical breakthrough of catalyst regeneration. Alkali metal catalyst is an alternative with good catalytic performance and also exhibits outstanding coke resistance. It is due to this that alkali metal could suppress directly decomposition of hydrocarbon by avoiding quick adsorption of tar components. But alkali metal evaporates under high temperature gasification condition. In many practical process, biomass ash has been reused as an alkali catalyst because most biomass contains abundant alkali metal elements and it is believed that this type of natural catalyst with properties of low cost and disposability should attract special attention

In the future, the development of novel and economic catalysts is still a promising option for tar elimination. At this stage, the biggest barrier for the catalyst development is the unclear mechanism of complex tar reformation. Therefore, employing model tar components for the study of coke formation mechanism is still very important and will be an effective way out. For the catalyst synthesis, composite catalysts with different components should be considered. It is also favored that if the developed catalyst could be applied under a low temperature condition (400–600°C), it will minimize cost effectively in a practical operation by using waste heat. In addition, the practical application of the catalyst also requires solving many scale-up issues, such as variation of temperature and pressure, impurities, fly ash and catalyst collapse

4. Socio-environmental impact

Biomass gasification could exploit an abundant variety of waste materials as feedstock such as agricultural residues and food waste. It actually achieves resource recovery and mitigates CO_2 emission as an environmental benefit. However, power generation from biomass gasification poses several key hazards and socio-environmental impacts.

4.1. Health and safety hazard

One of the major risks is the potential emission of toxic producer gas and particulates. The production of CO, SO_x, NO_x and volatile organics involves incomplete combustion and oxidation of trace elements in feedstock [24]. As one of the most dangerous constituent, CO can permeate into human blood system and combine with hemoglobin to stop oxygen adsorption and distribution. Long-term exposure to CO causes asthma, lung inflammation, schizophrenia and cardiac defects. Toxic gases like SO_x, NO_x and volatile organics could also destruct inhalation, ingestion and dermal system of human [25]. Hence, the entire gasification process should prevent leakage and an efficient gas clean-up system is essential. In recent years, the hazard of particles emission ($PM_{2.5}$) attracts public attention increasingly, due to its carcinogenicity. $PM_{2.5}$ particles can adsorb many soluble organic compounds including alkanes,

carboxylic acid and aromatic compounds, which will damage human organs like lung and liver [26]. For control of these particles' emission, an efficient gas clean-up system with conditioning unit is necessary, as well as avoiding insufficient combustion and gasification. In addition, ashes and condensate from biomass gasification also contribute to environmental problems if they are not disposed properly. Especially the toxic condensate with high content of tar is very difficult to deal with and has higher risk of hazards.

Besides the risk of health hazards and environment, gasification is also confronted with risk of fire and explosion. Because the gasification system is normally operated at relatively high temperature and pressure, it also produces flammable gas mixture with a great portion of hydrogen gas. However, explosion is not easy to be created even air leakage into the gasification system, which could raise a partial combustion. This will only lead to lower quality and higher temperature of producer gas [1], unless there is a large amount of air which enters with feedstock from the feeding system or massive leakage of flammable outlet gas occurs.

4.2. Social impact

The development of bioenergy will need a lot of land for energy-growing crops. This requirement will clash with other applications of farmland, like food and other cash crops. The competition with food agriculture must be intensive. The food shortage is still a big global issue nowadays. According to the data of World Hunger Education Service, the world's hungry population was 925 million in 2010. Besides this, the world population is still growing by rate of 1.2%. The natural disasters and climate change also affect agriculture. These three factors will decide that the demand of the farmland in the future will expand. Thus, transferring farmland for energy crop planting in a large scale would be difficult, especially in Europe.

4.3. Ethical issues

The bioethics report by Nuffield council points out that deployment of bioenergy should not violate the human right which is reflected in the Universal Declaration of Human Right (UDHR). In the UDHR, it states that every people can share and enjoy the protection of the moral and the any product from any scientific, literary or artistic which is owed by them. There are a lot of ethical issues referring bioenergy, like human rights, solidarity and sustainability. Biofuel production application will require land use, water supply and labor from local community. Destruction to the land and local ecosystem cannot be avoided. Also, land displaced for energy crops will not only bring food price increases; some local residents may face migration. All these could be regarded as the actions, which violate the human rights of citizens and non-citizens.

5. Conclusion

The commercialization of biomass gasification is still at the early stage of development and leaves a lot to be desired on the technology aspect. In particular, large-scale utilization of biomass still needs to overcome the challenge of biomass collection and transportation, due

to its low energy density. However, in some small communities, with large amount of local biomass materials, using biomass to replace polluting fossil fuels is a competitive way for providing reliable and clean power and heat.

This chapter provides the current technique status and development condition in China. It concludes that the gasification of biomass waste with distributed power generation would be a potential market. The properties of biomass feedstock have been analyzed and both advantage and disadvantage of biomass utilization were pointed out. Consequently, highly dispersed property and the low volumetric of biomass limit its large-scale application. Apart from that, this chapter also detailed some common types of gasifiers, except some emerging technologies, for meeting special requirements such as supercritical water gasification (SCWG) for wet biomass and plasma gasification for toxic organic waste. The tar issue, one of the most baffling problems in biomass gasification, is introduced briefly as well as its removal technologies. In our view, the socio-environmental impact is not the primary factor for restriction of biomass gasification development, while an objective financial return can actually attract investors and accelerate commercialization; in the meantime, it will also contribute to other technical breakthroughs.

Author details

Xiang Luo[1,2]*, Tao Wu[1,2], Kaiqi Shi[1,2], Mingxuan Song[3] and Yusen Rao[3]

*Address all correspondence to: xiang-luo@nottingham.edu.cn

1 A Key Laboratory of Clean Energy Conversion Technologies, The University of Nottingham Ningbo China, Ningbo, China

2 New Materials Institute, The University of Nottingham Ningbo China, Ningbo, China

3 Department of Chemical and Environmental Engineering, The University of Nottingham, Nottingham, UK

References

[1] Asadullah M. Barriers of commercial power generation using biomass gasification gas: A review. Renewable and Sustainable Energy Reviews. 2014;**29**:201-215

[2] McKendry P. Energy production from biomass (part 1): Overview of biomass. Bioresource Technology. 2002;**83**:37-46

[3] McKendry P. Energy production from biomass (part 2): Conversion technologies. Bioresource Technology. 2002;**83**:47-54

[4] Fallot A, Saint-André L, Le Maire G, Laclau J-P, Nouvellon Y, Marsden C, Bouillet J-P, Silva T, Piketty M-G, Hamel O. Biomass sustainability, availability and productivity. Revue de Métallurgie Paris. 2009;**106**:410-418

[5] Field CB, Behrenfeld MJ, Randerson JT, Falkowski P. Primary production of the biosphere: Integrating terrestrial and oceanic components. Science. 1998;**281**:237-240

[6] Gan M, Fan X, Chen X, Ji Z, Lv W, Wang Y, Yu Z, Jiang T. Reduction of pollutant emission in iron ore sintering process by applying biomass fuels. ISIJ International. 2012; **52**:1574-1578

[7] Demirbas A. Combustion characteristics of different biomass fuels. Progress in Energy and Combustion Science. 2004;**30**:219-230

[8] Demirbaş A. Biomass resource facilities and biomass conversion processing for fuels and chemicals. Energy Conversion and Management. 2001;**42**:1357-1378

[9] Faaij A. Modern biomass conversion technologies. Mitigation and Adaptation Strategies for Global Change. 2006;**11**:335-367

[10] van den Broek R, Faaij A, van Wijk A. Biomass combustion for power generation. Biomass and Bioenergy. 1996;**11**:271-281

[11] Lan P. Investigation of Hydrogen Production from Steam Reforming of Bio-oil and Catalytic Deactivation by Carbon Deposition, East China University of Science and Technology, East China University of Science and Technology; 2011. pp. 121

[12] Bridgwater AV, Meier D, Radlein D. An overview of fast pyrolysis of biomass. Organic Geochemistry. 1999;**30**:1479-1493

[13] Lin Y, Tanaka S. Ethanol fermentation from biomass resources: Current state and prospects. Applied Microbiology and Biotechnology. 2006;**69**:627-642

[14] Ruiz JA, Juárez MC, Morales MP, Muñoz P, Mendívil MA. Biomass gasification for electricity generation: Review of current technology barriers. Renewable and Sustainable Energy Reviews. 2013;**18**:174-183

[15] Sikarwar VS, Zhao M, Clough P, Yao J, Zhong X, Memon MZ, Shah N, Anthony EJ, Fennell PS. An overview of advances in biomass gasification. Energy & Environmental Science. 2016;**9**:2939-2977

[16] McKendry P. Energy production from biomass (part 3): Gasification technologies. Bioresource Technology. 2002;**83**:55-63

[17] Basu P. Biomass Gasification and Pyrolysis. Boston: Academic Press; 2010

[18] Maschio G, Lucchesi A, Stoppato G. Production of syngas from biomass. Bioresource Technology. 1994;**48**:119-126

[19] Luo S, Xiao B, Hu Z, Liu S, Guo X, He M. Hydrogen-rich gas from catalytic steam gasification of biomass in a fixed bed reactor: Influence of temperature and steam on gasification performance. International Journal of Hydrogen Energy. 2009;**34**:2191-2194

[20] Mahapatra S, Dasappa S. Influence of surface area to volume ratio of fuel particles on gasification process in a fixed bed. Energy for Sustainable Development. 2014;**19**:122-129

[21] Anis S, Zainal ZA. Tar reduction in biomass producer gas via mechanical, catalytic and thermal methods: A review. Renewable and Sustainable Energy Reviews. 2011; **15**:2355-2377

[22] Fagbemi L, Khezami L, Capart R. Pyrolysis products from different biomasses: Application to the thermal cracking of tar. Applied Energy. 2001;**69**:293-306

[23] Corella J, Orío A, Aznar P. Biomass gasification with air in fluidized bed: Reforming of the gas composition with commercial steam reforming catalysts. Industrial and Engineering Chemistry Research. 1998;**37**:4617-4624

[24] San Miguel G, Domínguez MP, Hernández M, Sanz-Pérez F. Characterization and potential applications of solid particles produced at a biomass gasification plant. Biomass and Bioenergy. 2012;**47**:134-144

[25] Kampa M, Castanas E. Human health effects of air pollution. Environmental Pollution. 2008;**151**:362-367

[26] Lewtas J. Air pollution combustion emissions: Characterization of causative agents and mechanisms associated with cancer, reproductive, and cardiovascular effects. Mutation Research/Reviews in Mutation Research. 2007;**636**:95-133

Chapter 2

Current Developments in Thermochemical Conversion of Biomass to Fuels and Chemicals

Chan Seung Park, Partho Sarothi Roy and Su Hyun Kim

Additional information is available at the end of the chapter

http://dx.doi.org/10.5772/intechopen.71464

Abstract

Biomass is one of the largest concentrated carbon source available for producing renewable energy. Thermochemical conversion of biomass has been used for centuries in various settings. Biomass typically has a higher oxygen and volatile matter content than other solid carbon feedstocks, resulting in increased reactivity during conversion by thermochemical pathways. Moisture content of the biomass feedstock exerts significant influence on the conversion process and is an important criteria used to classify various thermochemical conversion technologies. This chapter discusses the current status and future outlook of thermochemical biomass conversion processes.

Keywords: biomass, gasification, pyrolysis, hydrothermal treatment, steam hydrogasification, combustion

1. Introduction

Biomass has always considered as one of the major energy source for the world. Biomass can be defined as plant materials and animal waste, although broader definitions that include other forms of carbonaceous waste are used in the renewable energy context. Earth's primary source of biomass is the plant matter that grows through photosynthesis. The carbon stored in the biomass is from the carbon dioxide consumed during photosynthesis and is ultimately converted back to carbon dioxide during any energy generation processes. As is well known, biomass based processes are often carbon neutral, i.e., do not add additional carbon dioxide to the atmosphere, or have a very low carbon footprint. For these reasons, biomass is the largest and most widespread carbon source for producing renewable energy and is relatively free of fluctuation problems inherent to wind and solar energy. A comprehensive inventory of biomass

resources in the United States potentially available for energy production is available as so-called "billion-ton study" by the U.S. Department of Energy [1].

The oldest energy conversion process used by humans is biomass combustion in open air to produce heat. Biomass burning is still a dominant process in many parts of the world and thermochemical conversion of biomass to energy has a long scientific history. Since then, various thermochemical processes for biomass conversion have been developed to overcome the primary limitation of combustion; it only produces thermal energy along with the flue gases. Thermochemical biomass conversion to gaseous and liquid fuels has been studied and practiced for centuries. Production of a number of chemical compounds from biomass is also important application of the thermochemical process. The first such example is charcoal production from wood around 4000 B.C.

Compared to coal, which is the most widely used conventional solid fuel for energy production, biomass typically contains a higher oxygen and volatile matter content and lower ash [2]. This high oxygen content makes biomass a good fuel although oxygen itself does not contribute toward the energy value of the fuel. The higher oxygen content results in reduced air (oxygen) requirement during the combustion reaction. **Table 1** summarizes the Lower Heating Value (LHV) of different fuels. Coal has a higher LHV than biomass per unit mass of the fuel. However, once the volume of air required for complete combustion is taken into account (LHV per mass per air mix), biomass's value is higher than that of coal, and is even comparable to methane.

Nearly 80% of the carbon in the biomass is typically considered "organic," i.e., bounded to hydrogen or oxygen. Organic carbon is highly volatile compared to elementary carbon, resulting in improved reactivity and thus makes biomass an attractive feedstock for thermochemical production of fuels and chemicals, especially from the conversion perspective. **Table 2** summarizes the typical oxygen and volatile content of coal and biomass. Conversion of the volatile portion of the biomass feedstock into gaseous species starts around 225 to 300°C and is mostly complete around 500 to 600°C [4]. While elemental, non-volatile carbon decompose at temperatures above 800°C, much higher temperatures (>1200°C) are desirable to avoid potential problems associated with ash softening [5]. Thus, thermochemical conversion of biomass can be performed at the much lower temperatures than is needed for coal, with higher conversion efficiency.

LHV	Methane	Bituminous coal	Biomass	Hydrogen
MJ/kg fuel [3]	47	27	18	120
MJ/kg fuel/air mix	2.62	2.44	2.60	3.36

Table 1. Comparison of LHV values of methane, coal, biomass and hydrogen.

Components	Bituminous coal	Biomass
Oxygen (wt.%, dry ash free, daf)	14	43
Volatiles (wt.%, daf)	42	82

Table 2. Oxygen and volatiles content of coal and biomass.

From the thermodynamic point of view, at the typical biomass conversion temperature of 800°C, the product gas typically has higher concentrations of more valuable C_{2+} species. **Table 3** shows product gas composition of a biomass gasifier operated by the Milena project [6], a well-known biomass gasification demonstration project in Europe, along with the gas composition of a typical coal gasifier operated at higher temperatures (1400°C), which more closely represents the thermodynamic equilibrium values.

It also shows the product gas has lower syngas ratio (syngas or synthesis gas is a mixture of hydrogen and carbon monoxide and syngas ratio is the molar ratio of Hydrogen to CO), which typically provides more flexibility during use in downstream processes that require specific syngas ratios. Syngas ratio can be increased using the well-known, commercially matured, water-gas shift process. Syngas ratio reduction is achieved through techniques such as membrane separation, and presents a number of technical challenges [7]. Higher CH_4 content is also beneficial since the product gas is often used as a fuel in combustion engines or boilers. C_{2+}, i.e., gaseous carbon species with a higher carbon number, can potentially be used as a feedstock in chemical production. Such high value co-products often provide an additional revenue stream, improving the overall economics of the biomass gasification plant.

In conclusion, biomass is the only concentrated renewable carbon source that can be converted into fuels and chemicals with a zero or very low carbon footprint. Unlike biological processes that only convert part of the biomass, thermochemical processes can generally convert all the carbon in the feedstock. Biomass is a reactive, desirable feedstock for thermochemical processes due to the higher oxygen content compared to coal. Thermochemical conversion of biomass offers significant versatility since the product gas can be converted into fungible liquid fuels, thereby offering a pathway to reduce the carbon intensity of the transportation sector. The product gas from most thermochemical processes can also be converted into high value chemicals such as ethylene and BTX (Benzene, Toluene, and Xylene).

Some thermochemical process such as flash pyrolysis and hydrothermal liquefaction directly produce a liquid product. Thermochemical processes can also handle intermediate products and waste biomass from biological conversion processes [8]. High value chemicals production from biomass with energy as a major co-product may be the path to economic viability in the near future.

This chapter presents an overview of the different thermochemical processes that convert biomass into a high energy content gaseous or liquid product and/or additional thermal energy. A discussion of the unique aspects of different technologies from various perspectives, including energy storage and transportation is also provided.

Mole fraction, %	**H_2**	**CO**	**CO_2**	**CH_4**	**C_{2+}**
Equilibrium value	51	45	3	1	0
Measured (Milena FB gasifier) [6]	25	33	18	15	6

Table 3. Comparison of product gas composition under equilibrium conditions with those from a biomass gasifier.

2. Classification of thermochemical biomass conversion processes

Biomass is the only renewable resource that can be directly converted in to concentrated energy products using thermochemical conversion [9]. Biomass consists of organic and inorganic matter and often significant amounts of moisture. Organic matter in biomass contributes to its calorific value. Organic matter can be further classified into cellulose, hemicellulose, and lignin. The inorganic matter is conventionally referred to as ash. Compared to conventional fuels, the oxygen content of biomass is typically very high, approximately ranging from 20 to 50% by weight. The moisture content plays a very important role in selecting the appropriate thermochemical conversion process. Heating value of biomass is heavily dependent on the moisture content. The LHV value is negative for biomass with a high moisture content (80%), since the heat released during the combustion process is not sufficient to evaporate all the water [10]. Therefore, biomass is usually dried under sunlight or through other methods, e.g., using recycled thermal energy as part of feed preparation. Solar and air drying in the production field is the preferred method of drying, primarily due to the lower cost. However, there are several conversion routes that use wet biomass feedstocks without the need for drying. Whether a conversion process uses wet or dry biomass as the feedstock is an important criteria for the classification of biomass conversion processes. A technology is categorized as a wet biomass process based on whether the moisture in the feedstock plays an important role in the process, either as a major reactant, or as physical media to maintain the reaction environment. In other words, wet biomass processes do not benefit from drying the feedstock, and often require the feedstock to contain certain quantity of moisture. **Table 4** lists the wet and dry biomass feedstock processes, and these processes are discussed in detail in the rest of the chapter.

Feedstock	Technology	Features
Wet biomass	Biological*	Anaerobic digestion, or alcohol production from sugars by biomass hydrolysis and fermentation
	Hydrothermal conversion	High pressure conversion to a hydrophobic oil. Often involves further catalytic conversion to methane, liquid fuels or chemicals
	Supercritical gasification	Conversion occurs under supercritical conditions
	Steam hydrogasification	Uses hydrogen and steam as the gasifying agents
Dry biomass	Oil extraction form seeds*	Trans-esterification or hydrogenation of vegetable oil from oil seeds to produce bio-diesel
	Direct combustion	Generate heat or power through the direct combustion of biomass
	Slow pyrolysis	Heating up the biomass in the absence of air (or oxygen) with slow heating rates to produce biochar and gaseous products
	Fast pyrolysis	Extremely fast pyrolysis of biomass with very high heating rates resulting in crude oil like bio-oil and gaseous products
	Gasification	Biomass is converted into the syngas or Substituted Natural Gas (Bio-SNG) using air or oxygen or hydrogen as the gasifying agent

*These processes are outside the scope of this chapter and are not covered.

Table 4. Classification of biomass conversion processes.

Recently, the bio-refinery concept has emerged as an important option. A bio-refinery integrates several conversion and resource recovery processes with the aim of maximizing process efficiency, minimizing waste and improving profits [9]. An integrated bio-refinery may use additional feedstocks besides biomass and will produce multiple products including fuels, chemicals and thermal or electrical energy. The bio-refinery concept is still evolving, and has the potential to be an important biomass utilization option in the future that incorporates a wide range of options including biological and thermochemical processes to overcome the limitations of specific technologies.

3. Wet biomass conversion processes

3.1. Hydrothermal conversion process

Hydrothermal conversion has been studied for more than a 100 years. Friedrich Bergius, who would later receive the 1931 Nobel Prize in Chemistry along with Carl Bosch, developed the Bergius process that produces liquid fuel through hydrogenation of crude oil derived from hydrothermal treatment of coal. The technology was also applied to peat and plant material [11]. Hydrothermal conversion converts biomass into "bio-crude" through thermal depolymerisation under high pressures and moderate temperatures and has since then been studied by several research groups. A comprehensive review of the hydrothermal conversion process of the biomass is provided by Peterson et al. [12].

Hydrothermal processes can convert all types of biomass, including wet organic biomass, and typically involves the use of a catalyst to improve conversion efficiency. Hydrothermal liquefaction study conducted by Yang et al., shows that the process produces larger amount of oil product compared to other methods [12]. The product liquid fuel is easy to separate, for once it is cooled downed to the room temperature the gaseous product is emitted very quickly [13]. The product bio-crude, can be further processed into high-quality diesel or kerosene. The fast pyrolysis process, discussed later, is a dry conversion process that produces a bio-crude (or bio-oil) from dry biomass feedstock. Hydrothermal conversion process has lower efficiencies caused by the significant energy requirement of water evaporation.

Hydrothermal conversion processes can be further divided into supercritical hydrothermal and subcritical conversion processes. A supercritical hydrothermal conversion process developed by Aalborg University and commercialized by Steeper Energy under the name of "Hydrofraction" converts organic wastes into a raw bio-crude under supercritical conditions in the presence of K_2CO_3 catalyst [14]. Another process, referred to as the "Catliq" process uses Zirconia catalyst under supercritical conditions to produce a bio-crude with less than 6% oxygen content [15].

Shell research group has demonstrated a subcritical process named Hydro Thermal Upgrading (HTU) that converts the biomass into bio-crude with and without a catalyst [16]. Research has shown that in the presence of a catalyst with adequate activity, conversion could be accomplished at conditions that are less severe than supercritical. A number of catalysts including ones based on Ru, Carbon, and Ni have been proposed with the ultimate goal of developing an optimal hydrothermal conversion process under subcritical conditions [17].

3.2. Supercritical gasification

The supercritical condition for water is the combination of T > 374°C and P > 218 atm. Under these conditions, distinct liquid and vapor phases do not exist and the water exists as a single phase fluid [18]. The general reason to use supercritical conditions for wet feedstocks is to minimize the energy loss associated with water evaporation. Study performed by Demirbas [19] and Gadhe, & Gupta [20] shows that the supercritical water behaves as an organic solvent and exhibits extraordinary solubility toward organic compounds containing large nonpolar groups and most permanent gases. Transition of liquid water to the gas phase (steam) requires a large amount of heat, so-called "the heat of vaporization," which can be recovered in theory, but needs very efficient heat exchanger design. By operating the conversion process under supercritical conditions, uniform temperature profile along the reactor can be expected without the formation of multi-phase of water (liquid water, steam and/or superheated steam), which in turn results in efficient heat transfer between the product gas and feed inlet of the gasifier.

Supercritical biomass gasifiers typically operate around 500 to 750°C without a catalyst or at temperatures below 500°C in the presence of a catalyst. The presence of supercritical water leads to rapid hydrolysis of biomass and high solubility of intermediate reaction products including gaseous species. These features make supercritical gasification as excellent tool for the conversion of very wet biomass feedstocks such as aquatic species and sewage sludge (a.k.a. biosolids), which normally require considerable drying before they can be gasified economically. Supercritical gasification also produces a high pressure product gas, thereby eliminating the need for the product gas compression required by most down-stream processes. A detailed discussion of process efficiency and other aspects of supercritical gasification is available in the article by [21]. For example, the gasification efficiency of a biomass feedstock with 80% water content using conventional steam reforming reaction is only 10%, while that of supercritical gasification can be as high as 70%. The main products are H_2 and CO_2 and the hydrogen is produced at very high pressure which is at the storage condition and reduces the storage cost. Also, the reactor operates at high reaction temperature, low residence time, and low biomass concentration.

However, there are several technological issues that must be overcome in order for supercritical processes to be commercially viable:

- Supercritical gasification processes need large heat input. Efficient design of heat exchanger is critical to achieve desired energy conversion efficiency.
- The feeding of wet biomass is another barrier, although slurry pump has been used to feed into the high pressure vessel. However, achieving reliable feeding into supercritical gasification reactor under a very high operating pressure is still a significant challenge.
- Other issues such as fouling, plugging of the feedstock, and corrosion are well reviewed by [22].
- Higher capital costs due the high operating pressure also have a negative impact on economic performance.

For these reasons, supercritical gasification processes are still in the development stage [23]. University of Twente operates a pilot plant and is involved in active research and development [24].

The VERENA group operates a somewhat larger pilot plant with 100 kg per hour throughput in Karlsruhe, Germany [25].

3.3. Steam hydrogasification

Steam hydrogasification uses steam and hydrogen as the gasifying agents and is especially suited for the conversion of wet feedstocks since it utilizes the water from the feedstock as a major reactant other than the physical media served as a thermal moderator [26]. Hydrogasification, using only hydrogen as the gasifying agent, is a well-known conversion technology but is not considered commercially viable due to several issues, including low conversion efficiencies and requirement of an external hydrogen source [27]. Research has shown that hydrogasification in the presence of steam significantly enhances the rate of methane formation under specific process conditions, thereby improving the overall process efficiency [28, 29]. This process, referred to as "steam hydrogasification," produces a product gas with a high methane content. The product gas also contains a considerable amount of unreacted steam along with CO, CO_2, H_2, and some higher molecular hydrocarbons. The product gas can then be converted into various fuels or chemical products. The impurities in the flue gas is significant during the steam hydrogasification. Cui et al., [30] developed Ni based catalyst and ZnO sorbent for contaminant and sulfur removal from the product gas and they were able to reduce the components significantly.

An example block flow diagram for Renewable Natural Gas (RNG) production is shown in **Figure 1**. The feedstock is turned into a slurry through a hydrothermal pre-treatment process (HTP) and is transported into the steam hydrogasification reactor (SHR) using a slurry pump. A portion of the necessary steam enters the reactor as water that is part of the slurry along with additional superheated steam and recycled hydrogen.

The methane-rich gasifier product gas is then subjected to warm gas clean-up in order to remove contaminants such as sulfur and other species. Following this, the excess steam and CO is converted into hydrogen in a water gas shift reactor (WGS). This is an important aspect of the process: Even though the steam hydrogasification process needs hydrogen, it does not require an external source of hydrogen. The hydrogen is separated and fed back into the gasifier, making the process self-sustained in terms of the hydrogen supply. The process is currently undergoing demonstration [31].

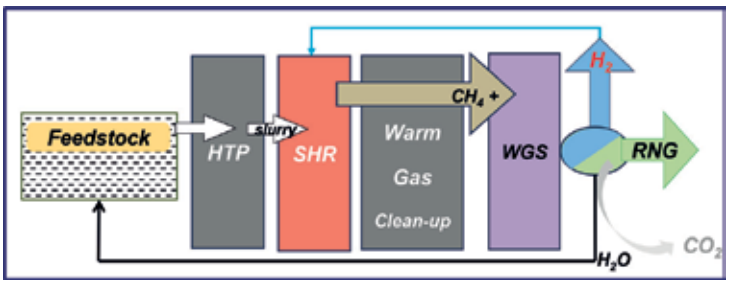

Figure 1. Block diagram of RNG production by steam hydrogasification process.

4. Dry biomass conversion processes

4.1. Gasification

Gasification, which implies incomplete combustion (also commonly referred to as partial oxidation) of the carbonaceous feedstock, is one of the most attractive options to convert biomass into various high value products such as liquid and gaseous fuels, chemicals and electricity. Gasification is the most popular among the thermochemical conversion processes with the exception of direct combustion. Gasification processes have several advantages and disadvantages over other conversion technologies. The main advantages are that the gasification feedstock can be any type of biomass including agricultural residues, forestry residues, by-products from chemical processes, and even organic municipal wastes. Moreover, gasification typically converts the entire carbon content of the feedstock, making it more attractive than enzymatic ethanol production or anaerobic digestion where only portions of the biomass material are converted to fuel. The second advantage is that the product gas can be converted into a variety of fuels (H_2, Bio-SNG, synthetic diesel and gasoline, etc.) and chemicals (methanol, urea). The other benefit of the biomass gasification process is lowered CO_2 emissions, compact equipment setup with higher thermal efficiency [32]. Thus gasification is most suitable to produce chemicals that can be alternatives to petroleum based products.

Gasification technology for biomass conversion is commercially applied in China: in 1990, China built more than 70 biomass gasification projects for household cooking and each of them can supply energy for 800–1600 families [32] whereas in India, a perspective way of electricity generation is gasification.

Gasification processes are primarily designed to produce synthesis gas (syngas, a mixture of hydrogen and carbon monoxide) by converting the feedstock under reducing (oxygen deficient) conditions in the presence of a limited amount of gasifying agent such as air or oxygen [5]. Gasification consists of three major steps. The first step is devolatilization of the dried feedstock to produce the fuel gas for the second step, which is combustion. The combustion step produces the necessary heat and reducing environment required for the final step. The final step (so-called reduction step, char gasification step or syngas production step), is the slowest reaction phase in gasification, and often governs the overall gasification reaction rate. These 3 steps can be shown as:

Devolatilization: Feedstock → Fuel gas +Char.

Combustion: Fuel gas + Air → Flue gas + Heat (~25% of carbon)

Reduction: Fuel gas, Char + Heat → Syngas (~75% of carbon)

Gasification: Feedstock + Air → Syngas + Flue gas + Ash.

Approximately 25% of carbon in the feedstock is consumed in the combustion step to provide the heat and reducing environment for the reduction step. A detailed discussion of gasification, including minor steps and considerations is available elsewhere [5].

The dual fluidized bed reactor configuration is a well-known option for the gasification of biomass feedstock. This configuration uses two separate reactors, one for the combustion and the other for the reduction reaction.

Benefits of the dual bed configuration for biomass gasification are [33]:

- Provides improved process efficiencies and avoids the challenges related to ash melting by operating at lower gasification temperatures (normally greater than 800°C but below the ash softening point).
- Other fuel sources can be used for the combustion step to overcome the low heating value of the biomass feedstock. These fuels include char by-product from the reduction reactor or other designated fuels such as methane.
- Air is only used in the combustion reactor and does not enter the reduction reactor, thereby preventing nitrogen dilution of syngas, a major problem in air blown gasifiers [34].

The heat required for the reduction reaction is supplied through the bed material (typically sand) from the combustion reactor. The bed material is continuously circulated between the two reactors while the ash is removed from the bed material using cyclones and the gases from the two reactors are not allowed to mix. The Milena project gasifier uses the two reactor configuration [35].

Tar formation in a gasifier during gasification process is significantly affected by reactor/gasifier configuration. Cao et al. [36] introduced an innovative fluidized bed gasifier which can produce tar free product flue gas. The factors that affects the biomass gasification process most are: the reaction temperature, residence time and oxygen to biomass ratio [37].According to this study, the optimum residence time is 1.6 s and the optimum oxygen to biomass ratio is 0.4.

A major challenge of biomass gasification is to overcome the higher specific capital and operating costs. This is due to the much smaller plant sizes (normally less than 500 tons per day) compared to coal gasification plants (tens of thousands of tons per day). The plant size is determined by biomass availability and related logistic issues and transportation costs inherent to any distributed resource. Other challenges include the presence of undesirable species such as alkali compounds in biomass ash. Alkali materials such as sodium and potassium cause slagging and fouling problems [38]. Most biomass gasifiers operate below the ash softening temperature to avoid ash melting. The lower temperatures also lead to lower capital cost requirement, resulting in favorable process economics. However, lower temperatures often result in the formation of undesired tar, which leads to severe operational problems. A number of catalysts and process configurations have been developed to address this issue, but tar problems still persist [39]. Addition of a catalytic tar cracker to the outlet of the gasifier to decompose the tars into smaller molecules has been considered [40]. Washing out the tars while the product gas is cooling down has also been proposed, but this approach requires rigorous treatment of the washing water. Tar formation is still a major challenge and is regarded as the "Achilles heel" of biomass gasification processes. These issues are not to be underestimated and careful attention is required in the design and operation of biomass gasifiers.

The study performed by van de Kaa, Kamp and Rezaei [41], investigated the technology dominance of the three different dry thermochemical conversion of biomass. They found that the gasification technology has the highest potential of becoming the commercial technology for biomass conversion in the Netherlands.

4.2. Bio-SNG production by gasification

4.2.1. Current status of bio-SNG R&D projects

Bio-SNG is a fuel made from syngas produced by biomass gasification with major constituent of natural gas for potential use in household or transportation. Various R&D projects on biomass gasification are underway in many EU nations with specific objectives of enhanced generation and distribution of renewable energy and consequent reduction in greenhouse gas evolution: Current status of 3 Bio-SNG projects in Austria, the Netherlands, and Sweden is introduced.

4.2.2. SNG demonstration plant (Austria, Güssing)

- Fluidized bed gasification demonstration plant in operation at Güssing, Austria burning wood chips. Details are summarized in **Figures 2–4** and **Tables 5–7**.

4.2.3. ECN SNG project (Netherlands)

- At present, EU is setting legally-binding objectives of 20% CO_2 reduction by 2020 and further 60–80% by 2050 and thus the Netherlands is planning to increase the bio-SNG portion to 20% of primary energy generation source in compliance. Dutch ECN [44] has already performed feasibility study on production of SNG from biomass gasification since 2002 with fluidized bed gasifier consisting of gas purification system, and subsequent methanation and SNG upgrading processes. Details of ECN-initiated bio-SNG plant R&D stages and unit processes are shown in **Figures 5** and **6**.

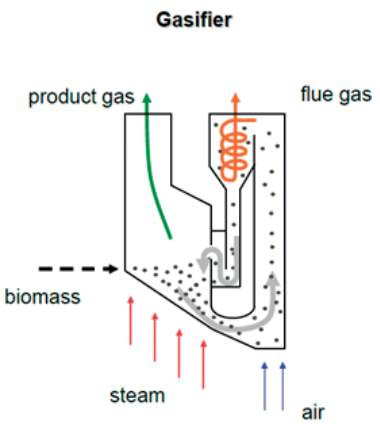

Figure 2. Gasifier type [42].

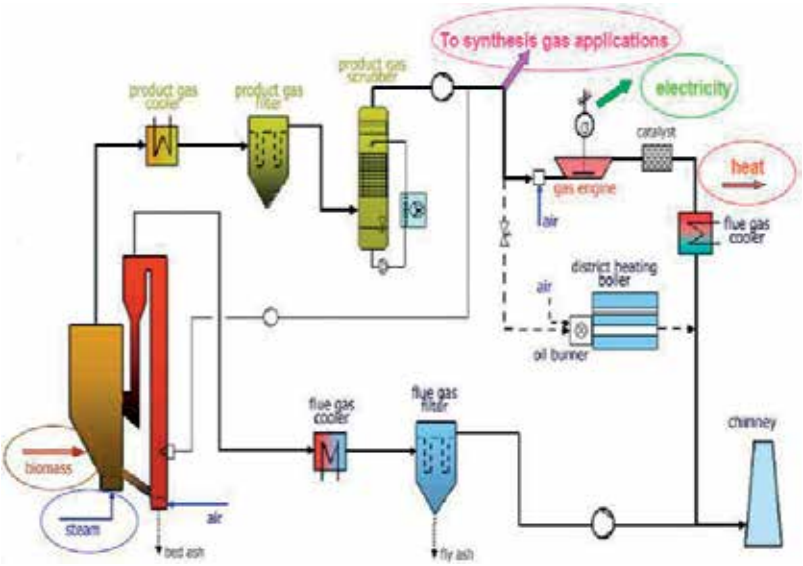

Figure 3. Process flow diagram of the gasification plant [43].

Figure 4. 1 MW capacity SNG demonstration plant [43].

The ECN bio-SNG plant gasifier is named as "MILENA," with circulating fluidized bed gasifier and bubbling fluidized combustor as main elements proper. The gasifier operates at 800°C, with various feedstocks. Overall gasification performance and processes of the ECN bio-SNG plant are shown in **Figure 7** and **Table 8**.

4.2.4. GoBiGas project (Sweden, Göthenburg)

- Sweden has currently set 50% proportion of renewable energy sources in the national energy generation and concomitant reduction of CO_2 evolution by 40%. Besides, they are planning to exclude reliance on fossil fuel sources in national transport system by 2030. Göteborg Energi initiated relevant R&D by performing feasibility studies on various

Items	Contents
Feedstock	• Wood chip(Moisture 20–30%) 2300 kg/h
Gasifier type	• Dual fluidized bed steam gasifier, • two-stage gas cleaning system • gas engine with an electricity generator • heat utilization system
Capacity	• 8 MWth(2MWe) • Commercial bio-SNG plants: announced as 20–200 MW
Final Product	• Currently used as power and heat by operation of gas engine • SNG synthesis is separately studied at Paul-Scherrer Institute, Sweden (1000 h demonstration experiment linked with slip stream • 1 MW demonstration SNG plant construction completed • 8-year of ongoing R&D in gas conditioning and synthesis of SNG
History	• R&D since 2002 • 10 M EURO invested (government subsidy of 6 M EURO inclusive) • Plant operation cost per annum at 15% of total investment • Recorded cumulative operation time of more than 60,000 h • R & D Project under name of "GAYA" as of 2010

Table 5. Summary of the project.

Main components (vol %)		
H_2	%	35–45
CO	%	22–25
CH_4	%	~10
CO_2	%	20–25
Minor components		
C_2H_4	%	2–3
C_2H_6	%	~0.5
C_2H_2	%	~0.4
O_2	%	<0.1
N_2	%	1–3
C_6H_6	g/m^3	~8
C_7H_8	g/m^3	~0.5
$C_{10}H_8$	g/m^3	~2
TARS	mg/m^3	20–30

Table 6. Syngas composition [43].

gasification technologies since 2006 and has completed fundamental engineering design as a result of primary stage progress during 2008–2013, thus enabling construction of a 20 MW bio-SNG demonstration plant. The production capacity of the 20 MW bio-SNG demonstration plant was equivalent to fuel 15,000–20,000 hydrogen fuel cell vehicles, based on the same type of gasifier as that of aforementioned Güssing, Austria. The bio-

Main components		
LHV	MJ/Nm^3	34.20
CH_4	%	94.81
CO_2	%	0.47
H_2	%	1.55
H_2O	%	0.16
N_2	%	2.67

Table 7. Bio-SNG composition [43].

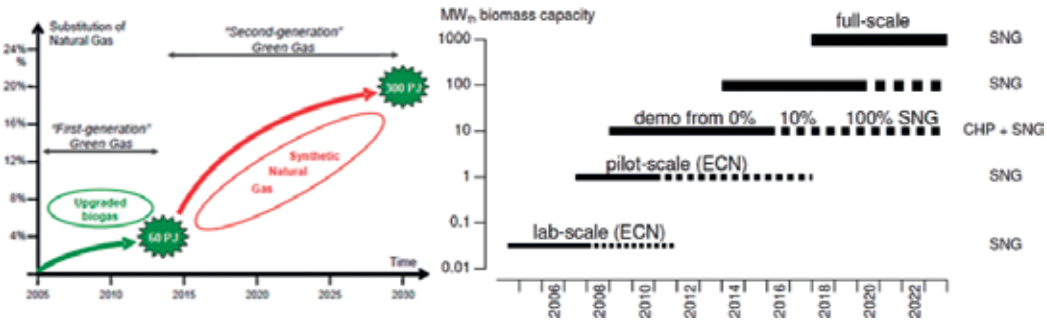

Figure 5. Overall timeline of the Dutch bio-SNG project [44].

SNG demonstration plant already supplied hydrogen fuel via natural gas distribution network with accumulated operation record exceeding 10,000 h. The methane concentration and calorific value of the SNG thus produced were 96.5–97.5% and 10.8 kWh/Nm^3 (HHV basis) which will be used as a basis for construction of a commercial scale gasifier with 80–100 MW capacity after successful operation of the demonstration plant for reliability substantiation. Overall unit processes and their flow diagram are illustrated in **Figure 8**.

4.3. Slow/fast pyrolysis

Pyrolysis is the thermal decomposition of the feedstock in the absence of oxygen. The products of biomass pyrolysis are char, bio-oil (also referred to as bio-crude) and gases including methane, hydrogen, carbon monoxide, and carbon dioxide. Pyrolysis can be further classified into slow and fast pyrolysis based on the residence time of the solid biomass in the reactor. Fast pyrolysis is normally conducted under medium to high temperatures (usually 450–550°C) at very high heating rates and short residence time (e.g., milliseconds to a few seconds).

The objective of the process is to maximize the liquid yield and minimize the production of char and gases. This requires fast heating of the biomass and produces bio-oil (~60% by weight) and other products including gas and char [49]. On the other hand, slow

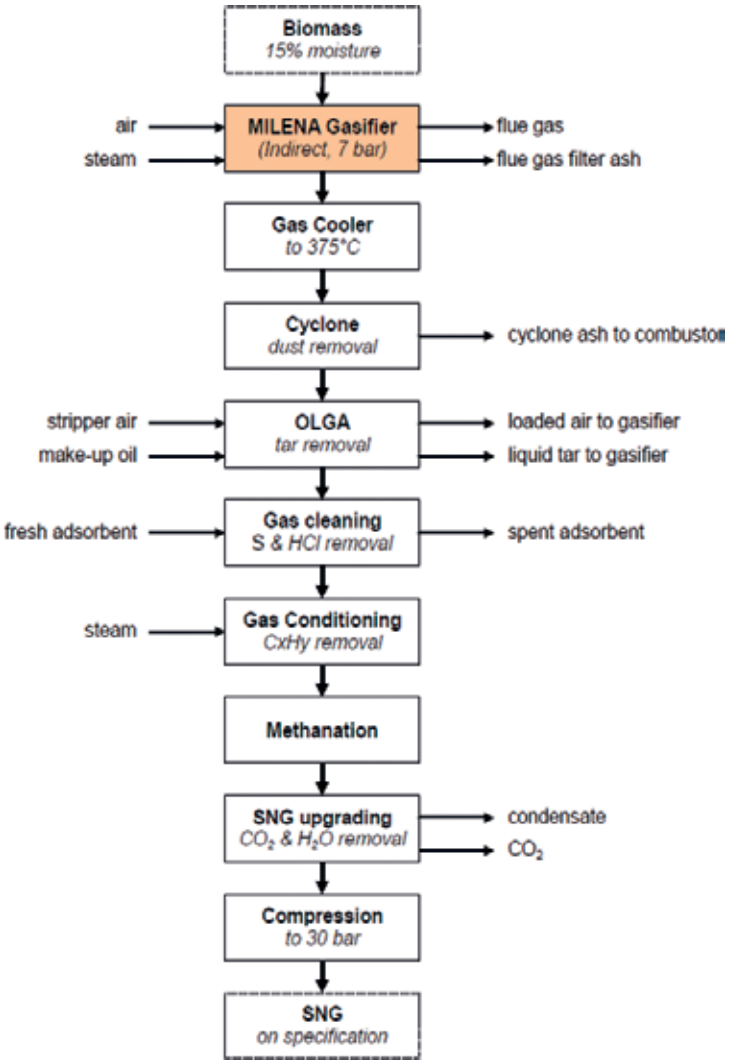

Figure 6. Process step of pilot and demo plants [45].

pyrolysis takes several hours to complete with bio-char being the main product. Pan et al. [50] performed the slow pyrolysis of Nannochloropsis sp. (a kind of green microalga) and showed that the catalytic pyrolysis can produce the fuel with low oxygen content and higher heating value than the pyrolysis product without catalyst. Fast pyrolysis has attracted considerable attention in recent years. Fast pyrolysis efficiency, in addition to the residence time and operating temperature, is strongly dependent on the particle size of the feedstock as rapid and efficient heat transfer through the particle is critical. Most fast pyrolysis processes use a maximum particle size of 2 mm. Pyrolysis processes can be built in relatively small scales and are well suited for lignocellulosic feedstocks. Efficient thermal energy input to the reactor is critical since the pyrolysis process is endothermic

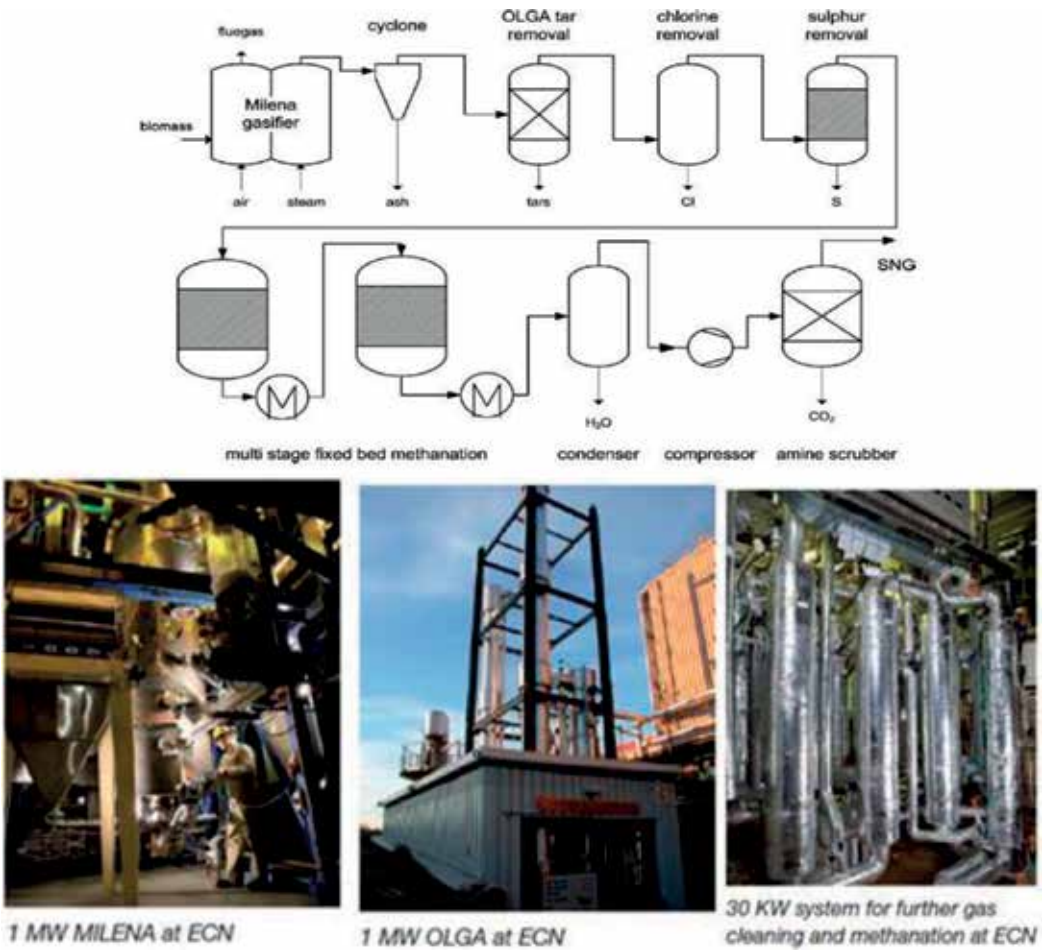

Figure 7. Process flow diagram and unit process of the ECN bio-SNG plant [47].

SNG-process characteristics	Milena
Carbon conversion (%)	80
Biomass-to-SNG efficiency (%)	66.3
Overall process efficiency (%)	82
Gas yield(Nm^3/kg biomass)	0.82

Table 8. Performance of the ECN bio-SNG plant [46].

and heat transfer rates play a major role in the conversion process. High moisture content biomass must be dried prior to the conversion process. Besides oil and gas, bio-char is an important pyrolysis product. Bio-char is well-known as a soil amendment as it is highly absorbent and increases the soil's ability to retain water and nutrients. This fast process product yields more than 70 wt.% biomass when operates at atmospheric pressure and

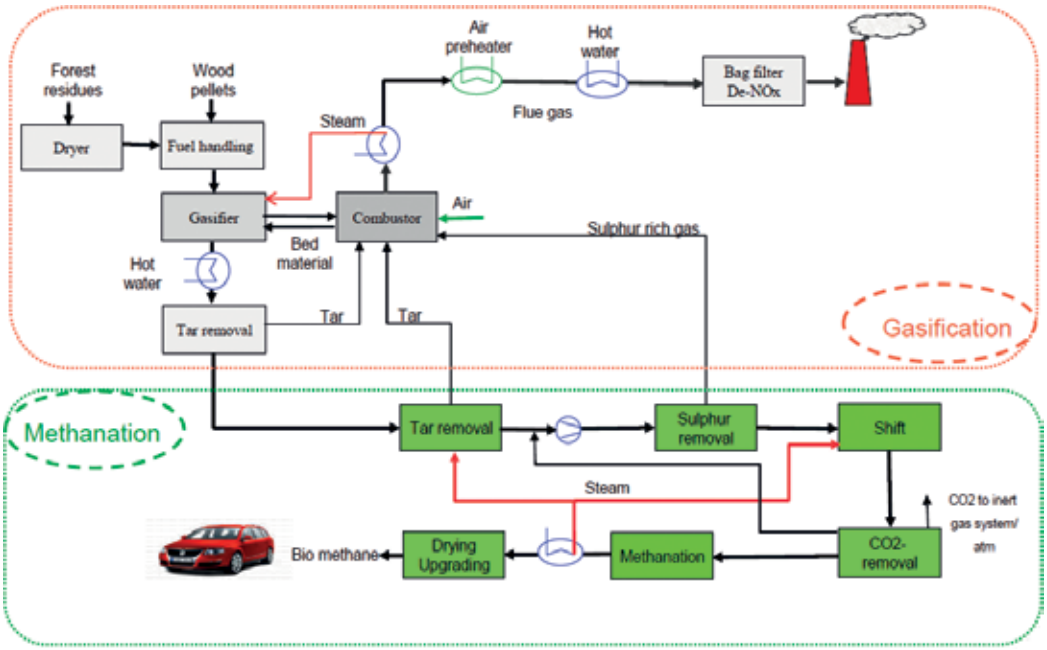

Figure 8. Process diagram of the Swedish GoBiGas plant [48].

moderate temperatures (450°C). Oxygen and water are major by-products during fast pyrolysis and these components degrades the fuel quality to the low-grade fuel compared to conventional hydrocarbon fuel [51].

Duman et al. [52] performed a comparison study of slow and fast pyrolysis: medium level of bio-oil is produced by slow pyrolysis of cherry seeds with only 21 wt.% yields whereas the bio-oil of 44% yield is produced by fast pyrolysis of the same feedstock.

Flash pyrolysis is an emerging technology and there are several key issues that need to be addressed. The most critical problems are associated with the quality of the "bio-oil," dictated by the physical and the chemical properties. Some of these problems are discussed below. Ideally, bio-oil should be interchangeable with petroleum crude oil so that the transportation and refining infrastructure can be used in existing form or with minor modifications. Based on this reasoning, the properties of bio-oil are often compared to that of petroleum crude oil. However, bio-oil has serious physical and chemical property issues and it is difficult to use it in existing petroleum refineries [15–18, 21–23].

Bio-oil is known to be extremely corrosive and this nature causes serious problems related to handling and transportation. The Total Acid Number (TAN) required for crude oil refineries is normally less than 2. Typical bio-oil TAN values range from 50 to as high as 200 [24]. Bio-oil typically contains 15–30% water. Besides water, components present in high concentrations are hydroxyl-acetaldehyde and acetic and formic acids. These oxygenated compounds along with various other species such as phenolic compounds contribute

toward the acidity of the bio-oil. Typical pH of the bio-oil is in the range of 2.0–3.0 [16]. The viscosity of bio-oils increases during storage and the physical properties undergo considerable changes [21]. The changes in the physical properties are attributed to the self-reaction of various compounds in the bio-oil including polymerization reactions [22, 25]. These reactions, occurring during storage, increase the average molecular weight of the bio-oil and also lead to other storage related issues such as phase separation.

The resulting corrosive nature presents serious obstacles to any efforts aimed at the transportation and centralized refining or upgrading of the bio-oils. Also, the unstable nature of bio-oils often necessitates minimizing storage times and local upgrading, instead of transportation to a centralized facility. Such local upgrading is done by means of hydro-deoxygenation using hydrogen, often in the presence of catalysts. This normally adds capital and operating cost to the bio-oil production process. Gasification and co-gasification of bio-crude to syngas have been tried, with reasonable success [5].

Most of the fast pyrolysis projects are still in laboratory scale with an exception of a few, including KIOR project [53] and BTG-BV in the Netherlands, which was originally developed by University of Twente [54]. These processes are regarded as pre-commercial, or demonstration stage technologies.

4.4. Direct combustion

Direct combustion of biomass is the oldest energy production process in human history. It is still by far the most widely used biomass conversion process. It is the most common biomass to power generation method commercially available [41]. The scale can be very small to relatively large, ranging from 1 MW up to 100 MW. Co-firing of biomass with coal is the effective way for lowering the greenhouse gas emissions. A wide range of technology options ranging from the simple fire stove to the advanced boiler system with fluidized furnace using pulverized fuel are available. Precise control of mixing between the biomass fuel and oxygen source (generally, air) is a critical aspect of advanced combustion systems in order to achieve improved thermal efficiency and minimize of criteria pollutant emissions including particulate matter (PM), nitrogen oxide (NOx), carbon monoxide (CO) and hydrocarbons.

For industrial and centralized domestic heat and power generation, several designs including stoker burners, grate boilers and/or dense fluid-bed combustor are used ranging from a few kilowatts to 10 MW. Combustion efficiency has improved remarkably in recent decades and has reached over 90% from around 55% in 1980 (FBC). Recently, development of combustion systems with pressurized fluidized beds have enabled direct electricity production without requiring steam generation, since process utilizes the fluidized bed as combustion chamber of the gas turbine [55].

For a very large-scale direct combustion (larger than 300 MW), co-firing biomass with pulverized coal has been recommended. Pulverized coal combustion technology is well established and co-firing is an attractive option that can reduce the carbon dioxide emissions

from coal. However challenges associated with co-firing with biomass such as changes in ash properties, fouling of heat exchanger, etc. still need to be addressed [56]. Biomass torrefaction is promising process that improves the usefulness of biomass as a fuel by heating the biomass in the absence of air under mild temperatures (230–300°C). The resulting biomass fuel is a desirable feedstock for entrained-flow reactors or in pulverized coal fired boilers with co-firing of biomass [57].

Arce et al., [58] studied the performance of the different types of biomass fuel combustion process in a counter-current fixed bed reactor in the temperature range of 740–1300°C to check the effects of different factors and find the optimum condition. According to the study, the ignition front propagation speed and the highest temperature that is reached at the fixed bed combustor affects the combustion process most.

Oxy-combustion is an emerging technology that uses pure oxygen in the combustor. The advantage is that after the cooling of flue gas, nearly pure carbon dioxide is produced without any nitrogen or nitrogen oxides. However, the use of pure oxygen (or oxygen enriched air) results in higher capital and operating costs. This needs to be balanced against the cost/energy savings related to carbon dioxide capture. This technology is still in the research and demonstration stage. As more cost effective processes for oxygen production such as membrane separation are developed, oxy-combustion will presumably become a more attractive option for both biomass and fossil feedstocks.

5. Conclusion

Energy sources from the renewable carbon are critical to address future energy needs, in the all energy consuming sector. Biomass is the largest and most widespread carbon source for producing renewable energy, fuels and chemicals and can be a constant, reliable resource compare to other renewable sources such as solar or wind energy. A wide range of biomass conversion processes are available and are under development. Among these, thermochemical processes offer several advantages, including product versatility, and high conversion rates and efficiencies, although challenges to commercialization still remain.

Wet thermochemical processes including hydrothermal conversion, supercritical gasification and steam hydrogasification are still under development, but have many attractive aspects for use in decentralized, low cost applications, especially for high moisture content biomass. Dry thermochemical conversion processes including direct combustion, gasification and pyrolysis have several specific technology options that are mature. However, economic viability issues and technical challenges related to tar formation and alkaline ash presence still need to be addressed.

New emerging approaches such as the bio-refinery concept which synergistically combines different conversion technologies and generate multiple products are expected to play a key role in addressing the technical and economic barriers of the current thermochemical biomass conversion processes.

Author details

Chan Seung Park[1]*, Partho Sarothi Roy[1] and Su Hyun Kim[2]

*Address all correspondence to: cspark@cert.ucr.edu

1 College of Engineering - Center for Environmental Research and Technology, University of California, Riverside, CA, USA

2 Institute for Advanced Engineering, Yongin-si, Gyeonggi-do, Korea

References

[1] Perlack RD, Wright LL, Turhollow AF, Graham RL, Stokes BJ, Erbach DC. Biomass as Feedstock for a Bioenergy and Bioproducts Industry: The Technical Feasibility of a Billion-Ton Annual Supply. Oak Ridge, Tennessee: Oak Ridge National Laboratory; 2005. DOE/GO-102995-2135

[2] Drift A. Role of gasification in a bio-based future. In: 24th European Biomass Conference and Exhibition; 1–4 June; Vienna, Austria; 2015. ISBN: ECN-L-15-063 EN

[3] GREET by Argonne National Laboratory. The Greenhouse Gases, Regulated Emissions, and Energy Use in Transportation Model. Argonne, IL: GREET 1.8d.1 ed; 2010

[4] Gaur S, Reed TB. Thermal Data for Natural and Synthetic Fuels. CRC Press: Marcel Dekker; 1998. pp. 102-108. ISBN 0-8247-0070-8

[5] Higman C, van der Burgt M. Gasification. Gulf Professional Publishing: Elsevier Science; 2011. 33, 167-173 p. ISBN 978-0-7560-8528-3

[6] Milena Indirect Gasifier. MILENA Biomass Gasification Process [Internet]. 2017. Available from: http://www.milenatechnology.com [Accessed: 2017-08-01]

[7] Peer M, Mahdeyarfar M, Mohammadi T. Investigation of syngas ratio adjustment using a polyimide membrane. Chemical Engineering and Processing Process Intensification. 2009;**48**(3):755-761. DOI: 10.1016/j.cep.2008.09.006

[8] Öhrman OGW, Weiland F, Pettersson E, Johansson A-C, Hedman H, Pedersen M. Pressurized oxygen blown entrained flow gasification of a biorefinery lignin residue. Fuel Processing Technology. 2013;**115**:130-138. DOI: 10.1016/j.fuproc.2013.04.009

[9] Patel M, Zhang X, Kumar A. Techno-economic and life cycle assessment on lignocellulosic biomass thermochemical conversion technologies: A review. Renewable and Sustainable Energy Reviews. 2016;**53**:1486-1499. DOI: 10.1016/j.rser.2015.09.070

[10] Swaaij W, Kersten S. Biomass Power for the World. CRC Press: Pan Stanford Publishing; 2015. p. 33. ISBN 978-981-4669-24-5

[11] Bergius FKR. Die Anwendung hoher Drucke bei chemischen Vorgangen und eine Nachbildung des Entstehungsprozesses der Steinkohle. Halle, Germany: Verlag Wilhelm Knapp. 1912; http://www.nobelprize.org/nobel_prizes/chemistry/laureates/1931/bergius-lecture.pdf [Accessed: 2015–12-04]

[12] Peterson AA, Vogel F, Lachance RP, Fröling M, Antal MJ Jr, Tester JW. Thermochemical biofuel production in hydrothermal media: A review of sub- and supercritical water technologies. Energy & Environmental Science. 2008;**1**(1):32-65. DOI: 10.1039/b810100k

[13] Yang YF, Feng CP, Inamori Y, Maekawa T. Analysis of energy conversion characteristics in liquefaction of algae. Resources, Conservation and Recycling. 2004;**43**(1):21-33. DOI: 10.1016/j.resconrec.2004.03.003

[14] Chen WH, Lin BJ, Huang MY, Chang JS. Thermochemical conversion of microalgal biomass into biofuels: A review. Bioresource Technology. 2015;**184**:314-327. DOI: 10.1016/j.biortech.2014.11.050

[15] Hoffmann J. Upgrading of bio-crude from hydrothermal liquefaction. In: TCBiomass. 2013; or http://www.steeperenergy.com

[16] Toor SS, Rosendahl L, Nielsen MP, Glasius M, Rudolf A, Iversen SB. Continuous production of bio-oil by catalytic liquefaction from wet distiller's grain with solubles (WDGS) from bio-ethanol production. Biomass and Bioenergy. 2012;**36**:327-332. DOI: 10.1016/j.biombioe.2011.10.044

[17] Berends RH, Zeevalkink JA, Naber JE. Results of the first long duration run of the HTU pilot plant at TNO-MEP. In: Proceedings of the 2nd World Biomass Conference: Biomass for Energy, Industry and Climate Protection; Rome; 2005. p. 535

[18] Elliott DC, editor. Hydrothermal Processing in Thermochemical Processing of Biomass: Conversion into Fuels, Chemicals and Power. Chichester, UK: John Wiley and Sons; 2011. pp. 200-231

[19] Demirbas A. Hydrogen production from biomass via supercritical water gasification. Energy Sources, Part A: Recovery, Utilization, and Environmental Effects. 2010;**32**(14):1342-1354. DOI: 10.1080/15567030802654038

[20] Gadhe JB, Gupta RB. Hydrogen production by methanol reforming in supercritical water: Catalysis by in-situ-generated copper nanoparticles. International Journal of Hydrogen Energy. 2007;**32**(13):2374-2381. DOI: 10.1016/j.ijhydene.2006.10.050

[21] Dinjus E, Kruse A. Hot compressed water—A suitable and sustainable solvent and reaction medium. Journal of Physics. Condensed Matter. 2004;**16**(14):S1161-S1169. DOI: 10.1088/0953-8984/16/14/026

[22] Marrone PA, Hong GT. Corrosion control methods in supercritical water oxidation and gasification processes. In: NACE International, editor. Corrosion. New Orleans; 2008

[23] Antal MJ, Allen SG, Schulman D, Xu X, Divilio RJ. Biomass gasification in supercritical water. Industrial and Engineering Chemistry Research. 2000;**39**(11):4040-4053. DOI: 10.1021/ie0003436

[24] Knezevic D. Hydrothermal conversion of biomass [thesis]. Ipskamp Drukkers B.V: Enschede; 2009. ISBN: 978-90-365-2871-9

[25] Fritz R. KIT-IKFT-VERENA Pilot Plant [Internet]. Available from: http://www.ikft.kit.edu/english/138.php. [Accessed: 2015–07-16]

[26] Hydrogasification/FT Production with Electricity & Electricity Only Cases CERT-1 thru CERT-6 Conceptual Study, [Internet]., DOE-NETL, 2010. Available from: http://www.netl.doe.gov/research/coal/energy-systems/gasification/gasifipedia/hydro. [Accessed: 2016-08-15]

[27] Mozafarrian M, Zwart R. Production of Substitute Natural Gas by Biomass Hydrogasification. Petten: Netherlands Energy Research Foundation, (ECN); 2000. ECN-RX-00-38

[28] Jeon SK, Park CS, Hackett CE, Norbeck JM. Characteristics of steam hydrogasification of wood using a micro-batch reactor. Fuel. 2007;**86**(17–18):2817-2823. DOI: 10.1016/j.fuel.2007.03.023

[29] Raju ASK, Park CS, Norbeck JM. Synthesis gas production using steam hydrogasification and steam reforming. Fuel Processing Technology. 2009;**90**(2):330-336. DOI: 10.1016/j.fuproc.2008.09.011

[30] Cui H, Turn SQ, Keffer V, Evans D, Tran T, Foley M. Contaminant estimates and removal in product gas from biomass steam gasification. Energy & Fuels. 2010;**24**(2):1222-1233. DOI: 10.1021/ef9010109

[31] Park C, Norbeck JM. Development of Steam Hydrogasification Process Demonstration Unit-5 Lb/Hr PDU Design Report. Sacramento, CA: California Energy Commission; 2011. DOI: CEC-500-2013-092

[32] Rezaiyan J, Cheremisinoff NP. Gasification Technologies: A Primer for Engineers and Scientists. CRC press; 2005. ISBN: 978-0-82-472247-0

[33] Basu P. Biomass Gasification and Pyrolysis: Practical Design and Theory. Academic Press: Elsevier Science; 2010. p. 167. ISBN: 978-0-12-374988-8

[34] Pröll T, Rauch R, Aichernig C, Hofbauer H. Fluidized bed steam gasification of solid biomass: Analysis and optimization of plant operation using process simulation. In: 18th International Conference on Fluidized Bed Combustion; ASME; 2005. pp. 763-770. DOI: 10.1115/FBC2005-78129

[35] Van der Meijden CM, Veringa HJ, Van der Drift A, Vreugdenhil BJ. The 800 kWth allothermal biomass gasifier MILENA. In: 16th European Biomass Conference and Exhibition. Valencia, Spain; 2008

[36] Yan C et al. A novel biomass air gasification process for producing tar-free higher heating value fuel gas. Fuel Processing Technology. 2006;**87**(4):343-353. DOI: 10.1016/j.fuproc.2005.10.003

[37] Zhou J, Chen Q, Zhao H, Cao X, Mei Q, Luo Z, Cen K. Biomass–oxygen gasification in a high-temperature entrained-flow gasifier. Biotechnology Advances. 2009;**27**(5):606-611. DOI: 10.1016/j.biotechadv.2009.04.011

[38] Huber GW, Iborra S, Corma A. Synthesis of transportation fuels from biomass: Chemistry, catalysts, and engineering. Chemical Reviews. 2006;**106**(9):4044-4098. DOI: 10.1021/cr068360d

[39] Knoef HAM, editors. Handbook of Biomass Gasification. 2nd ed. Netherlands: BTG Biomass Technology Group BV; 2012. Available from: http://www.btgworld.com/en/references/publications/handbook-biomass-gasification-second-edition [Accessed: 2015–12-05]

[40] Bridgwater AV, Boocock DGB, editors. Cleaning of Hot Producer Gas in a Catalytic Adiabatic Packed Bed Reactor With Periodic Flow Reversal, Development in Thermochemical Biomass Conversion Dordrecht. Netherlands: Springer; 1997. pp. 907-920. DOI: 10.1007/978-94-009-1559-6

[41] Van de Kaa G, Kamp L, Rezaei J. Selection of biomass thermochemical conversion technology in the Netherlands: A best worst method approach. Journal of Cleaner Production. 2017;**166**:32-39. DOI: 10.1016/j.jclepro.2017.07.052

[42] Aichering Ch. Indirect Gasification. 2011. [Internet]. Available from: http://www.marcogaz.org/egatec2011/PS2/PS2Eb_Aichernig_egatec2011.pdf [Accessed: November 29, 2017]

[43] Zweiler R. Best Practice Wood Gasification for CHP. 2011. [Internet]. Available from: http://abina.biomasseverband.at/de/veranstaltungen/tagungen-und-vortraege/archiv/cross-border-bioenergy-workshop/chp-workshop/ [Accessed: November 29, 2017]

[44] Zwart RWR. Synthetic Natural Gas. Large-Scale Introduction of Green Natural Gas in Existing Gas Grids (No. ECN-L–07-069). Energy Research Centre of the Netherlands ECN. 2007. [Internet]. Available from: ftp://ftp.ecn.nl/pub/www/library/report/2007/l07069.pdf [Accessed: November 29, 2017]

[45] Zwart RWR, Boerrigter H, Deurwaarder EP, Van der Meijden CM, Van Paasen SVB.. Production of synthetic natural gas (SNG) from biomass. Energy Research Centre of the Netherlands (ECN). 2006. [Internet]. . Available from: https://www.ecn.nl/docs/library/report/2006/e06018.pdf [Accessed: November 29, 2017]

[46] Bengtsson K. Twin-Bed Gasification Concepts for Bio-SNG Production. Lund Institute of Technology, Department of Chemical Engineering, Lund, Sweden. 2007. [Internet]. Available from: http://www.chemeng.lth.se/exjobb/E450.pdf [Accessed: November 29, 2017]

[47] Ahrenfeldt J, Jørgensen B, Thomsen T. Bio-SNG Potential Assessment: Denmark 2020. Risø Nationallaboratoriet for Bæredygtig Energi: Danmarks Tekniske Universitet; 2010. [Internet]. Available from: orbit.dtu.dk/files/5237878/ris-r-1754.pdf [Accessed: November 29, 2017]

[48] Hdenskog M. The GoBiGas-Project Gasification to Produce High-Quality Biogas. [Internet]. Available from: http://www.vtt.fi/files/projects/vetaani/malin_hedenskog.pdf [Accessed: November 29, 2017]

[49] Scott D, Piskorz J. The flash pyrolysis of aspen-poplar wood. The Canadian Journal of Chemical Engineering. 1982;**60**(5):666-674. DOI: 10.1002/cjce.5450600514

[50] Pan P, Hu C, Yang W, Li Y, Dong L, Zhu L, Fan Y. The direct pyrolysis and catalytic pyrolysis of Nannochloropsis sp. residue for renewable bio-oils. Bioresource Technology. 2010;**101**(12):4593-4599. DOI: 10.1016/j.biortech.2010.01.070

[51] Isahak WNRW, Hisham MW, Yarmo MA, Hin TYY. A review on bio-oil production from biomass by using pyrolysis method. Renewable and Sustainable Energy Reviews. 2012;**16**(8):5910-5923. DOI: 10.1016/j.rser.2012.05.039

[52] Duman G, Okutucu C, Ucar S, Stahl R, Yanik J. The slow and fast pyrolysis of cherry seed. Bioresource Technology. 2011;**102**(2):1869-1878. DOI: 10.1016/j.biortech.2010.07.051

[53] KiOR, Inc. - Home. Inaeris Technologies [Internet]. Available from: http://www.kior.com/ [Accessed: 2017–02-01]

[54] Wagenaar BM, Prins W, Van Swaaij WPM. Pyrolysis of biomass in the rotating cone reactor: Modelling and experimental justification. Chemical Engineering Science. 1994;**49**(24):5109-5126. DOI: 10.1016/0009-2509(94)00392-0

[55] Huang Y, McIlveen-Wright D, Rezvani S, Wang YD, Hewitt N, Williams BC. Biomass co-firing in a pressurized fluidized bed combustion (PFBC) combined cycle power plant: A techno-environmental assessment based on computational simulations. Fuel Processing Technology. 2006;**87**(10):927-934. DOI: 10.1016/j.fuproc.2006.07.003

[56] Loo S, Koppejan J. Biomass Power for the World. CRC Press: Pan Stanford Publishing; 2015. pp. 248-264. ISBN 978-981-4669-24-5

[57] Bach QV, Skreiberg Ø. Upgrading biomass fuels via wet torrefaction: A review and comparison with dry torrefaction. Renewable and Sustainable Energy Reviews. 2016;**54**:665-677. DOI: 10.1016/j.rser.2015.10.014

[58] Arce ME, Saavedra Á, Míguez JL, Granada E, Cacabelos A. Biomass fuel and combustion conditions selection in a fixed bed combustor. Energies. 2013;**6**(11):5973-5989. DOI: 10.3390/en6115973

Chapter 3

Development of Torrefaction Technology for Solid Fuel Using Renewable Biomass

Lola Domnina B. Pestaño and Wilfredo I. José

Additional information is available at the end of the chapter

http://dx.doi.org/10.5772/intechopen.76100

Abstract

Fossil fuel sources such as coal, crude oil and natural gas would eventually get exhausted and their price continuously fluctuates. During the past four decades, many researches have tried to find alternate fuel resources to satisfy the worldwide increasing energy demand as well as to minimize dependence on fossil fuels. Among many possible alternate fuel sources, agriculture biomass residues exhibit most promising possibility due to their inherent characteristics in storing solar energy and amenability in subsequent conversion into convenient solid, liquid and gaseous fuels. Torrefaction is a thermal method for the conversion of biomass operating in temperature range of 200–300°C under atmospheric conditions in the absence of oxygen. Agricultural crop residues that are abundant in the Philippines such as coconut leaves, cogongrass and rice husk were utilized to produce solid fuel by torrefaction for use as alternative source of energy. The key torrefaction products were collected and analyzed. Combustion characteristics of both torrefied and untorrefied biomass were investigated. Torrefaction of the biomass significantly improved the heating value, proximate compositions also improved and were comparable to coal and combustion characteristics were superior making it more suitable for fuel applications. The design of the torrefaction process was researched and developed.

Keywords: biomass, renewable energy, torrefaction, cogon grass, rice husk, coconut leaf

1. Introduction

The reserves of non-renewable energy sources (coal, crude oil, natural gas) gradually get exhausted and their price continually increases. Nevertheless, they cover about four-fifth of the energy consumption [1].

In the last four decades, researchers have been focusing on alternate fuel resources to meet the ever increasing energy demand and to avoid dependence on crude oil [2].

Among different sources of renewable energy, biomass residues are the most potential raw material due to their inherent capability to store solar energy and amenability to subsequent conversion to convenient solid, liquid and gaseous fuels. Further, biomass is a renewable source of carbon through a global carbon cycle and can be a source to make many chemicals.

With serious concern about deforestation as one of the causes of global warming, especially in developing countries, and need for reforestation to maintain global ecological balance, increasing demand is being made for proper utilization of agro and forestry biomass residues to play the role previously carried out by wood.

Torrefaction is a recently well-known technology which can change biomass properties to become a higher energy quality biofuel. From a viewpoint of chemical components, torrefaction process comprises mainly the removal of oxygen to yield a final solid product. The torrefied biomass product contains a lower O/C ratio compared to the original raw biomass.

Torrefaction occurs through the heating of biomass below 300°C in the absence of oxygen, where moisture and volatile materials are lost. It was first applied in 1939, then in 1984 but forgotten until recently. Published papers and patents issued were from late 2000s to present. It can convert biomass wastes to solid fuel affordably without complications.

The Philippines is mainly an agricultural country with a land area of 30 million hectares, 47% of which is agricultural. The total area devoted to agricultural crops is 13 million hectares distributed among food grains, food crops and non-food crops. Among the crops grown, rice, coconut and sugarcane are major contributors to biomass energy resources. The most common agricultural residues are rice husk, rice straw, coconut husk, coconut shell and bagasse [3].

In order to utilize agricultural crop residues and to improve its biomass properties, there is a need to create new knowledge and apply it to be more productive focusing on creativity and innovation. Agricultural crop residues that are abundant in the Philippines such as coconut leaves [4, 5], cogongrass [5], and rice husk [5], were utilized to produce solid fuel by torrefaction for use as alternative source of energy. The design of the torrefaction process based on the biomass characteristics was researched and developed.

2. Biomass upgrading as energy source

In future energy supply scheme, biomass can play an important role in supplying renewable energy [6]. Biomass is an attractive energy source as a renewable energy, especially as a sustainable carbon carrier.

2.1. Biomass

Biomass can generally be defined as any hydrocarbon material which mainly consists of carbon, hydrogen, oxygen and nitrogen. Sulfur is also present in less proportion. Biomass resources include many natural and derived materials such as woody and herbaceous species, wood wastes, bagasse, agricultural residues, waste paper, municipal solid wastes, sawdust, biosolids, grass, food wastes, animal wastes, aquatic plants, and algae, etc. Woody materials are preferred among biomass resources because they contain much higher energy value. Most important feature of biomass is its inherent climate neutral behavior. When biomass is grown in a sustainable way, during the life cycle of biomass production and application, no net amount of CO_2 emits into the atmosphere. The CO_2 released during the utilization of biomass is stored in return in the biomass resource through photosynthesis, which means a climate neutral carbon cycle of CO_2. Biomass is considered as an environmentally friendly alternative energy source replacing fossil fuels because it is produced in nature by photosynthesis from CO_2 and H_2O [7].

On the other hand, some biomass properties are inconvenient, particularly its high oxygen content, a low heating value, a hydrophilic nature and high moisture content. Also, the energy accumulation to biomass through photosynthesis has known to be a process of low energy efficiency. The overall energy efficiency from solar energy to biomass energy is 1–3% [8]. Typical disadvantages of biomass are its tenacious and fibrous structure and its heterogeneous composition that makes process design and process control more complicated.

Biomass has unique characteristics that necessitate pre-processing before it can be stored, transported or used in various applications. Unlike fossil fuels which are mined at one location, biomass is often available seasonally in small quantities scattered over many locations [9]. Biomass is highly heterogeneous in quality and nature, and is available in low energy density form [10]. It has relatively high moisture content and consequently lower heating value compared to fossil fuels [11]. It is therefore often needs to be pre-treated to improve handling [12].

2.2. Thermal conversion processes

Burning biomass in an oxidative environment is the oldest conversion process practiced by man. Combustion, however, does not intend to produce value-added products in the form of fuels, chemicals or materials, as other thermochemical conversion technologies, but only heating value [13].

Thermal conversion processes can be categorized into combustion, gasification, pyrolysis and the emerging torrefaction technology according to the operating conditions. The products of the thermochemical processes are divided into a volatile fraction consisting of gases, vapors and tar components and a carbon rich solid residue [4].

3. The torrefaction technology

Torrefaction is a recently well-known technology to upgrade biomass for combustion and gasification applications. It is a thermal pre-treatment technology carried out at atmospheric pressure in the absence of oxygen. Torrefaction of biomass can be described as a mild form of pyrolysis that occurs at temperatures between 200 and 300°C [4]. During torrefaction, the more easily combustible components of biomass (i.e. hemicelluloses) are decomposed first and most vigorously, through carbonization. Only minor decomposition of lignin and cellulose occur at torrefaction temperatures but rate of decomposition depends on the type of biomass [14]. Their chemical structure is changed but no significant mass losses occur [15, 16]. The solid uniform product that is produced has a very low moisture content, high heating value [17] and less hydrophilic compared to the untreated biomass to fresh biomass [1]. Furthermore, the fibrous and tenacious nature of the biomass is reduced, resulting in a brittle material that can easily be comminuted into smaller particles [18].

4. Renewable biomass sources

Like any developing country, the Philippines is facing a formidable challenge of promoting sustainable energy options to support the energy requirements of its economic and social development goals with minimal adverse effects on the environment. The Philippines utilizes renewable energy sources including hydropower, geothermal and solar energy, wind power and biomass resources. In 2015, these sources contributed 20,963 GWh of electrical energy, out of which, 41% is hydropower while 53% is geothermal power. Solar energy, wind power and biomass energy application accounts for around 6% of the primary use in the country. These renewable energy sources represent 25.44% of the country's energy needs [19].

4.1. Coconut leaf, cogongrass and rice husks as a renewable source of energy

Among the coconut farm wastes such as husks, shell, coir dust and coconut leaves, the latter is considered either the most grossly under-utilized or completely un-utilized, only to be utilized by in situ burning at the coconut farm in order to dispose. A study conducted by Banzon [20] considered only the petiole to assess the fuel potential of the coconut leaf. Banzon reported that 376.9 million trees each producing at least 12 leaves a year or a total of 45×10^8 leaves with a total weight of 4000 kcal/kg (16.7 MJ/kg) makes the energy available from the coconut petiole equal to 39×10^{12} kcal [20, 21].

Imperata cylindrical, or cogongrass grows all around the world, including the Philippines. In general, cogongrass is composed of three main components: **C**ellulose, hemicellulose, and lignin [22]. Cellulose and hemicellulose can be converted into fermentable sugars and produce a large amount of fuels and chemicals by fermentation and chemical processes [23]. *Imperata*

is being considered as a feedstock for bioethanol. Very few studies have reported the use of cogongrass as a renewable energy source.

Agricultural wastes such as rice husks are now used as a source of energy that helps advance the agriculture industry, particularly on rice mechanization and post production operations. The Philippines produces an average of 2 million metric tons of rice husks annually. A kilo of rice husk basically contains about 3000 kcal of heat energy and can provide sufficient amount of clean gaseous fuel when gasified. Converting this available biomass waste into energy by gasification can provide about 25 pJ of energy which can be utilized for various heat and power applications, especially in rice farming and rural-based operations [24].

5. Methodology

5.1. Sample production of biomass

Dried coconut leaves were collected in a coconut farm in Calauan, Laguna (CALABARZON, Region IV-A). Cogongrass and rice husks were collected from Puerto Princesa, Palawan [5]. The dried biomass was air dried and cut into small pieces. The cut biomass was stored in plastic containers at room temperature.

5.2. Characterization of the raw biomass

5.2.1. Thermogravimetric analysis (TGA)

The thermal behaviors of dried coconut leaves [4, 5], cogongrass [5] and rice husks [5] (about 5.769 mg milled using a Thomas Willey mill) were investigated at the Polymer Materials Laboratory at the Institute of Chemistry, College of Science, University of the Philippines, Dilijan, Quezon City using a TGA Q50 (TA Instrument). The heating program consisted on a 5 min hold at 30°C, ramp up to 800°C at a heating rate of 10°C/min, and then the weight difference was recorded as a function of temperature profile. Nitrogen was used as a purging gas at a flow rate of 50 ml/min [4].

5.2.2. Heating value

The calorimetric experiments were performed using the raw and torrefied biomass. About 1 g size sample was placed in a nickel crucible introduced into a Parr 1356 Oxygen Combustion Bomb Calorimeter. The experiments were performed at 25°C. The bomb was filled with oxygen at a filling pressure of 30 atm. The calorimeter was placed in an isothermal-jacket with an air-gap separation of 10 mm between all surfaces. The calorimeter was filled with two liters of de-ionized water. The fuel was ignited through external electric connections. Temperature of this water was measured to 10^{-4}°C at intervals of 10 s at the start of ignition to calculate the heating value for each sample [4].

5.2.3. Proximate analysis

Samples of the feedstock or raw biomass and the solid product or torrefied biomass were analyzed at the Analytical Services Laboratory at the Institute of Chemistry, U.P. Diliman, QC for moisture content using a micro thermogravimetric analyzer according to Method 925.45 B "Official Methods of Analysis of AOAC International (17th edition Revision 1)" and ash content according to Methods of Analysis of AOAC International (17th edition Revision 1)" and ash content according to method 923.03 Ibid [4].

5.3. The torrefaction reactor

The torrefaction batch reactor was developed and fabricated for the laboratory scale. The reactor which is of rotary drum type (capable of approximately 200–500 g per batch, depending on material) is made of stainless steel with an inside diameter of 20 cm, length of 30 cm and thickness of 1 cm. It consists of (1) an air locked feeder cover where the feedstock is fed; (2) the heating chamber where torrefaction process of the biomass takes place; (3) rotor blades that allows uniform heating of the biomass; (4) the thermometer that displays the temperature in the heating chamber; and (5) a tachometer that measures the rotation speed of the shaft [4]. **Figure 1** shows the schematic diagram of the torrefaction reactor and its parts. **Figure 2** shows the fabricated torrefaction batch reactor.

5.4. The torrefaction experiment

Figure 3 shows the experimental set-up of the torrefaction experiment. Raw biomass was torrefied using the lab-scale torrefaction unit. Four torrefied samples were prepared with different feedstock conditions and different operating temperatures based on the TGA results of the untorrefied (raw) biomass (see **Table 1**).

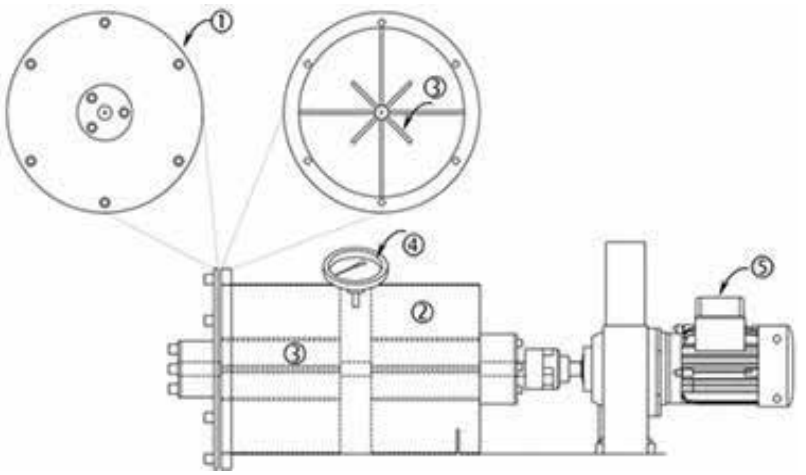

Figure 1. Schematic diagram of torrefaction reactor and its parts.

Figure 2. The fabricated torrefaction reactor.

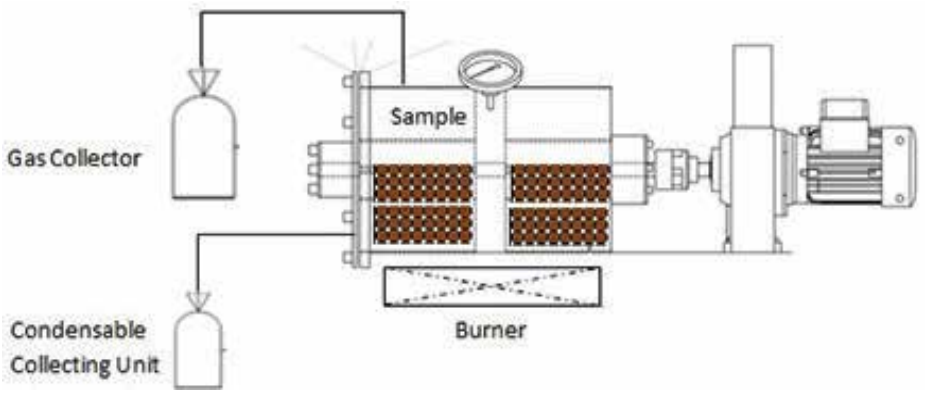

Figure 3. The experimental set-up of the torrefaction experiment.

Property	Coconut leaves	Cogongrass	Rice husk
Operating temperature (°C)	245–290	247–298	238–293

Table 1. Torrefaction operating temperature conditions.

The reactor was heated, at the rotating speed of the shaft of about 23 rpm. When the desired reaction condition was reached, the set-up was allowed to cool, the solid product or the torrefied biomass was weighed. The condensate was collected throughout the process by connecting the condensate collecting unit to a condenser. The volume and weight of the condensate were measured. The collected gas and the condensate were disposed properly. Bomb calorimetry and proximate analysis were used in determining the physical and fuel properties of the torrefied biomass. Fuel characteristics (heating value, moisture content, fixed carbon content, and ash content) of the raw and torrefied biomass were compared. Design engineering principles were used to develop a process design of the production of solid fuel from renewable biomass.

6. Results and discussion

6.1. Characterization of the raw and torrefied biomass

6.1.1. TGA

TGA is very important in the torrefaction of renewable biomass to establish the thermal properties of the dried biomass [4].

The thermogravimetry profile of dried coconut leaves in **Figure 4** shows an onset temperature of 245°C that denotes the temperature at which weight loss begins. Starting from 5.679 g, a weight loss of 7.436% was observed. After which the weight drastically falls down until a temperature of 350°C is reached when a weight loss of 53.33% of its weight was recorded. This is called the first derivative peak temperature, also known as the inflection point. This indicates the point of greatest rate of change on the weight loss curve. It was reported that the higher the cellulosic content of the dried coconut leaves, the higher was the thermal degradation rate and the initial degradation temperature [4].

The TGA results for dried coconut leaves [4, 5], cogongrass [5] and rice husks [5] shown in **Table 1** provided the basis for the optimum operating temperatures (between 245 and 298°C) that were utilized in the torrefaction experiment.

6.1.2. Heating value, proximate analysis

The heating value obtained in a bomb calorimeter test represents the gross heat of combustion for the sample. This is the heat produced when the sample burns, plus the heat given up when the newly formed water vapor condenses and cools to the temperature of the [4].

The results of the experiments showed that torrefaction can improve the fuel properties of the biomass. The fuel characteristics of the raw and torrefied biomass are shown in **Figure 5**. **Figure 5(b)** shows the moisture content was reduced by an average of 67%. The heating values were increased to 20–26 MJ/kg, see **Figure 5(a)**. The fixed carbon was increased to 44–46%, see **Figure 5(d)**. The ash content increased to 9–28%, see **Figure 5(c)**. These values approach that of subbituminous coal that coal contains 42–52% carbon (on a dry, ash-free basis) and has calorific values ranging from about 19 to 26 MJ/kg.

The raw biomass low heating values are due to low fixed carbon content of about 45% and relatively high moisture content, typically about 50% [25]. Torrefaction significantly improved the heating values of the biomass (see **Figure 5a**). Improvement of heating value is due to increased fixed carbon. The fixed carbon content of torrefied biomass is high (25–40% depending on reaction conditions) [12, 15, 26]. The combustion property also improved; torrefied biomass burns longer due to larger percentage of fixed carbon [27]. Torrefaction reduces the O/C ratio and this makes the biomass better suited for gasification [26]. Gasification also produces less smoke during the process since smoke causing volatiles are driven off during torrefaction [28, 29].

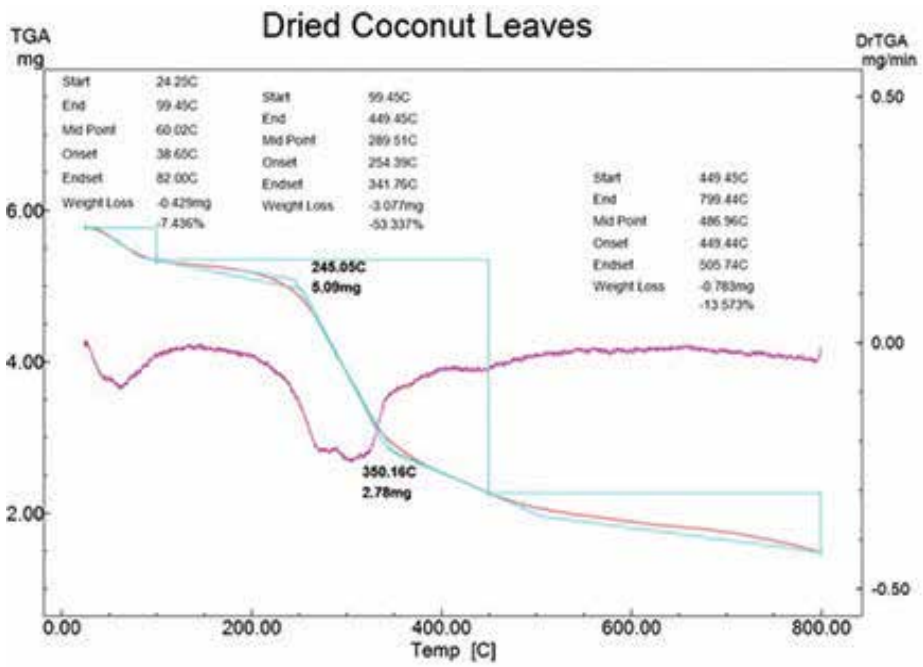

Figure 4. Thermogravimetric profile of dried coconut leaves.

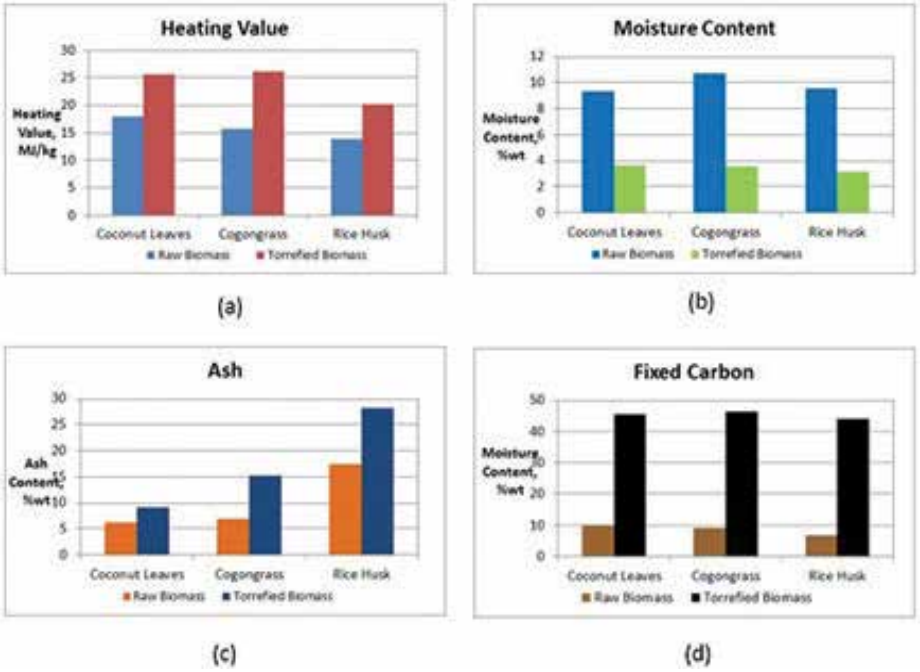

Figure 5. Fuel characteristics of the raw and torrefied biomass.

In some plant species, a significant fraction of the total biomass is not combustible and is recovered as ash from bioenergy processes. The amounts range from about 6% of dry weight in dried coconut leaves to about 9% in torrefied coconut leaves. Generally, the ash content of herbaceous biomass is higher than that of woody biomass. While ash weight content (in dry basis) values of less than 1% are expected for wood, different herbaceous biomass types have reported values ranging from less than 2% up to 8–10% or even up to 25% for rice husks. In waste fractions, the ash content may often be as high as 30–50% and is only scarcely less than 10% [30].

6.2. The torrefaction process design

6.2.1. Feedstock grinding

Standard-sized pellet mills generally require biomass that is ground to particles that are no more than 3 mm in size. Several types of equipment are available to carry out this task.

6.2.2. Moisture control

Maintaining an appropriate moisture level in your feedstock is vital for overall quality of the final pellets. For wood, the required moisture level of the feedstock is at or near 15%. Other types of biomass have other requirements—you may need to experiment a bit. Moisture can be removed from the feedstock by oven-drying or by blowing hot air over or through the particles. If the feedstock is too dry, moisture can be added by injecting steam or water into the feedstock [31].

6.2.3. Torrefaction

Torrefaction is usually performed in inert atmosphere at temperature below 300°C that aims to remove mostly the major hemicellulose contents from biomass structure [32, 33].

A typical torrefaction process is presumed to comprise drying of the biomass feedstock to have a biomass feed of constant moisture content to torrefaction, which also implies a more or less constant heat duty to be delivered to the torrefaction reactor. Furthermore, it is expected that the best destiny for the liberated torrefaction gas is to combust it to generate heat for the drying and torrefaction processes, which requires a combustible torrefaction gas [34].

6.2.4. Pulverizing and pelletizing

Torrefied biomass can be subjected to pulverizing and pelletizing to produce fuel pellets. A roller is used to compress the biomass against a heated metal plate called a "die." The die includes several small holes drilled through it, which allow the biomass to be squeezed through under high temperature and pressure conditions. If the conditions are right, the biomass particles will fuse into a solid mass, thus turning into a pellet [35].

The torrefaction process is quite simple as **Figure 6** shows. Our pre-feasibility study for a commercial plant shows an investment of USD 1 million, whereas a Belgian company offers USD 25 million. We are designing small-scale units that can be operated by Local Government Units (LGUs) at subsidized cost.

In order to promote the wider use of biomass resources for energy generation, three A's have to be satisfied: A—appropriate to varying local conditions, A—affordable to a wide sector of the population and A—available along with the necessary support services and program back-up.

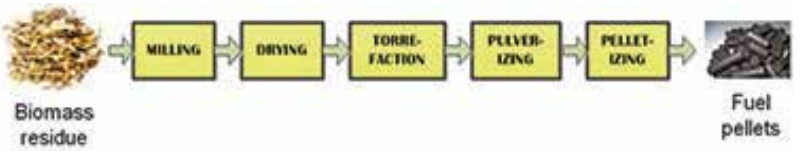

Figure 6. The complete torrefaction process.

Above measures will make biomass technologies as an attractive option to potential users [36].

7. Conclusion

Torrefaction can convert low-grade biomass to solid fuel with properties similar to subbituminous coal that can be used for industrial and domestic applications. Torrefaction results on coconut leaves showed that the moisture content was reduced by 67% compared to the raw material, and the heating values, fixed carbon, and ash content were increased from 20 to 26 MJ/kg, 44 to 46%, and 9 to 28%, respectively. These values approach that of typical subbituminous coal with calorific values ranging from about 19 to 26 MJ/kg. The proposed torrefaction process is cheaper, less complicated, and more convenient to handle compared to the pyrolysis or gasification. It is appropriate and suitable for application with biomass.

Author details

Lola Domnina B. Pestaño[1,2]* and Wilfredo I. José[2]

*Address all correspondence to: lbpestano@ust.edu.ph

1 Department of Chemical Engineering, University of Santo Tomas, Manila, Philippines

2 Department of Chemical Engineering, National Graduate School of Engineering, University of the Philippines, Quezon City, Philippines

References

[1] Brožek M, Nováková A, Kolářová M. Quality evaluation of briquettes made from wood. Research Agriculture Engineering. 2012;**58**(1):30-35

[2] Karunanithy C, Wang Y, Muthukumarappan K, Pugalendhi S. Physiochemical characterization of briquettes made from different feedstock's. Hindawi Publishing Corporation Biotechnology Research International. 2012;**2012**:165202. 12 pages

[3] Bioenergy Consult. Biomass Energy Potential in the Philippines [Internet]. May 12, 2015. Available from: https://www.bioenergyconsult.com/tag/biomass-energy-in-philippines/ [Accessed: Sept. 13, 2017]

[4] Pestaño LDB, José WI. Production of solid fuel by torrefaction using coconut leaves as renewable biomass. International Journal of Renewable Energy Development. 2016;**5**(3):187-197

[5] José WI, Banta MT, Palanca AG, Tamisin A, Pestaño LDB. Torrefaction of biomass residue technology uncovered using a novel idea generating method. Poster presented at the Scientific Conference & 82nd NRCP General Membership Assembly Summit C & D, Philippine International Convention Center-Pasay City. March 11, 2015

[6] IEA (International Energy Agency). Chapter 1—Introduction and Scope. In: Energy and Climate Change: World Energy Outlook. Paris, France; 2016

[7] Davis SC, Anderson-Teixeira KJ, De Lucia EH. Life-cycle analysis and the ecology of biofuels. Trends in Plant Science. 2009;**14**:140-146

[8] Herman WA. Quantifying global exergy resources. Energy. 2006;**31**(12):1685-1702

[9] Junginger M, Faaij A, van den Broek R, Koopsmans A, Hulscher W. Fuel supply strategies for large scale bio-energy projects in developing countries. Electricity generation from agricultural and forest residues in northeastern Thailand. Biomass & Bioenergy. 2001;**21**(4):259-275

[10] Tapasvi D, Khalil R, Skreiberg O, Tran K, Gronli M. Torrefaction of Norwegian birch and spruce: An experimental study using macro-TGA. Energy Fuels. 2012;**26**:5232-5240

[11] Ben H, Ragauskas AJ. Torrefaction of loblolly pine. Green Chemistry. 2012;**14**:72-76

[12] Park S, Jang C. Effects of pyrolysis temperature on changes in fuel characteristics of biomass char. Energy. 2012;**39**:187-195

[13] Basu P. Biomass Gasification and Pyrolysis: Practical Design. Burlington, MA: Academic Press; 2010

[14] Almeida G, Brito JO, Perre P. Alterations in energy properties of eucalyptus wood and bark subjected to torrefaction: The potential of mass loss as a synthetic indicator. Bioresource Technology. 2010;**101**:9778-9784

[15] Bergman P, Kiel J. Torrefaction for Biomass Upgrading. 2005

[16] Tumuluru JS, Sokhansanj S, Wright CT, Boardman RD. Biomass torrefaction process review and moving bed torrefaction system model development. US: Idaho National Laboratory; 2010. 57 p. INL/EXT-10-19569-1

[17] Ustu A, Faaij APC, Bergman PCA. Pretreatment technologies, and their effect on international bioenergy supply chain logistics. Techno-economic evaluation of torrefaction, fast pyrolysis and pelletization. Energy. 2008;**33**(8):1206-1223

[18] Van der Stelt MJC, Gerhauser H, Kiel JHA, Ptasinski KJ. Biomass upgrading by torrefaction for the production of biofuels: A review. Biomass and Bioenergy. 2011;**35**:3748-3762

[19] 2015 Philippine Power Statistics

[20] Banzon JA. The coconut as a renewable energy. Philippine Journal of Coconut Studies. 1980;**5**(1):31-36

[21] Banzon JA. Harvestable energy from the coconut palm. Energy in Agriculture. 1984;**3**:337-344

[22] Lin YS, Lee WC. Simultaneous saccharification and fermentation of alkali pretreated cogongrass for bioethanol production. BioResources. 2011;**6**:2744-2756

[23] McMillan JD. Pretreatment of lignocellulosic biomass. American Chemical Society. 1994;**566**:292-324

[24] Gagelonia E. Rice husk as sustainable energy source [Internet]. Philippine Rice Research Institute; Nov. 23, 2016. Available from: http://www.philrice.gov.ph/rice-husks-sustainable-energy-resource/ [Accessed: Sept. 16, 2017]

[25] Crocker M, Andrews R. The rationale for biofuels. In: Crocker M, editor. Thermochemical Conversion of Biomass to Liquid Fuels and Chemicals. Cambridge, UK: The Royal Society of Chemistry; 2010. pp. 1-25

[26] Medic D, Darr M, Shah A, Potter B, Zimmerman J. Effects of torrefaction process parameters on biomass feedstock upgrading. Fuel. 2012;**91**:147-154

[27] Bridgeman TG, Jones JM, Shield I, Williams PT. Torrefaction of reed canary grass, wheat straw and willow to enhance solid fuel qualities and combustion properties. Fuel. 2008;**87**:844-856

[28] Tumuluru JS, Hess JR, Boardman RD, Wright CT, Westover TL. Formulation pretreatment, and densification options to improve biomass specifications for co-firing high percentages with coal. Industrial Biotechnology. 2012;**8**(3):113-132

[29] Patel B, Gami B, Bhimani H. Improved fuel characteristics of cotton stalk, prosopis and sugarcane bagasse through torrefaction. Energy for Sustainable Development. 2011;**15**:272-275

[30] Nadav S, Yeats T, Szemenyei H, Youngs H, Somervile C. The implications of lignocellulosic biomass chemical composition for the production of advanced biofuels. Biofuels. 2014;**64**(3):192-201

[31] Ciolkosz D. Manufacturing fuel pellets from biomass. In: Penn State Extension. Renewable and Alternative Energy Fact Sheet. 2009. pp. 1-3

[32] Ramiah MV. Thermogravimetric and differential thermal analysis of cellulose, hemicellulose and lignin. Journal of Applied Polymer Science. 1970;**14**:1323-1337

[33] Worasuwannarak N, Sonobe T, Tanthapanichakoon W. Pyrolysis behaviors of rice straw, rice husk, and corncob by TG-MS technique. Journal of Analytical and Applied Pyrolysis. 2007;**78**:265-271

[34] Bergman P, Kiel J. Torrefaction for biomass co-firing in existing coal-fired power stations. Biocoal. Paris, France: Published at 14th European Biomass Conference & Exhibition, Paris, France, October 2005. pp. 17-21

[35] Dara, B., Manufacturing Process for Wood Pellets. 2015

[36] Cruz I. Utilization of biomass resources for energy. In: Energy Research and Development Center (PNOC-ERDC), editors. PCIERD Symposium on "Technology Thrusts Towards Productivity"; July 12, 1985; Bicutan, Taguig, M.M; 1985

Chapter 4

Thermodynamic and Kinetic Study of Lignocellulosic Waste Gasification

Rosa Ana Rodriguez, Germán Mazza,

Marcelo Echegaray, Anabel Fernandez and

Daniela Zalazar García

Additional information is available at the end of the chapter

http://dx.doi.org/10.5772/intechopen.73288

Abstract

In this chapter, the kinetic behavior during the steam gasification of sawdust, plum, and olive pits was investigated by thermogravimetric analysis where the weight loss is measured with the temperature variation at different heating rates (5, 10, and 15 K/min). The weight loss and their derivative curves show that the gasification takes place in three visible stages. The kinetic study was carried out using Coats-Redfern methods. The Ginstling-Brounstein model showed better fit. The obtained activation energy values vary between 70 and 100 kJ/mol for the pyrolysis stage for all studied agro-industrial wastes. On the other hand, a thermodynamic model was proposed to predict the five waste gasification processes, considering the char and tar production. The proposed model allows it to perform a parametric study, analyzing the process variables' effect on the exergetic efficiency. The higher temperatures favor the endothermic reactions as the H_2 and CO formation reactions. Therefore, in the product, moles of H_2 and CO increase and consequently the exergy efficiency of the process. Increasing the equivalence ratio value, H_2, CO, and CH_4 contents decrease; thus the calorific value of the produced gas and the exergetic efficiency decrease. In addition, the CO_2 and H_2O presences in the syngas composition diminish its calorific value and the exergetic efficiency. Considering the influence of supply steam/biomass ratio, the exergetic efficiency decreases with the growth of this parameter.

Keywords: gasification, lignocellulosic wastes, kinetic analysis, thermodynamic analysis

1. Introduction

Energy demand has gradually become a critical factor for the international industrial sector. For this reason, technologies based on renewable-energy sources, such as biomass residues, have been developed and promoted. Biomass has the potential to become one of the main sources of energy worldwide; it is estimated that by 2050, its contribution to the global energy model could be between 100 and 400 EJ/year [1].

The biomass waste utilization, as a substitute for fossil biofuels, has the advantage to produce environmentally beneficial fuel, due to the energy production, and its sustainable use allows the emitted CO_2 to be absorbed during the biomass growth. In short time periods, this cycle was fulfilled, which allows confirming that the energetic biomass uses under these conditions in neutral with respect to the CO_2 emissions [2]. One of the main disadvantages for the biomass waste utilization is its low production per unit area, causing high costs related with the collection and the transport from the origin to the consumption place [3]. Due to this reason, the systems using biomass must have a high efficiency.

Recently, to develop the energy obtaining from waste biomass, several works have been carried out; particularly about pyrolysis and gasification because these thermal processes are effective and attractive methods [4, 5]. Considering the gasification, it converts biomass wastes into low heating value gas generally called syngas. This product is more suitably used to produce electricity through internal combustion engines or gas turbines [6].

Different operating variables have a high influence on the gasification behavior: biomass feedstocks, temperature (T), equivalence ratio (ER, supply air/stoichiometric air), and supply steam/biomass ratio (SBR) [7]. In order to evaluate the gasification performance, the exergy analysis can be employed (based on the second law of thermodynamic).

On the other hand, considering the kinetic behavior, the biomass waste gasification occurs in three stages: drying (evaporation of moisture contained in the solid), pyrolysis (thermal decomposition in the oxygen absence), and the last step associated with the reaction of the char by CO_2 to produce CO. When the solid fuel is heated to temperatures between 473 and 648 K in the absence of an oxidant agent, it is pyrolyzed. The process products are a solid (char), condensable hydrocarbons (tar), and gases. Then, at higher temperatures, the condensable fraction and the gases form part of the volatile phase of the pyrolysis. The additional permanence of the solid and volatile phases in the reaction zone allows their conversion to a fraction of gases (gasification) [8].

The tar presence in the gas mixture is the main problem in the technological development of the gasification systems of biomass. The generated char during the pyrolysis stage can react with water vapor, CO_2, and oxygen. These reactions occur slower than that corresponding to the volatile phase; however, these contribute significantly to increase the amount and calorific value of the syngas.

Considering the gasification process description above, the involved reaction number, and their unknown mechanisms, simple kinetic models cannot describe the global reactions.

In this chapter, the kinetic characterization of different lignocellulosic waste gasification processes by thermogravimetric techniques using the Coats-Redfern method is presented [8]. The experimental data were fitted with several models, and each one was evaluated with different statistical parameters. Using the model with the best fit, the activation energy and pre-exponential factor were calculated, and their variation with the heating rate was evaluated [9]. On the other hand and in order to extend and improve the basic knowledge on composition and properties and to apply this knowledge for the most advanced and environmentally safe utilization, an exergy analysis of a gasification process is presented, taking into account different byproducts' production.

2. Kinetic analysis

Coats and Redfern [8] method has been widely applied to study the thermal decomposition kinetics of biomass. The reaction kinetic equation is

$$d\alpha/dt = k(T)\, f(\alpha) \tag{1}$$

where k(T) is the rate constant, $d\alpha/dt$ is the process rate, T is the absolute temperature, t is the time, $f(\alpha)$ represents function commonly used for description of biomass thermal decomposition, and α is the degree of transformation; α can be calculated from the corresponding TG curve by the following equation:

$$\alpha = (m_0 - m)/(m_0 - m_f) \tag{2}$$

$$\beta = dT/dt \tag{3}$$

where m is the mass of the sample at a given time t and m_0 and m_f refer to values at the initial and final mass of samples. For non-isothermal conditions, when the temperature varies with time with a constant heating rate defined by

$$k = A\, \exp(-E/RT) \tag{4}$$

According to Arrhenius expression:

where A is the pre-exponential factor, E is the activation energy, and R is the universal gas constant.

After a combination of Eqs. (1) and (4) and integrating, the following expression is obtained:

$$g(\alpha) = \int_0^{\alpha} d\alpha/f(\alpha) = \left(A/\beta\right) \int_0^{T} e^{(-E/RT)}\, dT \tag{5}$$

Eq. (5) can be integrated when the right hand side is expanded into an asymptotic series and higher order terms are ignored:

$$g(\alpha)/T^2 = \left(AR/E\beta\right)\left[\left(AE/E\beta\right) - (1 - 2RT/E)\right] - (E/RT) \tag{6}$$

The term 2RT/E can be neglected since it is much less than unity for the thermal decomposition of lignocellulosic materials. Plotting the left hand side of Eq. (6), which includes $g(\alpha)/T^2$ versus T, for the proposed models (**Table 1**), gives the E and A parameters. The least squares nonlinear regression was used by means of the Marquardt [10] and Levenvrg [11] algorithm using MATLAB software.

Table 1 lists several reaction models ($g(\alpha)$) used in this work to describe biomass thermal decomposition.

Reaction model	**g(α)**
Reaction order	
Zero order	α
First order	$-\ln(1-\alpha)$
Nth order	$(n-1)-1\,(1-\alpha)1-n$
Diffusional	
One-dimensional diffusion	$\alpha 2$
Two-dimensional diffusion	$(1-\alpha)\ln(1-\alpha)+\alpha$
Three-dimensional diffusion (Jander)	$[1-(1-\alpha)1/3]2$
Three-dimensional diffusion (Ginstling-Brounstein)	$(1-2\alpha/3)-(1-\alpha)2/3$
Nucleation	
Power law	αn n = 3/2, 1, ½, 1/3, 1/4
Exponential law	α
Avrami-Erofeev	$[-\ln(1-\alpha)](1/n)$, n = 1, 2, 3, 4
Contracting geometry	
Contracting area	$(1-\alpha)(1/n)$, n = 2
Contracting volume	$(1-\alpha)(1/n)$, n = 3

Table 1. Expressions for the most common reaction mechanisms in solid-state reactions.

3. Thermodynamic model

The proposed model in this work is derived from the thermodynamic equilibrium applying the following assumptions:

- The gasifier is considered as a system in stationary state, with homogeneous temperature and pressure.
- The C content in the biomass is converted in gases due to the gasification and combustion processes, and it can remain in the fly and bottom ash like char. The considered gaseous

products are CO, H_2, CO_2, CH_4, H_2O, and N_2. The quantities of other produced hydrocarbons are considered negligible. The tar production is considered in this model.

- The ash contents in the studied biomass are considered inert during all the process reactions.
- All gaseous products behave as ideal gases. This assumption error is not significant for the gasifiers operating at low pressure and high temperature.
- The S, Cl, and N contents in the biomass are negligible because they are very low compared with the C, H, and O contents.

The biomass is represented by the general formula CH_aO_b obtained from elemental analysis. The gasification process of the regional wastes can be characterized by the following global reaction:

$$\begin{aligned} CH_aO_b + wH_2O + m(O_2 + 3.76N_2) \rightarrow x_1CO + x_2H_2 + x_3CO_2 \\ + x_4H_2O + x_5CH_4 + x_6C + m3.76N_2 + x_{tar}CH_{1.003}O_{0.33} \end{aligned} \tag{a}$$

where w is the water mol/biomass mol; m is the air mol/biomass mol; x_1, x_2, x_3, x_4, and x_5 are unknown moles of exit gas composition; and x_6 and x_{tar} are char and tar exit moles, respectively.

Zainal et al. [12] presented a representative tar composition; this composition was used in this work. w and m are determined as function of the steam/biomass ratio (SBR, kg/kg) and ER (oxygen/biomass ratio, kmol/kmol). So, w and m expressions are

$$w = (SBR + w_w) \cdot \frac{M_{bm}}{18} \tag{7}$$

$$m = ER \cdot \left(1 + \frac{a}{4} - \frac{b}{2}\right) \tag{8}$$

where w_w is the mass faction of moisture content in the biomass and M_{bm} is reactant biomass quantity expressed as kmol of dry biomass/h:

$$M_{bm} = \frac{12 + a + 16b}{1 - w_w} \tag{9}$$

Taking into account global reaction (a), the balances for C, H, and O are

$$x_1 + x_3 + x_5 + x_6 + x_{tar} = 1 \tag{10}$$

$$a + 2w = 2x_2 + 2x_4 + 4x_5 + 1.003x_{tar} \tag{11}$$

$$b + w + 2m = x_1 + 2x_3 + x_4 + 0.33x_{tar} \tag{12}$$

Zainal et al. [12] considered the following reactions:

Water-gas-shift reaction:

$$CO + H_2O \overset{K_{wgs}}{\longleftrightarrow} CO_2 + H_2 \tag{b}$$

Methane reaction:

$$C + 2H_2 \overset{K_{methan}}{\leftrightarrow} CH_4 \tag{c}$$

In these reactions, the oxygen is not involved directly, and the steam is implicated in a limited form (water-gas-shift reaction). So, the gasifying agent's effect on the equilibrium reactions is not important. The equilibrium constants as partial pressure function are

$$K_{wgs} = \frac{p_{CO_2} \cdot p_{H_2}}{p_{CO} \cdot p_{H_2O}} = \frac{x_2 \cdot x_3}{x_1 \cdot x_4} \tag{13}$$

$$K_{methan} = \frac{p_{CH_4}}{p_{H_2}^2} p_0 = \frac{x_5}{x_2^2} \frac{p_0}{p} x_{total} \tag{14}$$

where p and p_0 are the total and reference pressures, respectively. They are equal to 101.3 kPa. x_{total} is the mol quantity of produced gas, excluding the inert gas.

The variation of Gibbs free energy at a determined temperature was used in order to know the K_{wgs} and K_{methan} values, according to the following equations:

$$\ln K(T) = \frac{-\Delta G_T^0}{RT} \tag{15}$$

$$\Delta G_T^0 = \sum_i \nu_i \cdot \Delta G_{f,i,T}^0 \tag{16}$$

where $\Delta G_{f,i,T}^0$ is the free energy of each constituent formation at a temperature equal T, ΔG_T^0 is the standard free energy at a temperature equal T, and ν_i is the stoichiometric number of the reaction products.

The necessary thermodynamic data were obtained of Reid, Prausnitz, and Polling [13]. The equilibrium constants as temperature function can be expressed by

$$K_{wgs} = EXP\left(\frac{5872.45}{T} + 1.86\ln T - 2.69 \cdot 10^{-4}T - \frac{58200}{T^2} - 18\right) \tag{17}$$

$$K_{methan} = EXP\left(\frac{7082.842}{T} - 6.567\ln T + \frac{7.467 \cdot 10^{-3}}{2}T - \frac{2.167 \cdot 10^{-6}}{6}T^2 + \frac{0.701 \cdot 10^{-5}}{2T^2} + 32.541\right) \tag{18}$$

3.1. Nonequilibrium factors

The assumed thermodynamic equilibrium for these reactions is not valid for real process due to the reactions that are not complete and the mass transfer resistance, too [14]. The equilibrium constant is modified to consider the nonequilibrium behavior:

$$K_{wgs}^* = K_{wgs} \cdot f_{wgs} \tag{19}$$

$$K_{methan}^* = K_{methan} \cdot f_{methan} \tag{20}$$

where f_{wgs} and f_{methan} are the nonequilibrium factors of the water-gas displacement and methanation reactions, respectively. Lim and Lee [14] obtained the values of these factors analyzing the T, ER, and SBR influences on them, considering several biomasses. Thereby, two empirical equations of f_{wgs} and f_{methan} are obtained:

$$f_{wgs} = 0.0836 \cdot e^{2.882 \cdot ER} \tag{21}$$

$$f_{methan} = 38.75 - 30.70 \cdot ER \tag{22}$$

f_{wgs} is smaller than 0.5, and this reaction is close by to equilibrium. Since the CO production during the gasification decreases when ER increases, f_{wgs} augments with this parameter in order to promote the water-gas displacement reaction. However, ER significantly affects f_{methan} varying between 20 and 33 approximately [14].

3.2. C conversion fraction

C is partially converted into gas under substoichiometric conditions, and it is related with O concentration in the atmosphere and the gasification temperature. C conversion fraction (f_c) is defined as the ratio between the mol total number in the gas composition and the C concentration present in the biomass. The non-converted C will be [14]

$$x_6 = 1 - f_c \tag{23}$$

$$f_c = 0.901 + 0.439 \cdot \left(1 - e^{(-ER + 0.0003 \cdot T)}\right) \tag{24}$$

The empirical parameters of these correlations were determined considering the experimental results obtained during the biomass gasification using air/steam mixture as gasifier agent [14].

3.3. Tar formation

Abuadala [15] defined the tar yield as a percentage by weight of the total gasification products:

$$Tar_{wt,\%} = 35.98 e^{(-0.00298 \cdot T)} \tag{25}$$

The total weight of gasification products is obtained applying a global mass balance. The tar mass is obtained by

$$m_{tar} = \frac{Tar_{wt,\%}}{100}\left(M_{bm} + SBR \cdot M_{bm} + w_w \cdot M_{bm} + 29(m + 3.76m)\right) \tag{26}$$

where M_{bm} and w_w are the fed biomass mass flow and moisture fraction of fed biomass (dry basis), respectively. The tar moles can be calculated by

$$x_{tar} = \frac{m_{tar}}{PM_{tar}} \tag{27}$$

where PM_{tar} is the tar molecular weight. In this case, the considered tar chemical formula is

$CH_{1.003}O_{0.33}$ proposed by Allesina et al. [16]. Considering Eqs. (5)–(7), (13)–(15), (17), and (21), the syngas composition can be obtained as operative variable function, T, ER, and SBR.

3.4. Process performance condition

The performance condition used in this work is the exergetic efficiency (η_{ex}). It is defined as the ratio between the profitable exergy outputs flow from the gasifier and the necessary exergy input flow to the gasifier [18]:

$$\eta_{ex} = \frac{\varepsilon x_{gas} + \varepsilon x_{loss} + \varepsilon x_{tar} + \varepsilon x_{char}}{\varepsilon x_{biomass} + \varepsilon x_{steam}} \tag{28}$$

where εx_{loss}, is the loss exergy flow and, εx_{gas}, εx_{tar}, εx_{char}, $\varepsilon x_{biomass}$, and εx_{steam} are the loss exergy flow and exergy flows of gas, tar, char, biomass, and steam, respectively. There is a loss due to the entropy production, heat and mass transfers, and chemical reaction irreversibility [18]. Considering the gasification process, it must satisfy the first and second thermodynamic laws. The second law leads to the following expression:

$$\sum_{R} \varepsilon x - \sum_{P} \varepsilon x = I \tag{29}$$

where εx is the exergy and I is the irreversibility, and it represents the lost internal exergy as the material quality loss and energy due to dissipation. It is calculated basing to the generated entropy during the gasification process:

$$I = T^{\circ} \cdot Sgen \tag{30}$$

The exergy depends on the biomass composition (chemical exergy), temperature, and pression (physical exergy). The chemical exergy (εx_{ch}) can be calculated by

$$\varepsilon x_{ch} = \sum_{i} x_i \cdot \varepsilon x^{\circ}_{ch,i} + RT^{\circ} \sum_{i} x_i \cdot \ln x_i \tag{31}$$

where xi and $\varepsilon x^{\circ}_{ch,i}$ are the molar fraction and standard exergy of i species [19]. The produced gaseous and tar physical exergies (εx_{ph}) can be calculated by

$$\varepsilon x_{ph} = \left(H - H^{\circ}\right) - T^{\circ}\left(S - S^{\circ}\right) \tag{32}$$

where H and S are the enthalpy and entropy of a species when the gasifier operates at determined T and pression and H° and S° are the enthalpy and entropy when the reactor works under standard conditions (T° = 298 K and p° = 1 atm). The total exergy is

$$\varepsilon x = \varepsilon x_{ch} + \varepsilon x_{ph} \tag{33}$$

In order to carry out the analysis of the first and second thermodynamic laws, the entropy and

enthalpy values are necessary. The specific heat capacity of tar (kJ/kgtar·K) from biomass gasification process is [20]

$$Cp = 0.00422 \cdot T \tag{34}$$

The tar enthalpy and the entropy are calculated with the following expression [21]:

$$H_{tar} = H^{\circ}_{tar} + \int_{T^{\circ}}^{T} Cp \cdot dT \tag{35}$$

$$H^{\circ}_{tar} = -30.980 + x_{CO_2} \cdot H^{\circ}_{CO_2} + x_{H_2O} \cdot H^{\circ}_{H_2O} \tag{36}$$

where x_i and $H^{\circ}{}_i$ are the molar fraction and the standard formation enthalpy of i species, respectively. The tar entropy is

$$S_{tar} = S^{\circ}_{tar} + \int_{T^{\circ}}^{T} \frac{Cp}{T} \cdot dT \tag{37}$$

where S°_{tar} is the tar standard entropy (kJ/kmol·K), and it is calculated using the following expression:

$$\begin{aligned} S^{\circ}_{tar} = \quad & 37.1636 + (-31.4767)\exp\left[-0.564682\left(\frac{H}{C} + N\right)\right] \\ & +20.1145\left(\frac{O}{C+N}\right) + 54.3111\left(\frac{N}{C+N}\right) + 44.6712\left(\frac{S}{C+N}\right) \end{aligned} \tag{38}$$

where C, H, N, O, and S are the weight fraction of carbon, hydrogen, nitrogen, oxygen, and sulfur present in the biomass, respectively. Usually, the gasifier losses at the environment are negligible comparing with the incoming and leaving energy of the gasifier. Several researchers consider that these losses are between 1 and 2% [22]. On the other hand, it is assumed that the char is pure carbon. Its specific heat capacity (kJ/kmol·K) is

$$Cp = 17.166 + 4.271\frac{T}{1000} - \frac{8.79 \cdot 10^5}{T^2} \tag{39}$$

The char chemical exergy is equal to 410 kJ/kmol, according to Moran and Shapiro [19]. Cengel [23] listed the values of standard enthalpy, entropy, and chemical exergy for the gaseous components. The biomass wastes are fed at environment temperature; its physical exergy is negligible. Ptasinski [24] calculated the biomass chemical exergy according to the expression present:

$$\varepsilon_{ch,\,biomass} = m_{biomass} \cdot \beta \cdot LHV_{biomass} \tag{40}$$

β factor is calculated by the following Eq. (24):

$$\beta = \frac{1.0414 + 0.0177\left(\frac{H}{C}\right) - 0.3328\left(\frac{O}{C}\right)\left(1 + 0.0537\left(\frac{H}{C}\right)\right)}{1 - 0.4021\left(\frac{O}{C}\right)} \tag{41}$$

Similarly, the tar chemical exergy is calculated using the liquid combustible correlation [25]:

$$\varepsilon_{ch,\,tar} = LHV_{tar}\left[1.0401 + 0.1728\left(\frac{H}{C}\right) + 0.0432\left(\frac{O}{C}\right)\right] \tag{42}$$

To evaluate the biomass high heating value (HHV,MJ/kg), the correlations presented by Sheng and Azevedo [26] were used, Eq. (1). The biomass low heating value (MJ/kg) is calculated with the following expression:

$$LHV_{biomass} = HHV_{biomass}(1 - w_w) - 2.447 \cdot w_w \tag{43}$$

2 MJ/kg is the latent heat of water vaporization at 298 K. In order to calculate the tar HHV, the following correlation is applied [27]

$$HHV_{tar} = 340.95\ C + 1322.98\ H - 119.86\ O \tag{44}$$

According to Richard and Thunman [28], the tar mass fraction of C, H, and O fractions of the tar are 0.545, 0.065, and 0.39, respectively.

4. Kinetic model application to biomass gasification

4.1. Experimental weight loss

The experiments were carried out in a tubular reactor of 5 cm of internal diameter and 100 cm of height. It is heated by electrical resistance and is coupled to an analytical balance. This equipment is connected to a control system, through which it is possible to vary the heating rate and to register time, mass data, and temperature in a computer.

Experiments were carried out under air/steam atmosphere; the steam flow rate was 0.17 ml/min, guarantying the steam/biomass ratio equal to 2.5 [7, 17]. The temperature increased from ambient temperature (approximately 300 K) to 1173 K. This final temperature ensures the highest decomposition. Three heating rates, 5, 10, and 15 K/min, were used. In order to minimize heat transfer and mass phenomena, 5 g of sample with size between 0.212 and 0.250 mm was used. **Figures 1–3** show these experiments.

4.2. Kinetic parameter determination

To determinate of kinetic parameters for the two stages, such as E and A, the weight loss curves have been used. Eq. (6) was applied to the experimental data, and a plot of $g(\alpha)/T^2$ versus T for

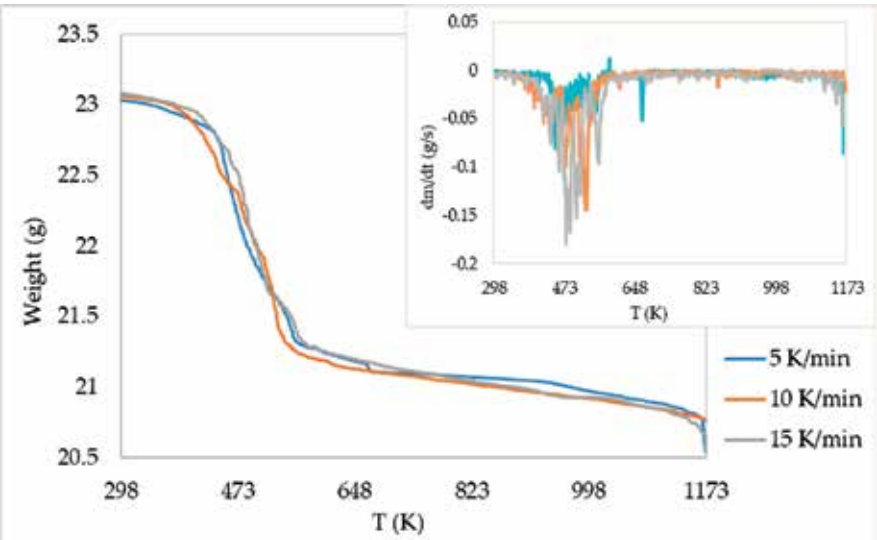

Figure 1. Weight loss and derivative curves for sawdust at different heating rates.

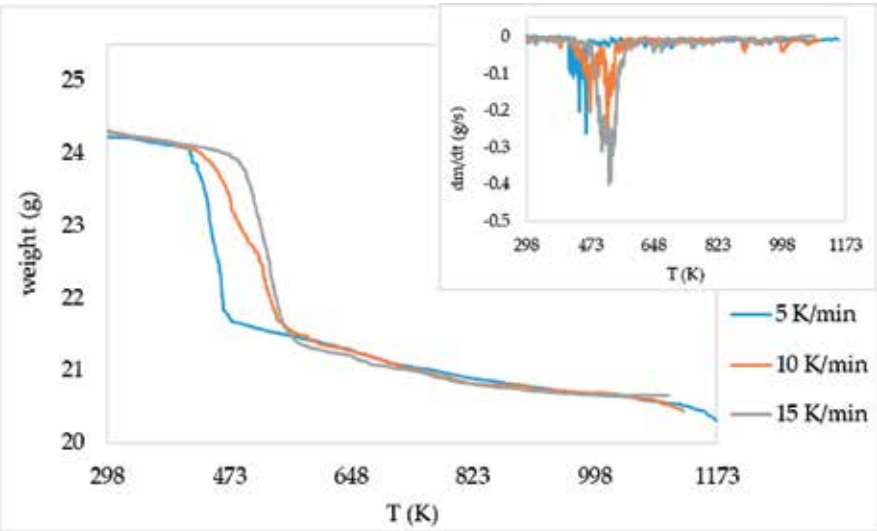

Figure 2. Weight loss and derivative curves for plum pits at different heating rates.

each biomass was obtained. **Figures 4–6** show the comparison of experimental data and the predicted values at different heating rates for the pyrolysis stage. The coefficient of correlation (R^2) for all cases is higher than 0.90, indicating a good fit.

The Ginstling-Brounstein model showed the better fit, and the obtained results are shown in **Table 2**.

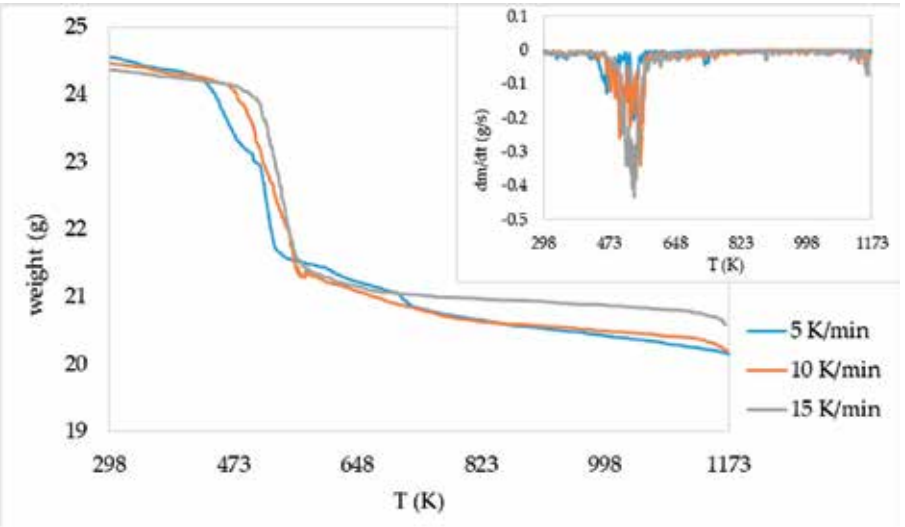

Figure 3. Weight loss and derivative curves for olive pits at different heating rates.

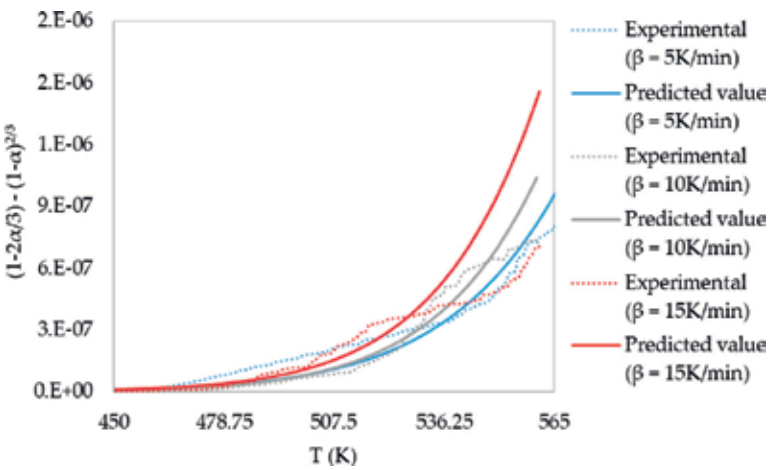

Figure 4. Comparison of experimental and predicted values of g(a) for sawdust at different heating rates for pyrolysis stage.

Figures 7–9 show the comparison of experimental data and the predicted values at different heating rates for the char combustion stage. The Ginstling-Brounstein model showed the better fit too, and the obtained results are shown in **Table 3**.

This model describes the biomass waste gasification characteristics, and it assumes that the process rate is limited by the diffusion of the reaction products from the surface, the reaction surface decreases during the process, and it can be assumed that the solid phase has the form of ball-shaped grains [29].

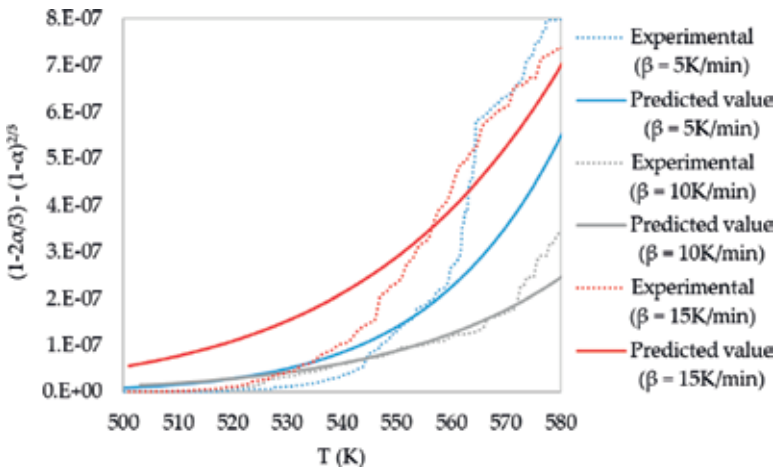

Figure 5. Comparison of experimental and predicted values of g(a) for plum pits at different heating rates for pyrolysis stage.

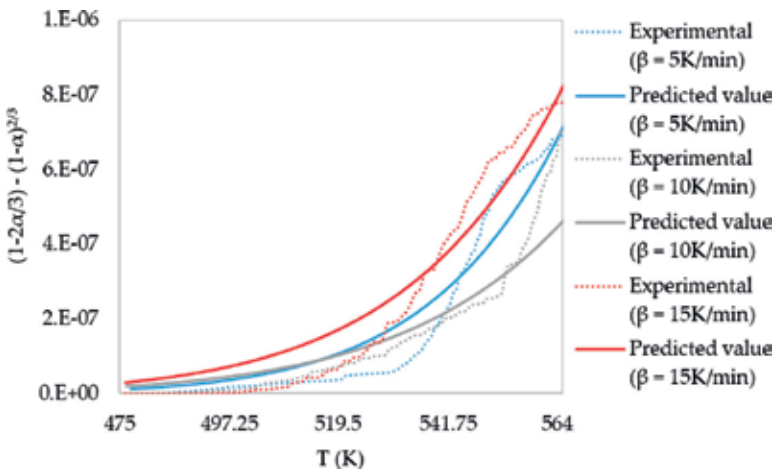

Figure 6. Comparison of experimental and predicted values of g(a) for olive pits at different heating rates for pyrolysis stage.

The obtained activation energy values vary between 70 and 100 kJ/mol and 24–98 kJ/mol for the pyrolysis and char gasification stages, respectively, for all studied agro-industrial wastes. The highest value of the energy activation was predicted for plum pits at heating rate of 15 K/min for pyrolysis stage. Also, the highest value for the same parameter was predicted for sawdust at 5 K/min for char combustion stage. The calculated values of E vary slightly with the heating rate for each biomass and indicate the existence of a complex multistep mechanism that occurs in the solid state. The increasing of heating rate leads to a simultaneous increase of the heat effect. So, the maximum decomposition rate tends to increase at higher heating rates because it provides a greater thermal energy facilitating the heat transfer around and

Agro-industrial wastes	Heating rate	Temp range	Kinetics parameters		Statistical parameters	
	β (K/min)	(K)	E (KJ/mol)	A (s−1)	R2	σ
Sawdust	5	450 565	90.96	1.34×10^{7}	0.90	7.31×10^{-8}
	10	450 560	98.62	1.91×10^{8}	0.98	3.44×10^{-8}
	15	442 561	99.80	5.10×10^{8}	0.91	6.13×10^{-8}
Plum pits	5	400 480	81.42	1.94×10^{7}	0.97	4.27×10^{-8}
	10	503 620	90.66	3.92×10^{6}	0.99	1.96×10^{-8}
	15	555 644	99.88	6.26×10^{6}	0.91	8.91×10^{-8}
Olive pits	5	387 477	70.23	1.59×10^{6}	0.91	7.09×10^{-8}
	10	476 679	80.45	1.22×10^{6}	0.98	3.21×10^{-8}
	15	488 578	87.46	1.07×10^{7}	0.92	8.91×10^{-8}

Table 2. Pre-exponential factor and activation energy obtained and the statistical parameter values for pyrolysis stage.

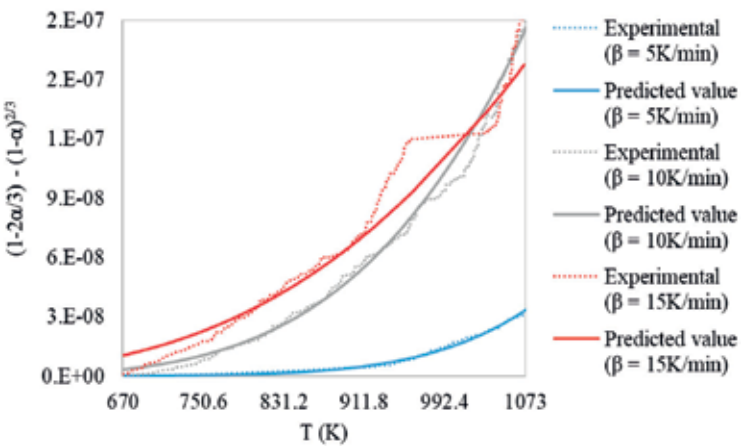

Figure 7. Comparison of experimental and predicted values of g(a) for sawdust at different heating rates for char gasification stage.

within the samples [30, 31]. The smallest value of this parameter was calculated for olive pit at 5 K/min. The found activation energy values are similar to obtained values by other authors [30, 32].

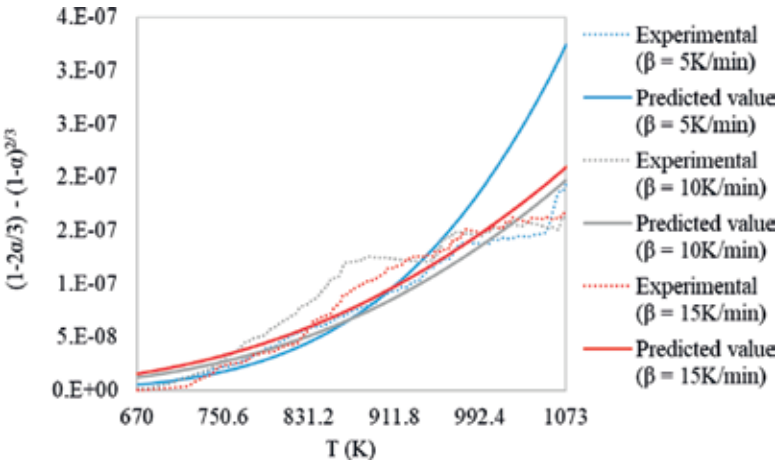

Figure 8. Comparison of experimental and predicted values of g(a) for plum pits at different heating rates for char gasification stage.

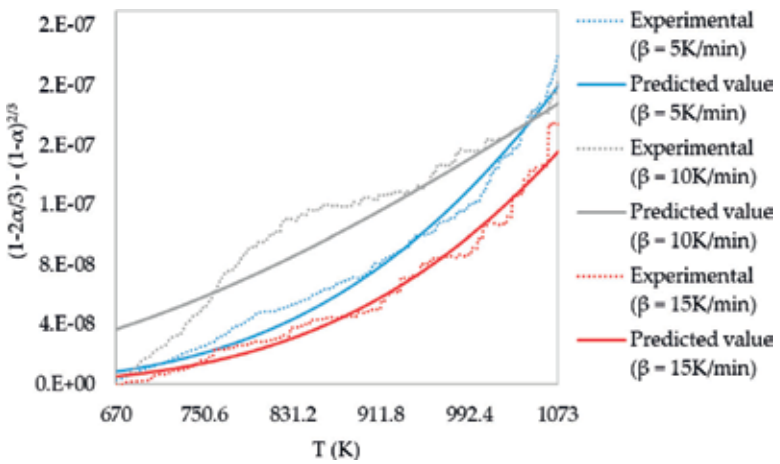

Figure 9. Comparison of experimental and predicted values of g(a) for olive pits at different heating rates for char gasification stage.

On the other hand, the pre-exponential factor value was obtained for each agro-industrial waste at the different heating rates. This parameter varies too with the heating rate; however, it is important to consider that it was obtained from a model-based method and it is tainted by association with the reaction model that must be assumed to permit its calculation.

5. Exergetic analysis to biomass gasification

The syngas composition and exergetic efficiency of the gasification process were studied with the lignocellulosic waste composition, gasifier temperature, and *ER* and *SBR* variation. *ER* was

Agro-industrial wastes	Heating rate	Temp range	Kinetics parameters		Statistical parameters	
	β (K/min)	(K)	E (KJ/mol)	A (s−1)	R2	σ
Sawdust	5	670 1073	98.19	1.20×10^{2}	0.97	2.85×10^{-9}
	10	670 1073	58.17	8.33×10^{0}	0.99	4.32×10^{-9}
	15	670 1073	40.11	1.03×10^{0}	0.95	6.67×10^{-9}
Plum pits	5	670 1073	60.25	1.00×10^{1}	0.90	8.15×10^{-9}
	10	670 1073	41.50	1.03×10^{0}	0.87	1.78×10^{-8}
	15	670 1073	38.64	1.11×10^{0}	0.92	1.49×10^{-8}
Olive pits	5	670 1073	46.40	1.01×10^{0}	0.98	6.44×10^{-9}
	10	670 1073	24.10	1.01×10^{0}	0.89	1.49×10^{-8}
	15	488 578	49.34	3.50×10^{0}	0.98	6.01×10^{-9}

Table 3. Pre-exponential factor and activation energy obtained and the statistical parameter values for char gasification stage.

varied from 0.15 to 0.3, SBR from 0 (gasification with air only) to 3, and gasifier temperature in the range of 650–950°C. The moisture content of wastes was set at about 6% by weight.

5.1. Influence of gasifier temperature

In order to analyze the syngas composition and exergetic efficiency with the gasifier temperature variation, SBR value was set at 2, and the ER value was 0.25. **Figure 10** shows that the

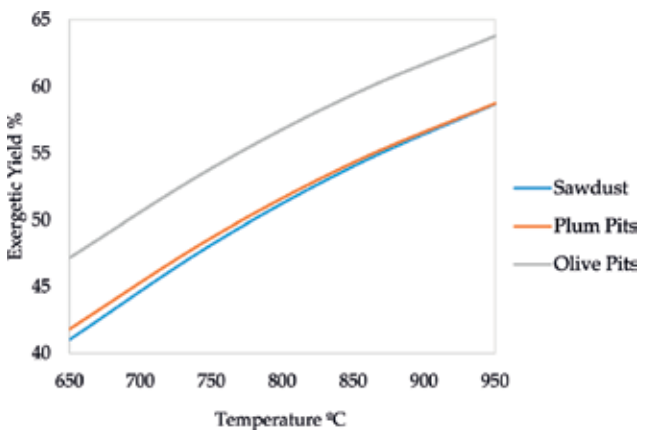

Figure 10. Exergetic yield vs. temperature.

exergetic efficiency increases when the gasifier temperature augments. This is consistent with Zhang results [33]; he informed that higher efficiencies can be achieved by increasing the gasification temperature. In the studied temperature range, the highest value to this parameter was calculated for olive pits (64% at a temperature equal to 950°C), and the lowest value was predicted for the sawdust (41% at a temperature equal to 650°C). The lower temperatures favor the exothermic reactions of CH_4 and CO_2 formations. The higher temperatures favor the endothermic reactions as the H_2 and CO formation reactions. Therefore, in the product, moles of H_2 and CO increase and consequently the exergy efficiency of the process. Therefore, the molar fraction of these gases in the syngas increases the process' exergy efficiency.

5.2. Influence of ER

To study the *ER* influence on the gasification efficiency and syngas composition, the gasifier temperature was set at 850°C and *SBR* at 1.5. **Figure 11** shows that the exergetic efficiency diminishes with the increase of *ER*. It is because the O_2 content in the gasifying agent promotes the combustion reactions. During the gasification process, these reactions are not desirable because they compete with the reactions to transform the biomass in syngas rich in H_2 and CO contents. Increasing the *ER* value, H_2, CO, and CH_4 contents decrease; thus the calorific value of the produced gas and the exergetic efficiency decrease. In addition, the CO_2 and H_2O presences in the syngas composition diminish its calorific value and the exergetic efficiency. For the Olive pits, when *ER* increases, the H_2 and CO contents in syngas decrease about 20% and 15%, respectively.

5.3. Influence of SBR

Considering the influence of *SBR* in the gasification efficiency and syngas composition, this parameter was varied when *ER* value was equal to 0.25 and the gasifier temperature equal to 850°C. **Figure 12** shows the exergetic efficiency decrease with the growth of *SBR*. The lowest value of this parameter corresponds to *SBR* = 1.5; then the exergetic efficiency value increases

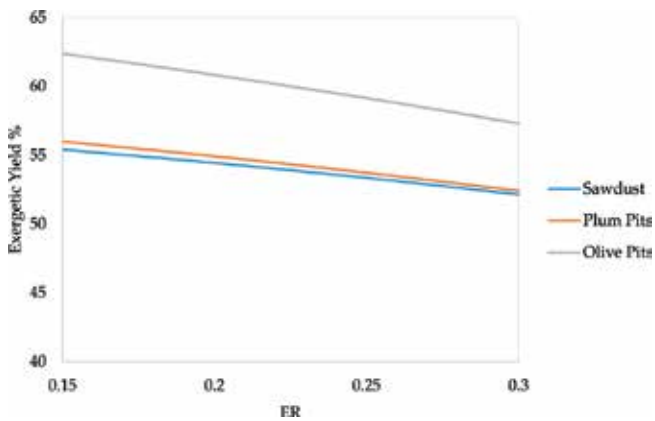

Figure 11. Exergetic yield vs. equivalent ratio (ER).

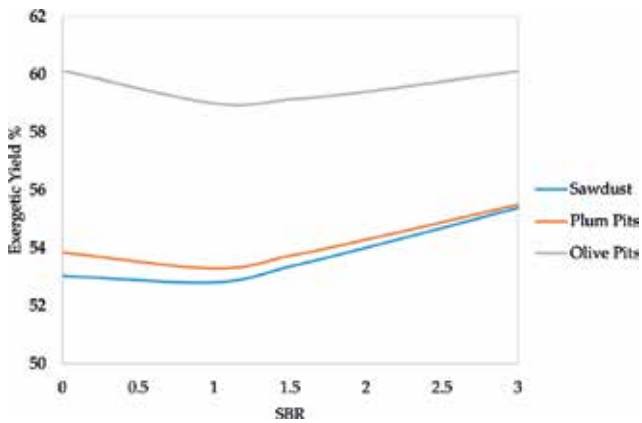

Figure 12. Exergetic yield vs. steam/biomass ratio (SBR).

softly. The decrease is due to the physical exergy of the steam used as the gasifying agent. This decrease is produced because it is necessary to supply energy to the water to transform it in steam. Then, it is partially offset by the increase of H_2 content in the produced syngas.

Comparing the gasification process of olive pits (*SBR = 0*) using air as gasifying agent and an steam–air mixture (*SBR = 1*), the CO content into the produced syngas decreases 38% approximately when the mixture is used; however, the H_2 content increases around 31%.

For the Olive pits, exergetic efficiencies equal to 60.13% and 60.11% were obtained for air and steam/air (SBR = 3) gasification, respectively, considering that the variation is not very noticeable. Physical exergy is related to the syngas sensible heat, and this is lost when the gas cools and it influences the exergetic efficiency value. Increasing the SBR value, the water content in the produced gas flow increases, and also it contributes to the physical exergy. The exergy content of syngas is the sum of physical and chemistry exergies. The physical exergy of biomass steam gasification is higher than the exergy of air gasification due to the higher temperature of the steam, resulting in the exergetic efficiency of air gasification higher to the efficiency of steam gasification.

6. Conclusions

- Two main stages defined the thermal process, named pyrolysis and gasification.
- When heating rate increases, the TG curves are shifted to the right, to the higher temperature region, and the peak height of the DTG curves increases. This shifting occurs because sample solid requires more reacting time at high heating rates.
- To describe the kinetic behavior during the pyrolysis stage, different models were selected. The three-dimensional diffusion (Ginstling-Brounstein) model showed the best fitting for all experiments, assuming that the diffusion is the controlling step of the reaction rate. The kinetic parameters were calculated using this model.

- The variation of E values with the heating rate indicates the existence of a complex multistep mechanism that occurs in the solid state.
- The results of the proposed model suggest to work at high temperatures using an air-vapor mixture as gasifying agent. While the vapor increases the H_2 content in the produced syngas, the exergetic efficiency decreases due to the necessary energy to convert water into steam.

Author details

Rosa Ana Rodriguez*, Germán Mazza, Marcelo Echegaray, Anabel Fernandez and Daniela Zalazar García

*Address all correspondence to: rrodri@unsj.edu.ar

Instituto de Ingeniería Química, Facultad de Ingeniería, Universidad Nacional de San Juan, San Juan, Argentina

References

[1] Berndes G, Hoogwijk M, van den Broek R. The contribution of biomass in the future global energy supply: A review of 17 studies. Biomass and Bioenergy. 2003;**25**:1-28

[2] Ma L, Wang T, Liu Q, et al. A review of thermal–chemical conversion of lignocellulosic biomass in China. Biotechnology Advances. 2012;**30**:859-873

[3] McKendry P. Energy production from biomass (part 1): Overview of biomass. Bioresource Technology. 2002;**83**:37-46

[4] Ellis N, Masnadi MS, Roberts DG, et al. Mineral matter interactions during co-pyrolysis of coal and biomass and their impact on intrinsic char co-gasification reactivity. Chemical Engineering Journal. 2015;**279**:402-408

[5] Han J, Kim HJ. Pyrolysis characteristic and kinetic of sawdust-polypropylene blend. Energy Sources, Part A: Recovery, Utilization, and Environmental Effects. 2009;**31**: 364-371

[6] Edreis EMA, Yao H. Kinetic thermal behaviour and evaluation of physical structure of sugar cane bagasse char during non-isothermal steam gasification. Journal of Materials Research and Technology. 2016;**5**:317-326

[7] Echegaray ME, Castro CM, Mazza GD, et al. Exergy analysis of syngas production via biomass thermal gasification. International Journal of Thermodynamics. 2016;**19**: 178-184

[8] AW C, JP R. Kinetic parameters from thermogravimetric data. Nature. 1964;**201**:68-69

[9] Fernandez A, Saffe A, Pereyra R, et al. Kinetic study of regional agro-industrial wastes pyrolysis using non-isothermal TGA analysis. Applied Thermal Engineering. 2016;**106**: 1157-1164

[10] Marquardt DW. An algorithm for least-squares estimation of nonlinear parameters. Journal of the Society for Industrial and Applied Mathematics. 1963;**11**:431-441

[11] Levenvrg K. A method for the solution of certain non-linear problems in least squares. Quarterly of Applied Mathematics. 1944;**2**:164-168

[12] Zainal ZA, Ali R, Lean CH, et al. Prediction of performance of a downdraft gasifier using equilibrium modeling for different biomass materials. Energy Conversion and Management. 2001;**42**:1499-1515

[13] Ried P, Prausnitz. The Properties of Liquids and Gases. 5th ed. New York: The McGraw-Hill; 2001

[14] Il LY, Do LU. Quasi-equilibrium thermodynamic model with empirical equations for air-steam biomass gasification in fluidized-beds. Fuel Processing Technology. 2014;**128**:199-210

[15] Abuadala A, Dincer I, Naterer GF. Exergy analysis of hydrogen production from biomass gasification. International Journal of Hydrogen Energy. 2010;**35**:4981-4990

[16] Allesina G, Pedrazzi S, La Cava E, et al. Energy-based assessment of optimal operating parameters for coupled biochar and syngas production in stratified downdraft gasifiers. In: The 15th International Heat Transfer Conference Proceedings of the 15th International Heat Transfer Conference. Kyoto, Japan Connecticut: Begellhouse, 2014. Epub ahead of print 2014. DOI: 10.1615/IHTC15.ees.008280

[17] Wu Y, Yang W, Blasiak W. Energy and exergy analysis of high temperature agent gasification of biomass. Energies. 2014;**7**:2107-2122

[18] Prins MJ, Ptasinski KJ, Janssen FJJG. Thermodynamics of gas-char reactions: First and second law analysis. Chemical Engineering Science. 2003;**58**:1003-1011

[19] Moran S. Fundamentals of Engineering Thermodynamics. 5th ed. The Atrium, Southern Gate, Chichester: Wiley; 2006

[20] Hyman D. Heat capacity and content of tars and pitchs. Industrial and Engineering Chemistry. 1959:1764-1768

[21] Eisermann W, Johnson P, Conger WL. Estimating thermodynamic properties of coal, char, tar and ash. Fuel Processing Technology. 1980;**3**:39-53

[22] de Souza-Santos ML. Solid Fuels Combustion and Gasification–Modeling Simulation and Equipment Operation. Boca Raton: CRC Press; 2004 Epub ahead of print 2004. DOI: 176548

[23] Cengel Y, Boles M. Loose Leaf for Thermodynamics: An Engineering Approach. 8th ed. New York: McGraw-Hill Education; 2014

[24] Ptasinski KJ, Prins MJ, Pierik A. Exergetic evaluation of biomass gasification. Energy. 2007;**32**:568-574

[25] Stepanov VS. Chemical energies and exergies of fuels. Energy. 1995;**20**:235-242

[26] Sheng C, Azevedo JLT. Estimating the higher heating value of biomass fuels from basic analysis data. Biomass and Bioenergy. 2005;**28**:499-507

[27] Mason DM, Gandhi KN. Formulas for calculating the calorific value of coal and coal chars: Development, tests, and uses. Fuel Processing Technology. 1983;**7**:11-22

[28] Richard N, Thunman H. General equations for biomass properties. [Internet]. 2002. Available from: http://www.unece.lsu.edu/biofuels/documents/2003-2006/bf03_011.pdf

[29] Amutio M, Lopez G, Aguado R, et al. Kinetic study of lignocellulosic biomass oxidative pyrolysis. Fuel. 2012;**95**:305-311

[30] Jayaraman K, Gökalp I. Pyrolysis, combustion and gasification characteristics of miscanthus and sewage sludge. Energy Conversion and Management. 2015;**89**:83-91

[31] Sanchez-Silva L, López-González D, Garcia-Minguillan AM, et al. Pyrolysis, combustion and gasification characteristics of Nannochloropsis gaditana microalgae. Bioresource Technology. 2013;**130**:321-331

[32] Baker EG, Mudge LK. Mechanisms of catalytic biomass gasification. Journal of Analytical and Applied Pyrolysis. 1984;**6**:285-297

[33] Yaning Z, Bingxi L, Hongtao L, et al. Exergy analysis of biomass gasification with steam/air: A comparison study. 2010 International Conference on Digital Manufacturing & Automation 2010;**1**:678-681

Chapter 5

Experimental Observation on Downdraft Gasification for Different Biomass Feedstocks

Edris Madadian

Additional information is available at the end of the chapter

http://dx.doi.org/10.5772/intechopen.77119

Abstract

With the need for developing a more sustainable world, there is a desire to shift from fossil fuels to biofuels, produced using the concept of biorefineries. Within the last few decades, thermochemical conversion technologies have gained a great deal of attention for producing advanced biofuels. In this context, this chapter elaborates different aspects of biomass gasification technology, as a representative of thermochemical pathways, and suggested potential solutions to enhance the efficacy of the process. To fulfill this goal, different types of biomass feedstock are employed to examine the potential of each in bioenergy production through gasification process. The chapter is consisting of a series of dependent studies to investigate the path for advancements in the gasification process. The first study investigates the parametric effect of experimental conditions during gasification of individual biomass feedstocks to select the best biomass feedstock for next study. It is also demonstrated that how the variation in the syngas composition interacts with H_2/CO ratio. The other study investigates the potential of composite feedstocks based on the results from the first study. The last study investigates the potential failure scenarios and the likelihood of their occurrence are explored.

Keywords: biomass, plastic waste, gasification, downdraft, syngas, bridging, clinker

1. Introduction

Sustainable development is a multi-aspect concept which demands a variety of decision makers from different sectors to play a role in saving the resources for future generations. Environment, Economy and Society are three key elements in Sustainable development. There are a variety of environmental issues, such as air pollution, water pollution, waste and land contamination and climate change, which threaten both the natural resources and the human.

To a great extent, fossil fuels consumption is the cause of the environmental issues. The context of sustainability, as it relates to energy, requires considering potential replacements for the fossil fuels. Renewable resources of energy are the solution for solving this problem. The renewable resources do not interfere the carbon balance and therefore are so-called "carbon neutral" resources (**Figure 1**).

Owing to the depletion of fossil resources and the increasing demand on fuels, it is important to develop renewable resources to produce fuels and chemicals for energy security. Biobased materials, including biomass and wood pellets, are one of the most promising sustainable energy resources to replace expensive fossil fuels, which are threatening our environment and global climate. Biobased residues and waste, as renewable multifunctional resources, can not only be used for heating and power generation but also for greenhouse carbon dioxide enrichment and the improvement of soil structure or soil aeration via biochar production.

Bio-based materials have been introduced as one of the energy resources for producing advanced biofuels. Advanced biofuels are technically referred to non-food biomass materials which can potentially be used for producing bioenergy. Advanced biofuels derived from biomass feedstock, such as agroforestry, municipal and industrial residues, each of which has the biological source for bioenergy production purposes [1]. The definition of advanced biofuels as defined in European Union (EU) Commission is "every type of biomass typically derived from plant material which does not have an alternative use as food; they can be based on waste biomass, cereal stalks, other dry plant matter, or crops grown especially for fermentation into biofuels (algae, Miscanthus)" [2].

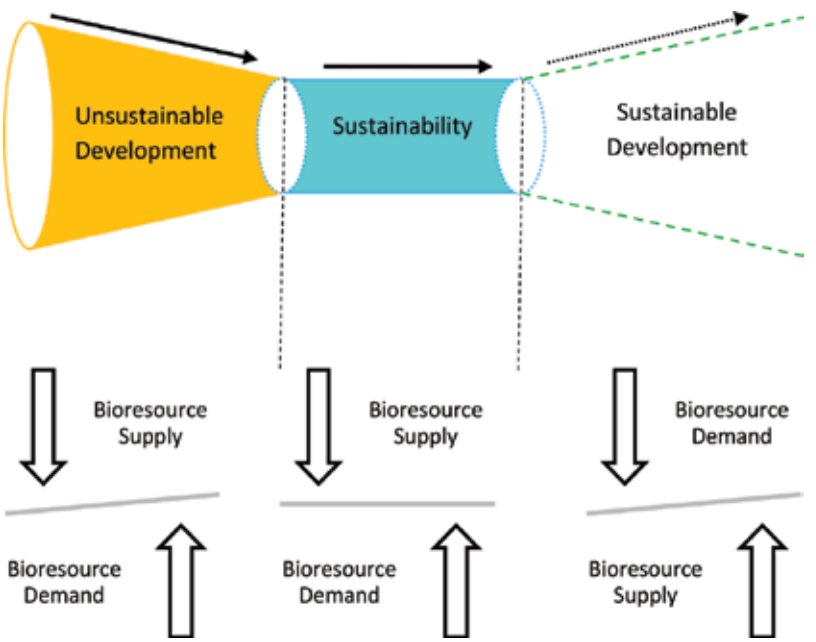

Figure 1. A developmental perspective on the transition from unsustainable era to sustainable era and sustainable development.

Biofuels have emerged as one of the most strategically important sustainable fuel sources and are considered an important way of progress for limiting greenhouse gas emissions, improving air quality and finding new energy resources. Advanced biofuels are referred to as liquid, gas and solid fuels predominantly produced from biomass, which are not in conflict with food security. A variety of fuels can be produced from biomass such as ethanol, methanol, biodiesel, Fischer-Tropsch diesel, hydrogen and methane. Renewable and carbon neutral biofuels are necessary for environmental and economic sustainability. Gasification is an environmentally friendly method which enables producing a wider range of products depending on the ultimate application.

There has been a great deal of attention from different authorities devoted to enhancing the share of advanced biofuels in the next decade. For instance, the Renewable Energy Directive (RED) stablished overall policy for the advancement of energy from renewable sources in the European Union (EU) which requires deployment of renewable energy for the share of 20% of the total energy needs of the union. RED also requires that all the members of the union to ensure use of renewable sources in the transport sector upward of 10% by 2020 which is twice of its share in 2009 [3]. Moreover, the U.S. Environment Protection Agency (EPA) mandates the increment in the share of biofuels in transportation sector from 41.9 (in 2009) to 136 billion liters (in 2022) under Renewable Fuel Standard (RFS2) [4, 5].

There are two major processes which can be served for converting biomass into useful forms of energy. The choice of conversion process could be performed by considering different parameters such as type and quantity of feedstock, the end-use applications, the local and national environmental regulations and the financial and economic conditions. Thermochemical and biochemical conversion pathways are categorized as the most well-known techniques for producing the desired form of the energy from biomass feedstocks [6, 7]. An overview of different technologies which falls under thermochemical and biochemical conversion pathways is presented in **Figure 2**.

Gasification technology represents an effective thermochemical conversion method which converts carbonaceous into synthetic feedstock. Gasification technology has been receiving a great deal of attention in the past few decades. Gasification converts carbon-based materials into gaseous products using a gasifying agent such as air, oxygen, steam and carbon dioxide. When air is used as the oxidant, the gaseous product is usually called producer gas, and when oxygen or steam is used, the product is termed synthesis gas (syngas). Syngas is an important feedstock for the chemical and energy industries, along with hydrocarbons traditionally produced from petroleum oil that can also be produced from syngas [1, 8]. During gasification, feedstock is partially oxidized. A gas medium—air, pure oxygen, steam or a mixture of these gases—is required to maintain the process. Biomass feedstock and gasification reactants, which accelerate ignition of the feedstock, typically enter the gasifier at the top and travel in the same direction down the gasifier. It should be noted that feeding points for biomass gasifiers can be from the top or from the side depending on the process.

Compared to combustion, gasification has higher efficiency due to exergy (i.e. the energy that is available to be used) losses, mainly from lower internal thermal energy exchange of expended exergy. The losses due to internal thermal energy exchange may be lowered by changing the

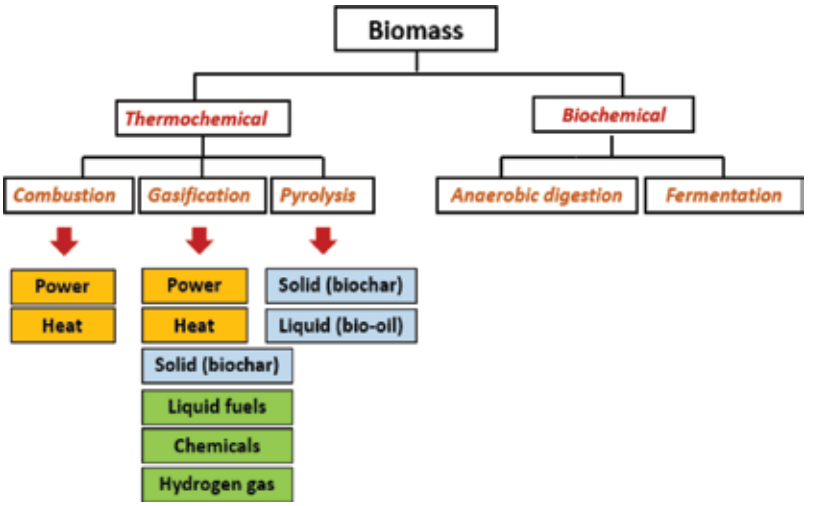

Figure 2. Biomass conversion pathways for producing bioenergy.

gasifying agent [9]. The gas composition evolved from biomass gasification strongly depends on the gasification process, the gasifying agent, and the feedstock composition [9].

The production of renewable energy from biomass using a gasification system is an environmentally friendly method that helps reduce dependence on fossil fuels. Biomass gasification offers advantages over the direct burning of biomass in a boiler. The sustainability of biomass utilization will greatly increase the overall sustainability of biomass management. In this chapter, the technical aspects of sustainable biomass management, with specific focus on recycling and energy recovery via gasification technology, are investigated. The Chapter is consisting of four interconnected studies to examine the basics towards advancements in the gasification process.

2. Gasification of individual biomass feedstocks

The first study begins with the first set of experimental studies using a 10 kW energy output down-draft gasification system (**Figure 3**). The type and characteristics of biomass can significantly affect the performance of gasification process and consequently result in different reaction temperatures, synthesis gas high heating value and tar content [10–12].

As shown in **Figure 3**, the complete system for syngas production from the gasification unit is composed of six major parts: (1) feeding; (2) main reactor; (3) filtering system, (4) burner assembly, (5) calorimetric units, and (6) purification system.

Feeding consists of a cylindrical painted steel drum bolted to a double layer drying bucket for drying of raw material. The main purpose of the painted steel drum is to increase the biomass storage capacity of the gasifier which multiplies by 6 the continuous operational time in comparison of using only the storage capacity of the main reactor. The drying bucket is used

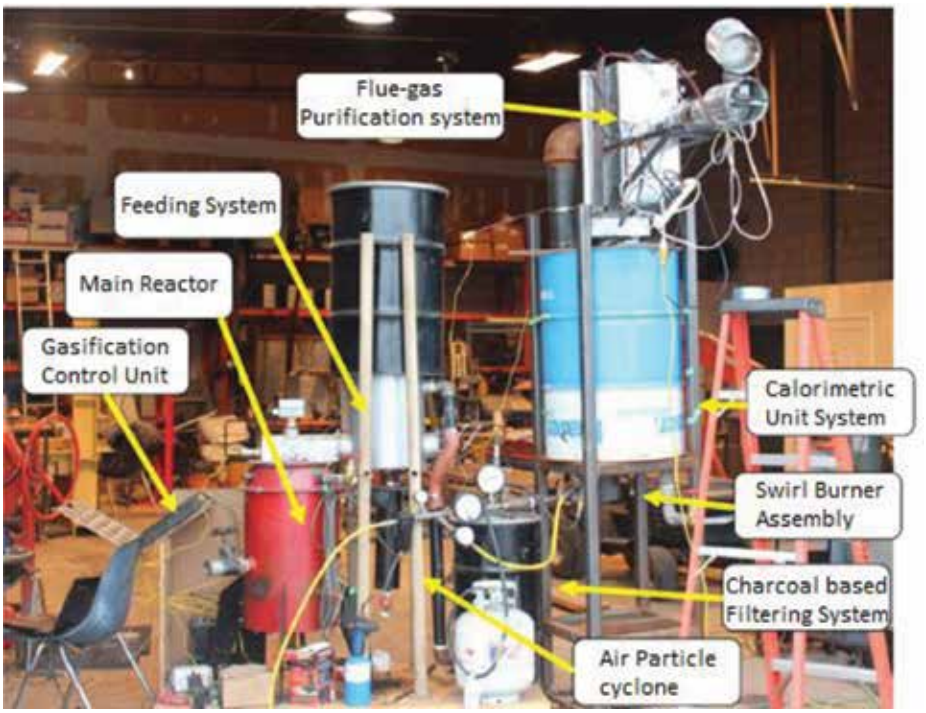

Figure 3. A downdraft gasification unit for producing advanced biofuels (McGill University, Canada).

to reduce the moisture content of the biomass that will enter the main reactor. The drying bucket is a double layer container with the biomass feedstock in the middle and hot syngas coming from the cyclone in a separate compartment surrounding the feedstock. From feeding point of view, the capacity of the employed mini-scale gasification system ranges averagely between 2.45 and 3.75 kg hr^{-1} of biomass. However, this range may change depending on the conditions of the reactor as well as the biomass feedstock.

The main reactor, which is a cylinder-shaped vessel, receives the gasifying medium (i.e. air, oxygen, steam or carbon dioxide) using internal pipes rolled around the reactor. These pipes are used to preheat the air prior the injection at the top of the reduction bell allowing a more stable gasification. Thermocouples are installed at different heights into the reactor to monitor the gasification process. An ignition port provides an access to introduce a flame directly at the top of the reduction bell to start the gasification process. The pressure into the reactor is maintained at atmospheric pressure by an ejector venturi located prior the swirl burner. This negative pressure siphons the syngas produced at the bottom of the reduction bell into the air particulate cyclone. There is a reticular grate under the reduction bell that allows the ash to be separated from the unprocessed feedstock. The ash accumulates under the grate and can be removed from the reactor by the ash trap. The compartment comprised between the reduction bell and the grate is filled with wood charcoal. A bed of pyrolysis materials facilitates the ignition of the system. The compartment between the lid and the reduction bed is filled with the biomass that will be gasified. A manometer is connected to the reactor frame to measure the

vacuum pressure inside the reactor. A schematic view from cross section of the reactor along with the different zones during the gasification is shown in **Figure 4**.

The filtering system consists of an air particulate cyclone and a charcoal filtering system. The filtration process assists to remove particulates of larger diameters than 5–25 μm. The efficiency of the particulate removal varies between 50 and 90% depending on the conditions of the gaseous entered into the cyclone.

The burner assembly consists of an ejector venturi and a swirl burner. Compressed air is provided to the ejector venturi by a compressor capable of delivering an air flow between 10.2 and 13.6 $m^3 hr^{-1}$ at a pressure of 750 kPa as specified by the manufacturer's recommendations.

The calorimetric unit consists of an insulated drum filled with water in which a spiral chimney is installed. The swirl burner is connected at the bottom of the drum to the chimney. The flue gas produced by syngas-air combustion travels inside the spiral chimney and transfers its heat to the water surrounding the chimney. The calorific value of the syngas is calculated based on the calculation of the rejected heat from the flue gas and the change in temperature of the water [13].

Low energy density of biomass is a major restriction for using biomass which typically ranges from 60 to 400 kg m^{-3} for different feedstocks [10]. There are also two operational parameters bed temperature and pressure across the reactor which affects the process of gasification as well as ultimate heating values and the syngas composition. The pressure gradient, which is monitored using pressure sensors positioned at different levels across the reactor, is a function of system configuration, geometry, feedstock porosity, permeability and physical properties of the feedstock [14].

A variety of biomass feedstock is deployed for the gasification process. In the first step, pelletized woody biomass is selected as the primary biomass of interest to run in the reactor. Forests are a major source of wealth for Canadians, providing a wide range of economic, social and environmental benefits. Therefore, choosing woody biomass to run the gasifier for baseline tests matches with the available natural resources in Canada. This section elaborates

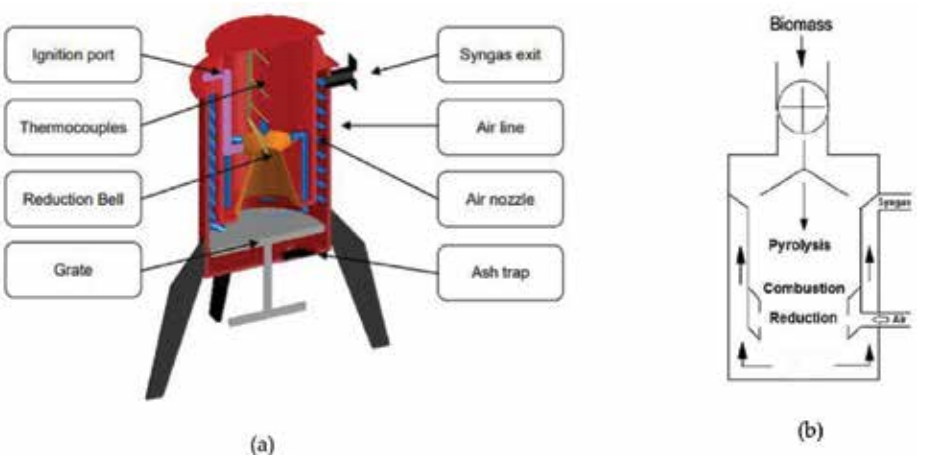

Figure 4. (a) Cross section view of the main reactor of the downdraft gasifier, (b) different zones across the gasifier [10].

the development, detailed technical aspects, and potential failure scenarios of the gasification process using woody biomass. The wood pellets are cylindrical in shape and are characterized according to American Society for Testing and Materials (ASTM) for finding out the proximate and ultimate analysis (**Table 1**).

The pressure fluctuations between the top and bottom pressure sensors cause material jamming such as bridging. Bridging of the feedstock results in a stopping of the downward flow of the pellet biomass inside the main reactor. A schematic of bridging scenario is depicted in **Figure 5a**. As can be seen, the bridging happens in the above-side zones of the reactor where only drying and pyrolysis take place. Bridging starts at early stage of gasification when the raw biomass is not yet influenced by the heat from the combustion zone (**Figure 5b**). The materials are however impacted by the gaseous products generated from the pyrolysis zone (**Figure 5c**). The pyrolysis does not take place completely due to the feedstock bridging. Therefore, the blocked materials do not allow an appropriate flow of heat towards drying and pyrolysis zones. As a result, the level of biomass does not change across the reactor in different times while the materials are slightly impacted by incomplete pyrolysis products and only transforms to darker color after a while. It should be noted that there is no chemical transformation happening under this scenario.

The gasification temperature controls the equilibrium of the chemical reactions [15, 16]. The results for five different types of feedstocks including switchgrass (representative of energy crops), woody materials (representative of agro-forestry), chicken manure (representative of animal waste) and fiber and cardboard (representative of municipal solid waste) are presented in **Figure 6** [17]. The gas compositions are recorded at five different instant temperatures of 600, 700, 800, 900 and 1000°C during the operation and at an air-biomass ratio of 0.3. All the feedstock reached instantaneous temperature over 1000°C while the average bed temperature measured is different for each feedstock. It is of worth mentioning that depending on the type of the feedstock and the conditions of the reactor in the time of operation, the producer gas flow into the swirl burner rate was recorded averagely in the range of 9.6–11.4 $Nm^3\ hr^{-1}$.

The desired element in the syngas composition is producing hydrogen (first preference) and then carbon monoxide (second preference). The production of hydrogen is so appropriate for using in the secondary combustion chamber downstream to the gasification unit for conditioning the syngas and producing ultimate end-products. This, however, never happens in practice to have only these two elements in the syngas. There have been numerous studies working on the composition of syngas [17–21] at which there are always four components hydrogen, carbon monoxide, carbon dioxide and methane reported. Majority

Properties (%)	Value	Properties (%)	Value
Moisture content	5.2	Carbon	42.64
Ash content	1.2	Hydrogen	8.5
Fixed carbon content	21.1	Oxygen	42.40
Volatile matter	72.45	Nitrogen	0.06

Table 1. Proximate and ultimate analysis of pelletized woody biomass.

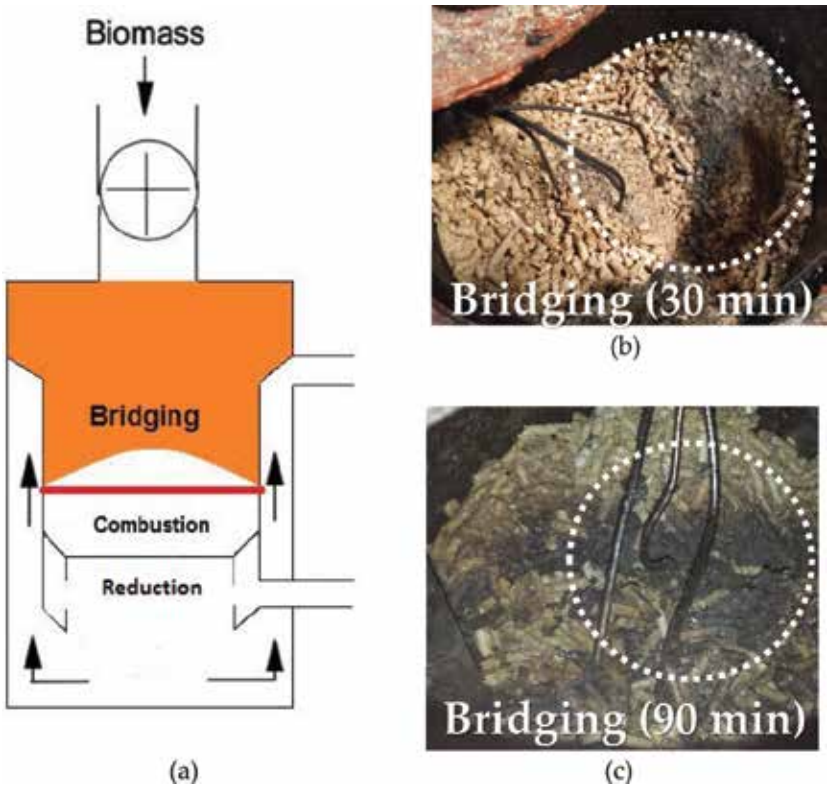

Figure 5. (a) Schematic of bridging formation across the reactor [10], (b) bridging after 30 minutes from beginning of the gasification process, (c) bridging after 90 minutes from beginning of the gasification process.

of studies have shown only up to 50% of the syngas composition filled with hydrogen and carbon monoxide, and the rest is contaminated with the other elements. As can be seen in **Figure 6**, energy crops (switchgrass) along with municipal solid waste (fiber and cardboard) showed promising performance in hydrogen and carbon monoxide. It should be also noted that the ratio of hydrogen to carbon monoxide is an important factor for condition the syngas. Madadian et al. reported that a higher percentage of hydrogen to carbon monoxide does not necessarily indicated a rich syngas [17]. This could be the main reason that the gas needs a secondary conditioning after production. Furthermore, the syngas heating values measured using the calorimetric unit fell in the range 16.84–9.24 MJ kg^{-1} which belongs to switchgrass and chicken manure, respectively. The heating values of the other biomass were recorded at 15.7, 14.45, 14.19 and 13.94 MJ kg^{-1} for hardwood, cardboard, softwood and fiber. The values may be found to some extent lower from what is reported in literature which is mainly attributed to the calorimetric unit errors which was developed by the author.

For the abovementioned biomass feedstocks in this section, the ratio of hydrogen to carbon monoxide is presented in the range of 0.15–1.5 under different temperatures. As shown in **Figure 6**, there is a proportional relationship between the value of hydrogen to carbon monoxide and the temperature profile within the reactor. In higher temperature, the

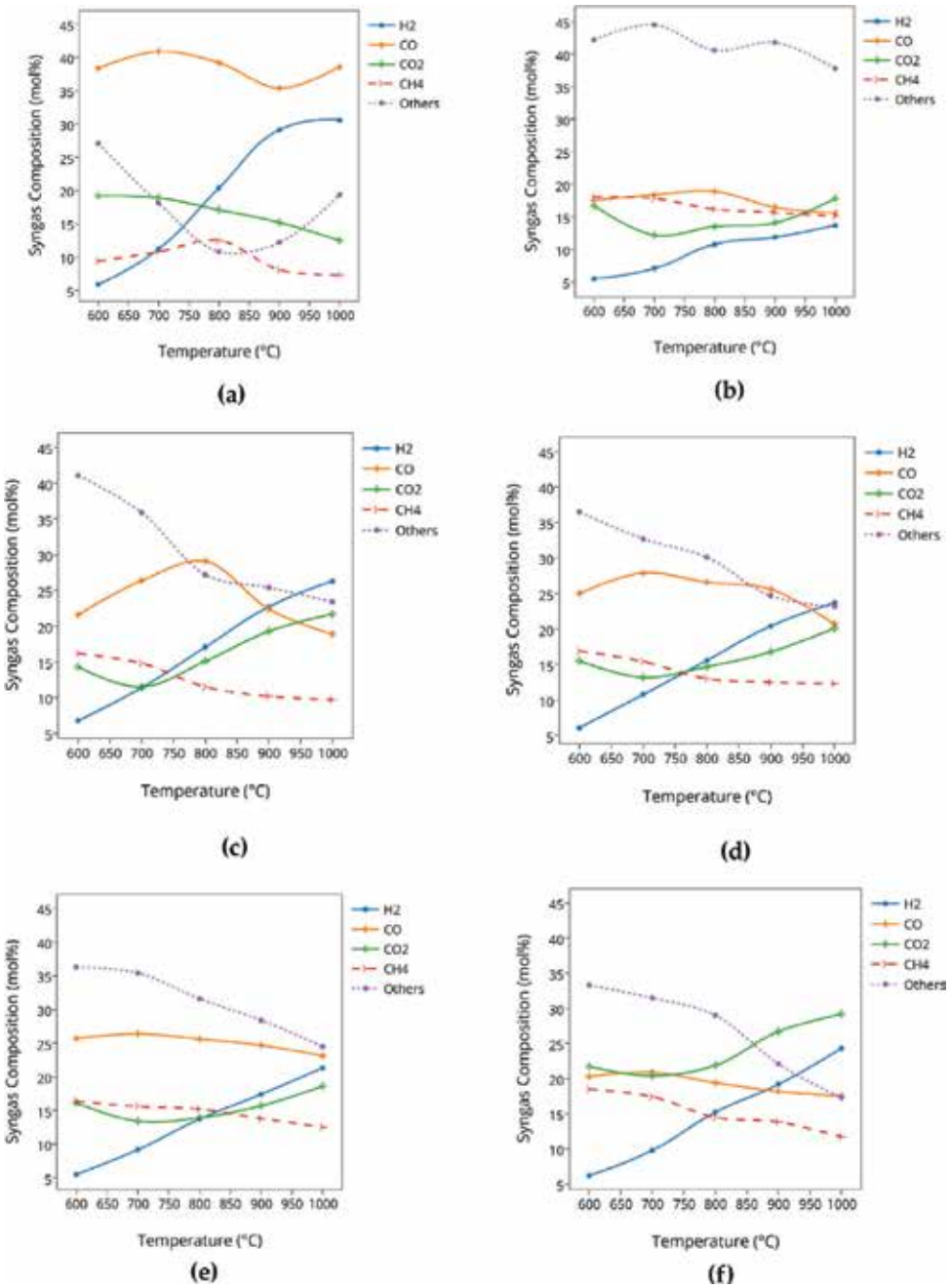

Figure 6. The recorded variations in syngas composition with respect to temperature profile during gasification of (a) switchgrass, (b) chicken manure, (c) soft wood, (d) hardwood, (e) fiber, and (f) cardboard [17].

amount of carbon monoxide drops which can be related to the reduced environment at higher elevation within the reactor. The step-by-step procedure under which this observed phenomenon took place is explain below:

a. By increasing the elevation across the reactor (from top to bottom), the temperature initially rises particularly in combustion zone where the reduction bell and air nozzles are positioned. At this step, a rich combustion process happens due to excess of air.

b. Over the time, and by controlling the amount of air getting into the reactor, oxygen-starved environment forms in higher elevation where the air enters the reactor. The immediate impact of reduced environment is an increment in the level of carbon monoxide.

c. However, the value of carbon monoxide drops gradually as the formed gaseous products react with the generated steam and/or moisture from the biomass and produce higher amount of hydrogen and carbon dioxide.

3. Gasification of composite biomass feedstocks

In this part, gasification of composite biomass feedstock is investigated. The blending of biofuels is one of the solutions for the suppliers of conventional fuel to alleviate the greenhouse gas intensity originated from the fossil fuels. As an example, a composite biomass composed of paper fiber and plastic waste originating from a municipal waste stream is tested to investigate the role of adding dissimilar agents on the productivity of the gasification technology. The study also elaborates the failure scenario of "Clinkering" and investigates the thermo-chemical properties of the generated by-products through gasification of composite fiber and plastic.

To date, experimental indices based on feedstock composition have been used to predict ash deposition and slagging potential [22]. Ash deposits or agglomerates are a major problem in the continuous operation of a thermo-chemical conversion reactor such as a gasification and combustion system [23]. There are several major factors in the bed representative agglomeration phenomenon such as particle size, feeding mode, reaction environment (oxidation/reduction), temperature, fluidization velocity, and contents of alkaline earth and alkali mineral [23]. Although downdraft gasifiers are known to have their limitations such as a feed size requirement, low ash content, decreased scale-up potential and increased risk for bridging and clinkering, this technology normally produces less tars and is less complex which could be applied for smaller scale systems [24].

The composition of the current experimental biomass includes a blend of the fibrous and plastic portions of post-consumer solid waste in Montreal, Quebec, Canada. The majority of the feedstock (90–100%) is comprised of fiber, which includes newspaper, cardboard, office paper, flyers, etc. Plastics are included as the remainder and consists of a blend of mixed polymers that include HDPE, LDPE, PET, trace PVC, etc. The plastics portion combined with fiber does not account for the level of plastic contamination that already exists in recycled municipal solid waste fiber. This portion may be as high as 2–5 wt%.

The proximate and ultimate analysis to understand the elemental matters in the individual and composite biomass feedstock is listed in **Table 2**.

As shown in **Table 2**, the ash content of plastic is much less than paper fiber waste which causes a lower ash content in the matrix of the composite pellets. Furthermore, the higher

	Testing item (%)	Plastic waste	Paper waste	Composite biomass*
Proximate analysis	Moisture content	4.78	6.27	6.12
	Volatile matter	94.19	85.78	86.62
	Fixed carbon content	<0.01	3.45	3.11
	Ash content	1.03	4.5	4.15
Ultimate analysis	Carbon	77	44.95	48.16
	Hydrogen	13.97	5.92	6.73
	Nitrogen	0.29	0.18	0.19
	Sulfur	0.19	0.19	0.19
	Oxygen	2.93	38.18	34.66
	Higher heating value (MJ kg^{-1})	40.01	17.09	19.38

*Ratio 1:10 for plastic to paper.

Table 2. Proximate and ultimate analysis of composite pelletized paper and plastic waste [25].

heating value of plastic waste is notably higher (over double) than the one for paper waste which also adds value to the composite pellet. Therefore, the lower ash content and higher heating value of plastic waste show the promising potential of making their composite pellets for producing biofuels [26]. The lower heating values of plastic waste and paper waste were calculated at 36.91 and 15.38 MJ kg^{-1}. It should be noted that gasifying the plastic is not practical as single biomass despite its high heating value. Hence, it is inevitable to blend the plastic waste with other biomass to reduce its potential emissions.

The excess of plastic content in the composition of composite matrix results in production of contamination in different forms. In the case of composite pellet, the plastic content was mixed in the ratio of 10% and resulted in producing metallic chunks of semi-burnt pellet mixed with some other elements called as clinker. The clinkering or so called "agglomeration" happens after ash is generated within the reactor when ash sintering begins at higher temperatures. The clinker forms initially in combustion zone where the highest temperature resides. By increasing clinker formation, some move downward with the help of biomass flow and deposit on top of the bed material. Therefore, the developed clinker is less porous compared to the original one formed in combustion zone. This can be due to longer distance in which they travel resulting in increased retention time in a high temperature zone which would lead to more viscous slag, along with lower heat transfer when entering the reduction zone. At the highest plastic levels tested (10%) one big ball of aluminum slag with an average of around 912 g was generated from a 15 kg start sample. The clinkers are shown in **Figure 7** [25]. One possible source of aluminum component can be from the coated plastic, however, other small contaminants during the experiment and from the fibrous feedstock might be another reason for observing contamination in the clinker. The detailed analysis of the clinker is explained in the next two paragraphs.

The organic content and minerals of the biomass feedstock have different level of persistency in leaving the matrix of the composite pellets at different temperatures. Organic content of biomass has fairly lower resistance against high temperature gasification and is fully consumed in the combustion region of the reactor where highest temperature takes place. At higher temperature, the mineral content of the biomass transforms into ash and prepares the ash sintering process at which liquid and viscous slag is generated. The formation of slag is due to the interactive reaction between the melted ash and the mineral matter content of the ash matrix. This process continues until the generated molten ash accumulates and makes the chunk of clinkers which deposits in the bottom part of the reactor. It is also reported that liquid slag flows under the force of gravity and out of the bottom of the gasifier into a water quenching system which is not the case for the current system [25].

The inductively coupled plasma (ICP) mass spectrometry analysis of individual and composite paper and plastic waste indicates presence of six major elements in the matrix of the composite pellet including sodium (Na), magnesium (Mg), aluminum (Al), potassium (K), calcium (Ca) and silicon (Si). The majority of the contaminants (i.e. Na, Mg, Al, K and Ca) originates from paper fiber existed in the municipal waste stream, and silicon is derived from plastic wastes. It is reported that these elements could be detected in typical paper waste such as brown toilet paper, cardboard, industrial paper towel, magazine paper and printer papers. The use of these elements is for the purpose of grading and sizing of the papers [25, 27]. Characteristics of the clinker are also a function of degradation mechanism depending on the composition of volatiles and consequently the gaseous phased products are affected. The thermal degradation of polymers and plastics typically begins with random scission followed

Figure 7. Clinkering during gasification of composite pellet of fiber and plastic (unit: cm) [25].

by direct scission, 1,5-radical transfer scission, and multiple step-radical transfer scissions as temperature climbs over 800°C [27].

4. Conclusion

In this chapter, the potential of bioenergy production from each of which was investigated. The failure scenario of "bridging" was observed in this stage. Next, multiple feedstocks were examined for seeking the possible improvement in the quantity and quality of the produced gas. This chapter also aimed to find how the increase in plastic specifically in the recycled fiber stream would affect the performance of a downdraft gasifier. The failure scenario of "clinkering" was observed in this stage which could be considered as an individual project to work on. The chapter also showed that a mixture of silicon with aluminum, calcium and sodium under high temperatures would result in the generation of a solid clinker that ultimately moves through the reactor and is deposited at the bottom of the reactor. It may be concluded that due to the presence of plastic, the generated ash is superheated and melts into glass-like materials causing formation of metallic chunk. The chunk is cooled down through partially endothermic nature of the gasification and results in generation of clinker. This chapter presented informative tools for improving advanced biofuel production through gasification technology and using different types of biomass feedstock which can be continued in further researches.

This study also focused on the development of gasification technology to enhance the efficiency of biomass conversion within the process. In a nutshell, the following recommendations are offered for future research:

1. Although this study worked on gasification of different types of biomass feedstock and identified the potential failure scenarios, it is still essential to elaborate the post-gasification process for syngas conditioning to produce enriched gas. This will have a significant contribution to approaching integrated gasification combined cycle (IGCC) concept.
2. Developing/re-designing the down-draft gasification unit is recommended to examine the possibility of process optimization. The new design might apply a coupled reactor in which one produces the syngas and the other one works as a downstream unit to condition the produced gas.
3. Designing a burner is recommended to enhance the efficiency of the process where the syngas comes out. A good burning process helps to preserve the syngas produced in the reactor and boost the performance of the technology.
4. Developing a feeding system which is independent of the physical properties of feedstock is strongly recommended. This will help to reduce the cost related to supply chain.
5. A detailed investigation of tar and char modeling through different types of reactor configurations could help to understand the formation process and minimize the detrimental effects of by-products.

Author details

Edris Madadian[1,2]*

*Address all correspondence to: edris.madadian@mail.mcgill.ca

1 Department of Mining and Materials Engineering, McGill University, Montreal, Canada

2 Department of Process Engineering and Applied Science, Dalhousie University, Halifax, Canada

References

[1] Madadian E et al. Green energy production: The potential of using biomass gasification. Journal of Green Engineering. 2014;**4**(2):101-116

[2] Bourguignon D. EU biofuels policy. Dealing with indirect land use change. In: European Parliament Research Service, EPRS Briefing. 2015. Available at: http://www.europarl.europa.eu/RegData/etudes/BRIE/2015/545726/EPRS_BRI(2015)545726_REV1_EN.pdf

[3] European Parliament. Directive 2009/28/EC of the European parliament and of the council of 23 April 2009 on the promotion of the use of energy from renewable sources and amending and subsequently repealing directives 2001/77/EC and 2003/30/EC. Official Journal of the European Union. 2009;**L140**(16):16-62

[4] USEPA, Renewable Fuel Standard Program (RFS2) Regulatory Impact Analysis. Ann Arbor, MI: Assessment and Standards Division, Office of Transportation and Air Quality; 2010

[5] Menten F et al. A review of LCA greenhouse gas emissions results for advanced biofuels: The use of meta-regression analysis. Renewable and Sustainable Energy Reviews. 2013;**26**:108-134

[6] Madadian E et al. Energy production from solid waste in rural areas of tehran province by anaerobic digestion. In: Proceedings of the 6th International Conference on Bioinformatics and Biomedical Engineering; Shanghai. 2012

[7] Amiri L et al. The effects of co-substrate and thermal pretreatment on anaerobic digestion performance. Environmental Technology. 2017;**38**(18):2352-2361

[8] Basu P. Biomass Gasification, Pyrolysis and Torrefaction: Practical Design and Theory. Elsevier, Academic press; 2013

[9] Jangsawang W, Laohalidanond K, Kerdsuwan S. Optimum equivalence ratio of biomass gasification process based on thermodynamic equilibrium model. Energy Procedia. 2015;**79**:520-527

[10] Madadian E et al. Gasification of pelletized woody biomass using a downdraft reactor and impact of material bridging. Journal of Energy Engineering. 2016;**142**(4):04016001

[11] Rivas J, Mc Carty A. The Effect of Biomass, Operating Conditions, and Gasifier Design on the Performance of an Updraft Biomass Gasifier. USA: Kansas State University; 2012

[12] Madadian E et al. Pelletized composite wood fiber mixed with plastic as advanced solid biofuels: Physico-chemo-mechanical analysis. In: Waste and Biomass Valorization; 2017. pp. 1-12

[13] Roy Y et al. Biomass combustion for greenhouse carbon dioxide enrichment. Biomass and Bioenergy. 2014;**66**:186-196

[14] Sharma AK. Experimental investigations on a 20 kWe, solid biomass gasification system. Biomass and Bioenergy. 2011;**35**(1):421-428

[15] Begum S et al. Performance analysis of an integrated fixed bed gasifier model for different biomass feedstocks. Energies. 2013;**6**(12):6508-6524

[16] Cimini S, Prisciandaro M, Barba D. Simulation of a waste incineration process with flue-gas cleaning and heat recovery sections using aspen plus. Waste Management. 2005; **25**(2):171-175

[17] Madadian E, Orsat V, Lefsrud M. Comparative study of temperature impact on air gasification of various types of biomass in a research-scale down-draft reactor. Energy & Fuels. 2017;**31**(4):4045-4053

[18] Sur R et al. TDLAS-based sensors for in situ measurement of syngas composition in a pressurized, oxygen-blown, entrained flow coal gasifier. Applied Physics B. 2014;**116**(1):33-42

[19] Bhaduri S et al. The effects of biomass syngas composition, moisture, tar loading and operating conditions on the combustion of a tar-tolerant HCCI (homogeneous charge compression ignition) engine. Energy. 2015;**87**:289-302

[20] Pinto F et al. Effect of syngas composition on hydrogen permeation through a Pd–Ag membrane. Fuel. 2013;**103**:444-453

[21] Shabangu S et al. Techno-economic assessment of biomass slow pyrolysis into different biochar and methanol concepts. Fuel. 2014;**117**:742-748

[22] Lee B-H et al. Ash deposition characteristics of Moolarben coal and its blends during coal combustion. Korean Journal of Chemical Engineering. 2016;**33**(1):147-153

[23] Namkung H et al. Effect of bed agglomeration by mineral component with different coal types. Journal of the Energy Institute. 2016;**89**(2):172-181

[24] McKendry P. Energy production from biomass (part 3): Gasification technologies. Bioresource Technology. 2002;**83**(1):55-63

[25] Madadian E, Crowe C, Lefsrud M. Evaluation of composite fiber-plastics biomass clinkering under the gasification conditions. Journal of Cleaner Production; 2017

[26] Madadian E, Akbarzadeh A, Lefsrud M. Pelletized composite wood fiber mixed with plastic as advanced solid biofuels: Thermo-chemo-mechanical analysis. In: Waste and Biomass Valorization; 2017. pp. 1-15

[27] Lopez G et al. Recent advances in the gasification of waste plastics. A critical overview. Renewable and Sustainable Energy Reviews. 2018;**82**:576-596

Section 2

Wastes Gasification

Chapter 6

Recent Trends in Gasification Based Waste-to-Energy

Muhammad Saghir, Mohammad Rehan and
Abdul-Sattar Nizami

Additional information is available at the end of the chapter

http://dx.doi.org/10.5772/intechopen.74487

Abstract

Addressing the contemporary waste management is seeing a shift towards energy production while managing waste sustainably. Consequently, waste treatment through gasification is slowly taking over the waste incineration with multiple benefits, including simultaneous waste management and energy production while reducing landfill volumes and displacing conventional fossil fuels. Only in the UK, there are around 14 commercial plants built to operate on gasification technology. These include fixed bed and fluidized bed gasification reactors. Ultra-clean tar free gasification of waste is now the best available technique and has experienced a significant shift from two-stage gasification and combustion towards a one-stage system for gasification and syngas cleaning. Nowadays in gasification sector, more companies are developing commercial plants with tar cracking and syngas cleaning. Moreover, gasification can be a practical scheme when applying ultra-clean syngas for a gas turbine with heat recovery by steam cycle for district heating and cooling (DHC) systems. This chapter aims to examine the recent trends in gasification-based waste-to-energy technologies. Furthermore, types of gasification technologies, their challenges and future perspectives in various applications are highlighted in detail.

Keywords: waste-to-energy (WtE), waste, gasification, fuel cell

1. Introduction

Anthropogenic activities associated with increasing global population, living standards, desire for better economic growth, energy demands, and global trade are some of the critical factors that inevitably lead to massive waste generation [1]. The environmental challenges associated with growing waste generation are further exacerbated by lack of waste planning and policy, poor waste management practices, open dumping of waste residues leading to pollution, low

or no landfilling and cheap energy costs in some regions around the world. It is inevitable that waste generation cannot be eliminated to support the human development [2].

A study by International Solid Waste Association (ISWA) showed that annual global waste generation accounts for 7–10 billion tonnes in total, of which approximately 2 billion tonnes is made up of municipal solid waste (MSW). The typical waste is made up of 24% MSW, 21% industrial waste, 36% construction and demolition (C&D) waste, 11% commercial waste, and 5% arises from wastewater treatment. Only 3% of the total solid waste is used for energy production, and there is a considerable potential to use the remaining waste for energy recovery [3].

There is an increasing momentum to reduce, reuse and recycle the waste (3R's approach), but more efforts are required to minimize the environmental impacts of residual waste disposal. When the efforts to reduce the waste generation are exhausted, plastics, glass, paper, and metals are more attractive materials for reuse and recycling purposes. A vast quantity of mixed waste still remains that becomes a nuisance and thus destined to landfills if not left to decay naturally in the immediate environment [4]. Energy generation from residual waste provides an excellent waste management solution especially after all the waste management hierarchical efforts are made and when further waste recycling is not economically viable. These mixed waste streams, commonly known as residual waste, are heterogeneous, very complex to recycle and are well suited for waste-to-energy (WtE) application. After energy conversion, the remaining waste is reduced to a tiny fraction of the original volume, and the rest can be easily disposed of in the landfills.

Many factors influence the effectiveness and routes of energy recovery from waste. Awareness to greenhouse gases (GHG's) effects from increasing emissions of waste, access to conventional energy resources, waste management costs and practicality of WtE technologies are some of the key factors that influence the energy recovery from waste. For maximizing the resource efficiency of waste feedstocks, all efforts are made to manage the waste during its life cycle. A standard waste management hierarchy includes, prevention of waste generation, reduce, reuse and recycle, conversion to energy and disposal of remaining residues throughout the waste life cycle. This chapter aims to examine the recent trends in WtE, primarily based on gasification technologies with an ambition to produce clean energy and solve waste disposal issues.

2. Trends in waste management

Historically waste was an undesirable by-product of human development and was considered as a nuisance. However, rising or unstable conventional energy costs in some parts of the world, geopolitical instability of the supply and costs of conventional energy resources, increasing waste landfills costs, and reducing landfill capacities led to a change in the waste management strategies. As a consequent, the trends in waste management have shifted from waste dumping to waste disposal for the landfill, and from waste destruction by incineration to WtE generation. Therefore, waste is no longer an undesirable by-product but one of the very

profitable business in some developed countries due to its high potential for energy and resource recovery.

2.1. Waste types and composition

Waste is a general term and encompasses a wide range of materials originating from various sources associated with human development. Waste is heterogeneous in nature [5] and very troublesome to separate down to individual waste types. Readily separable waste streams are sorted and separated at a material recovery facility (MRF), and remaining residue waste that is complex and un-economical to separate is left for energy recovery. **Table 1** provides waste types and their sources that shows the diversity of waste materials in the MSW. Typical composition of MSW varies from country to country and can have high moisture content up to 50 w/w %.

2.2. Waste treatment options

As shown in **Table 1**, the diversity of materials in the waste and complexity of separation leads to a variety of waste treatment options. Since no single waste treatment option can address all types of waste, hence different waste types attract different treatments. Source segregation has made it possible to separate waste streams that can be destined for a waste treatment facility. For example, in an MRF or waste-based biorefinery, most of the readily separable waste streams are separated for reuse and recycling such as metals, plastics, glass, aggregates,

Source	Type	Composition
Municipal solid waste (MSW)	Residential	Food wastes, paper, cardboard, plastics, textiles, leather, yard wastes, wood, glass, metals, ashes, special wastes (e.g., bulky items, consumer electronics, white goods, batteries, oil, tires), household hazardous wastes, e-waste.
	Industrial	Housekeeping wastes, packaging, food wastes, wood, steel, concrete, bricks, ashes, hazardous wastes.
	Commercial & institutional	Paper, cardboard, plastics, wood, food wastes, glass, metals, special wastes, hazardous wastes, e-waste.
	Construction & demolition	Wood, steel, concrete, soil, bricks, tiles, glass, plastics, insulation, hazardous waste.
	Municipal services	Street sweepings, landscape & tree trimmings, sludge, wastes from recreational areas.
Process waste		Scrap materials, off-specification products, slag, tailings, topsoil, waste rock, process water & chemicals.
Medical waste		Infectious wastes (bandages, gloves, cultures, swabs, blood & bodily fluids), hazardous wastes (sharps, instruments, chemicals), radioactive wastes, pharmaceutical wastes.
Agricultural waste		Spoiled food wastes, rice husks, cotton stalks, coconut shells, pesticides, animal excreta, soiled water, silage effluent, plastic, scrap machinery, veterinary medicines.

Table 1. Types and sources of waste [2].

e-waste, and liquid waste [4–9]. Medical waste is sent for incineration with or without energy recovery with minimal ash residues left for landfilling [6, 8, 10]. Organic liquid waste such as waste cooking oils and fats are sent for conversion to biodiesel and glycerol [7, 9]. Food waste, wastewater, and some agricultural wastes are sent for anaerobic digestion (AD) to be turned into biogas and digestate [11]. Solid green waste is composted and turned into a standardized compost product for horticulture applications [12]. Most of the MSW can be incinerated [13] with or without energy recovery or can be subjected to advanced conversion technologies such as gasification [14, 15] and pyrolysis [16, 17]. Incineration of MSW has been practiced in developed and developing countries as an effective waste management solution, but it leads to toxic emissions [18, 19]. These emissions are produced when the waste residue is burnt at high temperatures that lead to the formation of toxic gases such as dioxins [20], furans, polycyclic aromatic hydrocarbons (PAH), oxides of sulfur, and nitrogen [21].

2.3. Waste-to-energy (WtE)

WtE is promising because most of the waste originates from urban and industrial areas, which are close to large urban populations and where there is a great need for energy. Waste treatment and energy conversion close to the waste source help to reduce transportation costs, provide energy locally, reduce transportation-related GHG emissions and can offset fossil fuel based GHG emissions by taking a large portion of energy from waste in the form of organic biomass waste. Another advantage is that since the WtE power plants can be built close to urban areas, this leads to a reduction in the electricity distribution losses, and there is a greater likelihood of using the waste heat from the plant for district heating and cooling (DHC) purposes. Waste management at local level further supports the concept of the circular economy where resource potential of the waste feedstocks is maximized. Another critical aspect that can partially be addressed by effective waste management is the Energy Trilemma; energy security, social equity and environmental impact mitigation [22]. Conversion of residual waste-to-energy is highly desirable because of environmental benefits and income generation from energy production and sales and gate fees [23] associated with the diversion of wastes from landfill, as can be seen in some developed regions such as the European Union (EU). Similarly, in some other countries like India, China, and Pakistan, it is an excellent option to divert waste from landfill for environmental benefits as well as displacing some fossil fuel based energy production.

3. Gasification of waste

Gasification was used during the Second World War to run engines on fuelwood. It was due to lower fossil fuel prices that lead to the demise of wood gasification. However, coal gasification is well known and is still used around the world. Gasification of waste feedstocks is no different in this, as they are hydrocarbons which are used to produce syngas. Gasification of waste is preferred over incineration because it provides a syngas product that can be used in many ways as opposed to hot combustion gases. Gasification provides a uniform quality syngas from a heterogeneous and complex residual waste. Gasification is the only option that

can provide multimodal products such as heat, power, cooling, gaseous and liquid fuels as well as chemicals [24, 25]. Moreover, gasification provides the feedstock flexibility with varying qualities. Gasification also enables to produce power efficiently with an excellent ability for integration with existing power production equipment such as steam cycle, gas turbines, and gas engines. As gasification can be deployed on a local level, thus it provides efficient DHC potential from waste heat by maximizing the energy conversion efficiency. Waste gasification is a precursor for large-scale biomass gasification, and it will enable the carbon capture and storage (CCS) that otherwise lead to harmful GHG's emissions.

There is a significant rise in urbanization that is commensurate with waste generation, thus waste energy through gasification became an obvious trend. Waste is attractive for energy recovery due to huge volumes produced in urban areas. However, waste is not uniform in quality, and its moisture content varies from season to season and between geographic locations. Waste gasification can also be integrated with biomass blending to deliver low carbon energy and chemicals. Gasification processes are extensively studied where researchers have tried to optimize the gasification conditions using thermal and catalytic treatments in order to enhance the gas quality by reducing the tar content in the syngas [26, 27], along with increasing the hydrogen content and reducing the processing steps to name a few. Furthermore, various studies have focused on the effect of gasifier types [28], effect of processing temperatures [29–31], effect of feedstock types and their particle sizes [31], effect of gasifying (oxidant) agents [30, 31], effect of the bed materials [32, 33], and combining gasification with other processes to enhance the process economics and efficiency. During gasification, various complex homogeneous and heterogeneous reactions take place; some of these are shown in **Table 2**.

Reaction	Heat of reaction (MJ/kmol)	Reaction name
Heterogeneous reactions:		
$C + 0.5O_2 = CO$	−111[a]	Char partial combustion
$C + CO_2 \leftrightarrow 2CO$	+172	Boudouard
$C + H_2O \leftrightarrow CO + H_2$	+131	Water-gas
$C + 2H_2 \leftrightarrow CH_4$	−75	Methanation
Homogeneous reactions:		
$CO + 0.5O_2 = CO_2$	−283	CO partial combustion
$H_2 + 0.5O_2 = H_2O$	−242	H_2 partial combustion
$CO + H_2O \leftrightarrow CO_2 + H_2$	−41	CO shift
$CH_4 + H_2O \leftrightarrow CO + 3H_2$	+206	Steam methane reforming
Hydrogen sulfide (H_2S) and ammonia (NH_3) formation reaction:		
$H_2 + S = H_2S$	nr[b]	H_2S formation
$0.5N_2 + 1.5H_2 \leftrightarrow NH_3$	nr	NH_3 formation

[a]Negative sign indicates an exothermic reaction, and the positive sign indicates an endothermic reaction.
[b]nr = Not reported.

Table 2. List of reactions in gasification process [34, 35].

Gasification involves four different steps that are drying of feedstock, pyrolysis, oxidation, and finally the reduction [36]. These are further explained below.

Drying: Feedstocks with varying moisture content are dried in a drying process at temperatures above 100°C. In this step, no chemical reactions take place, and phase change between liquid water and vapor steam is the main cause of energy requirement in the drying process.

Pyrolysis: In this step, feedstock starts to decompose [37] in the absence of oxidant at elevated temperatures and vapors are released from the feedstock using primary reactions. The proportions of vapors and char produced are influenced by process conditions such as the heating rate and temperature. In addition, product distribution is also affected by feedstock composition and feedstock size.

Oxidation: At elevated temperatures and in the partially oxidized environment, heterogeneous reactions take place between oxidant and feedstock forming carbon monoxide (CO) and water vapor. Oxidation is influenced by the chemical composition of feedstock, type of oxidants (oxygen, steam, CO_2 or air) and operating conditions. This step is mostly exothermic and results in heat energy released for energy self-sufficiency to sustain the process heating needs.

Reduction: This is a net endothermic step during which high-temperature chemical reactions take place in the absence of oxygen. Various reactions between products of oxidation and char take place to form new hydrocarbons. Ash and some char are the by-products of this reaction step [36, 38, 39].

Gasifier selection involves a detailed understanding of different types of gasification systems and feedstocks. Selecting a gasifier type with an atmospheric or pressurized gasifier will have cost implications as pressurized systems tend to cost slightly more. Selecting between a fixed bed and fluidized bed gasifier system will be influenced by the scale of the process as well as the upstream and downstream processing requirements such as upstream air preheating for fluidized bed gasifier and downstream heavy air suction requirement for fixed bed gasifiers. Choosing between different oxidant types such as air, oxygen, steam or carbon dioxide (CO_2) will be influenced by capital costs, syngas product quality and its application. Using air as an oxidant is a cheaper option with regards to capital investment, but it may not give high calorific value syngas, and hence a compromise needs to be made during the selection process [40]. Syngas heating values have a huge influence when selecting a gasifier because syngas heating value ranges between 4 and 40 MJ/kg. End applications of syngas will dictate certain heating values, e.g., syngas for heating applications can be accepted with a low heating value gas whereas Fischer-Tropsch diesel and another chemical synthesis will require fairly high heating value syngas [41].

Various types of gasification system configurations exist that are preferred for various reasons; these are presented in **Table 3**. Most notably, they include (1) fixed-bed downdraft gasification where feedstock and syngas flow downward in a co-current direction, (2) updraft gasification where feedstock and syngas flow are in counter directions, and syngas flows upward in the gasifier, and (3) fluidized bed gasification involves a moving (catalytic or non-catalytic) bed material in addition to feedstock and oxidant. Fluidized bed gasifiers involve bubbling and circulating fluidized bed. In a bubbling fluidized bed gasifier, there is rapid mixing of feedstock and bed material by the oxidant, which leads to high heating rates and somewhat uniform distribution of temperature within the system [44]. Notable differences between the

Gasifier	Flow direction		Support	Heat source
	Fuel	Oxidant		
Fixed bed-Updraft	Descending	Ascending	Grate	Coal partial combustion
Fixed bed-Downdraft	Ascending	Descending	Grate	Volatile partial combustion
Fluidized bed-Bubbling	Descending	Ascending	None	Coal and volatile partial combustion
Fluidized bed-Circulation	Descending	Ascending	None	Coal and volatile partial combustion

Table 3. Types of gasifiers, fuel, and oxidant flow configuration [42, 43].

different types of gasifiers arise due to variations in bed support for feedstock material in the gasifier, direction of flow of material and oxidant and the heat supply and control in the gasification process. **Table 3** lays out the most common gasifier configurations [42, 43].

3.1. Differences between pyrolysis, gasification, and combustion

The main differences between pyrolysis, gasification, and combustion based on oxygen demand can be explained as below:

- In pyrolysis there is no air or oxygen allowed in the reactor with feedstock and the ultimate objective is to produce liquids (bio-oil) for further upgrading as a fuel, small quantity of char and syngas. Most of the energy in starting feedstock is condensed in a liquid that is a complex mixture of more than 300 compounds. It is red-brown in appearance with high acidity or low pH, high viscosity and lower calorific value in comparison to crude oil. It is a mixture of organic compounds such as carboxylic acids, alcohols, aldehydes, esters, ketones, sugars, phenols, guaiacols, syringol, furans, terpenes and other minor compounds [45, 46]. Bio-oil can be used as a fuel in diesel engines with some modifications or after blending with conventional diesel or as a fuel in furnaces; oil-fired boilers and turbines. Due to the characteristics of bio-oil, some improvements are necessary to enable its applications as a liquid fuel [45, 47–49].
- In combustion, the feedstock is completely combusted with excess air or oxygen, and hot combustion gases are produced. Heat produced during combustion is the end product and is used in boilers for steam generation to convert to power. The hot combustion gases are mainly made up of CO_2, water vapor, and nitrogen.
- In gasification, the feedstock is partially burned with limited oxygen or air, and fuel gas (syngas) with a calorific value greater than 4 MJ/m^3 is produced. This syngas is then further cleaned for other uses in boilers, engines, turbines, fuel cells and chemical synthesis. It is mainly composed of CO, CO_2, water vapor, hydrogen, nitrogen, and C_2H_n gases in varying concentrations [45]. Syngas (CO & H_2) is a precursor for the production of liquid fuel through Fischer-Tropsch (FT) synthesis process [50]. The gaseous product from gasification can be used in many different ways such as in heating applications (furnaces, boilers), power applications (gas engines, integrated gasification combined cycle (IGCC)) or in chemical synthesis through catalyst reactions for producing ammonia, hydrogen, FT hydrocarbons and methanol [51].

3.2. Trends in waste gasification

As highlighted earlier, MSW has vast variations in material composition, particle size, density, calorific value, contamination and ash and moisture content composition. Due to these variations in MSW, waste feedstock after sorting valuable components such as metals, plastics, and paper is standardized into solid recovered fuel (SRF) or refuse-derived fuel (RDF). This standardization has led to waste being a commodity and is sold in the international market. Also, to reduce transportation costs, SRF and RDF are pelletized to increase energy density. The international movement of waste is widespread among the EU countries [52]. The huge size of installed incineration capacity within EU attracts waste movement on the mass scale. In continental Europe, cement kilns are regularly co-fired with RDF as these facilities have sophisticated emissions cleaning equipment. However, due to Waste Incineration Directive, there is an increasing shift towards advanced conversion treatment such as pyrolysis and gasification within EU.

There is an increasing policy shift towards sustainable energy production at reduced carbon footprint. For example, the United Kingdom (UK) of Great Britain under its Climate Change Act 2008 committed to reducing its 80% of carbon emissions to 1990 level by 2050 [53]. The UK government has provided subsidies in the form of Renewables Obligation Certificates (ROC) for biomass waste utilization contained within the residual waste to support the low carbon energy production. This has created a big shift towards the UK becoming a market leader in WtE. There are currently 14 such WtE plants, mostly based on gasification technology, are operational in the UK alone, and much more are under construction [52].

3.3. Tars and their associated problems in gasification

Tars are defined by Milne et al. [54] as "the organics produced under thermal or partial-oxidation regimes (gasification) of any organic material are called "tars" and are assumed to be largely aromatic." Other researchers have described tars as a very complex mixture of aromatic and oxygenated hydrocarbons having a molecular weight higher than that of benzene of [55–57]. Benzene and other heavier molecular weight compounds are present in pyrolysis bio-oil, and their presence in syngas tends to cause problems. As previously said, intermediate pyrolysis is based around the concept of encouraging secondary reactions between the evolved vapors from biomass and resulting char. Some tars present in the bio-oil can have their molecular weight up to 500 Daltons [58]. The presence of these very high molecular weight tars in bio-oil and syngas lead to incomplete combustion when these fuels are used. High molecular weight tars act as promoters of high viscosity, and limit the atomization of the fuel, and cause blockages in fuel pipes and injector lines by condensation [45, 54, 59].

Tar levels as reported by Milne et al. [54] exhibit a wide range of various gasification processes. For example, updraft gasifier tar content in the raw syngas is reported between 1 and 150 g/m^3. Whereas, in a downdraft, it is 0.04–6 g nominally, and in the fluidized bed gasifiers it is 0.1–23 g/m^3. Milne et al. [54] also reported various tar tolerance levels from various authors in the syngas for multiple applications such as for engines, turbines, fuel cells, and compressors. It is

imperative to bring the tar levels in the syngas as low as possible to avoid associated problems in the downstream processing equipment.

4. Types and applications of gasification systems

Numerous researchers are looking into alternative ways to make use of low-grade biomass and wastes by avoiding the need even to produce bio-oils while still pyrolyzing and gasifying these materials [59–68]. One such system is the Viking gasifier [61] that is a two-stage process to crack the tars thermally. This system works by a screw pyrolysis system that produces hot vapors and char at a temperature of 500–600°C at the top of the gasifier to be partially oxidized and tar fractions to be broken down into syngas. The char from the pyrolysis unit is transferred into fixed bed of the gasifier to act as a tar cracking unit where further tar cracking occurs. This system is reported to have a nominal tar content in syngas as low as 15 mg/m^3. Tar sampling has been performed in various stages of this process in another study [1, 59–68], which shows a progressive decrease in tar levels starting from the pyrolysis stage to partial oxidation to gasification stages and decreasing to 5 mg/m^3 tar levels.

4.1. Fluidized bed gasifiers

Fluidized bed gasifiers are used for commercial applications >5 MW as they are only economical at large scale as compared to downdraft gasification that is economical up to 5 MW maximum. Such systems consist of a vessel with an air distributor nozzle assembly at the bottom of the vessel. Feedstock enters the bed and finely ground bed material is fluidized by air or oxidizing agent. The temperature of the bed in the gasifier is regulated by the air/feedstock ratio within 700–900°C. Biomass is thermally broken down into gaseous compounds, and char is produced. The hot char and fluidizing bed material cause further reactions to break long-chain hydrocarbons or tars into syngas components. Thus, a syngas product with very low tar content is produced with tar content less than 3 g/Nm^3.

Advantages of fluidized bed gasifiers include uniform syngas product composition, uniform temperature distribution throughout the gasifier, rapid heat transfer between the feedstock, bed material, and oxidant. It is also possible to achieve high conversion efficiency and low tar content in the syngas. The effectiveness of tar removal can be further enhanced by using catalytic bed materials such as olivine, dolomite, and other industrial nickel-based catalysts. Disadvantages include problems with low ash melting point materials and large bubble size bypassing the bed [43]. Examples of these gasifiers include Royal Dahlman [69] bubbling fluidized bed gasifier and Gussing circulating fluidized bed gasifier [70].

4.1.1. Type 1 gasifier

Two-stage close coupled gasification/combustion is used within the fluidized bed reactor with a multi-level injection of air. Primary air/oxygen injection in gasification level and secondary air injection is used in the combustion level for complete combustion of gases. Hot gases

exiting the reactor are fed into a steam generator to produce steam which then drives a steam turbine to generate electricity. Minimal gas cleaning takes place in this type of gasifier configuration. This process layout suits steam turbines and usually have low overall efficiency up to 20%. Example include Energos process [71] where the objective is to reduce capital costs of downstream gas cleaning equipment.

4.1.2. Type 2 gasifier

This kind of gasifier is usually better equipped as compared to type 1 gasifier. After waste feedstock entry into gasifier, air or oxygen is introduced to run the gasifier for converting waste into syngas. There is catalytic fluidized bed environment to crack tars, and the resulting syngas is then cooled to 400°C and hot filtered and then combusted in the boiler to produce steam for electricity generation using a steam turbine. The excess heat is also recovered and used in district heating system. An example of this system is a Lahti gasification process [72].

4.1.3. Type 3 gasifier

Only this type of gasifier can deliver the future promise of meeting the need of syngas utilization for multi-modal products. This is due to the ultra-clean and tar-free syngas it can produce through various syngas tar cracking and polishing stages. In this type of gasifier setup, the waste feedstock is fed into the fluidized bed gasifier where oxygen or air/steam react with it in the presence of a catalyst bed such as dolomite or olivine to produce syngas. After removing solids through hot gas filtration, thermal tar cracking is performed by oxygen injection to raise the temperature (1200°C) of the syngas. The higher calorific value of the syngas is maintained as nitrogen input through the air is kept minimal. The resulting syngas is then further cleaned and polished before being used either in the gas engine, gas turbine or in chemical synthesis. This syngas can be converted into Fischer Tropsch diesel, methanol or hydrogen. The tar free nature of syngas provides excellent future proofing potential for the product flexibility. The engine efficiency on this syngas can be as high as 35% [73], and with heat recovery or through methanation for synthetic natural gas (SNG) production, even higher efficiencies are easily achievable. An example of this system is Lurgi fluidized bed gasification system.

4.2. Plasma gasification

Plasma gasification is preferred for mixed waste such as MSW or hazardous waste (asbestos and radioactive) where high temperatures are used to produce syngas and a melt arising from inorganic species of feedstock. A distinctive feature of plasma process resides in its ability to produce very high temperatures that are not achievable with conventional gasification and combustion; these high temperatures help to reduce tars and convert all the organic material into syngas. Tar content as reported by Refs. [54, 74] is shown to be 1000 times less than that of auto-thermal gasification processes. Arc discharges obtain thermal plasmas from DC or AC current or through radio frequency or microwaves. Mostly DC plasma technology is preferred for waste gasification plasma processes. Plasma is formed by high energy from AC or DC sources through the plasma torch close to the bottom of reactor and fuels are gasified through the plasma flames. The oxygen demand in this process is small as compared to conventional

gasification as most of the thermal energy is coming from external energy source rather than through exothermic reactions between the fuel and oxygen. Oxygen is only used to convert the fuel into syngas [75]. Commercial scale examples of operating plants are Advanced Plasma Power and Alter NRG (Westinghouse) [76].

4.3. Waste gasification for fuel cell application

Although waste gasification plants are mostly feeding the syngas to turbine or engine for electricity, however, there is a significant interest in using the ultra-clean syngas in high-temperature solid oxide fuel cells (SOFC) [77]. This is because CO being the main constituent of the syngas does not poison the fuel cell electrodes as it happens to be in polymer electrolyte fuel cells. The interest is due to the high electricity conversion efficiency that can be achieved by using fuel cells. However, so far most of the development for fuel cell application is based on individual biomass feedstocks as opposed to mixed waste feedstocks. The sulfur poisoning of SOFC is one big hurdle that needs to be overcome for waste gasification. SOFC usually are tolerant to sulfur content in parts per billion (ppb) range. Nagel et al. [78] have studied the biomass integrated syngas fuel cell setup with an electrical power output of 1 MWe. In another development, Lobachyov and Richter [79] explored the integration of a biomass-fuelled gasifier to Molten Carbonate fuel cell (MCFC). With the trends of waste gasification leading to producing ultra-clean tar-free syngas, the quality of syngas permits to use it in high-temperature fuel cells. The need to clean the syngas with sulfur impurities down to ppb level is achievable through a separate sulfur removal process. Given the high electrical efficiency of fuel cells and excess heat available from such integrated system, it all lends to perfect combined heat and power (CHP) system through fuel cell application in urban areas [80].

4.4. In-situ oxygen separation from air for gasification

Separating oxygen from the air through pressure swing adsorption and cryogenic methods is all very well known for large-scale oxygen production. As the waste gasification is trending towards ultra-clean tar-free syngas with high calorific values, this demand can only be met by oxygen gasification rather than air. In all oxygen separation processes, the high costs of oxygen production are associated with high-pressure air, low-temperature cooling and or membranes. New techniques of oxygen separation from the air are emerging where oxygen can be separated using a ceramic ionic membrane separation at high temperatures [81]. Since gasification takes place at temperatures above 800°C, this has attracted a lot of interest from industry to generate in-situ oxygen while gasifying the feedstocks. This mixed ionic-electronic conducting (MIEC) technology is based on dense ceramic membranes to separate the oxygen from air at temperatures around 800–900°C [82]. Since these membranes are made up of ceramics, they can tolerate high temperatures and do not need electrodes for oxygen separation [83, 84]. These ion transport membranes (ITM) work on electronic conductivity principle that creates a short circuit that involves oxygen partial pressure gradient from high to low. Oxygen permeates from high partial pressure to low partial pressure side while the flux of electrons balances overall charge neutrality. Air

Products and Chemicals and Praxair have developed ionic transport based ceramic membranes driven by high process temperature. In an ideal environment, compressed air at 7–20 Bar is heated in-situ to the gasifier where heat is applied from the gasifier to enable electronic conductivity and oxygen transport from high partial pressure atmosphere to low-pressure atmosphere. Oxygen production in this way will only require compressed air at moderate to low pressures, and the remaining energy is supplied from gasifier process heat generated by exothermic reactions.

5. Conclusions

With increasing shift towards sustainable energy production, waste gasification is certainly providing multiple solutions such as sustainable waste management and clean energy production. In Europe, district heating schemes are now regularly powered by combined heating and power (CHP) plants. Therefore, gasification to steam cycle experienced a shift towards ultra-clean syngas injection into CHP plant with heat recovery for district heating and cooling (DHC) systems. Moreover, there is a significant interest in high-temperature fuel cell applications of syngas with heat recovery after the emergence of solid oxide fuel cells (SOFC). As the carbon capture and storage is becoming high on the strategic agenda, the use of oxygen during gasification is becoming the norm. Therefore, emerging research into ceramic ionic transport membranes (ITM) to produce high purity oxygen for gasification at elevated temperature is leading the way into the new market.

Author details

Muhammad Saghir[1], Mohammad Rehan[2] and Abdul-Sattar Nizami[2]*

*Address all correspondence to: nizami_pk@yahoo.com

1 European Bioenergy Research Institute (EBRI), Aston University, Birmingham, UK

2 Centre of Excellence in Environmental Studies (CEES), King Abdulaziz University, Jeddah, Saudi Arabia

References

[1] Rehan M et al. Waste to biodiesel: A preliminary assessment for Saudi Arabia. Bioresource Technology. 2018;**250**:17-25

[2] Hoornweg D, Bhada-Tata P. What a Waste: A Global Review of Solid Waste Management. Urban Development Series Knowledge Papers. World Bank. Report no. 15. March 2012

[3] ISWA: International Solid Waste Association. Austria: ISWA Report 2015; 2015. p. 37

[4] Jambeck JR et al. Plastic waste inputs from land into the ocean. Science. 2015;**347**(6223): 768-771

[5] Nizami AS et al. Developing waste biorefinery in Makkah: A way forward to convert urban waste into renewable energy. Applied Energy. 2017;**186**(2):189-196

[6] Miandad M et al. Effect of plastic waste types on pyrolysis liquid oil. International Biodeterioration & Biodegradation. 2017;**119**:239-252

[7] Shahzad K et al. Biodiesel production potential from fat fraction of municipal waste in Makkah. PLoS One. 2017;**12**(2):e0171297

[8] Rehan M et al. Effect of zeolite catalysts on pyrolysis liquid oil. International Biodeterioration & Biodegradation. 2017;**119**:162-175

[9] Nizami AS et al. The potential of Saudi Arabian natural zeolites in energy recovery technologies. Energy. 2016;**108**:162-171

[10] Ouda OKM et al. Waste to energy potential: A case study of Saudi Arabia. Renewable and Sustainable Energy Reviews. 2016;**61**:328-340

[11] Khan MD et al. Effect of co-substrates on biogas production and anaerobic decomposition of pentachlorophenol. Bioresource Technology. 2017;**238**:492-501

[12] Waqas M et al. Resource recovery of food waste through continuous thermophilic in-vessel composting. Environmental Science and Pollution Research. 2017. DOI: 10.1007/s11356-017-9358-x

[13] Sadef Y et al. Waste-to-energy and recycling value for developing integrated solid waste management plan in Lahore. Energy Sources, Part B: Economics, Planning, and Policy. 2015;**11**(7):571-581

[14] Eghtedaei R et al. Co-gasification of biomass and municipal solid waste for hydrogen-rich gas production. Energy Sources, Part A: Recovery, Utilization, and Environmental Effects. 2017;**39**:1-6

[15] Materazzi M, Lettieri P, Taylor R, Chapman C. Performance analysis of RDF gasification in a two stage fluidized bed–plasma process. Waste Management. 2016;**1**:256-266

[16] Miandad R et al. Influence of temperature and reaction time on the conversion of polystyrene waste to pyrolysis liquid oil. Waste Management. 2016;**58**:250-259

[17] Miandad R et al. Catalytic pyrolysis of plastic waste: A review. Process Safety and Environmental Protection. 2016;**102**:822-838

[18] Malakahmad A et al. Assessment of carbon footprint emissions and environmental concerns of solid waste treatment and disposal techniques; case study of Malaysia. Waste Management. 2017

[19] Morin NA et al. The presence and partitioning behavior of flame retardants in waste, leachate, and air particles from Norwegian waste-handling facilities. Journal of Environmental Sciences. 2017

[20] Akele ES, Tarekegn MM. Assessment of dioxin and furan emission levels and management practices in Addis Ababa, Ethiopia. Journal of Health and Pollution. 2017;**7**(15):85-94

[21] Gatti MG et al. Human biomonitoring of polycyclic aromatic hydrocarbonsand metals in the general population residing near the municipal solid waste incinerator of Modena, Italy. Chemosphere. 2017;**186**:546-557

[22] Miandad M et al. Plastic waste to liquid oil through catalytic pyrolysis using natural and synthetic zeolite catalysts. Waste Management. 2017;**69**:66-78

[23] Nizami AS et al. Waste biorefineries: Enabling circular economies in developing countries. Bioresource Technology. 2017;**241**:1101-1117

[24] Prins MJ, Ptasinski KJ, Janssen FJ. From coal to biomass gasification: Comparison of thermodynamic efficiency. Energy. 2007;**32**(7):1248-1259

[25] Rauch R et al. Biokerosene production from bio-chemical and thermo-chemical biomass conversion and subsequent Fischer-Tropsch synthesis. In: Biokerosene. Springer; 2018. pp. 497-542

[26] Erakhrumen AA. Biomass gasification: Documented information for adoption/adaptation and further improvements toward sustainable utilisation of renewable natural resources. ISRN Renewable Energy. 2012;**2012**:8. Article ID 536417

[27] Wongsiriamnuay T, Kannang N, Tippayawong N. Effect of operating conditions on catalytic gasification of bamboo in a fluidized bed. International Journal of Chemical Engineering. 2013;**2013**:9. Article ID 297941

[28] Gómez-Barea A, Leckner B. Modeling of biomass gasification in fluidized bed. Progress in Energy and Combustion Science. 2010;**36**(4):444-509

[29] Ciferno JP, Marano JJ. Benchmarking Biomass Gasification Technologies for Fuels, Chemicals and Hydrogen Production. US Department of Energy. National Energy Technology Laboratory; 2002

[30] Rapagna S, Latif A. Steam gasification of almond shells in a fluidised bed reactor: The influence of temperature and particle size on product yield and distribution. Biomass and Bioenergy. 1997;**12**(4):281-288

[31] Mohammed M et al. Air gasification of empty fruit bunch for hydrogen-rich gas production in a fluidized-bed reactor. Energy Conversion and Management. 2011;**52**(2):1555-1561

[32] Mahishi MR, Goswami D. An experimental study of hydrogen production by gasification of biomass in the presence of a CO_2 sorbent. International Journal of Hydrogen Energy. 2007;**32**(14):2803-2808

[33] Hanaoka T et al. Hydrogen production from woody biomass by steam gasification using a CO_2 sorbent. Biomass and Bioenergy. 2005;**28**(1):63-68

[34] Ahmad AA et al. Assessing the gasification performance of biomass: A review on biomass gasification process conditions, optimization and economic evaluation. Renewable and Sustainable Energy Reviews. 2016;**53**:1333-1347

[35] Doherty W, Reynolds A, Kennedy D. The effect of air preheating in a biomass CFB gasifier using ASPEN Plus simulation. Biomass and Bioenergy. 2009;**33**(9):1158-1167

[36] Demirbas A. Biomass gasification for power generation in Turkey. Energy Sources, Part A: Recovery, Utilization, and Environmental Effects. 2006;**28**(5):433-445

[37] Bridgwater AV. Renewable fuels and chemicals by thermal processing of biomass. Chemical Engineering Journal. 2003;**91**(2):87-102

[38] Maschio G, Lucchesi A, Stoppato G. Production of syngas from biomass. Bioresource Technology. 1994;**48**(2):119-126

[39] André RN et al. Fluidised bed co-gasification of coal and olive oil industry wastes. Fuel. 2005;**84**(12):1635-1644

[40] Gañan J et al. Energy production by means of gasification process of residuals sourced in Extremadura (Spain). Renewable Energy. 2005;**30**(11):1759-1769

[41] McKendry P. Energy production from biomass (part 3): Gasification technologies. Bioresource Technology. 2002;**83**(1):55-63

[42] Couto N et al. Influence of the biomass gasification processes on the final composition of syngas. Energy Procedia. 2013;**36**:596-606

[43] Bridgwater AV, Evans G, Teknik D. An Assessment of Thermochemical Conversion Systems for Processing Biomass and Refuse. Harwell: Energy Technology Support Unit; 1993

[44] Rampling T, Gill P. Fundamental Research on the Thermal Treatment of Wastes and Biomass: Thermal Treatment Characteristics of Biomass. Vol. 208. Harwell Laboratory, Energy Technology Support Unit; 1993

[45] Hossain A, Davies P. Pyrolysis liquids and gases as alternative fuels in internal combustion engines – A review. Renewable and Sustainable Energy Reviews. 2013;**21**:165-189

[46] Zhang Q et al. Review of biomass pyrolysis oil properties and upgrading research. Energy Conversion and Management. 2007;**48**(1):87-92

[47] Veses A et al. Production of upgraded bio-oils by biomass catalytic pyrolysis in an auger reactor using low cost materials. Fuel. 2015;**141**:17-22

[48] Bridgwater A. Principles and practice of biomass fast pyrolysis processes for liquids. Journal of Analytical and Applied Pyrolysis. 1999;**51**(1):3-22

[49] Bridgwater AV. Review of fast pyrolysis of biomass and product upgrading. Biomass and Bioenergy. 2012;**38**:68-94

[50] Lam SS et al. Progress in waste oil to sustainable energy, with emphasis on pyrolysis techniques. Renewable and Sustainable Energy Reviews. 2016;**53**:741-753

[51] Center, B.E. Biomassenergycentre.org.uk. Retrieved on, 2012. pp. 02-28

[52] Unknown. Residual Waste Infrastructure Review; 2017. p. 22

[53] Climate Change Act 2008. Chapter 27 of 2008. United Kingdom. 2016. Available from: http://www.legislation.gov.uk/ukpga/2008/27/pdfs/ukpga_20080027_en.pdf

[54] Milne TA, Abatzoglou N, Evans RJ. Biomass Gasifier "Tars": Their Nature, Formation, and Conversion. Vol. 570. Golden, CO: National Renewable Energy Laboratory; 1998

[55] Maniatis K, Beenackers A. Tar protocols. IEA bioenergy gasification task. Biomass and Bioenergy. 2000;**18**(1):1-4

[56] Suzuki T, Ohme H, Watanabe Y. Alkali metal catalyzed carbon dioxide gasification of carbon. Energy & Fuels. 1992;**6**(4):343-351

[57] Devi L, Ptasinski KJ, Janssen FJ. Pretreated olivine as tar removal catalyst for biomass gasifiers: Investigation using naphthalene as model biomass tar. Fuel Processing Technology. 2005;**86**(6):707-730

[58] Brage C, Yu Q, Sjöström K. Characteristics of evolution of tar from wood pyrolysis in a fixed-bed reactor. Fuel. 1996;**75**(2):213-219

[59] Al-Rahbi AS, Onwudili JA, Williams PT. Thermal decomposition and gasification of biomass pyrolysis gases using a hot bed of waste derived pyrolysis char. Bioresource Technology. 2016;**204**:71-79

[60] Lu Q, Li W-Z, Zhu X-F. Overview of fuel properties of biomass fast pyrolysis oils. Energy Conversion and Management. 2009;**50**(5):1376-1383

[61] Gassner M, Maréchal F. Thermodynamic comparison of the FICFB and Viking gasification concepts. Energy. 2009;**34**(10):1744-1753

[62] Henriksen U et al. The design, construction and operation of a 75kW two-stage gasifier. Energy. 2006;**31**(10):1542-1553

[63] Neumann J et al. Production and characterization of a new quality pyrolysis oil, char and syngas from digestate – Introducing the thermo-catalytic reforming process. Journal of Analytical and Applied Pyrolysis. 2015;**113**:137-142

[64] Brandt P, Larsen E, Henriksen U. High tar reduction in a two-stage gasifier. Energy & Fuels. 2000;**14**(4):816-819

[65] Wu C, Williams PT. Hydrogen production by steam gasification of polypropylene with various nickel catalysts. Applied Catalysis B: Environmental. 2009;**87**(3):152-161

[66] Milhé M et al. Autothermal and allothermal pyrolysis in a continuous fixed bed reactor. Journal of Analytical and Applied Pyrolysis. 2013;**103**:102-111

[67] Tumiatti V. A flexible three-stage thermochemical conversion process; 2015

[68] Malkow T. Novel and innovative pyrolysis and gasification technologies for energy efficient and environmentally sound MSW disposal. Waste Management. 2004;**24**(1):53-79

[69] Dahlman. Gasification. 2017 [29/09/2017]

[70] Kraft S, Kirnbauer F, Hofbauer H. CPFD simulations of an industrial-sized dual fluidized bed steam gasification system of biomass with 8MW fuel input. Applied Energy. 2017; **190**:408-420

[71] Energos. [29/09/2017]. Available from: http://www.energos.com/energos-technology/the-process/

[72] Energia, L. Kymijarvi II Power Plant. [cited 2017]. Available from: https://www.lahtigasification.com/

[73] Evans G. Targeting New and Cleaner Uses of Wastes and Biomass Using Gasification. Loughborough: Energy Technologies Institute; 2017

[74] Fabry F et al. Waste gasification by thermal plasma: A review. Waste and Biomass Valorization. 2013;**4**(3):421-439

[75] Yoon SJ et al. Hydrogen and syngas production from glycerol through microwave plasma gasification. International Journal of Hydrogen Energy. 2013;**38**(34):14559-14567

[76] Power, A.P. Our Technology; 2017 [29/09/2017]

[77] Rokni M. Thermodynamic analyses of municipal solid waste gasification plant integrated with solid oxide fuel cell and Stirling hybrid system. International Journal of Hydrogen Energy. 2015;**40**(24):7855-7869

[78] Nagel FP, Schildhauer TJ, Biollaz SM. Biomass-integrated gasification fuel cell systems–part 1: Definition of systems and technical analysis. International Journal of Hydrogen Energy. 2009;**34**(16):6809-6825

[79] Lobachyov KV, Richter HJ. An advanced integrated biomass gasification and molten fuel cell power system. Energy Conversion and Management. 1998;**39**(16):1931-1943

[80] Panopoulos K et al. High temperature solid oxide fuel cell integrated with novel allothermal biomass gasification: Part I: Modelling and feasibility study. Journal of Power Sources. 2006;**159**(1):570-585

[81] Badwal SP, Ciacchi FT. Ceramic membrane technologies for oxygen separation. Advanced Materials. 2001;**13**(12–13):993-996

[82] Liu S, Gavalas GR. Oxygen selective ceramic hollow fiber membranes. Journal of Membrane Science. 2005;**246**(1):103-108

[83] Hashim S, Mohamed A, Bhatia S. Oxygen separation from air using ceramic-based membrane technology for sustainable fuel production and power generation. Renewable and Sustainable Energy Reviews. 2011;**15**(2):1284-1293

[84] Breeze P. Power Generation Technologies. Newnes; 2014

Chapter 7

Gasification of Municipal Solid Waste

Yong-Chil Seo, Md Tanvir Alam and
Won-Seok Yang

Additional information is available at the end of the chapter

http://dx.doi.org/10.5772/intechopen.73685

Abstract

Gasification of municipal solid waste (MSW) is an attractive alternative fuel production process for the treatment of solid waste as it has several potential benefits over traditional combustion of MSW. Syngas produced from the gasification of MSW can be utilized as a gas fuel being combusted in a conventional burner or in a gas engine to utilize the heat or produce electricity. Also, it can be used as a building block for producing valuable products such as chemicals and other forms of fuel energy. This book chapter covers the properties of MSW, gasification mechanism, chemistry, operating conditions, gasification technologies, processes, recovery system, and most importantly by reviewing the environmental impacts of MSW gasification. As one of recent advanced technologies, a case study of pilot-scale MSW gasification is introduced, which could be one of the most efficient pathways to utilize the technology to produce electricity with a newly developed gasification process by reducing tar and pollutant emission.

Keywords: municipal solid waste, gasification, waste to energy

1. Introduction

Gasification of municipal solid waste (MSW) is an attractive alternative fuel production process for the treatment of solid waste as it has several potential benefits over traditional combustion of MSW. The so-called "syngas" obtained by gasification has several applications. It can be utilized as a gas fuel being combusted in a conventional burner or in a gas engine and then connected to a boiler and a steam turbine or gas turbine to utilize the heat or produce electricity. Also, it can be used as a building block for producing valuable products such as chemicals and other forms of fuel energy, as discussed in the following literature

review [1]. This reference, called *Waste to Energy Conversion Technology*, introduces the theory behind gasification and pyrolysis and outlines the key differences between them and conventional combustion in Chapter 9, "Gasification and pyrolysis of MSW." This chapter also provides an overview of the types of products that can be made from gasification, and the applications of these products are presented. In addition, different types of gasification processes are addressed. However, it fails to discuss the properties of MSW, also gasification principles were not described in details into the chapter. Most importantly, environmental impacts of MSW gasification were not addressed in the chapter. Therefore, an up-to-date book chapter on gasification of MSW was much needed. To address this issue, an initiative was taken to write a book chapter on MSW gasification by assessing the present contents of MSW gasification by covering the properties of MSW, gasification mechanism, chemistry, operating conditions, gasification technologies, processes, recovery system, and most importantly by reviewing the environmental impacts of MSW gasification. The properties of MSW are discussed in Section 2. In Section 3, we discuss gasification principles such as the mechanism, chemistry (reactions), and operating parameters (equivalent ratio, temperature, residence time, cold gas efficiency, carbon conversion efficiency, tar content, etc.). Section 4 shows the MSW gasification technologies and processes, including plasma gasification, fixed-bed gasification, fluidized gasification, and worldwide plants of various types. Sections 5 and 6 describe energy recovery systems and environmental impacts of MSW gasification by reviewing available literatures and some case studies in recent practices and developments. Finally, a case study of a pilot-scale MSW gasification is introduced, which could be one of the most efficient pathways to utilize the technology to produce electricity with a newly developed gasification process with reducing tar and pollutant emission in Korea.

2. MSW properties

The design of a process for the management of MSW and the results for the economic evaluation and development of a feasible business plan require an introduction of the properties of MSW. Therefore, these are presented to support those who are performing such design and economic evaluations [2]. **Table 1** shows the density of various components such as some typical properties of the MSW of interest. **Table 1** also illustrates the typical moisture content with range for some specific properties of the MSW of interest. The typical values of elemental analysis and proximate analysis for some material of interest in MSW are also shown in **Table 1**. In the case of elemental analysis values for carbon (C), hydrogen (H), oxygen (O), nitrogen (N), sulfur (S), and ash; and in the case of proximate analysis values for moisture, volatiles, fixed carbon, and ash are shown on a percentage of weight basis [3].

Another important factor for evaluating and designing the process of MSW is calorific value of the appeared materials. **Table 2** shows some standard calorific value of various materials generally found in MSW [5].

Typical properties of uncompacted wastes (USA Data)-density						
	Density (kg/m³)					
Food wastes	288					
Paper	81.7					
Plastics	64					
Garden trimmings	104					
Glass	194					
Ferrous metal	320					
Typical moisture contents of wastes						
	Moisture content (wt.%)					
Residential	**Range**	**Typical**				
Food wastes (mixed)	50–80	70				
Paper	4–10	6				
Plastics	1–4	2				
Yard wastes	30–80	60				
Glass	1–4	2				
Typical proximate analysis values (% by weight)						
Type of waste	**Moisture**	**Volatiles**	**Carbon**	**Ash**		
Mixed food	70.0	21.4	3.6	5.0		
Mixed paper	10.2	75.9	8.4	5.4		
Mixed plastics	0.2	95.8	2.0	2.0		
Yard wastes	60.0	30.0	9.5	0.5		
Glass	2.0	—	—	96–99		
Residential MSW	21.0	52.0	7.0	20.0		
Typical elemental analysis (% by weight):						
Type of waste	**C**	**H**	**O**	**N**	**S**	**Ash**
Mixed food	73.0	11.5	14.8	0.4	0.1	0.2
Mixed paper	43.3	5.8	44.3	0.3	0.2	6.0
Mixed plastics	60.0	7.2	22.8	—	—	10.0
Yard wastes	46.0	6.0	38.0	3.4	0.3	6.3
Refuse derived fuel	44.7	6.2	38.4	0.7	<0.1	9.9

Table 1. Physical properties of MSW [4].

Material	Calorific value (BTU/lb)	Ash content (wt.%)	Moisture content (wt.%)
Soft wood	6330	0.1	19
Fiberboard, 90% paper	7600	4.6	7.5
Damp wood	5690	1.2	27.5
Leather trimmings	7670	5.2	10.4
Cotton seed hulls	10,600	2.47	8.9
Sludge material (steel mill)	9150	24.5	1.9
Nitrile rubber	15,240	3.4	
Cardboard, granulated	8592	12.3	6.4
Carbon residue	13,681	8.7	0.0
Wood waste, sawdust	7500	0.8	14
Nut shells	7980	1.75	11.85

Table 2. Calorific values of various materials [4].

3. Basics of gasification

3.1. Mechanism

Combustion, gasification, and pyrolysis are thermal energy conversion processes available for the thermal treatment of solid wastes. **Figure 1** introduces all the potential pathways to convert MSW or biomass into different energy forms using thermal, mechanical, and biological processes. **Figure 2** shows the schematic diagram of syngas production and how to utilize the gas for various purposes such as power generation, creating chemicals by upgrading steps, and further biochemical processing before producing fuels or chemicals. As shown in these figures, different products are obtained from the application of these processes, and different energy and residual material recovery systems can be used in various types of technologies.

Gasification is a thermochemical conversion process of carbonaceous materials into gaseous product at high temperatures with the aid of gasification agent. The gasification agent (another gaseous compound) allows the feedstock to be quickly converted into gas by means of different heterogeneous reactions [6–9]. The gaseous product obtained during this process is called synthetic gas (syngas) or producer gas, and it mainly contains hydrogen, carbon monoxide, carbon dioxide, and methane. Also, a small amount of inert gases, hydrocarbons, tar, and gas pollutants can be found [10]. Based on the effect of gasification agent, gasification can be divided into two categories. If the gasification agent partially oxidizes the feed material it is called direct gasification. During direct gasification, to maintain the temperature of the process, oxidation reaction supplies the required energy. If the gasification process takes place without the aid of gasification agent it is called indirect gasification [7, 11]. Usually steam is used for indirect gasification as it is easily available. Moreover, it increases the hydrogen content in the producer gas [7].

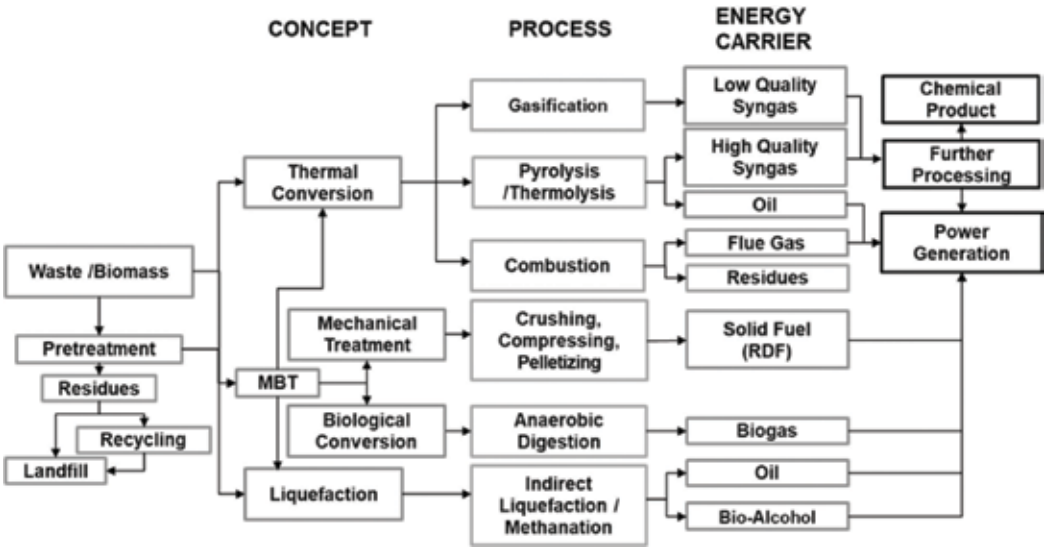

Figure 1. Pathways to convert MSW to different types of energy forms or chemicals through various conversion processes.

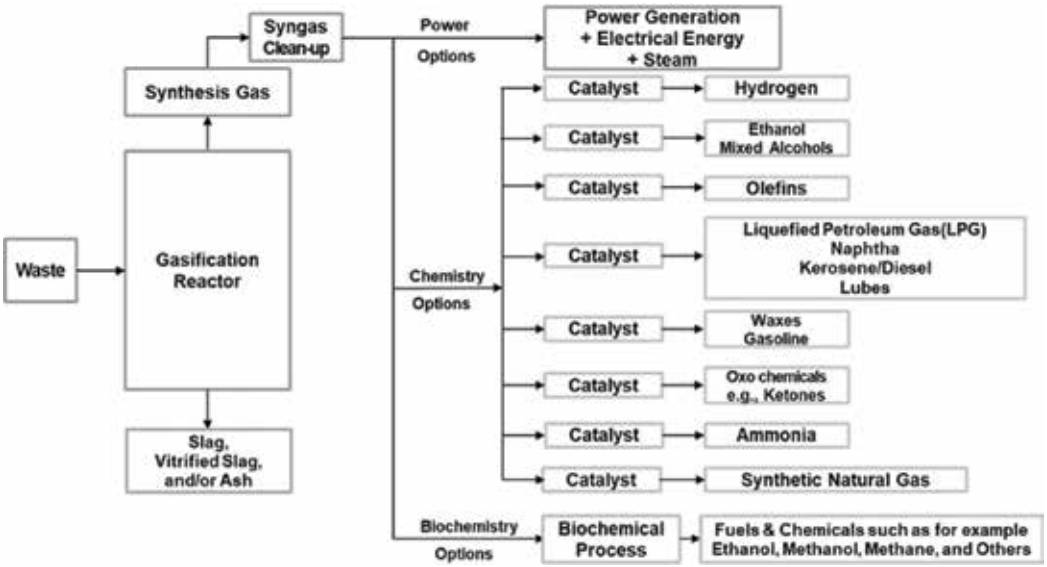

Figure 2. Pathway of waste to energy (gases, fuels, chemicals) by gasification.

As shown in **Figure 3**, two main gasification processes can be classified into direct and indirect gasification processes. Indirect gasification processes are conducted without air or oxygen injection. The heating value of the syngas is significantly affected by the presence of nitrogen. In the absence of nitrogen in indirect gasification process, the volumetric efficiency and higher heating value of producer gas both increases [12, 13]. Also, indirect gasification

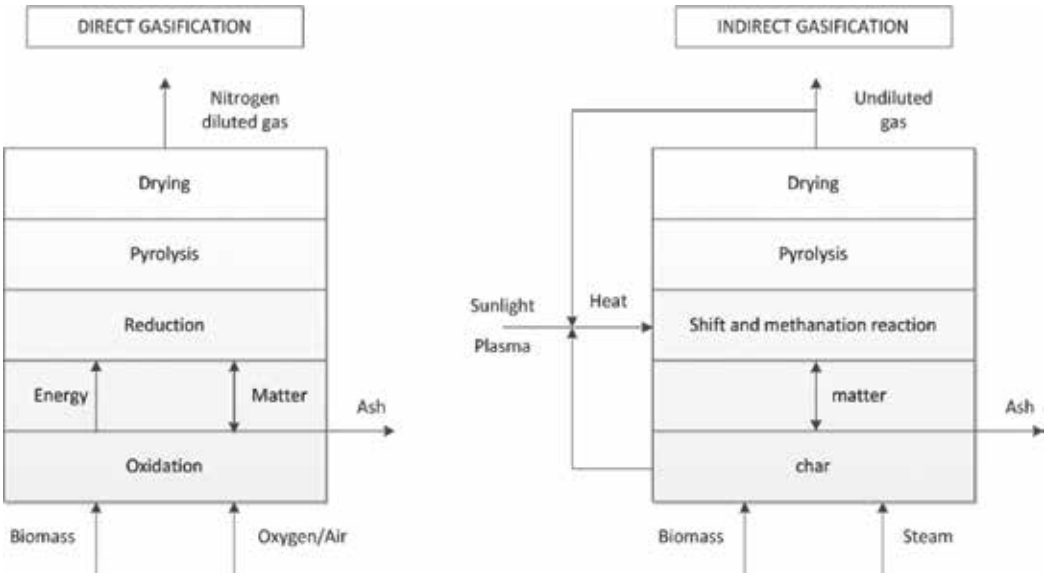

Figure 3. Direct and indirect gasification processes.

process decreases the cost of gas clean up and energy recovery by lowering the gas production rate. However, the process is quite complex and the investment cost is higher [7].

Pure oxygen gasification as direct gasification has same advantages over indirect gasification. However, the cost of producing pure oxygen is expected to account for more than 20% of the total cost of electricity production [14].

Generally, a gasification system is composed of three stages: (1) gasifier for useful producing syngas; (2) the syngas cleaning system for removal of pollutants and harmful compounds; (3) an energy recovery system such as a gas engine. Additionally, sub-systems are included to prevent environmental impacts such as air pollution, solid wastes, and wastewater.

3.2. Chemistry

3.2.1. Process steps

The gasification process of solid waste has endothermic and exothermic reactions, which are successive and repetitive [15, 16]. **Figure 4** describes the main reactants and steps of the gasification process.

• Heating and drying at about 160°C: In this stage, the moisture and steam from the feedstock are removed by the porous solid phase.

• Devolatilization (or pyrolysis or thermal decomposition) at about 700°C: This stage determines the thermal cracking reactions and conversion of heat and mass, including light permanent gases (such as H_2, CO, CO_2, CH_4, H_2O, and NH_3), tar (condensable hydrocarbon vapors), and char (residue emitted after devolatilization). Vapors produced in this stage undergo thermal cracking to gas and char. In the case of MSW, as described in **Figure 4**, high contents

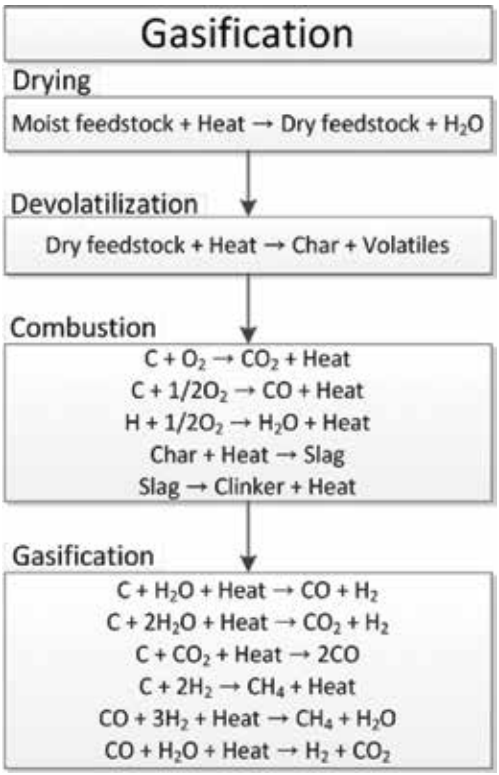

Figure 4. Main reactions and steps of gasification process.

of carbon and hydrogen, which are easily converted to combustible gases in volatiles, are included in the feedstock. The quantities, composition, and characteristics of chemical species released due to devolatilization are dependent on several factors such as original composition and structure of the waste, temperature, pressure, and heating rate imposed by particular reactor types. In devolatilization, various gas compositions are produced, and these gases are generated by the hydrogen and carbon in the waste [16, 17].

• Many chemical reactions occur in a reducing environment that is in remarkably lower oxidation (25–50%) than stoichiometric oxidation. Following **Table 3**, in an auto-thermal gasification process, the partial oxidation of combustible gas, vapors, and char are controlled by the amount of air, oxygen, or oxygen-enriched air. Also, this heat is necessary for the thermal cracking of tar hydrocarbons and char gasification by steam, and carbon dioxide maintains the operation temperature of the gasifier. Following the enthalpy of reactions 1, 2, and 3 in **Table 3**, in auto-thermal gasification processes, about 28% of the carbon heating value is invested in CO production, and the remaining 72% of the carbon heating value is conserved in the gas. The heating value of gas is generally between 75 and 88% of the original fuel because it also contains some hydrogen. If this value were 50% or lower, gasification using coal, biomass, and waste would probably never have become such an interesting process [18]. On the other hand, in an allo-thermal gasification process, the heat is supplied by external sources that are using heated bed materials, burning chars or gases, and utilizing plasma touch. The specific

Oxidation reactions			
1	$C + ½O_2 \rightarrow CO$	−111 MJ/kmol	Carbon partial oxidation
2	$CO + ½O_2 \rightarrow CO_2$	−283 MJ/kmol	Carbon monoxide oxidation
3	$C + O_2 \rightarrow CO_2$	−394 MJ/kmol	Carbon oxidation
4	$H_2 + ½O_2 \rightarrow H_2O$	−242 MJ/kmol	Hydrogen oxidation
5	$C_nH_m + {}^{n}/_{2}O_2 \rightarrow nCO + {}^{m}/_{2}H_2$	Exothermic	C_nH_m partial oxidation
Gasification reactions involving steam			
6	$C + H_2O \rightarrow CO + H_2$	+131 MJ/kmol	Waster-gas reaction
7	$CO + H_2O \rightarrow CO_2 + H_2$	−41 MJ/kmol	Water-gas shift reaction
8	$CH_4 + H_2O \rightarrow CO + 3H_2$	+206 MJ/kmol	Steam methane reforming
9	$C_nH_m + nH_2O \rightarrow nCO + (n + {}^{m}/_{2})H_2$	Endothermic	Steam reforming
Gasification reactions involving hydrogen			
10	$C + 2H_2 \rightarrow CH_4$	−75 MJ/kmol	Hydrogasification
11	$CO + 3H_2 \rightarrow CH_4 + H_2O$	−227 MJ/kmol	Methanation
Gasification reactions involving carbon dioxide			
12	$C + CO_2 \rightarrow 2CO$	+172 MJ/kmol	Boudard reaction
13	$C_nH_m + nCO_2 \rightarrow 2nCO + {}^{m}/_{2}H_2$	Endothermic	Dry reforming
Decomposition reactions of tars and hydrocarbons[a]			
14	$pC_xH_y \rightarrow qC_nO_m + rH_2$	Endothermic	Dehydrogenation
15	$C_nH_m \rightarrow nC + {}^{m}/_{2}H_2$	Endothermic	Carbonization

[a]Note that C_xH_y represents tars and, in general, the heavier fuel fragments produced by thermal cracking, and C_nH_m represents hydrocarbons with a smaller number of carbon atoms and/or a larger degree of unsaturation than CxHy.

Table 3. Main reactions in the heterogeneous and homogeneous phases during the solid waste gasification process.

gasification reactions are those taking place between the devolatilized solid waste (char) and gases excluding oxygen.

3.2.2. Gasification reactions

The gasification reactions have various reactions, but **Table 3** shows just three independent gasification reactions: the water-gas reaction, the Boudard reaction, and hydrogasification. In the gasifier, where there is no more carbon in the feedstock, only two reactions are produced: the water-gas shift reaction, which is the combination of the water-gas and Boudard reactions, and methanation, which is the combination of the water-gas and hydrogasification reactions. These reactions are a simple framework related to reactants and products of H, N, O, S, etc. in the feedstock [16]. Also, CO is produced instead of CO_2, H_2 instead of H_2O, and for other elements, H_2S instead of SO_2, and NH_3 or HCN instead of NO. Moreover, the formation of

dioxin strongly declines because of the oxidation reactions of the dioxin synthesis mechanism [19–21]. All gasification reactions except oxidation reactions create equilibrium. In fact, the final gas composition is determined by reaction rates and catalytic effects, rather than by the chemical equilibrium after an infinite period of time [22–24].

3.3. Operating and performance parameter

3.3.1. Equivalent ratio

Equivalent ratio (ER) is defined as the ratio of the actual amount of oxidant to stoichiometric oxidant for complete combustion. This parameter is the most important operating parameter in gasification process because it affects syngas composition, tar content, gas yield, and its chemical energy. The pyrolysis process is operated at close to ER zero, and the combustion process is operated at more than ER one for complete combustion. In **Figure 5**, the conversion of char in the gasification process at ER 0.25 to 0.35 appears to maximize even though these gasifiers and those that are used in large-scale commercial plants (following **Table 4**), namely, moving grate gasifiers [25] and fluidized bed gasifiers [26] operated with wet fuels, are operated at about ER 0.5. With a lower ER, the gas yield from char is reduced, and the tar in syngas increases while with a higher ER, the oxidation reactions in the gasification process improve

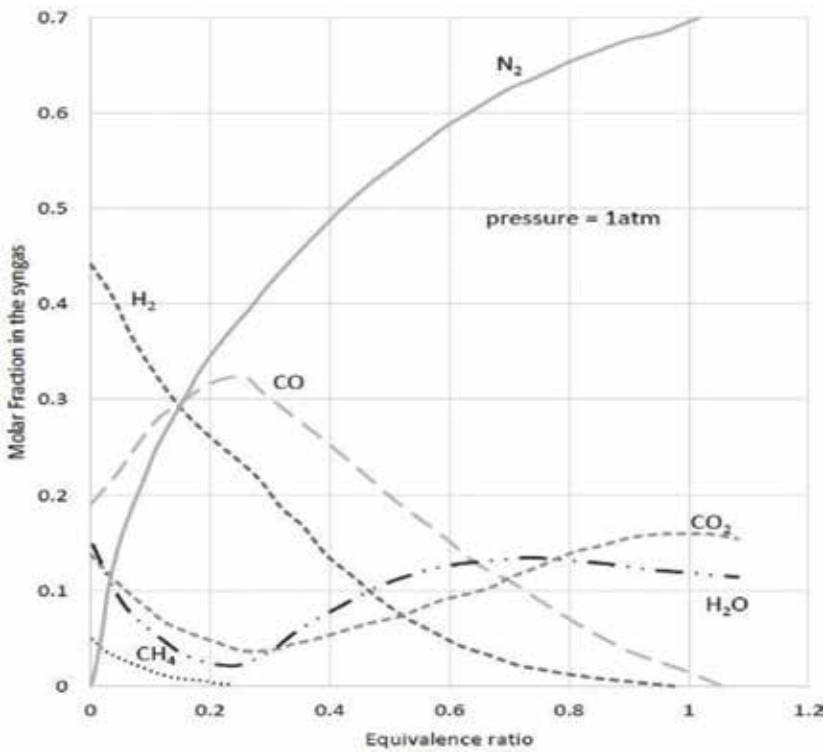

Figure 5. Syngas composition at chemical equilibrium as a function of ER for the gasification of wood at 1 atm [29].

Operating parameters	
Equivalence ratio, –	0.25–0.35[a]
Waste low heating value, MJ/kg_{waste}	7–18
Process performance parameters	
Carbon conversion efficiency, %	90–99
Cold gas efficiency, %	50–80
Syngas low heating value, MJ/m^3_N	4–7[b]
Net electrical efficiency, %	15–24
Specific net energy, kWh/t_{waste}	400–700

[a]This value is typically equal to 0.50 in moving grate gasifiers.
[b]This value can increase to about 10 MJ/m^3_N in oxygen gasification processes.

Table 4. Typical ranges of operating and process performance parameters in air/ oxygen-enriched gasification of MSW [30].

and the heating value of syngas is reduced; this could cause incomplete combustion in a flare or syngas combustor, which is generally downstream from the gasifier [24, 27, 28].

3.3.2. Reactor temperature

Temperature profile along the reactor is another important characteristic of both allo-thermal (indirectly heated) gasifier and auto-thermal (directly heated) gasifier. The reactor temperature profile is considered as a state variable of the process, and it is affected by different parameters, such as ER, residence time, waste chemical energy, composition, inlet temperature of the gasifying medium, quality of the reactor insulation, etc. Moreover, the state of the bottom ash and the content of tar in the syngas can also be determined by the temperature profile of the reactor [24, 27].

3.3.3. Residence time

Generally, the residence time of gases and waste in the reactor is determined by the reactor type and design. Also, a fixed reactor type and design have limitations in terms of varied residence times: for example, the superficial gas velocity is varied in a fluidized bed and the velocity of grate elements is varied in the moving grate reactor [25, 31, 32].

3.3.4. Cold gas efficiency

Cold gas efficiency (CGE) is defined as the ratio between the heating value of the syngas produced and the heating value of the feedstock fed into the gasification process, that is, $CGE = (Q_{syngas}\ LHV_{syngas})/(Q_{waste}\ LHV_{waste})$. This is called "cold gas efficiency" since it does not take into account the gas sensible heat but only its potential chemical energy, that is, those related to the combustion heats of obtained syngas and fed waste.

3.3.5. Carbon conversion efficiency

Carbon conversion efficiency (CCE) is defined as how many carbons in the waste gets converted to carbon in the syngas such as CO, CO_2, CH_4, C_2H_6, C_3H_8, etc., that is, CCE = $(Q_{syngas}\ C_{carbon\_syngas})/(Q_{waste}\ C_{carbon\_waste})$; C_{carbon_waste} is the carbon fraction in the waste and C_{carbon_syngas} is the carbon fraction in the syngas with no dust or tar. This parameter shows the amount of the unconverted portion, which has to be treated by other processes or sent for disposal (such as in a landfill) as well as the chemical efficiency of the process.

3.3.6. Tar content

In the case of tar, if possible, the content and composition of the tar is analyzed. These tars, which are condensable heavy hydrocarbon materials, including oxygen-containing hydrocarbons and polyaromatic hydrocarbons, are an important parameter because they cause problems in all gasification processes, including the end of process [33]. The occurrence of excessive slag in boilers can cause blockages, corrosion, and also reduces the overall efficiency of the process. The amount of other metals and refractory surfaces increase and can also causes of ruin reforming catalysts, sulfur removal system, ceramic filters, etc. Also, if these tars are removed by a wet system using water, the tar is just moved from the gas to the water, and this water changes to wastewater with a loss of chemical energy of the gas and the generation of hazardous wastewater. Therefore, the content and composition of tar in syngas is an important factor in determining the energy conversion device that can be utilized, taking into consideration the cleaning system, and the technical and economic performance. These cleaning systems can be applied inside the reactor (primary measures) and/or downstream from it (secondary measures) [24, 27].

3.3.7. Other parameters

Other parameters are the heating value of the syngas (kJ/Nm^3), the flow rate of the specific syngas (Nm^3/kg waste), and the specific energy production, that is, the chemical energy of the syngas produced by the mass unit of waste fed to the gasification process (kJ/kg waste).

4. MSW gasification technologies

4.1. Overview of existing gasification technologies

Gasification can be considered as a process between pyrolysis and combustion in that it involves the partial oxidation of the material. This means that oxygen is injected but not enough to cause complete combustion. The temperatures are typically above 650–800°C. Although this process is mostly exothermic, it may be required to initialize and maintain the gasification process.

Raw MSW is not appropriate for the gasification process, so generally a separation is needed, including mechanical homogenization and the separation of glass, metals, and inert materials

before the treatment of residual waste. The main gasification syngas product contains carbon monoxide, hydrogen, and methane. Generally, the gas generated from gasification has a net calorific value (NCV) of 4–10 MJ/Nm^3. The calorific value of syngas from pyrolysis and gasification is lower than that of natural gas, which has a NCV of approximately 38 MJ/Nm^3 [34]. As mentioned earlier, an important issue in using syngas in alternative thermal treatment facilities is a problem related to tar. The tar can cause blockages and other operational problems, and it is associated with plant failures and inefficiencies in many pilot and commercial-scale facilities. The application of the high-temperature secondary processing phase can be used to "crack" the tars and purify the syngas before applying the energy recovery systems. This process is referred to as "gas clean up" or "polishing," and can enable higher efficiency energy recovery than can be applied through other waste heat treatment processes.

However, most commercial gasification facilities processing MSW-derived feedstock (SRF) utilize a secondary combustion chamber to burn the syngas and recover energy from a steam circuit, seeking to recover more energy. Other major products produced by gasification include solid residues of noncombustible materials (ash) that contain a small amount of carbon. Also, high-temperature plasma gasification technologies are being used at various stages of gasification process. Using this plasma technologies, tar-free clean syngas can be produced, as well as the ash can be fused into glassy or vitreous residue [35]. To recover high energy efficiency from hydrogen fuel cells attached with gasifiers and engines, different pathways are available. Waste to energy (WTE) processes are a combination of partial oxidation and volatilization of the contained organic compounds. The first gasification furnace is the combustion of the volatile gases and the steam generation of the second furnace. Japan is the world's largest producer of MSW gasification. However, the main technology used in Japan is the grate combustion of "as-received MSW," but there are more than 100 thermal treatment plants based on relatively novel processes such as direct smelting, the Ebara fluidization process, and melting process such as Thermoselect gasification [36, 37]. These processes produce glass fibers that are less hazardous than conventional WTE combustion processes and can be used advantageously in external landfills.

Transportation of as-collected MSW from one location to another is not permitted in Japan. Consequently, the grate combustion facilities are relatively small. In addition, the MSW is transported to a central WTE facility that serves as a SRF in local SRF facilities and in several communities. Additionally, all WTE facilities are used to vitrify their ash after combustion by means of electric furnaces, thermal plasma melting, or other means.

The following sections introduce several technologies available in worldwide.

4.2. Energos grate combustion and gasification process

The Energos grate combustion and gasification technology is currently operating one plant in Germany, six plants in Norway, and one in the UK. This technology was developed in Norway in the 1990s to provide an economical alternative to reducing greenhouse gas emissions such as those from gasoline. All operating plants handle MSW and commercial waste or industrial waste. The current operating plants range in capacity from 10,000 to 78,000 tons per year.

Energos plant is using a mixture of post recycled MSW and industrial waste residue from material recovery facility as a feedstock. However, the amount of industrial waste is smaller compared with MSW. Before applying thermal treatment, using a low rpm and high torque shredder the feedstocks are shredded. After that ferrous metals are removed magnetically. Partial oxidation of the feedstock at sub-stoichiometric oxygen conditions (air to fuel ratio, k = 0.5–0.8), and combustion of the fixed carbon on the bed results in total organic carbon (TOC) of less than 3% from WTE ash in the first chamber of Energos process. In the adjoining chamber, the syngas generated during gasification are combusted completely, and the heat generated during combustion of the syngas is sent to the heat recovery system. During this process, temperatures climb up to 900 and 1000°C in the gasification chamber and oxidation chamber, respectively. All dioxins formed in this process are destroyed in combustion chamber and rapidly cooled in the heat recovery steam generator, which minimizes dioxin formation. NO_x formation was also kept comparatively low in this process (around 25% of the EU limit). A schematic diagram of the gasifier and the combustion chamber is shown in **Figure 6** [38].

After passing through the heat recovery steam generator, the flue gas enters into a dry flue gas cleaning system, which consists of a bag filter, an activated carbon injection, dry scrubbing with lime, and a filter dust silo. The lime absorbs the acidic compounds in the flue gas and the heavy metal molecules and activated carbon adsorb the dioxins. Emissions are continuously monitored. **Table 5** shows typical emission measurements at the Averoy Energos plant in Norway. These measurements were performed by TUV NORD Umweltschtz for the Norwegian Environmental Agency and reported an 11% oxygen concentration.

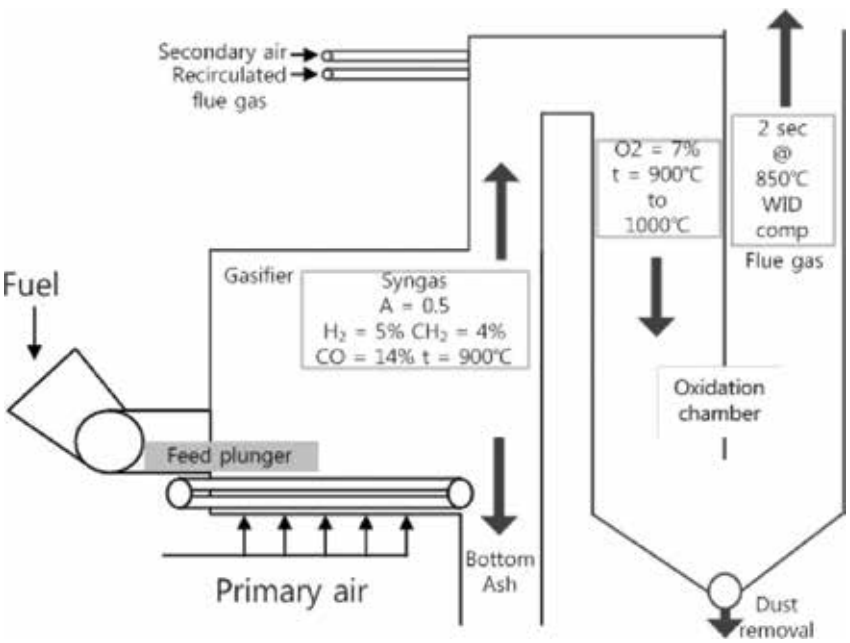

Figure 6. Flowchart of a model Energos plant.

Parameter	EU limits (mg/Nm^3)	Energos, Averoy
Particulate matter	10	0.24
Hg	0.05	0.00327
Cd + Ti	0.05	0.00002
Metals	0.5	0.00256
CO	50	2
HF	1	0.02
HCl	10	3.6
TOC	10	0.2
NO_x	200	42
NO_3	10	0.3
SO_2	50	19.8
Dioxins (ng/Nm^3 TEQ)	0.1	0.001

Table 5. Emissions from Energos plant (at 11% oxygen) [38].

The reported availability of the Energos plants is approximately 90% (8000 hours per year, similar to a typical combustion WTE plant).

4.3. Ebara fluidized bed process

The Ebara process (**Figure 7**) consists of partial combustion of shredded MSW in a fluidized bed reactor. The second furnace is where the gas produced in the fluidized bed reactor is combusted to generate temperatures up to 1350°C [36]. There is no oxygen enrichment. The largest application of the Ebara process is a three-line in Spain, with 900 tons per day.

In the reactor, the ash overflow from the fluidized bed is separated using a vibrating screen whose screen size is 3–4 mm. Metal particles are unable to pass it, however, sand particles can. The bottom ash produced during this process cannot be used for pavement construction purpose; it must be melted with slag, which is the final solid product used in construction areas. The Spanish plant using the Ebara process produces approximately 560 kWh per SRF ton.

4.4. Thermoselect gasification and melting process

Many plants, ranging from grate combustion to the Japan steel[Fe] engineering (JFE) direct smelting process and the seven JFE Thermoselect plants with a total capacity of 2000 tons per day, are operated by the JFE steel company of Japan [37]. In order to enter the gas turbines or engines, which generate electricity, the syngas produced in Thermoselect furnaces requires purification. Compared to conventional grate combustion, the amount of processed gas per ton of MSW is low. However, cleaning the reducing gas is more complicated than cleaning combustion processed gas. The Thermoselect process also produces industrial oxygen used for partial oxidation and gasification of MSW using part of the generated electricity. There is the possibility that the syngas product can be burned in a gas turbine to generate electricity

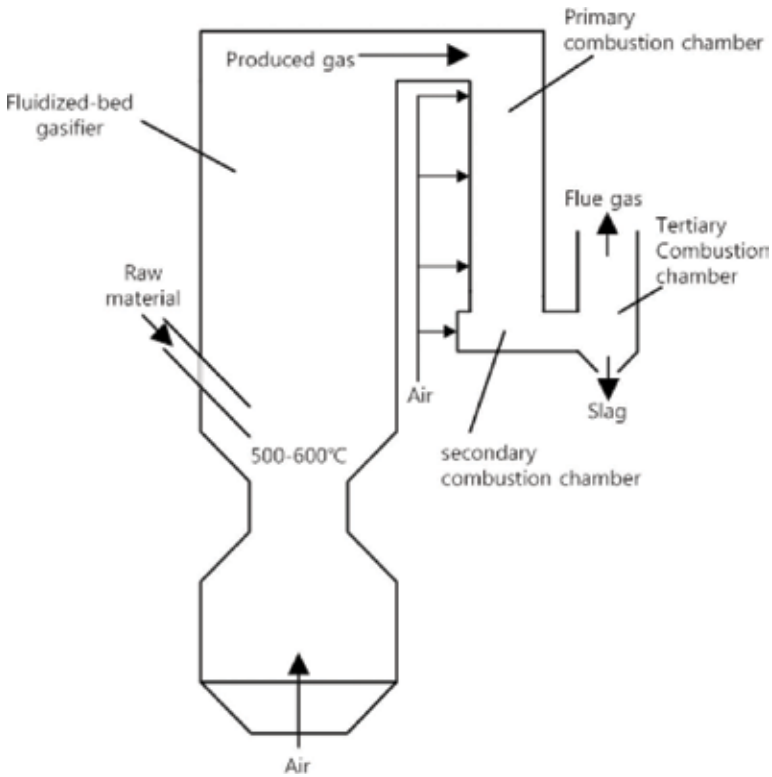

Figure 7. Ebara fluid bed gasification process.

at much higher heat efficiency than is possible in the conventional WTE plant using a steam turbine.

4.5. Plasma-assisted gasification WTE process

Recent research has shown there is a growing interest in plasma-assisted gasification of MSW. A plasma torch is a device that transforms electricity into heat by passing the current through a gas stream. Increased interest is focused on plasma-assisted gasification applied to the treatment of MSW. It might be a new way to increase WTE around the world. The Earth Engineering Center of Columbia University under the supervision of Professor Nickolas J. Themelis conducted a study of this technology. Plasma technology has long been used for the destruction of harmful materials such as asbestos, toxic wastes from hospitals, and surface coatings. Although plasma technology has been used for these purposes, its application in MSW has not yet been studied. Plasma-assisted gasification in the WTE process combines the partial oxidation of hydrocarbon in the MSW and the use of plasma. Using a relatively high voltage, high-current electricity is passed between two electrodes to create an electric arc. The inert gas is passed through the arc under pressure and is transferred to a closed container of waste, reaching a maximum temperature of 13,900°C in the arc heat. The temperature from the torch can reach 2760–4427°C. At this temperature, most types of waste are decomposed into gaseous elements, and complex molecules are separated into atoms. This arc decomposes

the waste with a device known as a plasma converter to a molecular gas and solid waste (slag). This process is for net generators of electricity depending on the composition of the input waste, and the amount of waste sent to landfills is reduced.

For MSW processing, a plasma torch can be used to gasify the solids, dissolve volatile gases, and electrify ash into slag and metal globules. A syngas product can be used to produce synthetic fuels or electricity in a gas engine or turbine generator. As mentioned in the previously discussed earth engineering center (EEC) study, the technology is a Westinghouse plasma owned by Alter NRG, Plasco Energy Group, Europlasma, and the In EnTec Process [39]. A major benefit to grate combustion is a dramatic reduction in process gas flow (up to 75%). In addition, the reducing atmosphere in the gasification process should reduce NOx emissions more than in the grate combustion process. However, this study showed that the cost of capital per ton of capacity is the same as that of grate combustion. Since electricity is used for high-temperature gas, energy production per ton of raw material is not expected to be higher than that of combustion. In a system such as the Alter NRG gasification process, it is expected to generate approximately 0.6 MWh/ton of MSW. Finally, the availability of these plants is different from the combustion process WTE plants (8000 hours annually).

5. Energy recovery systems

5.1. Steam cycle

In terms of energy recovery, steam is the simplest option. No gas pre-treatment is required because the burner burns the tar [40] so the tar cannot harm the boiler. The gasification-steam cycle plant shows approximately 23% of the maximum net electrical efficiency [41]. It is similar to the efficiency of the typical solid waste incinerator. Due to HCl that may be present in flue gas, corrosion of the tube occurs at temperatures above 450°C. It is a problem of traditional waste incineration and the gasification-steam cycle boiler. These limits reduce the vapor temperature for steam turbines and therefore lower the overall electrical efficiency of the plant [42]. However, through gas pre-treatment or integration with a thermoelectric power plant, this restriction can be overcome in a gasification-steam plant [14]. Prior to putting the gas into the burner, the HCl can be removed by pre-treating the gas. Therefore, in modern boiler combinations, the firing of the clean gas enables a steam temperature of 520°C and electric efficiency is improved by 6% [42].

Co-firing refers to integration with conventional power plants; it utilizes the high-efficiency steam cycle of the thermoelectric power plant to improve performance. In general, a co-firing system is performed in two possible configurations [41, 43]. For co-firing, one configuration is using a gas burner in a separate boiler that is only in the water evaporation phase, and the other is to use a gas burner in the same boiler as the primary fuel.

5.2. Engine

Gasoline and kerosene are usually used as fuel in the spark ignition engine. However it can also be operated using gas. For that, we need to install a spark ignition system, as well as we need

lower the compression ratio of diesel engine [40, 44]. Due to the lower heating value (LHV), untransformed engines show superior performance than engines converted to gas. Nevertheless, a correctly modified modern engine can allow more than 25% of the net power output [44]. The engine has the advantage of being stronger than gas turbines, and it is more resistant to pollutants [10]. Nevertheless, when the gas is compressed into a turbocharger, the same condition as in the gas turbine will occur [10, 44]. The main disadvantage of the gas engine is that the efficiency achieved using the combined cycle mode is low, and the economies of scale are poor [10].

5.3. Gas turbine

The power plants that build on advanced combined cycle gas turbines could enable an efficiency rate of approximately 60% [45]. Due to the consumption for gas pre-treatment, the effective net electrical output is below 40% [46, 47]. In fact, gas turbines allow extremely low levels of pollutants, mainly tar, alkali metals, sulfur, and chlorine compounds [10]. The chemical recovery cycle is an exciting and novel option. In this case, pre-treatment of the gas, which usually uses the tar or the catalytic cracking process of the steam reforming process, needs the energy content in the turbine exhaust gas [14, 48]. Typical gas turbines should be suitable for low LHV, for easy start-up, the burner must allow dual fuel operation, and a longer combustion chamber is needed to improve CO emissions control [49, 50].

6. Environmental impacts

6.1. Air pollution

Environmental performance in a MSW thermal treatment technology is important for the feasibility of the whole process. Recent research [51, 52] has shown that the operation of thermochemical and biochemical solid waste conversion processes poses little risk to human health or the environment compared to other commercial processes. Biochemical processes and those of anaerobic digestion have gained a wider acceptance in recent years [53]. The strong opposition to gasification processes from environmental organizations is the result of misunderstanding that these processes are only minor variations of incineration. As mentioned above, an important difference is that gasification is an intermediate process for producing fuel gas that can be used for various purposes. The most common process these days is the use of syngas for the production of on-site electricity and/or thermal energy, but there is a potential for chemical and fuel production due to the gasification of MSW, and this is possibly a true goal in the near future. The type of indirect combustion process discussed above is already emphasized in several important aspects that make it different from conventional incineration. Moreover, it makes air pollution control easier and cheaper compared with the conventional combustion processes. Although exhaust gas cleanup of thermochemical conversion processes is easier compared with incineration process, still a proper process and emission control system design is required to satisfy the safety and health requirements. The producer gas obtained from gasification process includes various air pollutants that must be controlled before being discharged to outside. These include hydrocarbons, carbon monoxide,

tars, nitrogen and sulfur oxides, dioxins and furans, and particle materials. Various strategies can be adopted to control exhaust gas in the gasification process, and, as mentioned above, they are rigorously dependent on the adopted plant configurations, especially regarding the particular requirements of the specific energy conversion device. In any case, an obvious advantage in that air pollution control is possible not only at the reactor outlet but also at the exhaust gas outlet through a variety of approaches. Furthermore, the low levels of oxygen (ER ranges between 0.25 and 0.50) in the gasification process strongly inhibit the formation of dioxins and furans even though hydrogen chloride in the syngas must be managed if combustion for heat or power follows gasification. Recently collected emissions data indicate that gasification technology meets emission standards [52]. A synthesis of these data is shown in **Table 6**, together with the limits of the European Community and Japanese standards.

6.2. Solid residue treatment

It is important to report some considerations regarding the management of solid residues such as bottom ash and air pollution control (APC) residues to define the environmental performance of gasification-based WTE facilities. Depending on the type of waste and on the specific gasification technology, the type and composition of these residues differ greatly [22, 51, 53, 58]. **Table 7** reports some leaching tests carried out on the slags of two large-scale, high-temperature gasification units. All values are significantly lower than the emission standard, and the low impurity content of the slag and its good homogeneity make it possible to sell for a variety of uses such as aggregates in asphalt pavement mixtures. The metals recovered from the melting section can be also recovered during the chemical treatment of fly ash and then landfilled.

Company, plant location	**Nippon Steel Kazusa, Japan**	**Thermoselect Nagasaki, Japan**	**Ebara TwinRec Kawaguchi, Japan**	**Mitsui R21 Toyohashi, Japan**	**Energos Averoy, Norway**	**Plasco En. Ottawa, Canada**	**EC/ Japanese Standard**	**Korea Standard**
Waste capacity	200 tons/day	300 tons/day	420 tons/day	400 tons/day	400 tons/day	100 tons/day		
Power production	2.3 MWe	8 MWe	5.5 MWe	8.7 MWe	10.2 MWe	—		
Emission, mg/m^3_N(at 11% O_2)								
Particulate	10.1	< 3.4	< 1	< 0.71	0.24	9.1	10/11	14.2
HCl	< 8.9	8.3	< 2	39.9	3.61	2.2	10/90	16.7
NOx	22.3	—	29	59.1	42	107	200/229	106.8
SOx	< 15.6	—	< 2.9	18.5	19.8	19	50/161	85.5
Hg	—	—	< 0.005	—	0.0026	0.0001	0.03/–	0.09
Dioxins/ furans, n-TEQ/m^3_N	0.032	0.018	0.000051	0.0032	0.0008	0.006	0.1/0.1	—

Table 6. Some certified emissions from waste gasification plants [30, 48, 52, 54–57].

Element (mg/L)	Regulation[a]	Measured[b]	Measured[c]	Korea standard[d]
Cd	< 0.01	< 0.001	< 0.001	< 0.03
Pb	< 0.01	< 0.005	< 0.005	< 0.1
Cr^{6+}	< 0.05	< 0.02	< 0.02	< 0.05
As	< 0.01	< 0.001	< 0.005	< 0.05
T-Hg	< 0.0005	< 0.0005	< 0.0005	< 0.001
Se	< 0.01	< 0.001	< 0.002	—
F	< 0.8	—	< 0.08	—
B	< 1.0	—	< 0.01	—

[a]Quality standard for soil (in agreement with Notification No. 46, Japanese Ministry of the Environment and the JIS-Japanese Industrial Standard K0058).

[b]Tests carried out in a Nippon Steel high-temperature shaft furnace with a capacity of 252 tons/day of MSW, bottom ash from other MSW incinerators, and residues from recycling centers [59].

[c]Tests carried out in a JFE high-temperature shaft furnace plant having a capacity of 314 tons/day of RDF from MSW [32].

[d]Recycling standard of waste (No. 5 of enforcement regulations in waste management law in Korea).

Table 7. Results of some slag leaching tests in two high-temperature MSW gasifiers [30].

Therefore, it can be deduced that the amount of solid residues generated in the MSW gasification process is reduced and the throughput at the landfill can be reduced.

6.3. Wastewater treatment

In the gasification process, wastewater produced by the gas cooler and the wet scrubber containing many soluble and insoluble pollutants such as acetic acid, sulfur, phenol, and other organic compounds [10]. The insoluble matter in this wastewater is mainly composed of tar. The amount of wastewater generated by removing tar through the scrubber is about 0.5 kg/Nm^3 of treated gas [60], and requires expensive treatment. There are also some minor problems such as high salt content and low pH associated with the wastewater generated in gasification process. However, these can be controlled easily by doing chemical precipitation and neutralization [61].

"In the gasification plant Thermie Energy Farm, one of the three IGCC projects selected for funding by the European Union, the sequence of treatment for tar-rich wastewater is: (a) precipitation of sulfur by iron sulfate addition; (b) recovery of sulfur and dust by filtering; (c) disposal of filter cake; (d) stripping off gases and the major part of the hydrocarbons dissolved in the water; (e) partial evaporation of water and usage of condensate as scrubber make-up; and (f) discharge of evaporator blowdown to conventional bio-treatment" [60, 62].

The recovered salts are treated through sanitary landfills because their potential for contamination is very low. The hydrocarbons and the recovered gas are decomposed and recovered as energy in the combustor [60, 62]. Recent trends due to difficulties in treatment and disposal are developing tar-free gasification technologies, but this is nonetheless possible only for wastes with low contaminant content [10].

7. Case study on the recent gasification technology for MSW to electricity

7.1. Introduction of MSW gasification pilot plant in Korea

The MSW gasification pilot plant in Korea, performed by the R&D project of the Korea Ministry of the Environment, was developed by the research team of the authors. This pilot gasification plant, installed in Y city of Korea, is composed of a fluff SRF manufacturing system and a fixed-bed gasification pilot system whose capacity is 8 tons/day. **Figure 8** shows the whole flow diagram of this plant. Generally, the economic efficiency of fluff SRF is higher than the economic efficiency of pelletized SRF due to skipping the pelletizing process. However, the fluff SRF created an issue for transporting and storage work because of its low density. In this process, manufactured fluff SRF was directly fed into the gasification process to overcome the transporting and storage problem.

7.2. Configuration of gasification system

This plant is divided into four sections, which are the feeding system, the gasifier, the cleaning system, and the gas engine generator. The feeding system is a two-step process of a conveyor for SRF transfer to the hopper and an input screw for continuous feeding into the gasifier. The gasifier is operated using a fixed-bed and downdraft concept. However, the gasifier can be converted to updraft depending on the operation conditions. The cleaning

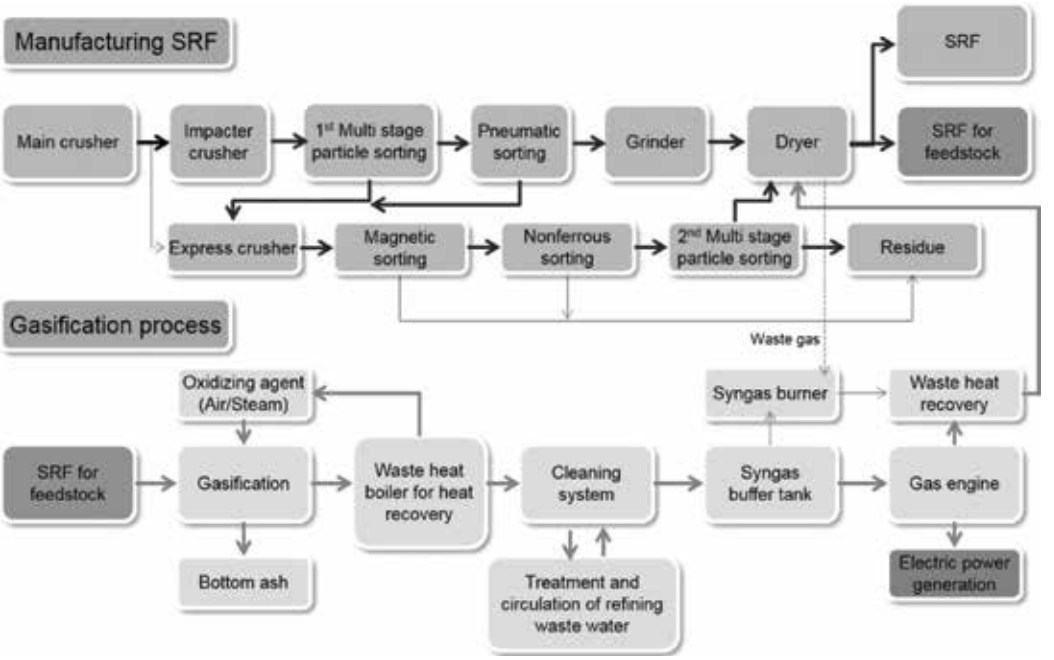

Figure 8. Overall diagram of pilot-scale SRF manufacturing system and gasification process.

system is composed of a cyclone, various scrubbers based on a wet system, and wet electric precipitation. All of the cleaning units except for the water used in the cyclone, which is recirculated by the water tank, and tar removal system for cleaning the produced gas. Lastly, the gas engine generator is installed for electricity production. For stable operation, this gas engine generator uses a low-speed gas engine that has a high-tolerance to tar and pollutants. The maximum power production of the gas engine is 300 kW but for stable power production, this is used at 100–250 kW.

7.3. Performance of gasification system

For the stable operation of this gasification process, the process was controlled by various factors that affected operation. These conditions were selected so that the charging rate of the gasifier was 50–60% and ER was 0.17–0.36. **Figure 9** shows a representative performance test result of the gasification system. The gasification process was operated for 63 hours and shows stable operation trends for the production of syngas and electricity. Among these results, the heat-keeping and check on facility were included for continuous operation. Average syngas composition in the producer gas was about 20% and the heating value of the syngas was

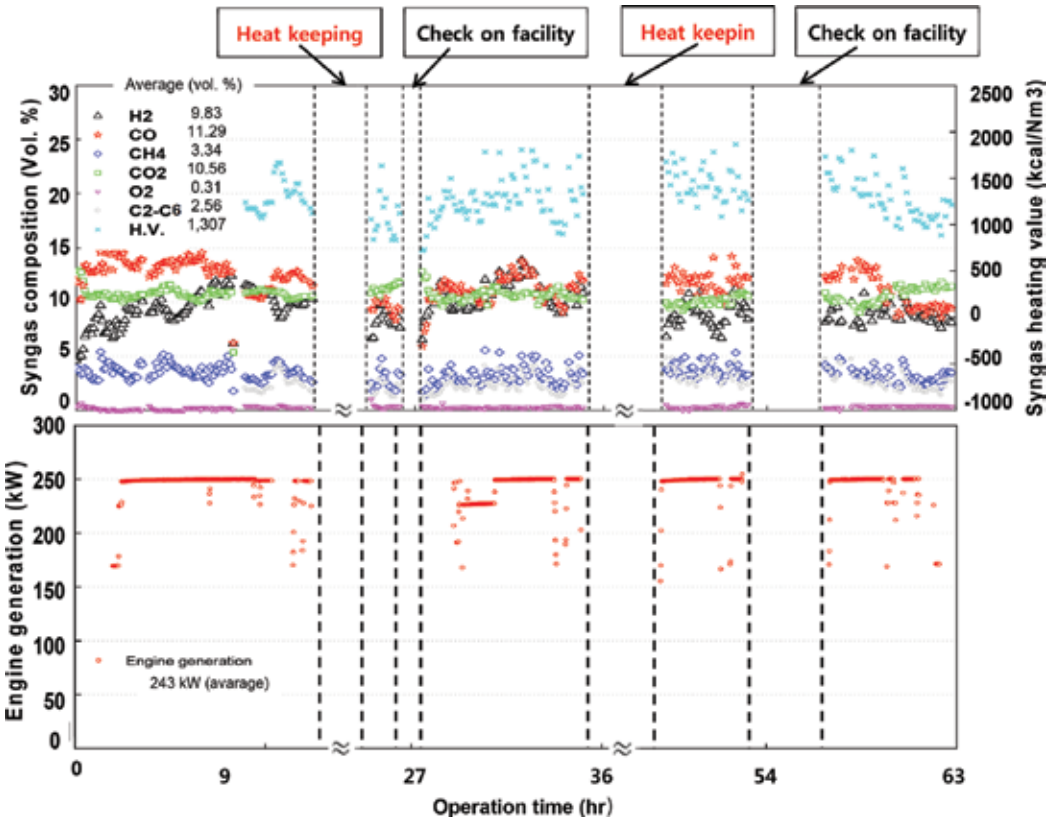

Figure 9. Reprehensive performance test results of the gasification system.

1307 kcal/Nm^3. Also, the average power generation by the gas engine was 243 kW. Following this result, the MSW gasification shows sufficient possibility and stable operation trends. Particularly in the case of power production, and even though this plant was on a pilot scale, the gas engine generator shows good performance using syngas from a gasification system.

8. Conclusion

In this book chapter, the properties of MSW have been discussed, which will help us to select the proper technology. Also, discussion on the gasification processes and technologies has been done to strengthen the basics on gasification. In addition, a review on energy recovery system has been made to guide and select the most viable option for energy recovery. The environmental benefits of MSW gasification has been also reported in this book chapter. Finally, a case study on pilot-scale MSW gasification to generate electricity has been presented to discuss one of the most efficient pathways to utilize it. Based on the above discussion, it is quite clear that gasification process offers considerable energy recovery and reduces the amount of potential pollutants emission. Moreover, gasification may be proposed as a viable alternative solution for waste treatment by converting waste into a gaseous energy form, syngas for further potential uses to energy production or chemicals. MSW gasification has some drawbacks due to the heterogeneous characteristics of MSW. However, a possible solution to address this issue could be production of solid refuse fuel (SRF) with homogeneous and controlled characteristics. The strongest point for gasifying MSW is its environmental performance. Several MSW gasification emission test results indicate that the gasification of MSW is able to meet the emission standard and can effectively reduce the environmental impacts, which can be considered as a sound response to the increasingly restrictive regulations applied around the world.

Acknowledgements

This work was supported by a grant from the Human Resources Development program (No. 20164030201250) of the Korea Institute of Energy Technology Evaluation and Planning (KETEP) funded by the Korean Ministry of Trade, Industry and Energy and the Korea Ministry of Environment (MOE) as a "Waste-to-Energy Technology Development Project".

Author details

Yong-Chil Seo*, Md Tanvir Alam and Won-Seok Yang

*Address all correspondence to: seoyc@yonsei.ac.kr

Yonsei University, Wonju-si, Republic of Korea

References

[1] Klinghoffer NB, Castaldi MJ. 9–Gasification and Pyrolysis of Municipal Solid Waste (MSW). Woodhead Publishing: Amsterdam; 2013. 146-176p

[2] Beck RW. Iowa Statewide Waste Characterization Study [Internet]. 2006. Available from: https://www.google.co.kr/url?sa=t&rct=j&q=&esrc=s&source=web&cd=2&cad=rja&uact=8&ved=0ahUKEwiirOrqvsnWAhWCwLwKHbfEDcAQFggqMAE&url=https%3A%2F%2Fwww.iowadnr.gov%2FPortals%2Fidnr%2Fuploads%2Fwaste%2Fwastechar05.pdf&usg=AFQjCNElkoeszk1PNFtmyIHGbJXHlGG91g [Accessed: 2017-09-29]

[3] Tchobanoglous G, Theisen H, Vigil SA. Integrated Solid Waste Management: Engineering Principles and Management Issues. New York: McGraw-Hill; 1993. 978 p

[4] Young GC. Municipal Solid Waste to Energy Conversion Processes: Economic, Technical, and Renewable Comparisons. Vol. 2010. New Jersey: John Wiley & Sons; 2010. pp. 135-154p

[5] Heat Treatment International. Michigan: Dutton; 2008

[6] Di Blasi C. Dynamic behaviour of stratified downdraft gasifier. Chemical Engineering Science. 2000, 2000;**55**:2931-2944. DOI: 10.1016/S0009-2509(99)00562-X

[7] Hauserman WB et al. Biomass gasifiers for fuel cells systems. La Chimica e l'industria. 1997;**79**:199-206. DOI: 10.1016/S1359-4311(97)00116-6

[8] Barducci G, Franchino R. The RDF gasifier of florentine area (Greve in chianti). I Simposio Italo-Brasiliano di Ingegneria Sanitaria-Ambientale SIBESA. 1992;**2**:80-94

[9] Baykara SZ, Bilgen E. A Feasibility Study on Solar Gasification of Albertan Coal. Alternative Energy Sources IV. Vol. 6. New York: Ann Arbor Science; 1981

[10] Bridgwater AV. Catalysis in thermal biomass conversion. Applied Catalysis A: General. 1994;**116**:5-47. DOI: 10.1016/0926-860X(94)80278-5

[11] Staniewski E. Gasification-the benefits of thermo chemical conversion over combustion. Hazardous Materials Management. October/November

[12] De Feo G et al. Solid wastes gasification. SIDISA international symposium on sanitary and. Environmental Engineering. 2000

[13] Paisley MA, Anson D. Biomass gasification for gas turbine-based power generation. Transactions-American Society of Mechanical Engineers Journal of Engineering for Gas Turbines And Power. 1998;**120**:284-288

[14] Della Rocca C. I Processi e le Tecnologie di Gassificazione Delle Biomasse e dei Rifiuti Solidi [Civil Engineering Degree Thesis]. Universitadegli Studi di Salerno; 2001

[15] Knoef H. Practical Aspects of Biomass Gasification. Handbook of Biomass Gasification. Enschede; 2005. pp. 13-37p

[16] de Souza-Santos ML. Solid Fuels Combustion and Gasification. Marcel Dekker; 2004

[17] Kawaguchi K, Miyakoshi K, Momonoi K. Studies on the pyrolysis behavior of gasification and melting systems for municipal solid waste. Journal of Material Cycles and Waste Management. 2002;**4**(**2**):102-110. DOI: 10.1007/s10163-001-0066-7

[18] Higman C, van der Burgt M. Thermodynamics of Gasification. Burlington: Gulf Professional Publishing; 2003. pp. 10-11p

[19] Stieglitz L, Vogg H. On formation conditions of PCDD/PCDF in fly ash from municipal waste incinerators. Chemosphere. 1987;**16**:1917-1922. DOI: 10.1016/0045-6535(87)90188-3

[20] McKay G. Dioxin characterisation, formation and minimisation during municipal solid waste (MSW) incineration. Chemical Engineering Journal. 2002;**86**:343-368. DOI: 10.1016/S1385-8947(01)00228-5

[21] Vehlow J. Dioxins in waste combustion–conclusions from 20 years of research. In: Bioenergy Australia; 12-13 December 2005. Melbourne; 2005

[22] Heermann C, Schwager FJ, Whiting KJ. Pyrolysis & Gasification of waste. In: A Worldwide Technology & Business Review. 2nd ed. Bengaluru: Juniper Consultancy Services Ltd; 2001

[23] C-Tech Innovation. Thermal methods of municipal waste treatment [Internet]. 2003. Available from: http://www.resol.com.br/textos/Thermowaste.pdf [Accessed: 2017-09-29]

[24] Arena U, Zaccariello L, Mastellone ML. Fluidized bed gasification of waste-derived fuels. Waste Management. 2010;**30**:1212-1219. DOI: 10.1016/j.wasman.2010.01.038

[25] Grimshaw AJ, Lago A. Small Scale Energos Gasification Technology. 3rd Int. Symposium on Energy from Biomass and Waste; 8-11 November 2010; Venice; 2010

[26] Hankalin V, Helanti V, Isaksson J. High efficiency power production by gasification. In: Thirteenth International Waste Management and Landfill Symposium; 3-7 October 2011; S. Margherita di Pula. Cagliari; 2011

[27] Devi L, Ptasinski KJ, Janssen FJ. A review of the primary measures for tar elimination in biomass gasification processes. Biomass and Bioenergy. 2003;**24**:125-140. DOI: 10.1016/S0961-9534(02)00102-2

[28] Li XT, Grace JR, Lim CJ, Watkinson AP, Chen HP, Kim JR. Biomass gasification in a circulating fluidized bed. Biomass and Bioenergy. 2004;**26**:171-193. DOI: 10.1016/S0961-9534(03)00084-9

[29] Kaupp A, Goss JR. State-of-the-Art Report for Small Scale (to 50 Kw) Gas Producer-Engine Systems. Davis: Dept. of Agricultural Engineering; California Univ.; 1981

[30] Arena U. Process and technological aspects of municipal solid waste gasification. A review. Waste Management. 2012;**32**:625-639. DOI: 10.1016/j.wasman.2011.09.025

[31] Arena U, Mastellone ML. Pyrolysis and gasification of solids wastes in fluidized bed reactors. In Industrial Fluidization Conference (IFSA-2005); November 2005; South Africa; 2005. pp. 15-17

[32] Suzuki A, Nagayama S. (2011, October). High efficiency WtE power plant using high-temperature gasifying and direct melting furnace. In: Thirteenth International Waste Management and Landfill Symposium; 3-7 October 2011; S. Margherita di Pula: Cagliari; 2011

[33] Milne TA, Evans RJ, Abatzaglou N. Biomass Gasifier "Tars": Their Nature, Formation, and Conversion (No. NREL/TP-570-25357; ON: DE00003726). National Renewable Energy Laboratory, Golden, CO (US); 1998

[34] Fichtner Consulting Engineers Ltd. The viability of advanced thermal treatment of MSW in the UK. ETSET: London; 2004

[35] Friends of the Earth. Pyrolysis, Gasification and Plasma [Internet]. 2009. Available from: https://www.foe.co.uk/sites/default/files/downloads/gasification_pyrolysis.pdf [Accessed: 2017-09-29]

[36] Suzuki S. The Ebara Advanced Fluidization Process for Energy Recovery and Ash Vitrification. In: 15th North American Waste to Energy Conference; 21-23 May 2007; Miami; 2007

[37] Delaware Solid Waste Management Technical Working Group. Interstate waste technologies thermoselect technology an overview [Internet]. 2006. Avaiable from: http://www.seas.columbia.edu/earth/wtert/sofos/IWTThermoselect.pdf [Accessed: 2017-09-29]

[38] Energos. Energos Gasification technology. In: Energy Recovery from Residual MSW and Commercial Waste [Internet]. 2009. Available from: http://www.all-energy.co.uk/__novadocuments/86899?v=635675612646970000 [Accessed: 2017-09-29]

[39] Ducharme C, Themelis N. Analysis of thermal plasma-assisted waste to energy processes. In: Proceedings of the 18th Annual North American Waste-to-Energy Conference; May 2010; Orland; 2010. pp. 11-13

[40] Quaak P, Knoef H, Stassen HE. Energy from Biomass: A Review of Combustion and Gasification Technologies. Washington D.C: World Bank Publications; 1999. p. 23-24

[41] Consonni S. Tecniche correnti ed avanzate per il recupero dell'energia. La termodistruzione del rifiuto urbano: recupero energetico ed emissioni. Ed. HYPER srl; 2000

[42] Rensfelt E, Everard D. Update on Project ARBRE: Wood Gasification Plant Utilising Short Rotation Coppice and Forestry Residues. Power Production from Biomass III; 1998

[43] Nieminen J, Palonen J, Kivelä M. Irculating fluidized bed Gasifier for biomass Thermie demonstration project in Lahti, Finland. VGB Powertech-English Edition. 1999;**79**:69-74

[44] FAO. Wood gas as engine fuel. FAO Forestry paper 72 [Internet]. 1993. Available from: http://www.fao.org/3/a-t0512e.pdf [Accessed: 2017-09-29]

[45] Najjar YS. Comparison of performance of the integrated gas and steam cycle (IGSC) with the combined cycle (CC). Applied Thermal Engineering. 1999;**19**:75-87. DOI: 10.1016/S1359-4311(98)00008-8

[46] De Lange HJ, Barbucci P. The Realisation of a Biomass-Fuelled IGCC Plant in Italy. In: 1st World Conference on Biomass for Energy and Industry; 5-9 June 2000; Sevilla: Earthscan; 2001. p. 1486

[47] Faaij A, Van Ree R, Waldheim L, Olsson E, Oudhuis A, Van Wijk A, et al. Gasification of biomass wastes and residues for electricity production. Biomass and Bioenergy. 1997;**12**:387-407. DOI: 10.1016/S0961-9534(97)00010-X

[48] Heppenstall T. Advanced gas turbine cycles for power generation: A critical review. Applied Thermal Engineering. 1998;**18**:837-846. DOI: 10.1016/S1359-4311(97)00116-6

[49] Zanforlin S. Use of crude-bio oil in gas turbine: description of experimental activities and tests results. In: Bio-Crude Oil Technology; 24-25 January 1995; Livorno: ENEL;1995

[50] Becker B, Schetter B. Gas turbines above 150 MW for integrated coal gasification combined cycles (IGCC). Journal of Engineering for Gas Turbines and Power. 1992;**114**:660-664. DOI: 10.1115/1.2906639

[51] E4tech. Review of Technologies for Gasification of Biomass and Wastes [Internet]. 2009. Available from: http://www.e4tech.com/wp-content/uploads/2016/01/gasification2009.pdf [Accessed: 2017-09-29]

[52] University of California Riverside, Riverside. Evaluation of emissions from thermal conversion technologies processing municipal solid waste and biomass [Internet]. 2009. Available from: http://dpw.lacounty.gov/epd/socalconversion/pdfs/UCR_Emissions_Report_62109.pdf [Accessed: 2017-09-29]

[53] Defra. Advanced biological treatment of municipal solid waste [Internet]. 2013. Available from: https://www.gov.uk/government/uploads/system/uploads/attachment_data/file/221037/pb13887-advanced-biological-treatment-waste.pdf [Accessed: 2017-09-29]

[54] Kenou-Kennan, Kankyou-Kumiai. Emissions Data of JFE Nagasaki Plant. In: Compliance Source Test report; April–June 2006

[55] Juniper Consultancy Services Ltd. Independent Waste Technology Report. In: Nippon Steel Gasification Process Review; 2007

[56] TUV Nord Umweltschutz. Report on emission measurements on Averøy Waste Incinerator; 2007

[57] Zeus GGD. Global Gasification Database [Internet]. 2011. Available from: https://stratasadvisors.com/Services/Energy-Perspectives [Accessed: 2017-09-29]

[58] Stantec. Waste to Energy. In: A technical review of municipal solid waste thermal treatment practices [Internet]. 2010. Available from: http://www2.gov.bc.ca/assets/gov/environment/waste-management/garbage/bcmoewteemmissionsrevmar2011.pdf [Accessed: 2017-09-29]

[59] Tanigaki N, Manako K, Osada M. Co-gasification of municipal solid waste and material recovery in a large-scale gasification and melting system. Waste Management. 2012;**32**:667-675. DOI: 10.1016/j.wasman.2011.10.019

[60] Barducci P, Neri G, Trebbi G. The Energy Farm Project. World gas conference; 1997; Copenhagen; 1997

[61] Cernuschi S. Processi e tecnologie per il controllo delle emissioni atmosferiche da impianti di termodistruzione di rifiuti. Fiftieth Environmental Sanitary Engineering Refresh Course, CIPA ed; Politecnico di Milano; 2000

[62] Barducci P, Neri G. An IGCC plant in Italy for power generation from biomass. In Bioelettrica Internal Report; 1997

Chapter 8

Analysis on High Temperature Gasification for Conversion of RDF into Bio-Methanol

Annarita Salladini, Emanuela Agostini,
Alessia Borgogna, Luca Spadacini,
Maria Cristina Annesini and Gaetano Iaquaniello

Additional information is available at the end of the chapter

http://dx.doi.org/10.5772/intechopen.74218

Abstract

Municipal solid waste (MSW) is one of the residue materials considered as a potential source for biofuel production in the EU Renewable Energy Directive (RED), which establishes that a minimum of 10% biofuels for transport shall be used in every Member State by 2020, thus promoting advanced biofuel from waste. A high-temperature gasification technology transforms MSW into a syngas rich in hydrogen and carbon monoxide and free of tar, char and harmful compounds like dioxins appearing as a promising root for methanol production. The overall process including MSW high-temperature gasification, syngas purification and conditioning up to methanol synthesis has been modeled with Aspen Plus analyzing the influence of waste composition and operating conditions on syngas composition and methanol yield. The evaluation of CAPEX and OPEX has been carried out to obtain a cost of production (COP) estimation. The greenhouse gas (GHG) emission has also been estimated and compared with the conventional waste incineration process and methanol production. The technology assessment shows interesting results technically and economically, when compared with waste to energy processes: over 50% of incoming carbon is fixed into methanol molecule, and due to the negative cost paid for RDF disposal, the bio-methanol COP provides a reasonable industrial margin.

Keywords: gasification, RDF, waste, biofuel, bio-methanol, aspen plus

1. Introduction

Municipal solid waste (MSW) disposal is a critical issue that all the cities have to tackle. Typical Italian municipal solid waste management includes landfill 26%, recycling 26%, biological

organic treatment 18%, incineration 19%, co-combustion 2%, mechanical and biological treatment 3%, exportation 1% and other 5% [1]. To limit the waste environmental impact, European legislations promote a hierarchy of actions for waste practices and treatments: the 4Rs of sustainability, in the order, reduce, reuse, recycle and recover [2]. According to this approach, landfill must be the last choice for waste disposal, also due to the landfill gas production with a high content of methane, which is considered a greenhouse gas (GHG) that is 25 times more dangerous than CO_2 [3]. Nowadays, mostly incineration is adopted as a waste treatment, since it has the benefit to reduce 80–90% of the waste volume and avoids sanitary issue related to waste putrefaction [4]. However, the incineration treatment leads to environmental issues regarding pollutions, high GHG emission and toxic substance formation. On the other hand, only a partial energy or thermal recovery could be achieved from incineration. Therefore, in a scenario where GHG and dioxin production is the main topic, incineration is not the proper solution for this issue. Under this prospective, a thermal conversion treatment, such as gasification, is suggested as a reliable Waste to Energy (WtE) process to produce steam and energy, avoiding any toxic substances formation. Gasification, widely reviewed by Arena [5], in contrast with incineration, provides the collection of ashes in an inert vitrified form and lowers pollutants emission and simpler combustion control, even though the thermal efficiency is comparable for both processes [6].

A further step is to move from the Waste to Energy process toward Waste to Chemicals (WtC) process, that is a process where syngas is not burnt, but used for chemical production purposes, complying as a good example of circular economy; some waste to chemical processes have been analyzed in engineering and economic terms [7, 8]. The chemical production occurring through gasification includes WtE process benefits of high-temperature destruction on pollutions formation. Moreover, the main advantage of WtC is that, in this process, the high carbon content of MSW, near to 50%, can be partially fixed in the molecule of the product and not all emitted as CO_2; this leads to consider MSW as a renewable carbon feedstock for chemical production. The MSW use as a potential source for biofuel production is promoted in the EU Renewable Energy Directive (2009/28/EC) [9]. In fact, within 2020, each Member State will have to achieve the target of 10% advanced biofuel used for transportation and double-counting biofuel produced from second-generation biomass, like waste. In this way, MSW turns from waste to a valuable resource able to compete with first biomass generation, whose production is becoming more and more controversial due to 'food competition' and intensive land use [10].

Generally, WtE or WtC processes require a first step to convert MSW into a higher calorific material named refused-derived fuel (RDF), whose lower heating value (LHV) is approximately equal to a classic fuel one. The MSW conversion to RDF is achieved with a mechanical-biological treatment that involves a preliminary sorting to separate the organic from the inorganic part, a magnetic separation to remove metals and a final shredding to get from rough to fine RDF, gathered with trommels and hammer mills. To convert RDF into energy or chemicals, a preliminary step involving its transformation into a combustible gas (syngas), rich in hydrogen and carbon monoxide, is required. This step is achieved, thanks to the gasification process itself: a thermochemical conversion of solid fuel by reaction with a controlled amount of oxidant agent. There are several currently gasification unit configurations, mainly obtained by varying the

reactor design or operating conditions such as temperature, pressure and the type of oxidant agent [5]. The choice related on gasification configuration and downstream scheme process strictly depends on the results of economic optimization and the required syngas composition for its forward use. Nowadays, gasification process in a WtC or WtE prospective is provided, for example, by Enerkem, a Canadian company specialized in a waste to fuel business (methanol, ethanol and green chemicals), which obtains syngas through a fluidized bed gasifier with air as the oxidant agent [11]. A different type of gasifier should be used, according to Energy Recovery System Ltd., for ammonia and urea production. The Thermoselect technology, a gasifier that works at high temperature with pure oxygen, is employed in the ammonia synthesis [12].

As mentioned before, the process scheme will be diversified according to the final product to achieve. Particularly, the methanol synthesis involves the following catalytic reactions:

$$CO + 2H_2 \rightleftarrows CH_3OH, \quad \Delta H(298\ K) = -90.7\ kJ/mol$$

$$CO_2 + 3\ H_2 \rightleftarrows CH_3OH + H_2O, \quad \Delta H(298\ K) = -49.8\ kJ/mol$$

$$CO_2 + H_2 \rightleftarrows CO + H_2O, \quad \Delta H(298\ K) = +40.9\ kJ/mol$$

Only two of this group of reactions are linearly independent. Accordingly, to the reaction stoichiometry, the number of hydrogen and carbon monoxide or of hydrogen and carbon dioxide combining to methanol is in the ratio of 2:1 and 3:1, respectively. Therefore, the stoichiometric value of the ratio

$$MM = \frac{H_2 - CO_2}{CO + CO_2}$$

named methanol module (MM) [13] is 2; generally, a value of MM just above it (about 2–2.4) is recommended in the industrial plant. Even the CO and CO_2 contents will influence the product distribution in the methanol synthesis; particularly, a syngas with a low CO_2 and a high CO content is more selective on methanol production than on water, but in the meantime, it will lead to an increased synthesis reactor outlet temperature due to the exothermicity of the methanol synthesis (reactions (1) and (2)); on the other hand, a high reactive feed (with a high CO content) may have a positive effect on the reactor sizing. A compromise, in an industrial plant, has been made by using a carbon ratio, CO_2/(CO + CO2), between 0.2 and 0.5 [14].

According to the reaction scheme reported earlier, a high CO_2 content negatively affects the methanol yield (referred to the hydrogen consumption) by promoting reaction (2); furthermore, this reaction produces water that promotes catalyst deactivation. Therefore, a carbon dioxide content and a water content less than 12 and 0.5%, respectively, are recommended at the inlet synthesis reactor. The main parameters required for methanol synthesis are shown in **Table 1**.

Finally, the gas fed to the synthesis reactor must be free from some contaminants like HCl, H_2S, COS and metals to preserve catalyst from deactivation.

For all these reasons, a deep purification and a conditioning step are needed, before methanol synthesis, in order to reach the mentioned requirements.

	Syngas from the gasifier	Requirements for methanol synthesis
Methanol module	0.41–0.54	2.1
$\frac{CO_2}{CO+CO_2}$	0.19–0.27	0.2–0.5
$\%CO_2$	9–14%	<12%
$\%H_2O$	5–6%	<0.5%

Table 1. Starting parameters describing syngas suitability for methanol synthesis, considering an RDF lower heating value between 14 and 18 MJ/kg, compared with required parameters.

In this work, a customized model developed within Aspen Plus environment is used to analyze the methanol production process from RDF, including RDF gasification, cleaning and purification, conditioning up to methanol synthesis and purification. The overall process has been also analyzed in terms of greenhouse gas emission and economic feasibility.

2. Process and model description

2.1. Process description

The proposed waste-to-methanol process is based on the following main steps, as shown in the block diagram depicted in **Figure 1**: RDF gasification and syngas cleaning, syngas purification, syngas conditioning, methanol synthesis and recovery. Gasification and cleaning steps are strictly connected and constitute a unique block. The core of this section is the gasifier: a high-temperature melting reactor able to convert the combustible fraction of RDF into syngas and in the meantime to transform the glassy and mineral waste components into an inert slag. At this scope, a proper temperature profile is required along the reactor, schematically represented in **Figure 2**. On the bottom, where the inert oxides are melted and then discharged, the temperature is maintained near to 2000°C due to the exothermic combustion reaction of RDF, obtained with the injection of a controlled amount of pure oxygen (gasifying agent) and methane. Pure oxygen is used for gasification step in order to ensure a higher syngas heating value and a lack of inert compound in the synthesis step. A temperature of about 1100°C is also maintained at the top of the reactor, in order to avoid the formation of pollutant compounds, such as dioxins, in the produced syngas [15]. The hot raw syngas, leaving the gasifier, is abruptly cooled in a quench settler, from 1100 to 90°C, freezing the gas composition and

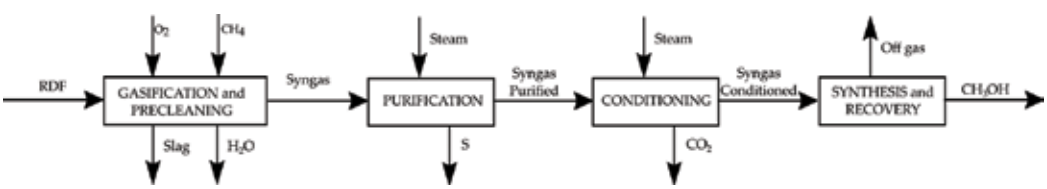

Figure 1. A block scheme of overall process.

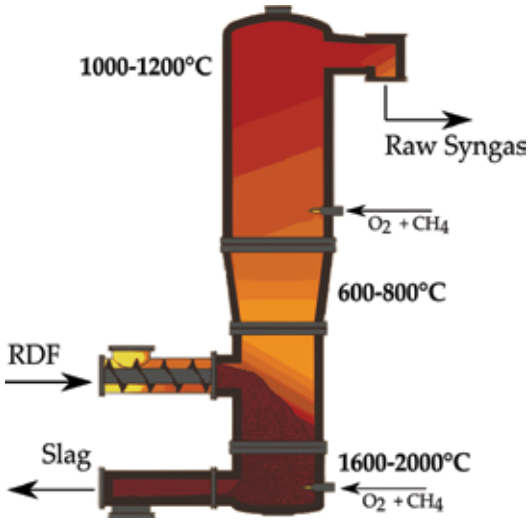

Figure 2. High-temperature melting gasifier.

avoiding dioxins formation. The syngas, properly cooled and coarsely cleaned from coarser combustion residues and powders, is then sent to two scrubbers built in series. The first one is an acid scrubber and the second one is an alkaline scrubber. At the end of this path, the syngas has been cleaned from thinner dust compound and from contaminants, particularly metals (Hg, Zn, Ti), ammonia and sulfur compounds. Before the subsequent steps, a part of the precleaned syngas is stocked in a gasometer in order to smooth the flow rate fluctuations, caused by the nonhomogeneous conditions set in the gasifier. The reactor works at a slightly higher atmospheric pressure in order to avoid any air entrance.

Despite the presence of preliminary cleaning in the gasification unit, the contaminants level, is still too high to use the syngas for methanol synthesis, especially in terms of H_2S and COS contents. For this reason, a deep purification step is required before the conditioning section. Firstly, COS is converted into H_2S, thanks to the hydrolysis reaction [16], carried out with medium pressure steam:

$$COS + H_2O \rightleftarrows H_2S + CO_2$$

Once the COS is converted, the overall H_2S content is removed by its conversion into solid elemental sulfur, by a catalytic oxidation system, named Lo-Cat. This particular system is composed of three sections that include an absorber, an oxidizer, for catalyst regeneration, and a sulfur-handling unit. In particular, when the gas stream enters in contact with the Lo-Cat solution in the absorber, the H_2S is converted into elementary sulfur; the latter leaves the absorber and enters the oxidizer, where the catalyst is regenerated by contact with the oxygen in air and the elemental sulfur is concentrated into slurry sulfur. Finally, the sulfur is washed to recover any entrained catalyst and converted in a solid form. In this way, a H_2S content down to 0.3 ppm is achieved [17]. To ensure ppb levels of H_2S, a polishing step is required by using an absorbent ZnO bed, which reacts with the remaining H_2S.

$$ZnO + H_2S \rightleftarrows ZnS + H_2O$$

All these treatments allow to reduce the sulfur content to ppb level, avoiding any detrimental effects for the downstream catalyst section.

The syngas compositions are mainly dependent on the lower heating value of the available solid waste, as widely discussed in Section 3. In any case, as shown in **Table 1**, the initial MM is too low to be suitable for methanol synthesis, due to the high amount of carbon present in the feedstock. To improve the MM ratio, hydrogen has to be added by using an external source or by converting the CO content present in the syngas via a water gas shift reaction:

$$CO + H_2O \rightleftarrows CO_2 + H_2$$

It is important to recognize that the shift reaction itself does not enhance the MM: in fact, this reaction converts CO in an equimolar mixture of H_2 and CO_2; therefore, a CO_2 removal unit is required to reach the right MM.

In the proposed process scheme, the conditioning is firstly carried out on a high-temperature shift reactor, operating with a steam/dry-syngas ratio equal to 1.5 and a CO_2 removal unit (amine scrubber), to remove the CO_2 produced by the shift reaction. To optimize the process scheme, only a fraction of the syngas from the gasifier is sent to the shift reactor, while the remaining fraction bypasses this step and is directly sent to the methanol synthesis reactor (see **Figure 3**). As a result, a MM value near 1.7 is achieved with this conditioning configuration. A further increase in the hydrogen content, up to a MM equal to 2.1, is achieved by adding a pure hydrogen stream to the stream entering the methanol synthesis reactor.

Methanol synthesis is carried out in an adiabatic catalytic reactor, operating at 55 barg. Due to the low one-pass conversion of syngas to methanol, a recycle loop is necessary. In detail, a portion of the recycle stream is sent to a Pressure Swing Adsorption (PSA) unit, where 85% of H_2 content is recovered in a pure hydrogen stream while CO and CO_2 are removed with the off-gas; the pure hydrogen stream is used to increase the MM to the reactor.

Raw methanol is finally recovered by condensation and purified via distillation up to fuel-grade methanol.

2.2. Process modeling

A steady-state simulation has been developed to describe the overall process of RDF conversion into methanol. The model, using Aspen Plus simulator [18], is divided into two main sections: the first one including the gasification and precleaning units, and the second one including the syngas conditioning and the methanol synthesis.

2.2.1. Gasification and precleaning unit

Waste, like biomass and coal, is a heterogeneous solid material that requires a specific step of characterization to be correctly represented in the simulation environment. RDF has been

introduced as a *non-conventional component* defining its elemental composition, moisture and ash contents and its calorific value. From these parameters, waste physical properties are estimated with HCOALGEN and DCOALIGT property methods. Even if these two methods have been developed to reproduce, respectively, the enthalpy of formation and the density of coal [19], they are able to fit well also the same properties of biomass and waste [20–22]. Meanwhile, IDEAL thermodynamic method has been used for physical properties of conventional components. Although ash is supposed to be inert in the gasification reactions, its content has been deeply characterized. In order to obtain a better definition of the heat amount required for melting process, ash composition has been modeled as a solid mixture composed by SiO_2, CaO, Al_2O_3 and Fe_2O_3, according to available experimental data from Malagrotta facilities. On composition basis, specific heat and enthalpy connected to melting process of the inert mixture have been estimated with the method proposed by Mills [23].

As first approach, already validated with experimental results, the attainment of thermodynamic equilibrium condition in the gasifier has been hypothesized, and a zero-dimensional and kinetic-free model has been developed. Four Aspen reactor blocks have been employed to model the complex gasifier behavior and the temperature profile, as shown in **Figure 3**. The RYIELD is required to simulate the waste decomposition. This block directly converts the non-conventional component (waste) into conventional elements (C, N, H, S, O, Cl, H_2O and ash mixture), without any kinetics or stoichiometric constrain but only defining mass yields according to ultimate analysis of waste. The enthalpy variation between the input and the output streams of this block just represents the heat required for bond-breaking step.

The gasifier itself is modeled as three Gibbs reactors, operating at different temperatures as follows:

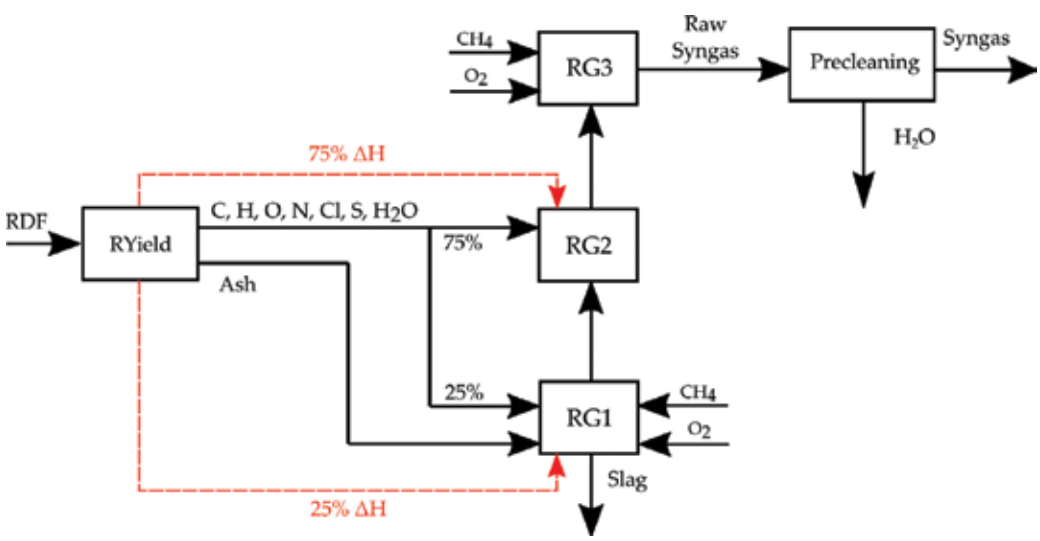

Figure 3. A block scheme reproducing gasification and cleaning unit in Aspen Plus environment.

- Melting zone RG1, where mainly heterogeneous combustion reactions and melting process occur at almost 2000°C; in this region, a fixed methane flow rate (as auxiliary fuel) is added, while the temperature is regulated with the introduction of a controlled amount of oxygen.
- Gasification zone RG2, where the oxygen amount decreases and a reduction atmosphere has been established; thus principally gasification reactions occur.
- Stabilization zone RG3, where a fresh amount of oxygen and methane, with a specified mass ratio, is introduced to raise the temperature near to 1100°C in order to enhance methane and tar decomposition and avoid dioxin formation.

The heat produced in the RYIELD reactor is proportionally added to RG1 and RG2 (as depicted in **Figure 3** with dashed red lines) in order to take into account all contributions for the right formulation of energy balance.

From the third Gibbs reactor, a hot raw syngas stream is obtained, which is suddenly cooled in quench equipment, modeled by a flash block. In a simplified way, also the acid and alkaline scrubbers have been simulated with flash blocks, neglecting the pH and composition variation, but mainly taking into account the decrease in water content in the syngas mixture.

2.2.2. Purification unit

The purification section is modeled using component separator, equilibrium and Gibbs reactor blocks of Aspen Plus simulator. The syngas obtained after the precleaning step is sent to a compression section to raise the pressure till 15 barg. To avoid deactivation of the catalyst used in the methanol synthesis reactor, a purification unit is necessary to decrease sulfur to ppb level (**Figure 4**). This purification unit is composed of the following:

1. Hydrolysis Gibbs reactor R-HYDRO is an adiabatic reactor where the hydrolysis reaction IV occurs, to convert COS to H_2S. Syngas and medium pressure steam are fed to this reactor, with a flow rate ratio depending on the COS content and set by a controller; a control is also placed to set the steam pressure in order to obtain an inlet gas temperature of 180°C, thanks to heat recovery.
2. Sulfur removal LO-CAT, modeled with a component separator, where 99.9% of H_2S is removed, according to the technical specifications provided by the vendor [17].
3. Sulfur-polishing step ZNO-BED, operating at 200°C, where 99.7% of residual H2S and 80% of residual COS are removed.

With all these units, a sulfur ppb level is obtained, so the syngas could be properly conditioned, avoiding any catalyst deactivation.

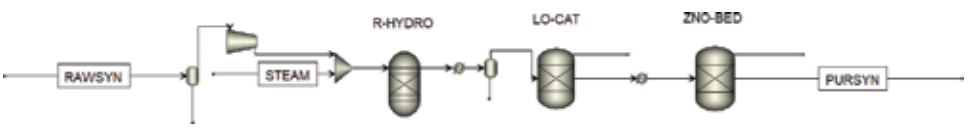

Figure 4. Syngas purification scheme.

2.2.3. Conditioning unit

As previously reported, in order to achieve a methanol module suitable for methanol synthesis, a portion of the purified syngas is sent to a shift reactor and a subsequent unit to remove carbon dioxide (**Figure 5**).

Simulation of this block in Aspen Plus is carried out with a split unit that separate the syngas stream sent to the shift reactor; a controller is used to define the flow rate of this stream, depending on the composition of the syngas, which in turn depends on the fluctuation of RDF composition. Superheated medium pressure steam is added to the split syngas; another controller is placed to define the right amount of steam that has to be added in order to respect a steam/dry-syngas molar ratio equal to 1.5 [24]. The inlet R-HTS temperature is 320°C, in order to activate the Fe/Cr/Al2O_3 catalyst. The R-HTS is an equilibrium reactor where the shift reaction is imposed. A CO_2 removal unit follows R-HTS to separate the carbon dioxide formed by reaction VI and thus increasing the MM value. The CO_2 REMOVAL is a component separator where a 95% of CO_2 removal is set. In detail, this separation consists of an amine (MDEA) unit absorber and a regenerator, with heat process recovery for the regeneration section, providing a pure CO_2 gas stream [25]. After this treatment, the conditioned syngas is reconnected to the split ones, reaching an MM value of 1.7.

2.2.4. Synthesis and recovery unit

The syngas is then compressed to be suitable for methanol synthesis till 56 barg. When methanol synthesis occurs, low methanol conversion is obtained, so to increase this, a recycle loop is required to circulate the unreacted reagents at the reactor entrance. In order to reach an MM equal to 2.1, part of the recycled stream is sent to the Pressure Swing Absorption system, modeled with a component separator where the 85% of H_2 recovery is set, while CO and CO_2 are removed with the off-gas. The conditioned syngas, added with the hydrogen stream, is now suitable for methanol synthesis, and after being preheated at 158°C, it is sent to the adiabatic Gibbs reactor R-MeOH. The referring reactor is a Davy-Johnson-Matthey isothermal reactor, where the reagents are heated in the reactor till 240°C by using the heat of synthesis reaction. The effluent of R-MeOH is cooled till 30°C and separated, using the block flash separator, to recover raw methanol as much as possible. To achieve a methanol fuel grade, the stream is purified using two distillation towers: the first one is just an exhaustion distillation, used to remove as much as possible the off-gas, while the second one is a typical methanol-water distillation column. The off-gas, depicted in **Figure 6**, coming from the purge of the PSA and the distillation column, is collected and sent to a boiler where steam is produced.

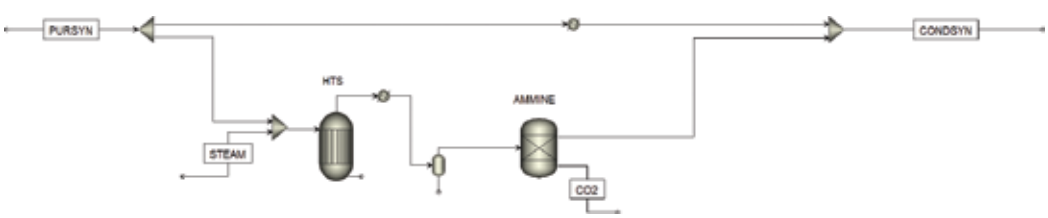

Figure 5. Syngas-conditioning scheme.

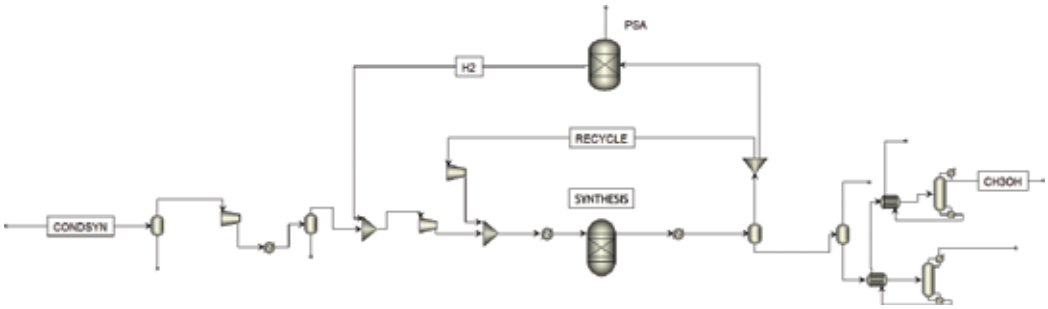

Figure 6. Methanol synthesis and purification scheme.

3. Process analysis

3.1. Influence on syngas composition

As already underlined, syngas composition plays a fundamental role in methanol synthesis step. Therefore, the optimization of the waste-to-methanol process requires analyzing the composition of syngas directly obtained from gasification unit and to investigate how the RDF composition and/or the gasifier-operating conditions can affect the syngas composition. In other words, it is interesting to investigate if a proper selection of RDF or an optimal choice of the gasifier-operating conditions can significantly improve the overall waste-to-methanol process efficiency.

3.1.1. Effect of RDF composition

According to its definition, waste is a solid mixture composed of variable quantities of refused materials belonging to different product classes [26]. However, its variable composition can be restricted to a reasonable limited range, as shown in **Table 2**; indeed, the waste composition can be defined in terms of three main mass fractions: the combustible fraction (CHO), the moisture fraction (MOI) and ash plus inert fraction (Ash&In). According to reasonable approximations, assuming in the combustible fraction, a carbon to hydrogen and a carbon to oxygen ratios, respectively, equal to 7.5 and 2, and a fixed composition of the Ash&In fraction. As reported in **Table 2**, waste ultimate analysis can be uniquely gathered from its composition in terms of CHO, MOI and Ash&In.

It is important to underline that the waste composition strongly affects the lower heating value (LHV) of the RDF; as evidenced in **Figure 7**, in particular, LHV is mainly dependent on the CHO fraction content of the waste. In this work, we assume an RDF with LHV in the range of 14 and 18 MJ/kg; therefore, only waste with composition in the highlighted color region in **Figure 7** is analyzed with our simulation tool.

The simulation of gasification unit has been carried out for several waste compositions derived from a fine discretization of the range depicted in **Figure 7**. As could be expected, syngas

CHO	50–80%	C/H = 7.5 C/O = 2	C	40–55%
			H	5–7.5%
			O	20–27.5%
Ash&In	10–25%	Cl = 0.75%		
		S = 0.15%		
		N = 1%		
		Ash = (Ash&In-Cl-S-N)	SiO_2 = 35.79%	
			CaO = 35.89%	
			Al_2O_3 = 13.32%	
			Fe_2O_3 = 15%	
MOI	10–25%			

Table 2. Waste composition range considered for feedstock characterization in the simulation tool.

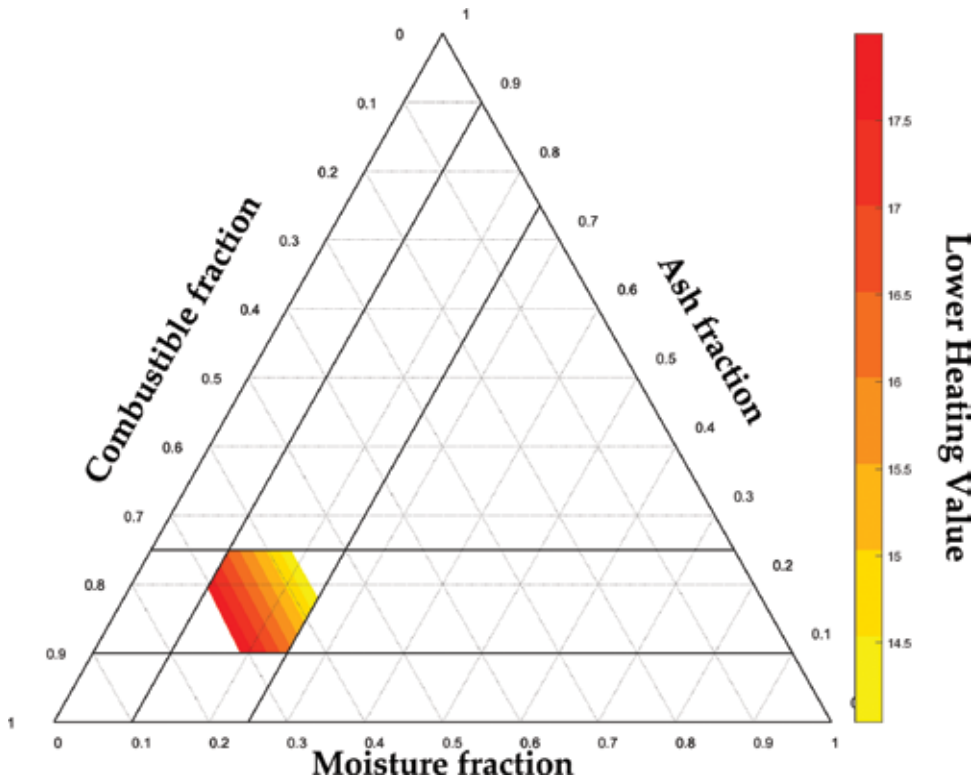

Figure 7. The lower heating value of waste as function of combustible, moisture and ash and inert contents.

composition is influenced by waste composition and LHV variation. Bearing in mind the requirements for methanol synthesis, it is useful to represent methanol module and carbon ratio—$CO_2/(CO + CO_2)$—variation as a function of waste LHV (**Figure 8**). Indeed, each LHV

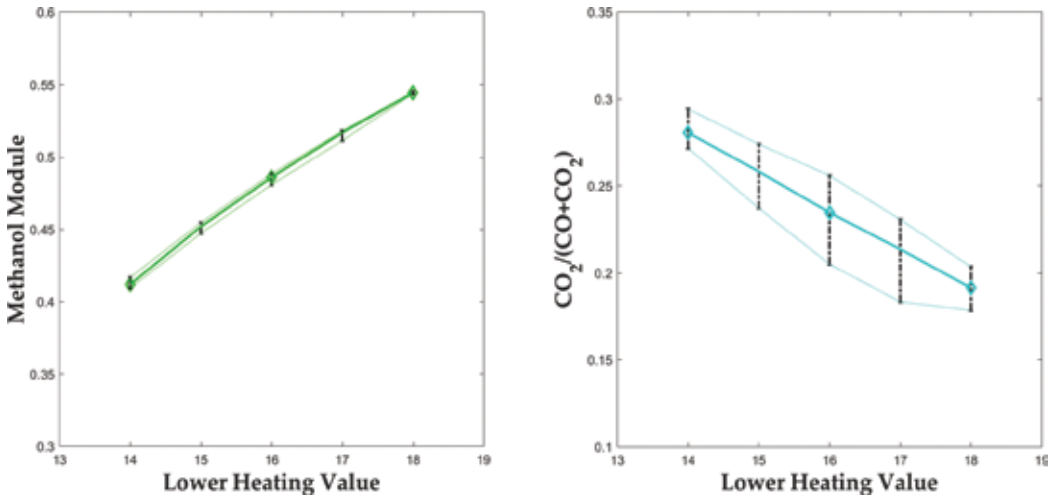

Figure 8. Methanol module and carbon ratio—$CO_2/(CO + CO_2)$—obtained with Aspen Plus simulation as functions of waste LHV (MJ/kg).

value can be obtained from different waste compositions (i.e. from waste with similar combustible fraction but different moisture or ash content) and can result in different syngas compositions; therefore, in each plot, a fixed LHV value corresponds to a range of MM or CO_2 content, actually depending on the MOI or Ash content. In the plots, the colored symbols '◊' represent the mean values of carbon ratio at LHV equal to 14, 16 and 18 MJ/kg. From the left panel of **Figure 8**, it is evident that for different waste compositions, with same LHV, methanol module values are very similar (i.e. MOI and Ash&In contents do not significantly affect the MM value), while a large variability is observed for the CO_2 to CO ratio (see the panel on the right). The strong correlation between methanol module and LHV is significant and supports the choice of LHV as a characterizing parameter for the feedstock, also for the analysis of the effects of RDF variability on the downstream process behavior.

Furthermore, as reported in **Figure 9** (left panel), the higher the waste LHV is, the higher the syngas yield is obtained, even if some variability related to the MOI and Ash content is observed. Finally, it is worth considering a gasification unit thermal efficiency defined as

$$\frac{LHV_{Syngas} \cdot kg_{Syngas}}{LHV_{RDF} \cdot kg_{RDF} + LHV_{CH_4} \cdot kg_{CH_4}}$$

where the heating value of the obtained syngas is compared with the total heating value of RDF and supplemental CH_4 fed to the gasifier. From the figure reported in the right panel of **Figure 9**, it is evident that the efficiency is strictly correlated to the LHV of RDF.

Comparing the obtained results with the technical requirements for methanol synthesis, it is evident that despite suitable $CO_2/(CO + CO_2)$ ratio that is always obtained, the MM values are always too low, even when RDF with a high heating value is used. That is why a conditioning step is required.

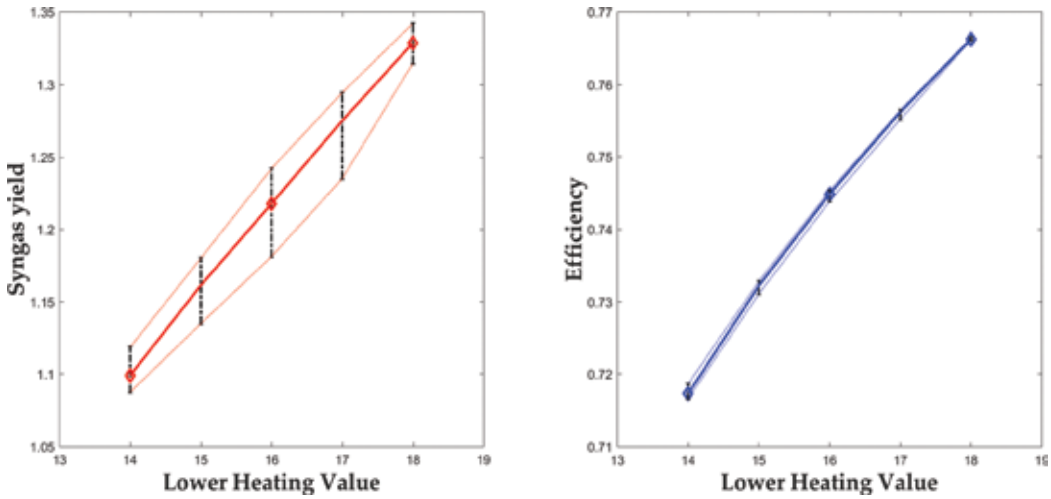

Figure 9. Syngas yield and efficiency obtained with Aspen Plus simulation as functions of waste LHV (MJ/kg).

3.1.2. Effect of operating condition

Usually, in gasification processes, the main examined operating conditions are operating pressure, temperature and gasification agent. In this case, the gasifier outlet temperature and the introduction of a supplementary steam stream have been deeply investigated.

3.1.2.1. Effect of temperature

The syngas composition and methanol synthesis parameters trends as a function of gasifier outlet temperature (i.e. equilibrium temperature of RG3 referred to **Figure 3**) are illustrated in **Figure 10**.

The represented trends show that both the methanol modulus and the ratio CO2/(CO + CO2) are improved at a lower gasification temperature, where the hydrogen content is higher. A reduction of the R-G3 temperature also reduces the oxygen consumption. However, a temperature higher than 1100°C must be provided in order to avoid dioxin formation and limit methane and tar content in syngas.

3.1.2.2. Effect of steam introduction

Steam is a possible oxidant [27], which can be additionally introduced in the gasifier with a controlled oxygen stream.

The results of the sensitive analysis made for different steam temperatures are depicted in **Figure 11**. Indeed, the steam injection results in two opposite effects: (1) an increase in H_2 production in the gasifier due to the shift reaction and (2) an increase in the heat required to maintain the top gasifier temperature equal to 1100°C, which in turn results in an increase in the oxygen consumption for exothermic reactions, including hydrogen combustion. These

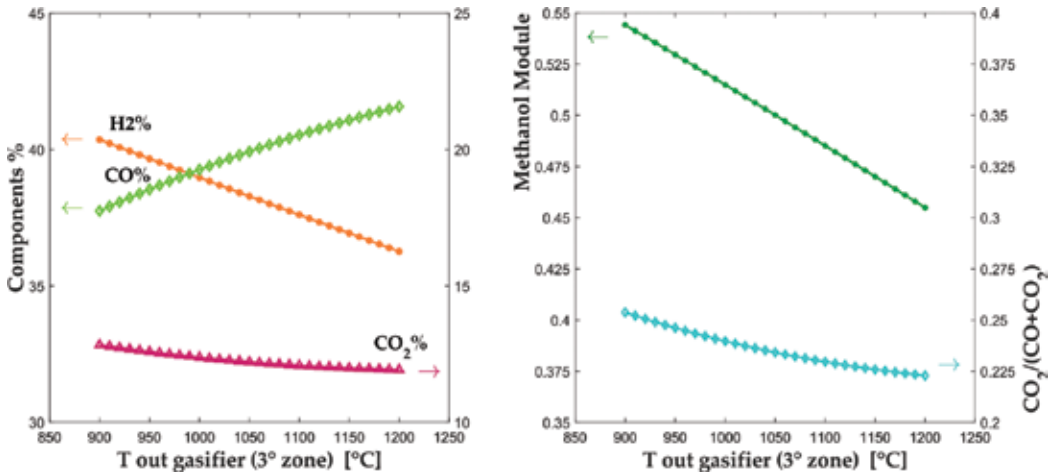

Figure 10. In the left panel, H_2, CO and CO_2% of syngas from gasifier as a function of its outlet temperature—third Gibbs reactor temperature (in Aspen Plus simulation). In the right panel, methanol module and carbon ratio as a function of syngas outlet temperature.

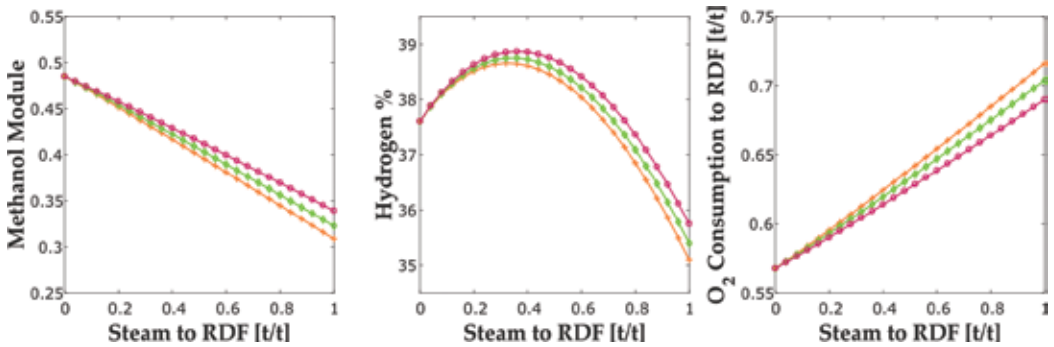

Figure 11. Methanol module, hydrogen % in syngas and O_2 consumption to RDF (t/t) as a function of steam to RDF (t/t) value, for different steam inlet temperature '+' 130°C, '◊' 210°C and 'o' 300°C.

mentioned factors explain the maximum hydrogen content, at steam to RDF ratio near to 0.35 and the increase in CO_2 content in syngas; on the whole, steam injection results in a reduction of methanol module. As results show, the increment of steam temperature is not enough relevant. On the other hand, steam might be able to destroy tar at a lower temperature and it could decrease the burner's outlet temperature which causes corrosion of refractory reactor covering. These possible benefits cannot be quantified with the support of the illustrated simulation that assumes thermodynamic equilibrium hypothesis. Obviously, a kinetic and fluid-dynamic model of the gasifier should be developed in the future to better analyze and optimize the process.

3.2. Influence on methanol production

Once the RDF is gasified, the obtained syngas has to be properly conditioned, as already described in Section 2. The syngas composition variation will cause the alteration of some

operating parameters of the conditioning section. Here, a controller is set to maintain MM equal to 2.1 at the inlet of the methanol synthesis reactor, by varying the percentage of syngas sent to the shift reactor. Consequently, the superheated stream to add to the shift reactor R-HTS, the methanol yield and CO_2 produced will be affected by this variation, depicted in **Figure 12**. As reported in Section 3.1.1, syngas composition depends on the RDF LHV. In particular, methanol module exhibits a linked correlation with LHV. For this reason, three main syngas compositions corresponding to RDF with LHV equaling to 14–16–18 MJ/kg have been selected, with the aim of analyzing the influence of feedstock variation on methanol production. **Figure 12** shows how the LHV values affect the main operating parameters of the conditioning section.

When waste LHV varies, also syngas flow rate is influenced and as a consequence methanol productivity. However, to better compare consumptions that occur for waste with different LHVs, it has been taken into account to obtain a fixed amount of methanol; in particular, when LHV decreases, a higher quantity of RDF to gasify is required. As represented in **Figure 12**, the values of operating parameters increase with the decrease in LHV. Then, we refer as design case to the process converting waste with lowest LHV of 14 MJ/kg.

3.3. Optimized process: mass and energy balance

The Italian municipal solid waste generated, expressed in kg per person per year, is equal to 529 [2]. With this number in mind, and considering that RDF represents a third of MSW quantity, a defined RDF quantity to gasify has been considered. A gasification line has a period of planned and unplanned maintenance. To avoid a plant arrest, three gasification lines working in parallel were adopted, so that when one of them stops, the other two work at their maximum capacity, providing only an 80% of turndown. For the design case, a gasification line with a normal capacity of 7.5 t/h is adopted, so that the available RDF (with 14 MJ/kg) is equal to 540 t/d.

Referring to **Figure 13**, a utility consumption has been performed for a further detailed economical evaluation. As shown in **Figure 13**, a 540 t/d feed is required to produce 225 t/d of

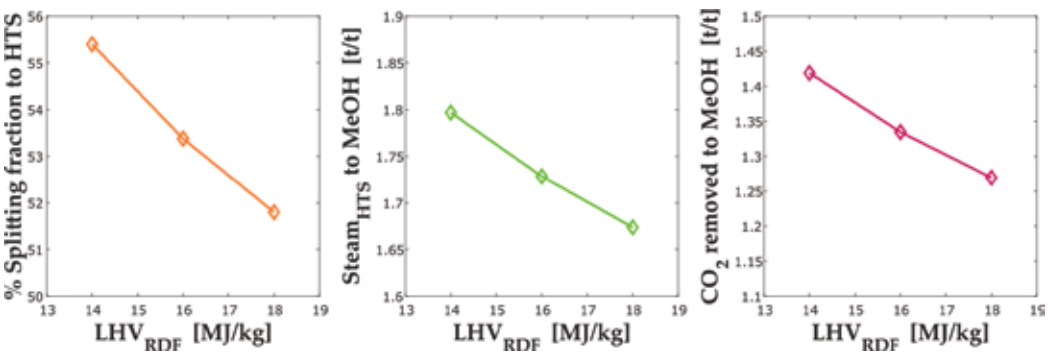

Figure 12. The variation of main operating parameters with a lower heating value.

bio-methanol. The CO_2 obtained comes from the CO_2 removal system and the flue gases of a boiler used to supply steam for the hydrolysis reactor, the HTS reactor, the CO_2 reboiler and the distillation reboilers. The cooling water (CW) reported in **Figure 13** is low because it just represents the reintroduction of water in the cooling tower system.

A comparison between a WtE and a WtC process with a typical incinerator, in terms of CO_2 emission and methane consumption, is necessary to understand the relevance of a waste to chemical conversion. To evaluate those parameters, the same gasified quantity has been assumed. In **Table 3**, CO_2 emissions of each process are reported in terms of CO_2 kg per kg of methanol.

A WtE process could be seen as a waste disposal method and as an energy production system; likewise, a WtC process could be seen as a waste disposal method and as a methanol production process. Therefore, in order to correctly compare them, CO_2 emission of WtE has to be added with the emission of a conventional methanol process, per unit of methanol produced. For that, waste combustion emission is equal to 2.96 kg CO_2/kg MeOH, considering that 2.4 kg RDF, which would be converted for 1 kg of methanol produced and that the direct emission of process is 1.23 kg CO_2/kg RDF. According to the same rules, WtC emissions are equal to the sum of the direct process emission (1.7 kgCO_2/kg MeOH) and the emission connected to the conventional energy production related to the same MW amount which would be produced by converting, through WtE, the RDF quantity, used for 1 kg of methanol synthesis (0.96 kg CO_2/

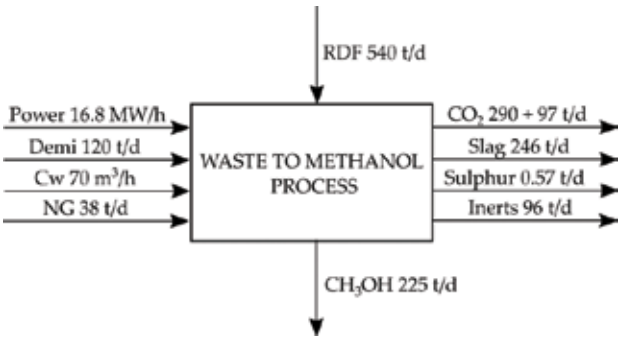

Figure 13. Overall process analysis consumption.

		$\frac{kgCO_2}{kgCH_3OH}$	$\frac{kgCH4}{kgCH_3OH}$
WtE	Conventional methanol production process	0.76	0.69
	Waste combustion	2.96	0.07
WtC	Conventional energy production	0.96	0
	Waste-to-methanol process	1.7	0.17

Table 3. Value considered to compare waste to energy and waste to chemical in terms of CO_2 emission [8] and CH_4 consumption.

kg MeOH). In this way, a reduction of 30% of GHG emission is obtained by comparing a WtC process with a WtE process.

Moreover, to evaluate CO_2 emission saved in a waste to chemical conversion, it is important to compare how much CO_2 is emitted when RDF is burnt and methanol is produced in a conventional way and with the waste-to-methanol process. Therefore, the following ratio is considered:

$$\frac{CO_2 \textit{ from a waste to methanol process}}{(CO_2 \textit{ from combustion} + CO_2 \textit{ from conventional methanol production}}$$

According to the value reported in **Table 3**, a saving of 54% is reached. Other than from an environmental point of view, even the consumption (in terms of methane usage) has been reported, to emphasize the importance of a WtC process.

4. Economical analysis

The process scheme reported in **Figures 1–6** provides an idea of the units required in a waste-to-methanol process. To evaluate the techno-economical feasibility of this process and decide whether or not this technology has a chance to be applied, a deep economical evaluation is required. Economic parameters used to estimate the cost of production (COP) are summarized in **Table 4**.

First of all, an analysis of the equipment employed is necessary to evaluate the CAPEX of the process.

As depicted from **Table 4**, the most relevant cost is related to the gasification lines, including the first purification treatment unit. Moreover, an Air Separation Unit is required when a gasification with pure oxygen is used. The additional costs for oxygen production appear justified on the basis that a higher syngas heating value is obtained [5] and less inert compounds circulate on the overall conditioning and synthesis unit. Once the total equipment cost is defined, an estimate of the total investment cost is predictable, as shown in **Table 5**. To define the CAPEX, an analysis of the total direct and indirect costs is necessary, including also the contract profit and the contingency.

	M €
HT converter reactor (3 lines)	25
ASU, gasometer and compressors	12
Syngas purification and conditioning	7
Methanol synthesis and purification	10
Total	**54**

Table 4. Total equipment cost.

	M €	% of delivered equipment cost
Equipment costs	54	100
Bulk materials (piping, instrumentation, electrical)	38	70
Building and civil works	16	30
Total Direct Costs	**108**	**200**
Engineering and site supervision	13	25
Construction	51	90
Total Direct Costs + Indirect Costs (TOT)	**172**	**315**
Contractors profit 7%	13	25
Contingency 10%	17	32
Fixed capital investment (CAPEX)	**202**	**372**

Table 5. Estimated investment cost.

The key assumption parameters used to make this evaluation are presented in **Table 6**.

The main advantage of producing bio-methanol by gasifying RDF is that according to UNI EN 15359, when an RDF with an LHV value less than a classified 'Type 3' is used, the process is considered as a disposal method and the usage of RDF becomes an income and not a cost. Moreover, nowadays, CO_2 with a high purity level is employed in many agro-industrial processes, so the CO_2 obtained from the CO_2REMOV UNIT could also be considered as an income, since it has a secondary usage. Therefore, the inert and sulfur compounds coming, respectively, from the gasification and the conditioning unit could also be used as an additional income, but they are less effective than RDF and CO_2, so they were not taken into account for the scope of this economical analysis.

RDF price (flock type), €/t (Italian basis)	85
Electricity price, €/MWh	50
Natural gas, €/kg (considering 115,000 kcal/kg)	0.30
Slag disposal costs, €/t	10
CAPEX, M€	202
RDF capacity, t/y	182,115
Methanol capacity, t/y	76,518
Slag capacity, t/y	33,691
Plant factor, h	7650
Depreciation factor (based on a 20-year life and 6% interest rate)	0.0875
Calculated cost of excess CO_2 capture, €/t	30

Table 6. Key economic assumption and parameters.

Costs	**M€/y**
Power consumption	6.0
Natural gas	1.74
Slag disposal	0.34
Maintenance	4.1
Other (including labor and chemicals)	2.96
Total costs	15.14
Depreciation rate	17.7
Total costs + Depreciation	32.84
Incomes	**M€/y**
RDF	15.5
CO_2 recovered	3.1
Total Incomes	18.6
COP	**€/t**
(Total Costs − Total Incomes)/Methanol capacity	**186**

Table 7. Cost of production per ton of methanol produced.

On this assumption, the total cost of production is equal to 186 €/t (**Table 7**). The selling methanol price (methanol produced in a conventional way) is 300–320 €/t, whereas the bio-methanol price is estimated as 464 €/t; in this way, a margin of 278 €/t of methanol is obtained.

The estimated Internal Rate of Return (IRR) is in the range of 22–23%, as shown in **Table 8**, which indicates a good profitability in the waste-to-methanol process. Moreover, the IRR value is strictly dependent on the price of RDF, here estimated as 85 €/t by increasing this, the IRR could become higher.

	M€
Profit from methanol	35.5
Other revenues (including ones from RDF and CO_2 certificate)	18.6
Total variable cost	(15.14)
Bank loan (considering 2/3 of the Capex as loaned)	(9.11)
Profit before taxes	**29.84**
Taxes (50%)	14.92
Net Profit	**14.92**
IRR%	**22.4**

Table 8. Calculation of return on investment.

5. Conclusion

The conversion of RDF into methanol, which can be termed bio-methanol due to its production from a renewable source, has the advantage of offering a new nontoxic-disposal methodology and of valorizing the feedstock by transferring the RDF carbon source into a valuable resource; in this process, in fact, the RDF carbon matrix is partially fixed in the methanol molecule and the remaining part is recovered in the form of pure CO_2. In this way, on one hand, an environmental-friendly process has been proposed, and, on the other hand, the target of providing 10% of advanced biofuel within 2020, disposed by Italian regulation, is achieved, taking into account the possibility of adding 'Bio-methanol' to transport fuel. Moreover, a reduction of 50% of GHG emission could be reached, comparing waste-to-methanol process with both methanol conventional process and RDF combustion as disposal method. From an environmental point of view, a good combination of the HT gasification process, proposed by 'OESA s.r.l., with the conditioning process is fundamental to lower as much as possible the GHG emission and avoid toxic substances formation, as dioxins which cause devastating effects on human health. All this could not be achievable without the combination of both sections: the gasification process itself could lead to syngas formation free of toxic substances but its conversion into energy, in a WtE optic, will contribute to the addition of GHG emission, whereas the syngas conversion into bio-methanol will provide a major contributor in environmental terms due to the GHG emission reduction. From an economical point of view, the bio-methanol cost of production allows a good margin, taking into consideration a major selling price of bio-methanol, mainly because RDF gasification is an income and not a cost. Moreover, bio-methanol produced from waste has the benefit of the double counting, as reported in the Renewable Energy Directive, so exploiting the fact that it counts double, it could be seen as an excellent investment considering the target to achieve through advanced biofuel by 2020.

Author details

Annarita Salladini[1]*, Emanuela Agostini[2], Alessia Borgogna[3], Luca Spadacini[4], Maria Cristina Annesini[3] and Gaetano Iaquaniello[5]

*Address all correspondence to: salladini.a@processiinnovativi.it

1 Processi Innovativi s.r.l., Rome, Italy

2 BIO-P s.r.l., Rome, Italy

3 Department of Chemical Engineering, 'La Sapienza' University, Rome, Italy

4 OESA s.r.l., Rome, Italy

5 KT Kinetics Technology S.p.A., Rome, Italy

References

[1] Rapporto Rifiuti Urbani. ISPRA; 2016

[2] Massarini P, Muraro P. RDF: From waste to resource–the Italian case. Energy Procedia. Elsevier. 2015;**81**:569-584

[3] Greenhouse Gas Emissions [Internet]. United States Environmental Protection Agency; 2017. Available from: https://www.epa.gov/ghgemissions/overview-greenhouse-gases

[4] Gohlke O, Martin J. Drivers for innovation in waste-to-energy technology. Waste management & research. Sage Publications Sage UK: London, England. 2007;**25**:214-219

[5] Arena U. Process and technological aspects of municipal solid waste gasification: A review. Waste management. Elsevier. 2012;**32**:625-639

[6] Consonni S, Viganò F. Waste gasification vs. conventional waste-to-energy: A comparative evaluation of two commercial technologies. Waste management. Elsevier. 2012;**32**:653-666

[7] Antonetti E, Iaquaniello G, Salladini A, Spadaccini L, Perathoner S, Centi G. Waste-to-chemicals for a circular economy: The case of urea production (waste-to-urea). ChemSusChem. Wiley Online Library. 2017;**10**:912-920

[8] Iaquaniello G, Centi G, Salladini A, Palo E, Perathoner S, Spadaccini L. Waste-to-methanol: Process and economics assessment. Bioresource Technology. Elsevier. 2017;**243**:611-619

[9] EU Renewable Energy Directive (2009/28/EC). European Union; 2009

[10] Lapola DM, Schaldach R, Alcamo J, Bondeau A, Koch J, Koelking C, et al. Indirect land-use changes can overcome carbon savings from biofuels in Brazil. In: Proceedings of the national Academy of Sciences. National Acad Sciences. 2010;**107**:3388-3393

[11] Biofuels and green chemicals [Internet]. Enerkem S.r.l.; 2017. Available from: http://enerkem.com/biofuels-and-green-chemicals/

[12] Energy Recovery System L.t.d. [Internet]. Energy Recovery System L.t.d.; 2017. Available from: http://www.ers-ksa.com/

[13] Aasberg-Petersen K, Nielsen CS, Dybkjær I, Perregaard J. Large scale methanol production from natural gas. Haldor Topsoe. 2008;**22**

[14] Grabow L, Mavrikakis M. Mechanism of methanol synthesis on Cu through CO_2 and CO hydrogenation. Acs Catalysis. ACS Publications. 2011;**1**:365-384

[15] McKay G. Dioxin characterisation, formation and minimisation during municipal solid waste (MSW) incineration. Chemical Engineering Journal. Elsevier. 2002;**86**:343-368

[16] Scheirer GE, Wu FS, Kiliany TR. Systems and processes for reducing the sulfur content of hydrocarbon streams. U.S. Patent No. 7,427,385. Washington, DC: U.S. Patent and Trademark Office. 2008

[17] LO-CAT® H2S Removal Technology [Internet]. Merichem; 2017. Available from: http://www.merichem.com/gas/upstream/natural-gas/lo-cat

[18] Aspen Plus [Internet]. Aspen Tech; 2017. Available from: http://home.aspentech.com/products/engineering/aspen-plus [Accessed 2018-03-28]

[19] Aspen Plus (2004). Getting Started with Modeling Processes with Solids. Cambridge, MA: Aspen Technology. Inc.; 2013

[20] Ilaiah S, Sasikanth DV, Satyavathi B. Process Simulation of a Entrained Fluidized Bed Biomass Gasification using Aspen Plus. In: Proceedings of 3rd International Conference on Recent Trends in Engineering Science and Management ICRTESM-16); Bundi, Rajasthan: Vedant College of Engineering and Technology; 10th April 2016

[21] Gopaul SG, Dutta A, Clemmer R. Chemical looping gasification for hydrogen production: A comparison of two unique processes simulated using ASPEN Plus. International Journal of Hydrogen Energy. Elsevier. 2014;**39**:5804-5817

[22] Emun F, Gadalla M, Majozi T, Boer D. Integrated gasification combined cycle (IGCC) process simulation and optimization. Computers & chemical engineering. Elsevier. 2010;**34**:331-338

[23] Mills KC. Physic-chemical properties of slags and ashes. ACS symposium series.Washington, DC, USA: American Chemical Society; 1986;**301**:195–214.

[24] Effendi A, Hellgardt K, Zhang Z-G, Yoshida T. Optimising H2 production from model biogas via combined steam reforming and CO shift reactions. Fuel. Elsevier. 2005;**84**:869-874

[25] Kohl AL, Nielsen R. Gas Purification. 5th ed. Houston: Gulf Publishing Co.; 1997

[26] Salladini A, Borgogna A, Spadacini L, Pitrelli A, Annesini M, Iaquaniello G. Methanol production from Refuse Derived Fuel: A preliminary analysis on the influence of the RDF composition on process yield. In: Proceedings of 5th International Conference on Sustainable Solid Waste Management (Athens). 2017

[27] Ramzan N, Ashraf A, Naveed S, Malik A. Simulation of hybrid biomass gasification using Aspen plus: A comparative performance analysis for food, municipal solid and poultry waste. Biomass and Bioenergy. Elsevier. 2011;**35**:3962-3969

Chapter 9

Efficiency of Plasma Gasification Technologies for Hazardous Waste Treatment

Victor Zhovtyansky and Vitas Valinčius

Additional information is available at the end of the chapter

http://dx.doi.org/10.5772/intechopen.74485

Abstract

The chapter is devoted to the development of technologies for the processing of carbonaceous wastes, including hazardous ones, using plasma energy sources. In particular, plasma-steam equipment provides complete environmental safety and high quality of the synthesis gas produced. Its application is also discussed to exclude the risk of environmental pollution by heavy metals, if they are contained in the recycled waste. The advantages of using oxygen instead of air as an additional reagent in gasification processes are underlined. It is shown that the proposed variant of the processing technology corresponds well to the general idea of numerous publications in the world scientific literature, known as the Waste-to-Energy. It has been shown that plasma equipment has significant advantages in terms of the commercialization of processes for the treatment of sewage sludge and some other hazardous waste.

Keywords: waste, biomass, solid fuel, plasma, gasification, plasma torch, syngas, gas engine, distributed energy

1. Introduction

The situation worldwide in the field of environmental protection and efficient energy use is constantly getting worse. In order to more efficiently reduce environmental pollution, traditional thermal methods are not enough. A whole complex of coordinated efficient measures should be applied.

In the last few decades, the problems of carbon-containing materials reforming into synthesis gaseous fuel—mixture CO and H_2—by means of plasma technologies were widely discussed in the scientific literature [1–14]. This syngas can be used for heat or electrical energy production [13].

The European Commission (EC) has defined the European Union (EU) objectives in the energy sector by 2020 (20% less greenhouse gas emissions, at least 20% of the EU's energy resources—renewable energy sources, a 20% reduction of primary energy consumption in the directive EU, COM (2008) 30) [15, 16]. To achieve these objectives, the Member States have to increase the share of renewable energy resources in electricity generation, fuel saving and waste management. At the same time, it should be taken into account about the most effective hazardous waste destruction technology such as a thermal treatment and gasification. Ukraine and Lithuania have approved the Community and follows the most important requirements and procedures of the EU.

It is well known that one of the most effective hazardous waste destruction technologies is a thermal treatment and gasification. However, there exist an entire group of substances any traditional treatment of which causes a threat to the environment and human health. Therefore, present research proposes to develop and implement plasma technology, which allows to remove all waste containing hazardous substances. Plasma decontamination technology of toxic materials allows to create a compact device, which can reliably neutralize all of types of hazardous waste. Such plasma device is characterized by a very high temperature, short reaction time, extreme activation energy, the ability to heat various gases, effective neutralization and independence from fuel sources.

Complete and safe hazardous waste (outdated medications, banned pesticides, plastic gears, pathological waste, container, etc.) removal method is high temperature (plasma) pyrolysis. It is already employed in many countries around the world: USA, Japan, France, Germany, Switzerland, Australia, etc. Many developing countries (India, China, Belarus, etc.) also seek to employ the plasma technology in this area. There is a shortage of detailed technology description in worldwide scientific literature because these research results some times are not made public. Medical wastes from hospitals, dental clinics and other health centers are collected and recycled in about 1500 large companies. Most of them are located in the USA, France, Great Britain and Japan [17, 18].

The interest in plasma technology in the application of harmful substances neutralization processes is huge. For example, the Japanese medical waste management company recently implemented a large project, whose main goal is to transform the infected local medical waste into useful products - glass, metal and syngas.

Environmental safety and technological advantages of plasma using plasma technology for this purpose are noted in many of the papers. However, the most important problem is their energy efficiency, because the efficiency of electricity generation to power the plasma torch (PT) is only about 30% [9]. Thus, in order to achieve the commercialization of such environmentally clean technologies, they need to simultaneously achieve high levels of their energy efficiency. The solution of this problem is also dedicated by this work.

2. Waste-to-energy process

Modern technologies of the waste treatment are oriented on the processes of their gasification. It has three interrelated advantages. First of all, the temperature range at which the gasification processes are effectively carried out is quite high and usually exceeds 1000°C. This automatically meets the requirements of the Directive 2000/76/EC [15], according to which the temperature should be maintained at 1100°C in case of incineration of waste containing more than 1% wt. of halogenated organic substances under conditions of chloride. This is necessary for dioxins and furans which are formed at lower temperatures, to be effectively decomposed into HCl.

Second, each local volume of gas produced in the processing has to be kept at this temperature over time ≥2 s. In this case, maximum permissible emission of dioxins and furans to the atmosphere in the refinement products do not exceed 10^{-10} g/m^3 [15]. This is very important as these compounds are among the most toxic ones. In addition, prolonged residence of reagents at high temperature ensures the completeness of gasification processes, and also allows accepting the assumption of equilibrium conditions when performing thermodynamic calculations.

Third, although gasification products must be cooled down quickly to avoid the reverse generation of dioxins and furans, the main energy is accumulated in chemical bonds. Even though syngas cooling leads to some losses of thermal energy, the share of which is small compared to the total energy content which consists of thermal and chemical energies.

Another problem appears when the waste contains in its composition heavy metals; using well known incineration for their utilization leads to formation of ash, which is itself a hazardous waste [19–21]. The latter environmental hazard is particularly dangerous in the case of recycling the sewage sludge of urban wastewater treatment plants [13].

The arc discharged plasma is an effective tool for many types of application including hazardous waste treatment. It is important to notice that there exist several unsolved problems in thermal treatment of sewage sludge area. During the combustion process, solid dispersed particles may be formed from the combustion products. Solid particles may penetrate into the human lungs and can cause serious illnesses. Incomplete combustion may also occur inside the furnace and form new chemicals that may appear to be more toxic than initial material. Therefore, flue gas is cleaned in multicyclones or fiber filters before discharge into the atmosphere. However, such types of filters are expensive and not very effective in the case of fine dispersed particulates. There does not exist means against newly formed hazardous chemicals at all. So the plasma treatment of exhaust combustion products is welcomed. Atmospheric pressure arc plasma is also a promising tool for the synthesis of catalytic coatings which could be successfully employed in the manufacturing of catalyst for flue gas treatment.

3. Plasma processing of hazardous waste

First in Ukraine, full-scale equipment for medical waste processing as well as another hazardous waste has been built by the E.O. Paton Electric Welding Institute of the National Academy

of Sciences of Ukraine (NASU) and the Institute of Gas, NASU [3, 9]. Its fundamental advantage is using water steam-plasma as a gasification agent, which allows to obtain the gasification products of maximum calorific value. Mode of the equipment operation satisfies all the requirements of the Directive 2000/76/EC [15].

The other type of experimental equipment for destruction of hazardous waste has been installed in Lithuanian Energy Institute (LEI) [11, 14]. It consists of a plasma jet reactor with DC arc plasma source capacity of up to 90 kW. The plasma process uses air, nitrogen, water vapor or their mixtures. The plasma-forming gas flow rate in the reactor reaches up to 2–7 g/s, the average exhaust mass temperature varies from 2800 to 3500 K. Experimental and numerical studies carried out upon the realization of the plasma decomposition process of organic and inorganic substances.

3.1. Plasma sources

Arc plasma torch (PT) is a key element of the equipment. It was made according to the two-electrode axial scheme with hollow copper electrodes. Compressed air and steam are used as the plasma-forming gases. PT ignition is carried out with air and then transition to steam occurs after the heating [9].

The linear DC arc heater was produced in LEI for heating air, nitrogen, steam or their mixtures up to 7000 K. It was connected to the reactor vessel. By achieving gas temperature over 4000 K, molecules of hazardous substances and waste decay to atoms, radicals, electrons and ions so that it appears ability to obtain simple combination of harmless chemicals. Several configurations of linear DC PT with hot cathode and step-formed anode were considered. As a sample, it could be mentioned PT 70 kW of power, with radial and tangential injection designed especially for the production of non-equilibrium plasma jet. Its analog was described elsewhere [22]. The novel PT (**Figure 1**) was manufactured and applied for the treatment of hazardous organic and inorganic compounds. It consists of a button type hafnium cathode, transitional copper anode for arc initiation 3, neutrode 5, insulation rings and step-formed copper anode 7. To increase the angular velocity of arc rotation, magnetic stabilization of flow was applied employing the coil 8 [22].

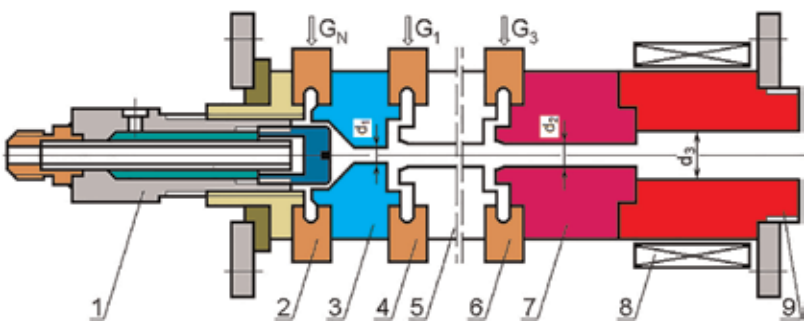

Figure 1. Schematic presentation of linear DC plasma torch. 1—Cathode junction with hafnium emitter; 2, 4, 6—Insulating rings with gas injection; 3—Intermediate anode; 5—Neutrode; 7, 9—Step-formed anode; 8—Magnetic coil.

A new PT is employed for heating the material that is injected into the reaction arc chamber. Both average and local heat losses of PT elements are necessary to know when the device is operating under extreme conditions to select operating and cooling regimes. Operating characteristics of the PT plasma flow and parameters were determined from the heat conservation calculations while measuring voltage drop, gas flow rate and arc current strength in the circuit. The preference has been given to the PT with neutral, fixed average arc length and step-formed copper electrode [22]. This enabled to reduce arc shunting after anode step and ensured the stability of length of the arc in the wide diapason of gas flow rates and current variation. The employed plasma source also is different comparing to ordinary plasma torches with the conical expanded anode. The anode step also serves for reduction of the pressure drop in the discharge channel and to fix the arc in the stable position. The total PT length is 0.25 m, the insular part anode diameter is 0.03 m and the diameter of extended part of the anode is 0.04 m. The neutrode makes separate neutral section of the torch and is isolated from the anode. It is located between insulating rings made of thermal resistant glass textolite. Each ring is also used for tangential air supply and contains a pair of tangential-oriented blowholes (as G_N, G_1 and G_3 in **Figure 1**) for the arc stabilization. The experimental equipment for producing arc plasma is comprised of rectifier for power supply, gas supply, water-cooling systems and airing devices.

The modified similarity theory has been applied for the analysis of operating and thermal characteristics and result generalization [22–24]. Voltage–current characteristic (VCC) of PT were generalized employing criterial equations and following expressions were established:

$$\frac{Ud_2}{I} = 1350\left(\frac{I^2}{Gd_2}\right)^{-0.55}\left(\frac{G}{d_2}\right)^{-0.14}(pd_2)^0. \tag{1}$$

PG performance and thermal characteristics can be evaluated by its efficiency η indicating what part of generated energy is transferred to gas:

$$\eta = GH(UI). \tag{2}$$

Generalization of the TC of PG is similar to generalization of the electric characteristic:

$$\frac{1-\eta}{\eta} = 5.5{*}10^{-3}\left(\frac{I^2}{Gd_2}\right)^{0.22}\left(\frac{G}{d_2}\right)^{-0.12}(pd_2)^0\left(\frac{l}{d}\right)^0. \tag{3}$$

Here U is arc voltage, I is arc current, G is total gas flow rate, d_2 is anode diameter and p is pressure. The value of η may be presented also as the Stanton number [23]:

$$\frac{1-\eta}{\eta} = \frac{4l}{d_2}St. \tag{4}$$

The research concludes that PT VCC depends on the following main factors: (i) radial and tangential injection of plasma-forming gas; (ii) gas flow rate of plasma-forming gas to produce the desired arc; (iii) arc chamber geometry and (iv) gas composition. The first factor was

evaluated during the experimental investigation of gas flow rate at the constant and various values of PT. In the present and previous [22] studies when the radial injection is not applied, operating characteristics were observed as decreasing in the current range between 150 and 250 A. This follows as a result of dropping electric field intensity which linearly depends on the arc current. It was also established that voltage drop and electric field intensity linearly decrease with increasing of gas flow rate in the range of 7–10 $\times$ 10^{-3} and 5–8 $\times$ 10^{-3} kg s^{-1}. When the radial and tangential injection in different locations is used, the arc is strongly turbulized and a possibility to heat up much larger amount of gas in the PT of reduced dimensions is available. Consequently, the voltage drop in such PT increases up to 70% and the possibility for better control of plasma-forming process appears.

When tangential injection of plasma-forming gas is applied inside the PT anode, the character of operating characteristics is slightly dropping or remains as stabile. The impact of gas flow rate, anode diameter and arc current on plasma generated electric characteristics and thermal efficiency for similar PT are described in Refs. [22, 23, 25]. It is important to notice that static PT characteristics may be also slightly rising with increase of arc current strength.

The present measurements over 120 experiments were carried out varying with the help of resistors arc current strength and injected air flow rate G_1 and G_3. Some geometrical PG characteristics and ranges of experiments carried out are summarized in **Table 1**.

3.2. Plasma chemical reactors

Technologically, the conversion process is carried out in a flow reactor. It has a metal case and is lined with the layer of fireproof and heat-insulating materials on the inside (**Figure 2**). PT

Power, *P* (kW)	33–78
Arc current, *U* (A)	175–245
Arc voltage, I	160–335
Cooling water flow rate, Gv (kg s^{-1})	0.16–0.18
Water temperature increment (deg):	
plasma torch	15–23
cathode	1.1–1.53
ignition section	1.08–2.16
neutrode	–
anode	13.0–19.3
Source gas flow rate (kg s^{-1}):	
cathode, G_N	0.54–1.0
neutrode, G_1	–
anode, G_2	1.85–7.6
Plasma jet average mass temperature (K)	3460–5200

Table 1. Plasma source technical parameters.

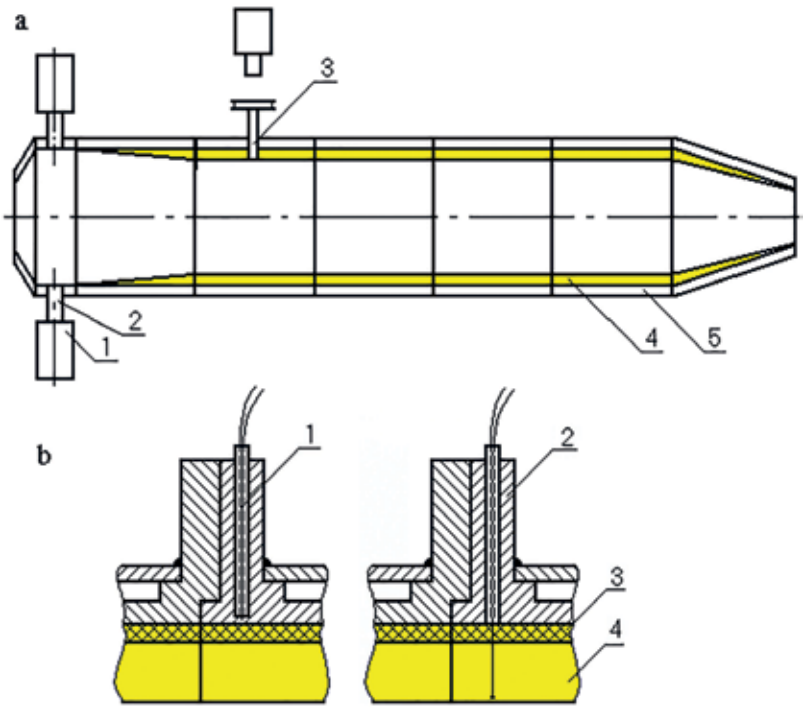

Figure 2. Schematic presentation of plasma jet reactor for treatment hazardous waste. (a) Stream reactor with: 1—Plasma torch; 2—Plasma torch and feeder connecting section; 3—Window for observation and measurement; 4—Layer of Zr_2O_3; 5—Cooling section (five units). (b) Construction of thermocouple's junction: 1—Thermocouple; 2—Frame; 3—Layer of insulating cover; 4—layer of ceramic cover.

electrical power reaches up to 160 kW with efficiency coefficient = 0.7–0.8. The equipment also includes lock-chamber for the periodic load of the packed medical waste, steam generator, power supply of up to 500 volts and a current up to 350 A, as well as the system for the gas quenching and cleaning. General view of equipment as well as PT is shown in paper [9].

The lock-chamber for medical wasteload is located in the upper part of the reactor. Unit management does not involve the full loading of the total reactor space with wastes. This is important for gasification products, if they move through a thick layer of raw materials, not to be cooled below 1100°C [15].

Table 2 presents the composition of the basic gasification products obtained from the medical waste in the equipment for plasma-steam gasification [9]. In these experiments, organic wastes of such average composition have been studied: 60% of cellulose $C_6H_{10}O_5$ + 30% of plastics based on polyethylene $(–CH_2–CH_2–)n$ + 10% water.

Components	H_2	CH_4	CO	CO_2	C_2H_4	C_2H_2	C_3H_6	H_2S	H_2O	Other
%. vol.	49.89	1.99	35.25	2.52	3.37	3.92	0.45	0.13	1.92	0.63

Table 2. Basic gasification products composition obtained from medical waste.

The main physical result of this experimental exploration was a possibility of self-power supply by syngas with gas-diesel engine system taking into account even low efficiency of electricity production ~30%. This fact was verified in Section 4.2 on the ground of thermodynamic calculations.

In general, the previous experience of using this equipment has confirmed the correctness of the basic technical solutions laid down therein. However, it also revealed some shortcomings of individual design solutions. They demand the revision process of further development. In particular, this applies to the high temperature thermal insulation of the reactor [9].

Three different plasma chemical reactors were designed in LEI:

- straight stream reactor for flue gas treatment;
- curved stream reactor for the treatment of gaseous, liquid and solid substances with small solid dispersed particles and
- steady ARC volume reactor, devoted for incineration of wide range of waste.

The last-mentioned is under reconstruction.

We have assumed the plasma flow has been characterized as optically thin. The transport coefficients and thermodynamic properties depend only on the temperature and pressure. The plasma flow in the reactor is also characterized with extremely high temperature gradients and recirculating turbulent flow with wall confinement. The flow inside the chamber was separated. Heat transfer characteristics in the entrance region of the reactor in this case of sudden expansion for the region of $x/d < 0.4$ could be described by the following equations:

$$Nu_{fd} = 0.006\mathrm{Re}_{fd}^{0.86}. \tag{5}$$

For the region of $x/d > 0.4$ described by the equation for entrance region of the pipe:

$$\mathrm{Nu}_{\mathrm{fd}} = 0.0256\mathrm{Re}_{\mathrm{fd}}^{0.8}\varepsilon_{\mathrm{l}}. \tag{6}$$

Here ε_l is the entrance factor, equal:

$$\varepsilon_l = 1.48(x/d)^{-0.15}. \tag{7}$$

Nu and Re are Nusselt and Reynolds criterions, respectively. Index *fd* means that Nu and Re are calculated according to the flow conditions in the entrance and reactor channel diameter.

4. Plasma application in sewage sludge treatment

During sewage treatment, the main pollutants are separated as sewage sludge. Depending on the original pollution load of the water being treated, they may include the heavy metals in

their composition. The Kyiv wastewater treatment plant (known as Bortnychi station of aeration) processes municipal and industrial sewage and run-off rain water. It accepts 9000 m^3 wastewater per day on an average. At present, 9 million tone of sewage sludge are accumulated on its territory [13].

Centralized wastewater treatment plants in Lithuania produce relatively small amounts of sewage sludge. The annual amount of dry sewage sludge produced in Lithuania is up to 50 thousand tons per year.

The special problem of this waste is heavy metals in its compound [16, 17]. The presence of these pollutants prevents the burial of sewage sludge and substantially limits its use in agriculture and forestry. A similar situation occurs when certain wastes (e.g., industrial, medical, military and sewage sludge) are destroyed in special devices known as incinerators, which leads to the formation of relatively high toxic waste in ash. Toxic residues (ash, slag, sediment of filters and sedimentation tanks) can be easily placed on landfills in case they were first immobilized and converted to non-leachable products. If these residues are heated to a very high temperature, then their main components, including minerals and toxic heavy metals, melt and take on a glassy appearance. This requires temperatures above 1700 K, which are not available in the most incinerators, but are easily achieved in plasma reactors [21]. The system of plasma vitrification of ash produces a chemically stable and mechanically strong substrate. After vitrification, this mineral product looks like a vitreous, similar in structure to basalt lava (even superior to basalt by mechanical strength); its main components are oxides of silicon, aluminum and calcium in the form of chemically inactive compounds that are resistant to washing. The effectiveness of this technology is convincingly confirmed by the data on the example of vitrification of the ash residue in a medical incinerator, given in Ref. [21].

A simple empirical estimate of the energy inputs required for the vitrification process is given in Ref. [26]:

$$\mathrm{M(kg)} = 0.35\mathrm{P(kWh)}, \tag{8}$$

where M is the mass of the vitrified product and P is the electrical energy consumed in the process. It is quite simple and allows you to calculate the energy required for the gasifier, regardless of the thermodynamic calculations associated with the conversion of carbon-containing raw materials.

4.1. Laboratory experiment

The equipment for hazardous waste processing created at the Institute of Gas, NASU was presented shortly above. Its fundamental advantage is using of water steam-plasma PT up to 160 kW of capacity. Nevertheless, such powerful and complex equipment cannot be used for laboratory studies to optimize the gasification processes of different types of carbon-containing raw materials. That is why relatively low-power industrial steam PT "Multiplaz 3500" up to 3.5 kW has been used in this research.

Components	H_2	CO	CO_2	CH_4
%. vol.	71.8	0.1	24.7	0.4

Table 3. Basic gasification products composition obtained from sewage sludge.

Quartz tube of inner diameter 3.2 cm and a length of 13 cm was used as a reactor model. It placed a portion of sewage sludge to be studied in the process of gasification. Aggregate data on the composition of treated dry products of gasification are presented in **Table 3** [13].

With these data, an equation for the reaction involving carbon, hydrogen, oxygen and organic matter was determined:

$$CH_{2.483}O_{0.530} + 1.334\ H_2O = 2.549H_2 + 0.111CO + 0.876CO_2 + 0.013CH_4. \tag{9}$$

Gross equation of sewage sludge in this reaction correlates well with the results of independent chemical study in Ukraine for their composition.

Analyzing the results of this experiment, it should be noted its main disadvantage associated with the overall low efficiency of the gasification process, despite even a relatively high yield of hydrogen. Indeed, most of the carbon in process (9) is directed to the production of a ballast gas CO_2, rather than a combustible CO. Thus, this experiment cannot be considered as too successful in terms of achieving the ultimate goal of the process – high energy efficiency.

The main reason for this result appears to be the low wall temperature of the reactor-quartz tube, which in these studies was 430–480°C. The two processes seem to contribute for the syngas production: the actual steam-plasma gasification of the raw material on the tube axis, where the temperature determined by the PT jet is quite high, and the so-called water gas shift reaction at the walls of the tube.

$$CO + H_2O \rightarrow H_2 + CO_2. \tag{10}$$

The optimal temperature for this reaction is just about 500°C [27]. This assumption is also supported by the very high content of CO_2 in the reaction products in a small diameter quartz tube (**Table 3**), if compared with our experimental data in the full-scale reactor presented in **Table 2**.

Equally important and negative factor was also the low reaction rate of carbon in such a system, which exponentially depends on the temperature. As a result, a significant part of steam as gasifying agent passes a small reactor, not reacting with the raw material, which in general predetermines the low energy efficiency of the process.

Already in appearance of the gross equation, it follows that sewage sludge should have good energy characteristics, based on the ratio of the hydrogen and oxygen components in its composition [27]. In the further basic thermodynamic estimates, we selected a simple and convenient for estimation the gross sewage sludge equation in the form of $CH_{2.5}O_{0.5}$ for which an analysis of the processes of plasma-steam gasification is performed later.

4.2. Thermodynamic calculation of the gasification process using plasma technologies

4.2.1. Generalized reaction of gasification

At present, quite a lot of software tools have been developed and used for quantitative analysis of gasification processes. However, with all the advantages of numerical calculations, such publications leave "in shadow" basic physical and chemical regularities. Just the knowledge of their characteristics built a clear understanding of the analyzed process. In reality, the basis of the quantitative description of gasification lie very simple thermodynamic relations arising from the laws of Hess used in thermochemistry [28]. It should be borne in mind only the features associated with the operation of the plasma source [29].

Following Refs. [29–31], the process of plasma-steam gasification can be represented by the gross equation in a sufficiently general form:

$$CH_xO_y + wH_2O + mO_2 = n_1H_2 + n_2CO + n_3CO_2 + n_4H_2O + n_5CH_4 + n_6C + Q_{TR}, \tag{11}$$

where $Q_{TR} = Q_R + \Delta Q$ is the total thermal energy that is released as a result of the chemical reactions Q_R and due to some additional source of heat energy ΔQ (so far we do not necessarily associate it with the energy of the plasma jet Q_{PL}), so that the reaction mixture reaches the desired temperature T_P of the gasification products, w and m—the amount of water and oxygen, per 1 kmol of waste, n_1, n_2, n_3, n_4, n_5 and n_6 are the coefficients for the corresponding reaction products. Among the latter are gases, most often obtained in the composition of gasification products and soot. In this formula, the energy term in the form presented was introduced in our paper [29]. It allows to distinguish the role of an additional source of energy ΔQ in viewpoint of achieving the optimal, predictably perceived, temperature T_P of the gasification process.

The "ideal" process of plasma-steam gasification would correspond to the case when only H_2 and CO would be present on the right side. Formally, it is possible to make many options of reaction (11) with various stoichiometric coefficients, including the relevant "ideal" process. However, in accordance with the second law of thermodynamics, nature chooses only such a path and the completion of the varying reactions, in which the principle of maximum entropy is realized:

$$\mathrm{dS} \geq \mathrm{dQ}/T. \tag{12}$$

Special software—"TERRA" thermodynamic calculations system is used for the conversion processes quantitative analysis with a glance of the accompanying reactions [32]. It also allows to determine the necessary amount of energy expenditure for carrying out reactions.

4.2.2. Plasma-steam gasification

Analysis of the process of plasma-steam gasification was made on a more optimal than (9) reaction:

$$CH_{2.5}O_{0.5} + 0.5H_2O = CO + 1.75H_2 \quad + Q_{TR}. \tag{13}$$

The heat of combustion of sewage sludge Q_{LSS} required to determine the energy of the process is determined on the basis of Mendeleev's Eq. [27]:

$$Q_{lSS} = -100\cdot(81\cdot c_C + 246\cdot c_H - 26\cdot(c_O - c_S) - 6\cdot c_W\ )\cdot 4.19\ kJ/kg, \tag{14}$$

where c_C, c_H, c_O, c_S and c_W are mass fractions of carbon, hydrogen, oxygen, sulfur and water. (Mendeleev's equation is an analog of the relations known in the Western scientific literature as Dulong or Milne equation.) As may be shown, this heat of combustion of sewage sludge is Q_{LSS} = −25.68 MJ/kg [33]. Following the law of Hess, its enthalpy of formation is $\Delta H^0_{CH2.5O0.5}$ = −76.8 kJ/kg [33].

The thermodynamic analysis of the sewage sludge conversion process carried out in the TERRA software [32] allows to determine the composition of its gasification products as a function of temperature. As it turned out, both for the reaction (12) and for other considered reactions, it is characterized by the practical completion of the gasification processes at 1250 K. More strictly, the mass fraction of the traces of CO_2, H_2O and CH_4 among the products of gasification at this temperature does not exceed 1–2%. As it turned out, the energy $Q_{PL}(T)$, which must be additionally introduced with a plasma torch per 1 kg of reagent mass in (12), to reach this temperature, is 0.785 kWh/kg. This parameter allows to determine the productivity of the gasifier at a given power of the PT.

Knowing the calorific values for CO and H_2, as well as the composition of the products obtained in the reaction (12), it is easy to determine the calorific value of the resulting syngas in this process W_{SG} = 6.23 kWh/kg. It allows to define the energy output of the gasification plant and its energy efficiency on the basis of a comparison with the specific energy Q_{PL} introduced into the reactor.

The value W_{SG} significantly exceeds the electricity consumption 0.785 kWh/kg by steam PT to produce 1 kg of syngas. Thus, even taking into account the relatively low efficiency of η_{EE} ~ 0.3 of electricity generation, the energy consumption is much lower than the level of energy of syngas produced. Indeed, taking into account also the efficiency of the PT at η_{PL} = 0.8, this is enough to ensure the operation of the PT, since it exceeds the value of ΔQ = 0.785 kWh/kg:

$$W_{SG}\cdot\eta_{EE}\cdot\eta_{PL} = 6.23 \times 0.3 \times 0.8 = 1.5\ kWh/kg > 0.785\ kWh/kg. \tag{15}$$

It is good preconditions for the energy self-sufficiency of the sewage sludge processing and the production of additional energy to compensate the role of raw materials moisture and ash residue vitrification or for the production of electricity for external consumers.

4.2.3. Plasma-steam-oxygen gasification in stoichiometric mode

Significant increase of conversion efficiency can be achieved by the addition of oxygen into the process. At the first stage, an "ideal" conversion reaction was considered, in which the number

of reagents, in contrast to (13), contained also oxygen, and among the reaction products syngas components only were present:

$$CH_{2.5}O_{0.5} + KH_2O + LO_2 \rightarrow CO + MH_2 + Q_{TR} \tag{16}$$

where *K, L, M* are coefficients that determine the content of components such as steam and oxygen, as well as the hydrogen one in the reaction products, respectively, under the stoichiometric reaction with respect to syngas production. Thus this reaction is stoichiometric as well as (13) for obtaining products of gasification as synthesis gas only. Nevertheless it has the most wide functional possibilities to achieve the best index of energy efficiency of the process as it allows varying the composition of the gasification agent. In determining the energy efficiency, naturally, the consumption of energy for oxygen production should also be taken into account. The range of possible specific energy consumption in the technological process of obtaining the oxygen itself is chosen as P_{O2} = 0.35–1 kWh/m^3. The first one corresponds to promising technologies, the second one is realistic today. Quantitative index of energy efficiency of the conversion process is the ratio

$$\eta = \left(P_{PL}^{C} + PO_2\right)/W_{SG}, \tag{17}$$

where $P_{PL}^{C} = \Delta Q/0.8$ is the electricity consumption for the production of plasma jet by efficiency of ~ 0.8 and for oxygen – P_{O2}. W_{SG} is the heat energy of syngas from 1 kg of the original raw mixture. In this form, it fully corresponds to the definition of energy saving (or energy efficiency) as energy costs (here, $P_{PL}{}^{J} + P_{O2}$) per unit productivity (here the product is syngas of energy W_{SG}).

The value of $L = 0$ in reaction (16) corresponds to the plasma-steam gasification (13), and the case $\Delta Q = 0$ is usual steam-oxygen technology, although their opposition does not make sense. Indeed, from the point of view of the process chemistry, in both cases, oxygen atoms, characteristic of these technologies, and hydrogen atoms, originally included in the gasified sewage sludge, are present in the reaction. For the noted limit values of *L*, the coefficient *K* takes the values $K_{max} = 0.5$ and $K_{min} = 0$, respectively. However, generally speaking, the reactions (16) can also correspond to the intermediate values of the coefficients *K* and *L*. Simple functions are determined on the basis of mass balances in reaction (16):

for oxygen

$$1{\cdot}0.5 + K + 2L = 1, or\ L = 0.25 - 0.5K; \tag{18}$$

for hydrogen

$$1{\cdot}2.5 + 2K = 2M, or\ M = 1.25 + K. \tag{19}$$

For clarity, the function (18), which characterizes the oxygen content of *L* as a function of the amount of steam *K* introduced by the PT, is shown in **Figure 3** as line 1. Line 4 represents the thermal power introduced into the reactor by a plasma jet at its nominal enthalpy of H_{PL} = 3.6 kW·h/kg in accordance with equation

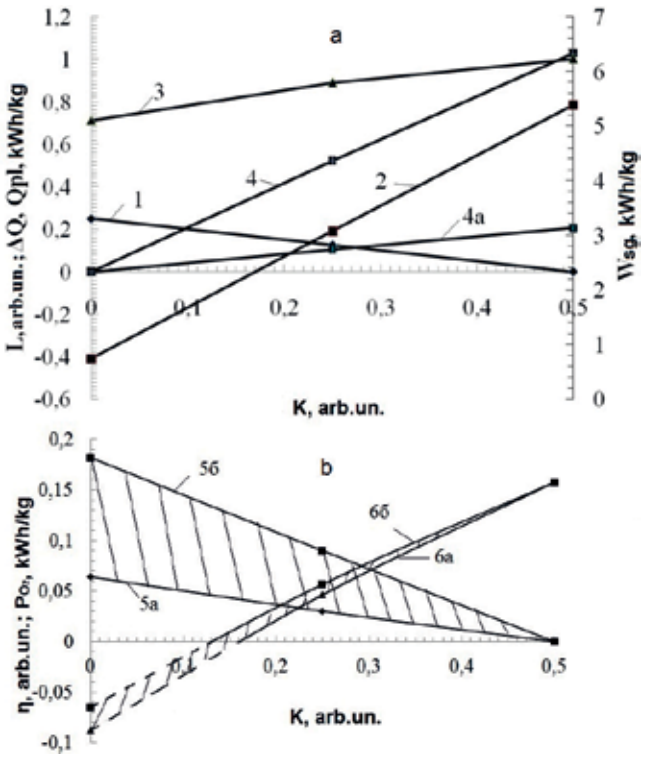

Figure 3. The main regularities characterizing the stoichiometric mode of gasification of the sewage sludge in the function of the amount of water introduced into the reaction K with plasma-steam jet – molar and energy ratios (a) and energy consumption for oxygen production and energy efficiency indicators of process (b): 1—oxygen content L introduced into the reactor; 2—additional energy ΔQ, which should be introduced in volume to achieve the operating temperature; 3—the energy of the producing syngas W_{SG}; 4, 4a—the energy introduced by the steam-plasma jet Q_{PL} with its enthalpy $H_{PL} = 3.6$ and 0.72 kWh/kg, respectively; 5a and 5b—energy consumption for oxygen production at a specific consumption of energy 0.35 and 1 kWh/Nm^3, respectively; 6a and 6b—indicators of energy efficiency of the process at the corresponding specified energy consumption for the production of oxygen.

$$Q_{PL} = H_{PL} m H_2O, \tag{20}$$

where mH_2O corresponds to the mass of water in the jet injected per kg of reagents. This enthalpy value corresponds to the moderate operating mode of the PT used in Ref. [9]. In principle, the higher values of plasma enthalpy, corresponding to the forced operating regime of the steam PT, can be achieved.

It can be concluded that the introduction of oxygen in the stoichiometric mode of gasification with the use of plasma technologies corresponds to an increase in the energy efficiency of the process. As it follows from **Figure 3b**, the maximum value η in the process (which corresponds to the highest value of the additional energy ΔQ and, consequently, the worst energy efficiency) occurs exactly when the oxygen content is $L = 0$, for which $K = 0.5$ corresponds—that is, on the right side of each graph. On the contrary, the value η decreases with a gradual increase of the oxygen content L (i.e., moving to the left along the abscissa).

Area $K < 0.17$ corresponds the negative values $\Delta Q < 0$ (**Figure 3**); this means that excess heat energy is released in the reaction zone, which can be used for the ash residue's vitrification. The level of energy consumption for this need is difficult to determine in general terms, but empirical ratio (13) is known for them. In this area, lines 6 characterizing the level of energy efficiency of the process η are indicated by a dashed line. This is emphasized by the fact that here the energy costs for maintaining the gasification process are negative. In other words, there is an energy release.

In the absence of a PT, the stoichiometric gasification regime according to the reaction (15) is realized for a single value $K_0 = 0.17$, corresponding to the intersection of line 2, which characterizes the required energy level ΔQ with the coordinate axis. It, in turn, corresponds to the moisture content of sewage sludge of about 10%, if it is determined from the composition of the reagents on the left side of the reaction (15). This moisture value is characteristic just for the conditioning of sewage sludge, which are currently dried with the help of those or other drying technologies.

However, the range of values $K = 0.17$ and near it for practical operation of the gasifier should be excluded, because the software TERRA reveals a significant soot formation, which makes it unacceptable for gasification. Thus, solving also the problem of obtaining more high quality syngas, it is expedient to move along line 2 to its maximum value corresponding to the stoichiometric regime at $K = 0.5$ (**Figure 3**). The results obtained are presented in **Table 4**. As can be concluded, an increase in the amount of water introduced into the process L is twice, corresponds to a worsening of energy efficiency of the conversion process η by a factor three.

4.2.4. Non-stoichiometric mode of plasma-steam-oxygen gasification

The introduction of a significant amount of energy with a plasma jet markedly worsens the indicator of the energy efficiency of the plant, as follows from **Figure 3b** and **Table 4**. Therefore, it is of interest to compare it with the non-stoichiometric regime, which can be easily

Parameter		**K, arb.un.**	
		0.25	**0.5**
L, arb.un.		0.125	0
ΔQ, kWh/kg		0.19	0.785
P_{PL}^{C}, кВт·ч/кг		0.24	0.98
P_{O2}, kWh/kg	$p_{O2} = 0.35$ kWh/Nm^3	0.03	0
	$p_{O2} = 1$ kWh/Nm^3	0.09	0
$W_{CГ}$, kWh/kg		5.79	6.23
η, arb.un.	$p_{O2} = 0.35$ kWh/Nm^3	0.046	0.15
	$p_{O2} = 1$ kWh/Nm^3	0.057	0.16

Table 4. Calculated parameters characterizing the stoichiometric process of conversion of sewage sludge at its humidity of 10% to synthesis gas using plasma technology, depending on the additional amount of water vapor introduced with the plasma jet.

realized for the same value of L_0 = 0.165, as in the stoichiometric regime at the point K_0 = 0.17, but at K > 0.17. Therefore, it is advisable to introduce excess oxygen into the reactor.

In this case, in order to optimize the plasma-steam gasification process of sewage sludge, the next reaction was analyzed:

$$CH_{2.5}O_{0.5} + KH_2O + LO_2 \rightarrow CO + MH_2 + ECO_2 + DH_2O + Q_{TR}. \quad (21)$$

This gasification mode is called "non-stoichiometric", as there are the products of partial combustion of sewage sludge—CO_2 and H_2O—among the products of gasification. In determining the parameters of the process in the non-stoichiometric mode of gasification, it should be taken into account that, in addition to the syngas, the ballast components are formed from the unit mass of the initial reagents. In other words, the correction factor should be taken:

$$W^*_{SG} = [(mCO + mH_2)/(mCO + mH_2 + mH_2O)]W_{SG} = k_{NS}W_{SG}, \quad (22)$$

where k_{NS} is the non-stoichiometric coefficient.

Recall that, in principle, it is possible to compose many variants of the reaction (21) with the different stoichiometric coefficients. However, in fact, only those are actually realized where maximum entropy principle is satisfied (see Eq. (12)). Examples of the resulting compositions of gasification products are shown in **Table 5**.

Using these data, the parameters of non-stoichiometric gasification regimes for K = 0.25 and 0.5 were calculated (**Table 6**).

Analyzing the results presented in **Table 6**, it should be borne in mind that they are not energetically self-consistent. Indeed, with an oxygen content L_0 = 0.165, a relatively small additional thermal energy ΔQ = 0.04–0.09 kWh/kg is required. **Table 6** also shows the energy introduced with a jet of a PT operating in our ordinary energetic mode with enthalpy H_{PL} = 3.6 kWh/kg [9] and – for comparisons – in a much less intense mode H_{PL} = 0.72 kWh/kg. One can conclude by comparing the values of ΔQ and H_{PL} between each other, that in this regime one can confine ourselves to a low-power PT. Otherwise, the excess energy of the plasma torch can be used to vitrify the ash residue. Thus, the final analysis causes a significant decrease in the value η compared with the data in **Table 4**. Here it should be taken into account that when working with moist sewage sludge, the energy introduced by the PT is proportional to $\Delta K = K - K_0$. The introduced thermal energy levels at K = 0.5 exceed the noted values ΔQ and, in the absence of

The water content in reagents, the mole fraction of K	Composition of gasification products, wt.			
	CO	H_2	CO_2	H_2O
0.25	0.84	0.089	0.034	0.032
0.5	0,.69	0.083	0.11	0.117

Table 5. Composition of gasification products in non-stoichiometric mode with oxygen content L_0 = 0.165 according to the calculated data in the TERRA software.

energy consumption for vitrification, would lead to overheating of the internal volume of the gasifier.

The consumption of electrical energy for the production of a plasma jet with a much lower enthalpy—0.72 kWh/kg is also shown in **Figure 3a**. Without even carrying out detailed calculations, it can be concluded that the use of a less powerful PT would lead to an improvement of the energy efficiency of the process, since it is the level of energy expenditure for the operation of the PT that determines its effectiveness.

The calculated data of **Table 6** can be useful for assessing the efficiency of the sewage sludge gasification installation, depending on the presence of the mineral mass, which requires vitrification, in its composition. For this, it should be taken into account that at $K = 0.5$, the next excess energy P is introduced into reactor:

$$P = (Q_{PL} - \Delta Q)/0.8 = (0.58 - 0.09)/0.8 = 0.6\,\text{kWh/kg} \tag{23}$$

(when recalculating to electrical energy to power PT). To determine the permissible content of the mineral part in the initial sewage sludge, it is necessary to use the relation (7). If there is a mineral mass in the composition of sewage sludge at a rate of M per 1 kg, the amount of excess energy produced is converted into electric energy, which will be *P(1 - M)*, and it, in turn, can be consumed for vitrification according to (7). Hence we can define M:

$$M(kg) = 0.35P(1 - M), \tag{24}$$

where the difference in parentheses characterizes the amount of syngas obtained from 1 kg of the mixture. It follows that $M = 0.17$ kg. Thus, the data of the last column of **Table 6** for the

Parameter		**K, arb. un.**	
		0.25	**0.5**
L_0, arb. un.		0.165	0.165
ΔQ, kWh/kg		0.04	0.09
Q_{PL}, kWh/kg	H_{PL} = 3.6 kWh/kg	0.16	0.58
	H_{PL} = 0.72 kWh/kg	0.03	0.12
P_{O2}, kWh	p_{O2} = 0.35 kWh/Nm^3	0.04	0.035
	p_{O2} = 1 kWh/Nm^3	0.114	0.1
k_{NS}, arb. un.		0.934	0.807
W_{SG}*, kWh/kg		5.44	5.11
η, arb. un.	p_{O2} = 0.35 kWh/Nm^3	0.015	0.023
	p_{O2} = 1 kWh/Nm^3	0.028	0.033

Table 6. Calculated parameters characterizing the non-stoichiometric process of sewage sludge conversion with its 10% humidity in syngas with oxygen content $L_0 = 0.165$ using plasma technology depending on the amount of water steam $K > K_0$ introduced with plasma jet.

index of the energy efficiency of the gasification equipment are valid up to 17% of the mineral content in sewage sludge to be vitrified.

A more rigorous problem of the non-stoichiometric gasification regime, self-consistent with respect to energy consumption, is also considered. It was solved on the basis of varying the values of L in the reaction (21) for a given value of K. The value of L was determined at which the compensation of the emerging thermal energy deficit ΔQ is attained due to the energy of the plasma jet introduced with the indicated quantity K of water steam at a certain enthalpy. In other words, it was determined at which values of L the condition $\Delta Q(L) - Q_{PL} = 0$ is reached.

The main regularities, which ultimately represent the efficiency of the non-stoichiometric gasification process with a small enthalpy of H_{PL} = 0.72 kWh/kg of the plasma jet and in its absence, that is, for wet bottom sludge are shown in **Figure 4**.

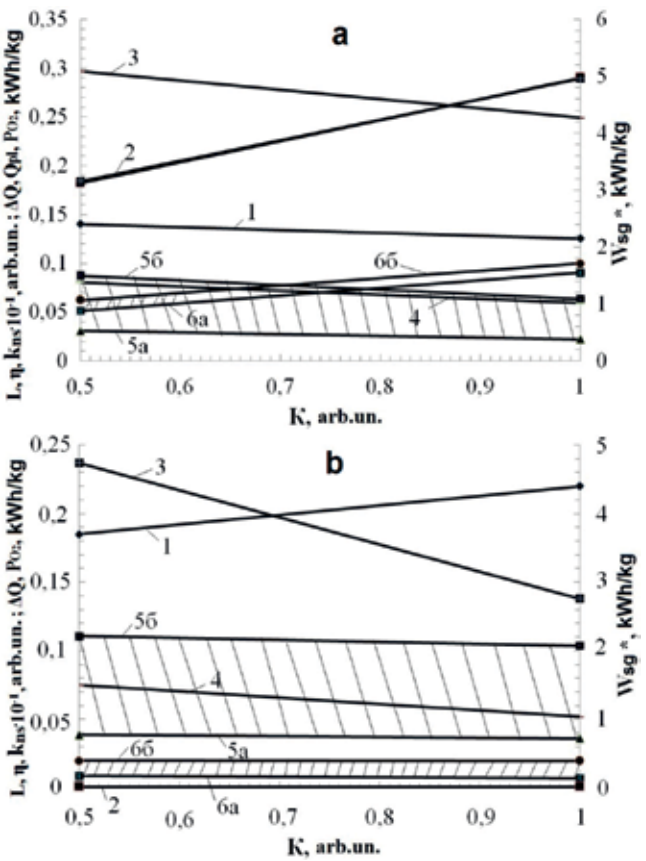

Figure 4. The main regularities characterizing the energy efficiency of non-stoichiometric modes of sewage sludge gasification as a function of the amount of water vapor K introduced into the reaction with the enthalpy of the plasma jet H_{PL} = 0.72 kWh/kg (a), and also, in its absence, for wet sewage sludge (b): 1—the oxygen content L introduced into the reactor; 2—additional energy ΔQ, which should be introduced into the volume to reach the operating temperature, equal to the energy introduced by the steam-plasma jet Q_{PL} (the latter—with the exception of wet sewage sludge); 3—the energy of the syngas W_{SG}*; 4—coefficient of nonstoichiometryk_{NS}; 5a and 5b—energy consumption for the production of oxygen at a specific consumption of 0.35 and 1 kWh/Nm^3, respectively; 6a and 6b—energy efficiency index of the process at the indicated energy inputs for the production of oxygen, respectively.

In the first of these cases, the energy efficiency index in the entire range of moisture content K in the reacting mixture does not exceed 0.1 (**Figure 4a**). Even better is the efficiency index of the steam-gasification, that is, in the second case, when its value does not exceed 0.05. However, one should realize that in the reactor space the vitrification and gasification zones are not so separated in space that some of the energy of the plasma jet is not consumed by the gasification processes. Therefore, we believe that, in general, the proposed technology can ensure the energy efficiency of the gasification process for sewage sludge with an index not worse than 0.1.

Thus, practically all cases presented in **Figure 4**, the consumption of syngas for the electricity generation by means of a gas-diesel power station is only a fraction of the total volume of its production

$$PO_2 + \Delta Q_{PL}/0.8)/\eta_{EE} = \eta W^*_{SG}/\eta_{EE} \approx 0.1\eta W^*_{SG}/0.3 \approx 0.33 W^*_{SG}. \tag{25}$$

In the variant represented by the last equation, this part is only 30% of the energy for the synthesis gas obtained (in deriving these relations, Eq. (17) was used). Accordingly, the remaining part of it can be spent, for example, for the production of electrical energy to external consumers, which will facilitate the commercialization of this development. Thus, in the variant proposed, the processing technology corresponds well to the general idea of numerous publications in the world literature, known as the Waste-to-Energy.

It should be emphasized that the sensitivity of the estimates has been obtained from the selected composition of carbon-containing gasified raw materials. Therefore, further development of these studies requires variation of this composition, as well as more strictly quantitative fraction of the mineral component of the sewage sludge. The same applies to other types of hazardous waste. This part of the publication is the methodological basis for such an analysis. In accordance with this, the role of the plasma part of the technology can also increase or, conversely, decrease. Nevertheless, especially for multi-purpose installations, its role from the point of view of the environmental safety of the process remains unchanged.

5. The state of design and construction of the shaft reactor for waste treatment plant based on plasma-steam-oxygen technology

5.1. Features of the project

In 2017, the Institute of Gas of the National Academy of Sciences of Ukraine completes the execution of the state order for development of steam-plasma technology for the processing of sewage sludge with the support of the Ministry of Education and Science of Ukraine. The result will be a reactor module for waste treatment based on plasma-steam-oxygen technology, which can become the core of plants for the recycling of hazardous waste: bottom sediments of aeration stations of urban water purification systems, unsorted solid household wastes (they are dangerous because of the risk of entering into their composition of chlorinated compounds), medical waste, overdue pesticides and chemical treatments for plants, etc. The module is designed in such a way as to ensure its payback through the production of electrical

energy through the products of gasification of carbon compounds in the waste. At the heart of the implementation of this project lie precisely the above calculations.

Unlike the previous development [9], the peculiarity of this shaft reactor is the loading of raw materials through its side wall. This will allow, on the one hand, to comply with the operating mode of the reactor, which meets the requirements of the Directive 2000/76/EC [15] for the processing of chlorine-containing waste. On the other hand, the operation of the PT will contribute to the achievement of the temperature regime characteristic for the vitrification of the ash residue, thus solving the problem of handling wastes containing heavy metals. The reactor capacity will be up to 500 kg/h depending on the type of waste. In terms of annual capacity, this will be up to 4000 tons per year, based on the 11-month cycle of work. The reactor will be tested this year, completely with equipment previously developed as part of a medical waste treatment plant [9]. The general view of the reactor of this plant is shown in **Figure 5**.

Researchers of LEI are also projecting a novel plasma volume reactor (**Figure 6**) to create steady non-transferred plasma ambient. It will allow the destruction wide range of hazardous substances.

The primary shield of the reactor is made up of steel (1500 mm of height × 1500 mm of width) with high temperature ceramic inner lining. Initially, it has hopper for waste feeding with single door arrangement. The door operation is manual. The chamber has several ports, 350 mm above the bottom of the chamber for mounting air or nitrogen PT. It is expected the plasma arc reactor have very high destruction efficiency and will be very robust. It is considered that it will be able to treat any waste with minimal or no pretreatment and produce a single waste form as gas and slag. The designed arc reactor has carbon anode and will strike an arc in a bath of molten slag. The higher temperatures will be reached by the arc convert the organic waste into light organics and primary elements. The system is under further development.

5.2. Economic assessments

Estimated construction cost of the plant for processing hazardous waste using the proposed reactor module will be about 1.2 million USD. If we compare it with the data of the publication

Figure 5. The reactor module body for plasma-steam-oxygen waste treatment in the stage of its installation.

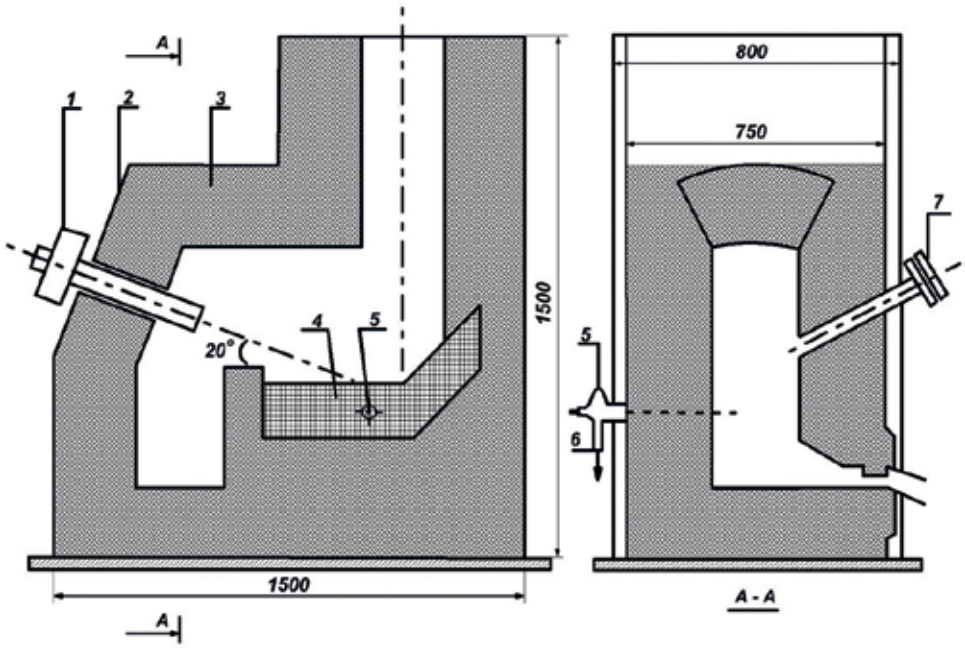

Figure 6. Plasma arc reactor. 1—Plasma torch; 2—Metallic shield; 3—Lining alloy; 4—Graphite plate; 5—Circular channel; 6—Observation window.

Youngchul Byun et al. [7], in terms of present value to the daily capacity of the reactor 12 TPD, this is noticeably less. The latter is due to the low cost of labor in present-day Ukraine. The estimates obtained in this article make it possible to compare its economic indicators with other developments presented in the Ukrainian market, among them, Waste-to-Energy Plant "Energy-2" from Brno [34], Integrated Multifuel Gasification technology (IMG) of Bellwether Recuparative Gasification Ltd. [35] and Westinghouse Plasma Corporation [36]. **Table 7** shows the main technical and economic indicators that characterize the operation of these plants according to the references given. These include: C—annual capacity of equipment (t/a), P—power generation of electricity to consumers per year (MW·h/a), I—investments. As can be

Indicator	Technology			
	"Energy-2" [34]	**IMG [35]**	**WPC [36]**	**IG NASU (project, this paper)**
C, t/a	224,000	100,000	534,000	4000
P, MW·h/a	63,000	68,000	427,000	4200
I, USD(€)	130 mln. €	65 mln. €	307.5 mln. USD	**1.2** mln. USD
I/C, USD(€)/t	580	650	575	300
P/C, kW·h /t	240	680	800	1050
Payback (in the absence of operating costs), years	61.9	28.7	20	8

Table 7. Comparison of the main technical and economic indicators of some waste-processing plants in Ukraine (see explanation in the text).

seen, the traditional waste-processing plant [34] "Energy-2" requires specific investments I/C, close to the plasma technologies [35, 36]. On the contrary, it has the worst indicators P/C concerning the possibility of investment return due to the production of additional electric energy for external consumers. All three samples of technologies [34–36] have a very high cost; it cannot be compensated by production of additional electric energy. Some additional reduction of payback is achieved by the presence of a "green tariff" in Ukraine for electric energy.

Thus, the proposed plasma-steam-oxygen technology of waste treatment has the highest calculated efficiency indicators compared with the developments under discussion. At the same time, it provides high levels of environmental safety. Further to improve the efficiency of this technology, it can facilitate the transition to more efficient methods of electricity production from syngas obtained [13]. This will lead to increasing value η_{EE} and, respectively, further decrease of the part of synthesis gas that is used for energy self-sufficiency of gasification equipment. Such prospects are associated primarily with fuel cell technology that has significantly greater efficiency than gas-diesel power stations.

6. Conclusion

Contrary to popular belief among experts in classical thermal physics, the process of plasma gasification, even in the absence of oxygen blasting, can be maintained in the regime of energy self-sufficiency.

The most general assessments of ecological benefits and energy efficiency of plasma-steam gasification technologies are presented. It is shown based on the thermodynamic study that processing of sewage sludge using plasma technologies can be commercially attractive.

The described hazards treatment system has the ability to accept a wide range of waste materials and as such can be regarded as a mobile and flexible treatment system. This system can be applied to treat high toxic wastes containing both organic and inorganic substances.

The results show that hazards treatment technology can process highly toxic organic and inorganic substances with the efficiency of 99.99%.

The results on heat balance and heat transfer point that the combustion process takes place over all the reactor volume. The incineration process finishes through the entrance section ($x/d < 1$) of the reactor chamber.

Acknowledgements

The study one of the authors (V. Zhovyansky) was supported by Ministry of Education and Science of Ukraine, project "The development of steam-plasma technology of aeration stations sewage sludge conversion" and the National Academy of Sciences of Ukraine, programs "Prospective study of plasma physics, controlled thermonuclear fusion and plasma technology" and "Basic aspects of renewable-hydrogen power and fuel cell technology".

Author details

Victor Zhovtyansky[1] and Vitas Valinčius[2]*

*Address all correspondence to: vitas@mail.lei.lt

1 Institute of Gas of the National Academy of Sciences of Ukraine, Kyiv, Ukraine

2 Lithuanian Energy Institute, Kaunas, Lithuania

References

[1] Gorokhovski M, Karpenko EI, Lockwood FC, Messerle VE, Trusov BG, Ustimenko AB. Plasma technologies for solid fuels: Experiment and theory. Journal of the Energy Institute. 2000;**78**(4):157-171

[2] Rutberg PG. Plasma pyrolysis of toxic waste. Plasma Physics and Controlled Fusion. 2003;**45**:957-969

[3] Chernets OV, Korzhyk VM, Marynsky GS, Petrov SV, Zhovtyansky VA. Electric arc steam plasma conversion of medicine waste and carbon containing materials. In: Jones JE, editor. Proceedings of XVII GD; 7–12 September, 2008; Cardiff, Wales: Cardiff University; 2008. pp. 465-468

[4] Hrabovsky M, Hlina M, Konrad M, Kopecky V, Kavka T, Chumak O, Maslani A. Thermal plasma gasification of biomass for fuel gas production. Journal of High Temperature Material Processes. 2009;**13**(3–4):299-313

[5] Ducharne C. Technical and economic analysis of Plasma-assisted Waste-to-Energy processes. Earth Engineering Centre, Columbia University. 2010. p. 50

[6] Brattsev AN, Kuznetsov VA, Popov VE, Ufimtsev AA. Arc gasification of biomass: Example of wood residue. High Temperature. 2011;**49**:244-248

[7] Byun Y, Cho M, Hwang S-M, Chung J. Thermal plasma gasification of municipal solid waste (MSW). In: Yun Y, editor. Gasification for Practical Applications. Rijeka, Croatia: InTechOpen; 2012. pp. 183-210

[8] Zhang Q, Dor L, Fenigshtein D, Yang W, Blasiak W. Gasification of municipal solid waste in the plasma gasification melting process. Applied Energy. 2012;**90**:106-112

[9] Zhovtyansky VA, Petrov SV, Lelyukh YI, Nevzglyad IO, Goncharuk YA. Efficiency of renewable organic raw materials conversion using plasma technology. IEEE Transactions on Plasma Science. 2013;**41**(12):3233-3239

[10] Fabry F, Rehmet C, Rohani V-J, Fulcheri L. Waste gasification by thermal plasma: A review. Waste and Biomass Valorization. 2013;**4**(3):421-439. DOI: 10.1007/s12649-013-9201-7

[11] Tamosiunas A, Valatkevicius P, Valincius V, Levinskas R. Biomass conversion to hydrogen-rich synthesis fuels using water steam plasma. Comptes Rendus Chimie. 2016; **19**:433-440. DOI: 10.1016/j.crci.2015.12.002

[12] Messerle VE, Mosse AL, Ustimenko AB. Municipal solid waste plasma processing: Thermodynamic computation and experiment. IEEE Transactions on Plasma Science. 2016; **44**(12):3017-3022

[13] Zhovtyansky VA, Kolesnikova EP, Yakymovych MV. Plasma-assisted waste-to-energy processes. Problems of Atomic Science and Technology. 2017;**1**(107):231-236

[14] Striugas N, Valincius V, Pedisius N, Poskas R, Zakarauskas K. Investigation of sewage sludge treatment using air plasma assisted gasification. Waste Management. 2017;**64**: 149-160. DOI: 10.1016/j.wasman.2017.03.024

[15] Council of the European Union. Directive 2000/76/EC of the European Parliament and of the Council of 4 December 2000 on the incineration waste. Official Journal of the European Communities. JOL. 2000;**L 332**:91-111. CELEX: 32000L0076

[16] Official Journal of the European Communities. Available from: http://eur-lex.europa.eu/LexUriServ/LexUriServ.do?uri=COM:2008:0030:FIN:en:PDF

[17] Gomez E et al. Thermal plasma technology for the treatment of wastes: A critical review. Journal of Hazardous Materials. 2009;**161**(2–3):614-626

[18] Materazzi M et al. Tar evolution in a two stage fluid bed–plasma gasification process for wastevalorization. Fuel Processing Technology. 2014;**128**:146-157

[19] McGrath S. Persistent organic pollutants and metals from sewage sludge: Their effects, on soil plants and food chain. In: Langenkamp H, Marmo L, editors. Workshop on Problems Around Sewage Sludge; 18–19 November, 1999; Italy Proceedings-European Commissions Joint Research Center; 2000. p. 242

[20] Balgaranova J. Plasma chemical gasification of sewage sludge. Waste Management & Research. 2003;**21**:38. DOI: 10.1177/0734242X0302100105

[21] Cedzynska K, Kolacinski Z, Izydorczyk M, Sroczynski W. Plasmavitrification of waste incinerator ashes. In: International Ash Utilization Symposium; Centre for Applied Energy Research; 1999

[22] Valinčius V, Krušinskaitė V, Valatkevičius P, Valinčiūtė V, Marcinauskas L. Electric and thermal characteristics of the linear, sectional DC plasma generator. Plasma Sources Science and Technology. 2004;**13**(2):199-206. ISSN 0963–0252

[23] Zhukov MF, Zasypkin IM. Thermal Plasma Torches: Design, Characteristics, Applications. United Kingdom: Cambridge International Science Publishing; 2007. 596p

[24] Solonenko OP. Thermal Plasma Torches and Technologies. Cambridge International Science Publishing; 2000. 410p

[25] Snapkauskienė V, Valinčius V, Valatkevičius P. Heat transfer in the arc discharge channel. Heat Transfer Research. 2009;**40**(5):399-413. ISSN 1064-2285

[26] Leal-Quiros E. Plasma processing of municipal solid waste. Brazilian Journal of Physics. 2004;**34**(4B):1587-1593

[27] Ravich M.B. Efficiency of fuel use. Moscow: Nauka; 1977. 258p

[28] Prigozhin I, Kondepudi D. Modern Thermodynamics. From Heat Engines to Dissipative Structures. Moscow: Mir; 2002. 461p

[29] Zhovtyansky VA, Orlyk VM, Petrov SV, Yakymovych MV. General principles of waste treatment with recycling their energy potential based on plasma technology. Part I. Ecological requirements, the thermodynamics of the process and its energy efficiency. Energy Technologies and Resources. 2015;**4**:24-46

[30] McAllister S, Chen JY, Fernandez-Pello AC. Fundamentals of Combustion Processes (Mechanical Engineering Series). New York: Springer Science and Business Media; 2011. DOI: 10.1007/978-1-4419-7943-8_2

[31] Mountouris A, Voutsas E, Tassios D. Solid waste plasma gasification: Equilibrium model development and exergy analysis. Energy Conversion and Management. 2006;**47**:1723-1737

[32] Vatolin NA, Moiseev GK, Trusov BG. Thermodynamic Modelling of High-Temperature Inorganic Systems. Moscow: Metallurgy; 1994. 353p

[33] Zhovtyansky VA, Orlyk VM, Petrov SV, Yakymovych MV. General principles of waste treatment with recycling their energy potential based on plasma technology. Part II. Gasification of sewage sludge from water treatment plants. Energy Technologies and Resources. 2016;**3**:25-42

[34] Technical Overview of the Waste-to-Energy Plant in Brno, Plant for Region with 2 mil. People [Internet]. [Updated: 2017]. Available from: http://www.sako.cz/page/en/607/waste-to-energy/

[35] Integrated Multifuel Gasification Technology (IMG) of Bellwether Recuparative Gasification Ltd [Internet]. [Updated: 2017]. Available from: http://bwrs.eu/

[36] Technology of Plasma Gasification Westinghouse Plasma Corporation [Internet]. [Updated: 2016]. Available from: http://www.cleandex.ru/articles/2016/03/07/zavody_po_pererabotke_othodov_proizvodstva_i_potrebleniya_v_elektroenergiyu

Chapter 10

Small-Scale Energy Use of Agricultural Biogas Plant Wastes by Gasification

Dariusz Wiśniewski, Mariusz Siudak and Janusz Piechocki

Additional information is available at the end of the chapter

http://dx.doi.org/10.5772/intechopen.71700

Abstract

In Poland, there are 78 biogas plants producing a total electrical power of 85.94 MW. The byproduct of biogas plants is called a digestate. A single biogas plant with a power of 500 kW produces more than 10,000 ton of digestate per year. The goal of this chapter is to present a low-cost method of raw digestate processing with water content of about 94.55%, and also the results of thermal gasification of dried and pelletized digestate. Initial dehydration method is based on mechanical separation of the solid fraction in screw separator with a slot filter. Pre-dewatered digestate had been dried in biodrying process in semi-technical scale bioreactor. Afterward, the digestate was dried in tubular dryer and pelletized. The chapter covers the energy consumption for each stage of preparation of digestate for thermal gasification process. The gasification tests were conducted in fixed bed downdraft reactor. The chapter also features the physicochemical properties of digestate used in gasification process. The result of research on the gasification of drier digestate was gaseous fuel that does not differ from the quality of fuels obtained from the thermal treatment of other types of biomass.

Keywords: gasification, digestate, wastes, solid fuels, syngas

1. Introduction

The biogas production from agriculture waste in anaerobic digestion is a profitable direction for their energetic use [1, 2]. The byproduct of anaerobic digestion is called a digestate, which consists of both liquid and solid fractions. They can be separated using screw separators, presses, or decanter centrifuges. Liquid fraction can be used to fertilize farmlands because it

contains substantial amount of the elements necessary for plant growth. Liquid fraction can also be further treated and recirculated to the fermenter [3]. Solid fraction can also be used for agriculture or as a solid fuel, e.g., in the combustion process [4].

1.1. Digestate treatment in Europe

Nowadays, the digestate in the regulations is considered as waste in Europe. It does not have the status of a biofuel or an alternative fuel and is most commonly used as a soil improver. Such use often requires additional tanks to store the digestate mass to allow it to be used during fertilization periods. This can generate significant capital expenditure on the construction of liquid fraction storage tanks [5]. Another problem that causes the necessity of processing digestate is too small cultivable area where it can be used directly. Agricultural use of digestate is limited by the maximum allowable nitrogen dose of 170 kg N ha^{-1} y^{-1} [6]. For this reason, European countries have begun to use the separation of digestate to solid and liquid fraction. These fractions differ in physicochemical properties. As a result, a much smaller area for storage of digestate is required, while liquid fraction is again used to dilute the substrates to the fermentation process to the required 12% of dry matter. Liquid fraction can also be used as fertilizer by acquiring mineral compounds. It is characterized by lower phosphorus content and a higher content of nitrogen and potassium. Solid fraction is used in areas with low phosphorus content, liquid fraction on the other hand—in phosphorus saturated areas [7].

For fertilizer purposes, the liquid fraction is used either directly or in the production of mineral fertilizers through further purification. Further purification can be achieved through ultrafiltration in order to remove solid particles, followed by the reduction of high concentrations of nitrogen through stripping or crystallization of struvite [8]. These methods are used extensively in Germany and the Netherlands, and are mainly derived from a pig farm where ammonia load is very high.

For separation, screw separators with slot filter are most commonly used, which have previously been used successfully to separate liquid manure. Those devices feature low energy consumption because of low pressure of pumped digestate and low rotational speed of the screw shaft. Dry matter content obtained is about 30% of the solid fraction, while the liquid fraction remains about 4% of the dry matter. More advanced equipment, such as decanter centrifuges or belt presses, allow more efficient operation, but are rarely used in small biogas plants because of high investment costs.

Often solid fraction of digestate is processed in composting process, which reduces its volume, moisture, and improves fertilizer and storage properties [9]. Separation devices are often directly integrated with composting reactor, e.g., container with moving floor and aeration system or drum reactor.

Another method often used is drying in belt or drum dryers using the heat from CHP units. Dried digestate is used to produce pellets for energy purposes or for use as bedding for animal farm [10].

2. The treatment of raw digestate

A digestate from a pilot biogas plant located at the Experimental Station in Bałdy, Poland (N54° 36′ 1.8073″, E20° 36′8.5295″) was used in this research. The following technological parameters of the fermenter were used [11]:

- Feedstock moisture—90%
- The total batch fed to a digester—1.2 m^3
- The total load of organic compounds—2.3 kg VS/m^3
- The set temperature during the fermentation process—35 to 40°C
- Residence time in the pre-fermentation tank—3 days
- Residence time in the fermentation chamber—20 days
- Residence time in the post-fermentation tank—20 days

Tables 1 and **2** show the properties of the raw digestate.

2.1. Mechanical dewatering of digestate

Raw digestate from biogas plant has been pre-dewatered in screw separator with slot filter with a filter gap of 0.5 mm. Raw digestate contained 94.55% of water. Energy consumption of the mechanical dehydration process was measured using the Schneider ION7650 electrical network meter. In separation process test 0.035 m^3 of raw digestate was used. **Figure 1** shows the photograph of the screw separator.

As a result of the separation process, 30 kg of liquid fraction and 5 kg of solid fraction was obtained. Energy consumption during the experiment was 0.02 kWh. The tests were carried out without the pump forcing the digestate pressure in the separator. Digestate was fed to the separator only under its hydraulic pressure. Absence of pressure force does not interfere with separation operation and performance results may be lower than expected. The usage of a forced pump can increase productivity but can also increase the energy consumption of the process.

Parameter									
pH	Water content	Loss of ignition	N	N-NH_4	P_2O_5	K_2O	MgO	CaO	Na_2O
pH	%	% D.M.	% D.M.	mg/kg D.M.	% D.M.	% D.M.	% D.M.	% D.M.	% D.M.
8.24	94.55	68.97	7.16	1830.0	2.38	6.61	1.28	3.48	1.28

Table 1. Properties of raw digestate.

Parameter						
Cu	Zn	Mn	Fe	Salinity	S	Cl
mg/kg D.M.	mg/kg D.M.	mg/kg D.M.	mg/kg D.M.	g/dm^3	% D.M.	mg/dm^3
8.24	94.55	68.97	7.16	1830.0	2.38	6.61

Table 2. Contamination content in raw digestate.

Figure 1. The photograph of a screw separator with slot filter.

Based on the power and energy measurements and mass of the separated fractions, the energy consumptions of the mechanical separation process in the screw separator with slot filter was determined. Energy consumed for separating 1 kg of solid fraction from raw digestate was 0.004 kWh (14.4 kJ), while the separation of 1 kg of liquid fraction consumed 0.00066 kWh (2.37 kJ). Solid fraction after mechanical separation process contained an average of 76.1% of water.

2.2. Biodrying of digestate

The pre-dewatered digestate was used as a feedstock in biodrying process. Biodrying technology is typically used in the mechanical and biological treatment of wastes [12]. This technology involves the usage of heat generated by aerobic microorganisms in organic matter decomposition processes [13]. The general stoichiometric equation for the decomposition of the organic matter has the following form [14]:

$$C_a H_b O_c N_d + 0.5(ny + 2s + r - c)\, O_2 \xrightarrow{heat} n\, C_w H_x O_y N_z + sC\, O_2 + r\, H_2 O + (d - nz) N\, H_3 \qquad (1)$$

The amount of heat released during biological transformation has been investigated by many authors. The range of this value is from 17.8 to 24.7 (kJ/g decomposed dry matter of organic), calculated as removed organic matter, it can reach up to 28.0 kJ/g organic dry matter [15].

To increase porosity and permeability of the feedstock, the digestate was combined with wood chips in 1:1 mass proportion. The addition of woods chips also intended to reduce the water content of pre-dehydrated digestate to create the mixture with the optimal water content for biodrying process—from 50 to 70% [16]. During biodrying process in the reactor the temperature was measured in four points on different heights. Volume flow rate of the air supplied to the reactor was measured by thermoanemometer. The reactor was set on strain gauges to measure the change of feedstock's mass during the process. During biodrying process, energy consumption was measured using the electricity meter. Stream of air was supplied by side channel blower through floor of the reactor. **Figure 2** presents schematic diagram of the biodrying reactor.

The biodrying process was carried out using 730 kg of mechanically dehydrated digestate and 730 kg of wood chips to ensure adequate porosity of the mixture. Aeration ratio was of average 0.025 m^3 kg^{-1} h^{-1}. The process took about 4 weeks. **Figures 3** and **4** show the results of the process.

As a result of the biodrying process was the weight loss of 500 kg—68% of the initial weight of digestate and 34% of initial weight of combination of wood chips and digestate. Total electricity consumption for the biodrying process was 17.792 kWh, equivalent to 0.0295 kWh/kg of reduced weight. **Table 3** shows the energy properties of digestate after the biodrying process.

2.3. Thermal drying of digestate

Digestate after biodrying process was isolated from wood chips by drum sieve and thermally dried in a flow-through tubular dryer. The drying process was controlled by changing the

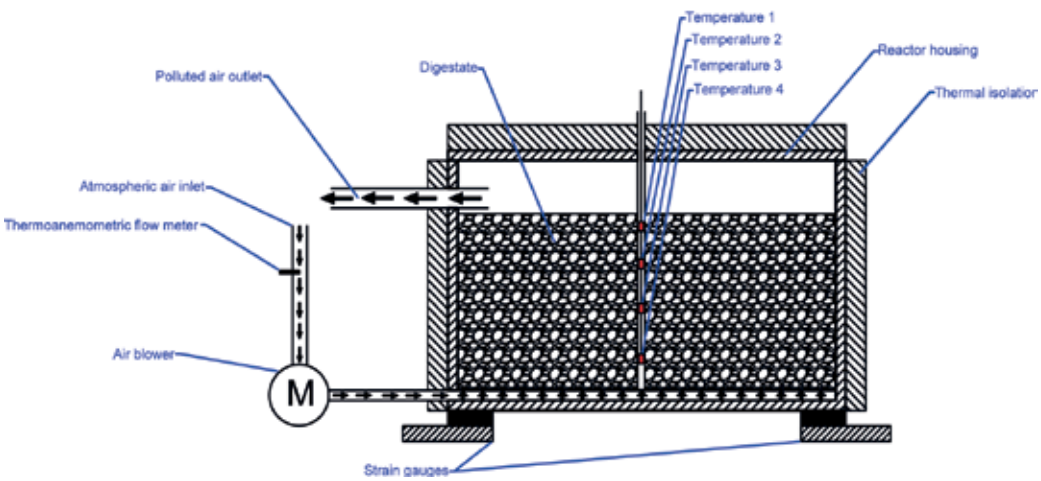

Figure 2. Schematic diagram of the biodrying reactor.

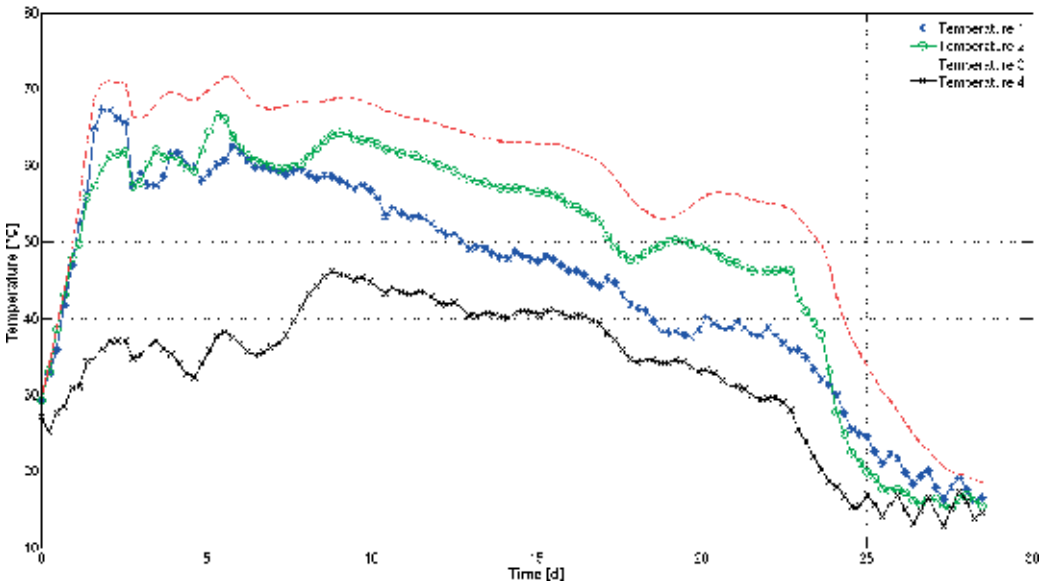

Figure 3. Temperature change graph during biodrying process.

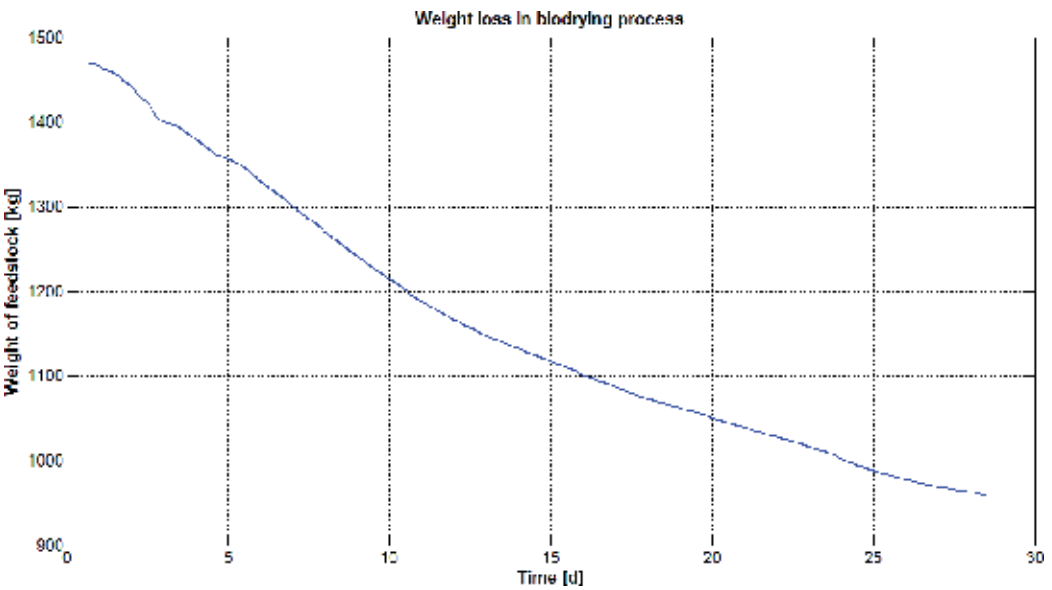

Figure 4. Mass change graph during the process.

feed rate of the dried material and the power of the electric heater. Energy consumption of the digestate thermal drying process was measured using the Schneider ION7650 electrical network meter. **Figure 5** shows a schematic of a tubular dryer.

Type of digestate	Parameter			
	Water content	Ash content	Heat of combustion	Calorific value
After biodrying	%	% D.M.	MJ/kg D.M.	MJ/kg
	43.67	18.07	17.82	8.97

Table 3. Energy properties of digestate after biodrying process.

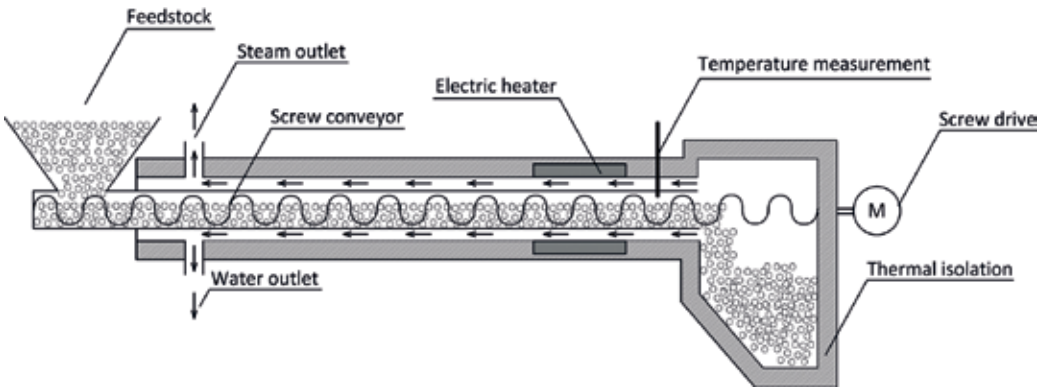

Figure 5. Schematic diagram of tubular dryer.

The tubular dryer was designed to allow steam and condensate drain-off in the initial part of the dryer. This design enables to transfer part of the heat energy of steam and condensed water to the dryer part before the electric heater, increasing the energy efficiency of the drying process.

Energy consumption test was carried out using 36.65 kg of digestate after biodrying process. The material feed rate was 2 m/min, temperature of drying process was about 150°C, and the ambient temperature was 12°C. The result of the drying process was mass reduction of 22.72 kg. The weight loss was 13.92 kg, and the water content of dried product was 9.15%. The drying process consumed 10.28 kWh, and the unitary electricity consumption for evaporation of 1 kg of water was 0.73 kWh/kg. The energy required to produce 1 kg of digestate with water content of 9.15% was about 0.136 kWh. **Table 4** shows the energy properties of digestate after thermal drying.

Type of digestate	Parameter		
	Water content	Ash content	Heat of combustion
After thermal drying	%	% D.M.	MJ/kg D.M.
	9.15	18.11	17.516

Table 4. Energy properties of digestate after thermal drying process.

Digestate after thermal drying process has been pelletized to increase of bulk density. Energy consumption for pelletization process was 0.085 kWh.

3. The gasification of digestate

3.1. Configuration of gasification system

Main features of the research gasification reactor:

- Reactor was designed and constructed as a downdraft
- Reactor without "throat" in oxidation zone
- Fixed bed reactor
- Thermal power about 200 kW
- Gasification agent—atmospheric air

Figure 6 shows schematic diagram of research gasification reactor. The reactor construction was mounted on strain gauges to real-time measurement of the reactor mass. This allows to determine the conversion speed of the batch material. The temperature measurement is carried out in four gasification zones and additionally in the outlet of syngas by thermocouples. Gasification agent is fed into the reactor by a side channel compressor, volumetric flow rate is measured by a rotameter. Syngas composition and calorific value are measured using the industrial GAS 3100R Syngas Analyzer.

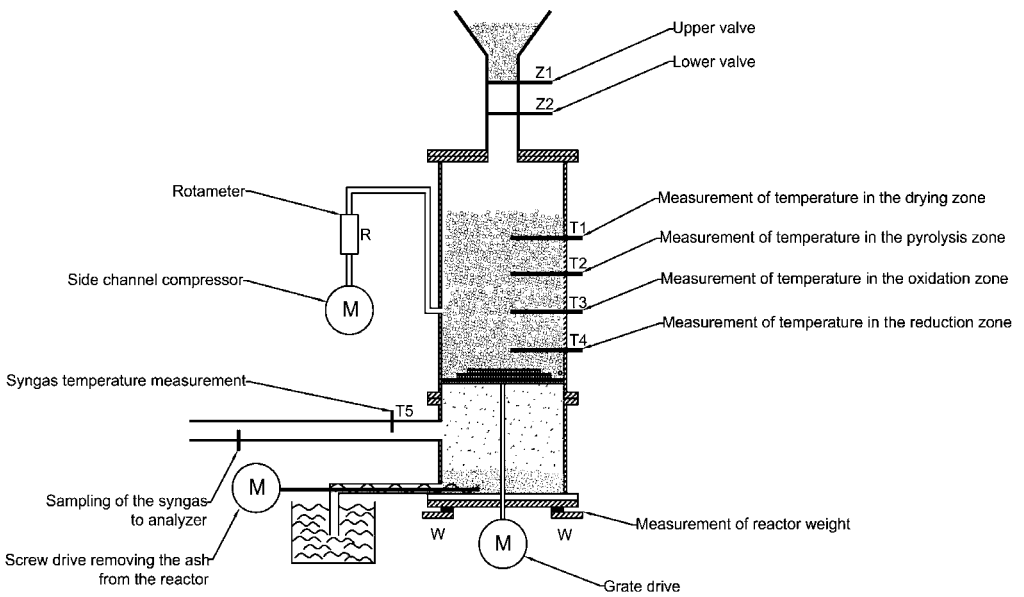

Figure 6. Schematic diagram of gasification reactor.

Reactor construction can be divided into:

- Biomass feeding unit
- Gasification agent supply system
- Ash removal unit
- Reactor chamber

Figure 7 shows 3D model of the gasification reactor with support frame. Biomass for the reactor is provided by screw feeder to the hopper and then through two knife gate valve to the interior of the reactor chamber. Such construction of the biomass feed system ensures the tightness of the installation.

Figure 7. 3D model of gasification reactor.

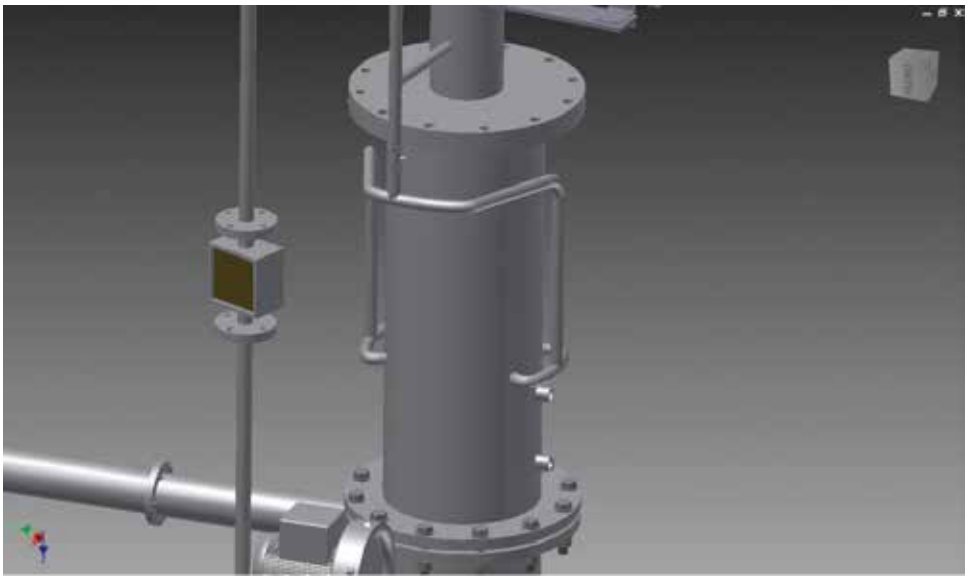

Figure 8. Air supply system to gasification reactor.

The gasification agent supply system consists of four nozzles arranged at the periphery of the oxidation zone (**Figure 8**). Atmospheric air as a gasification agent is forced into the oxidation zone of the reactor through a piping system using a side channel compressor. In order to achieve greater uniformity of the aeration, the nozzles were made at an angle of 15° to produce a vortex of air inside the reactor chamber.

The ash removal unit from reactor consists of a rotary grate integrated with an ash scraper and a screw conveyor (**Figure 9**). The ash removal rate mainly depends on rotational speed of the grate. The holes of grate were made in the form of cones increasing their diameter toward the bottom. Such a construction of the holes results in a lower risk of collimation and enables free removal of ash from the reactor space.

In order to achieve a high level of tar conversion, reactor structure was extended in relation to the diameter to increase the gas flow time through the hot zone. In the research reactor the internal diameter D = 300 mm, while the length of the gasification chamber L = 1200 mm.

3.2. Energy consumption for substrate preparation to gasification process

The substrate of the gasification process was pelletized digestate, after mechanical separation process, biodrying process, and thermal drying process. **Figure 10** shows energy consumption for each stage of preparation process to prepare 1 kg solid fuel from digestate. **Figure 11** shows picture of pelletized digestate. The total energy consumption for production 1 kg of fuel was 0.2545 kWh/kg. The largest part (about 53.43%) of energy was spent on thermal drying process in tubular dryer. Dehydration of digestate in mechanical separation process and in biodrying process was characterized by high energy efficiency of the processes.

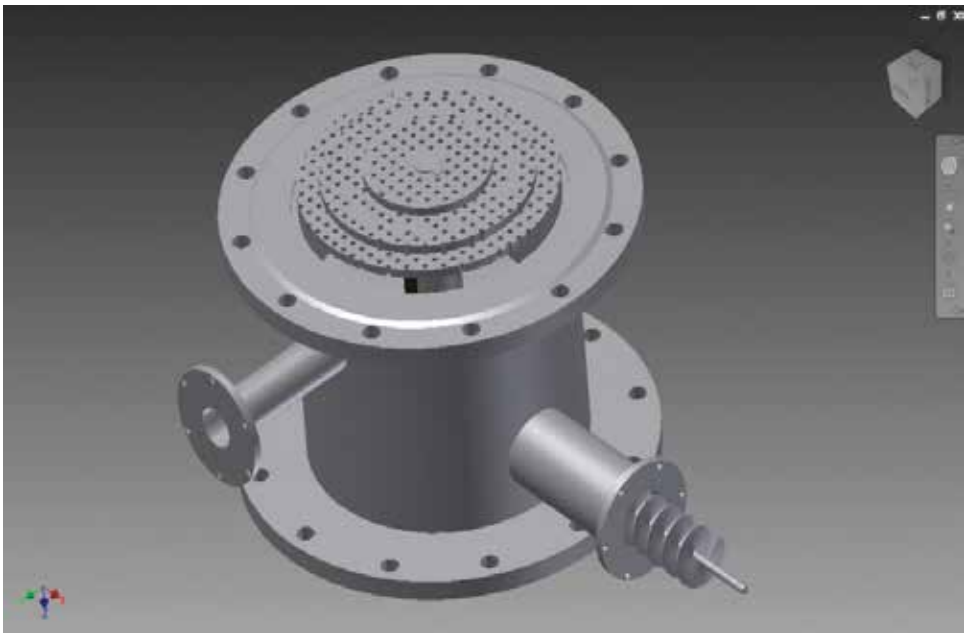

Figure 9. Ash removal unit from gasification reactor.

3.3. The gasification process

The main purpose of the experiments was to evaluate the gasification potential of the fuel produced from digestate and to analyze the obtained syngas. Gasification process was started using a wood pellet. After stabilizing the reactor work, supplying fuel from the digestate was started. Process was carried out with air volumetric flow rate of 30 m^3/h. The dispenser feeder has been setup to maintain fuel mass of about 30–31 kg. Syngas from gasification process was burned in atmospheric conditions immediately after leaving the reactor.

The results of the gasification process of the fuel produced from digestate include composition of syngas, calorific value (**Figure 12**), and the temperature in the oxidation zone of the process (**Figure 13**). In addition, the mass of the reactor measured by strain gauges during process is presented. From the chart, it is possible to read the conversion rate of biomass to syngas. For comparison purposes, the **Table 5** also shows composition of syngas from wood pellets.

During digestate gasification process a high fluctuation of temperature was observed in the oxidation zone of the reactor. Fluctuations reached ±50°C (**Figure 13**). The average temperature in the oxidation zone was 940°C. **Figure 14** shows fuel mass change in reactor chamber during gasification process. The thermal conversion speed of the digestate to syngas was average 26.63 kg/h.

Due to the low melting temperature of ash from digestate, during gasification process, ash slagging caused some problems. Because of this, temperature fluctuations in the oxidation zone probably occurred. During longer work of reactor, conglomerate prevented the

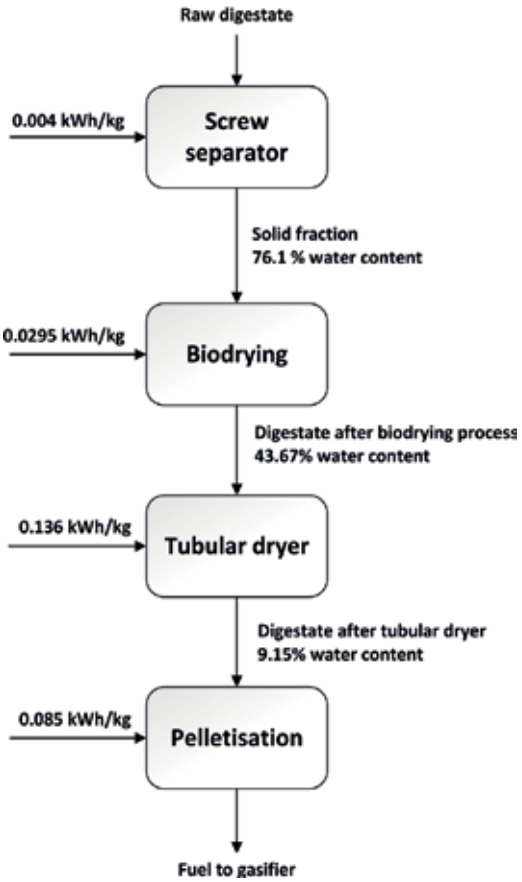

Figure 10. Scheme of digestate processing and energy consumption of each processing stages.

Figure 11. Photo of pelletized digestate—fuel for gasification reactor.

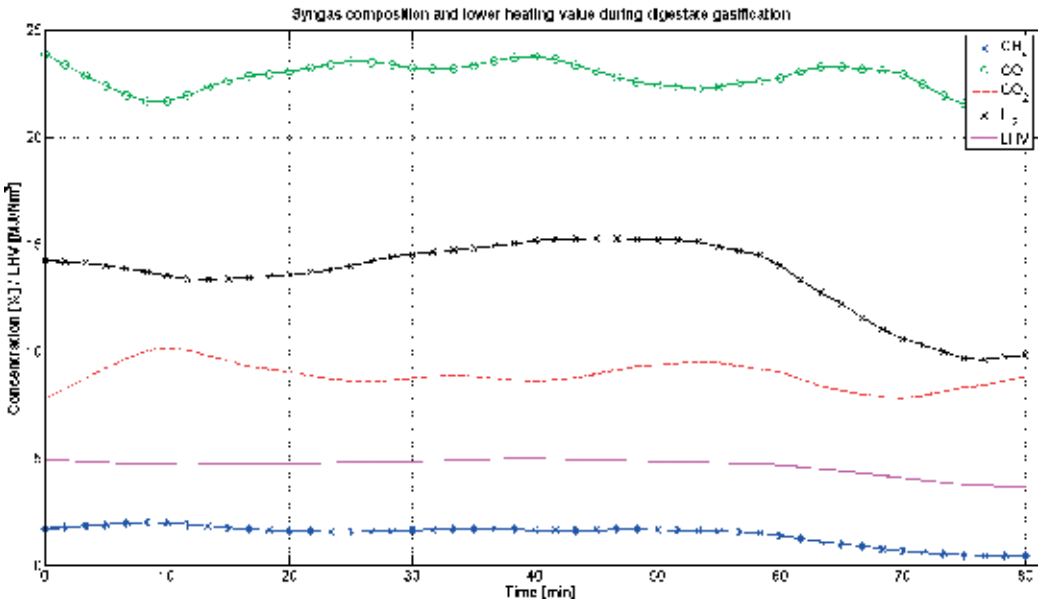

Figure 12. Syngas composition and its calorific value from the digestation gasification process.

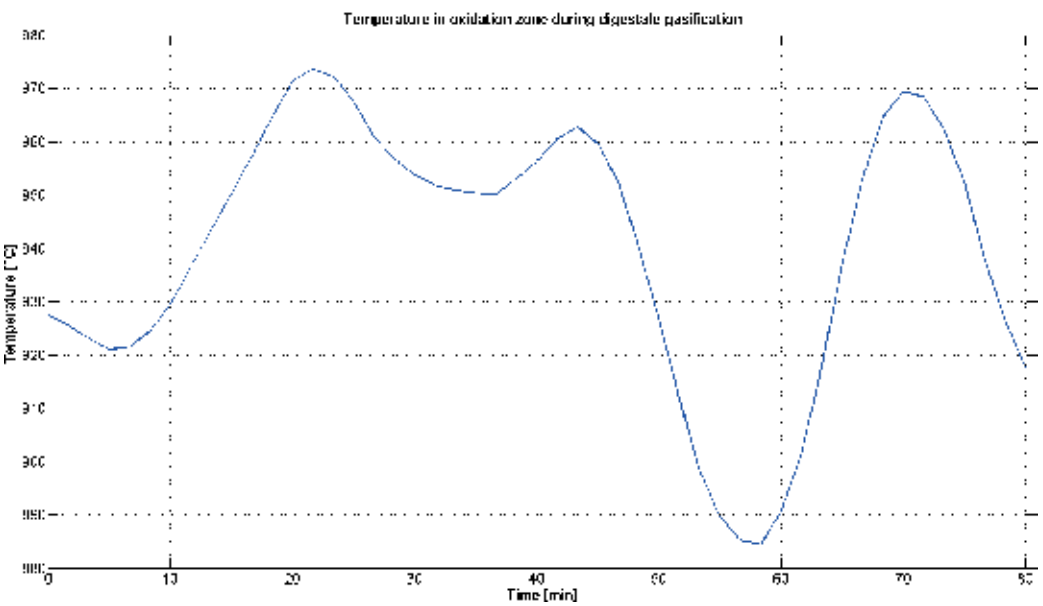

Figure 13. Temperature in oxidation zone during gasification process.

gasification reactor from working properly. A long-term operation of digestate gasification process would be possible by modifying the ash removal system for example by eliminating the solid grate. Some technological solutions of gasification reactors include a system of injecting pure oxygen below the oxidation zone. Molten ash is removed from reactor by

Parameter	Digestate	Wood pellet
CH_4	1.44%	2.3%
CO	22.75%	23.2%
CO_2	8.85%	9.5%
H_2	13.51%	11.0%
LHV	4.62 MJ/Nm^3	4.9 MJ/Nm^3

Table 5. Syngas composition and its calorific value—for comparison, table shows also syngas composition from wood pellets.

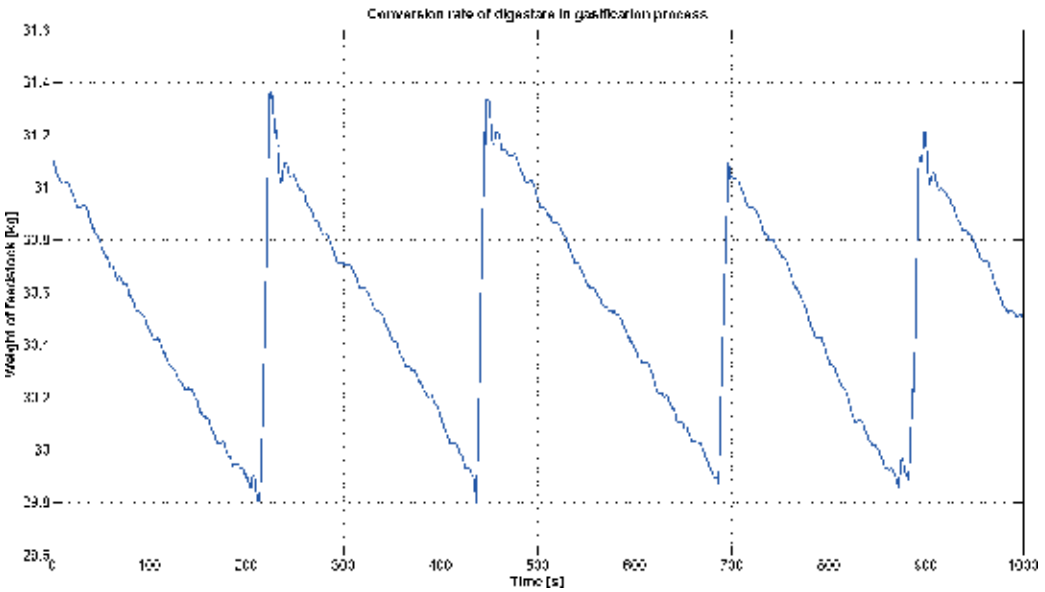

Figure 14. Slice of recorded mass change during gasification process.

a separate channel. This solution results in an increase of energy consumption for gasification process. To solve this problem, authors are currently working on the use of a double screw conveyor on the entire lower surface of the gasification reactor.

4. Summary

It is possible to produce second-generation fuels from dried digestate. The residues from thermal treatment of digestate can be used in the production of mineral fertilizers. Difficulties may occur during the gasification in downdraft reactors with fixed bed. High ash content, which in the case of biomass of agricultural origin features a low melting temperature, can cause problems with slagging.

The result of the research of the gasification of dried digestate was gaseous fuel that does not differ from the quality of fuels obtained from the thermal treatment of other types of biomass. The calorific value of obtained syngas was approximately 5 MJ/Nm^3. This type of fuels can be used for combustion in the engine or turbine systems; however, they require adequate conditioning in advance.

Author details

Dariusz Wiśniewski[1], Mariusz Siudak[2]* and Janusz Piechocki[1]

*Address all correspondence to: siudak.mariusz@gmail.com

1 Faculty of Technical Sciences, Department of Electric and Power Engineering, University of Warmia and Mazury in Olsztyn, Olsztyn, Poland

2 Faculty of Technical Sciences, Department of Systems Engineering, University of Warmia and Mazury in Olsztyn, Olsztyn, Poland

References

[1] Börjesson P, Berglund M. Environmental systems analysis of biogas systems—Part I: Fuel-cycle emissions. Biomass & Bioenergy. 2006;**30**(5):469-485. DOI: 10.1016/j.biombioe.2005.11.014

[2] Börjesson P, Berglund M. Environmental systems analysis of biogas systems—Part II: The environmental impact of replacing various reference systems. Biomass & Bioenergy. 2007;**31**:326-344

[3] Al Seadi T, Drosg B, Fuchs W, Rutz D, Janssen R. Biogas digestate quality and utilization. In: Wellinger A, Murphy J, Baxter D, editors. The Biogas Handbook. 1st ed. Woodhead Publishing; 2013. pp. 267-301. DOI: https://doi.org/10.1533/9780857097415.2.267

[4] Kratzeisen M, Starcevic N, Martinov M, Maurer C, Muller J. Applicability of biogas digestate as solid fuel. Fuel. 2010;**89**(9):2544-2548. DOI: https://doi.org/10.1016/j.fuel.2010.02.008

[5] Al Seadi T, Lukehurst C. Quality Management of Digestate from Biogas Plants Used as Fertiliser [Internet]. 2012. Available from: https://www.iea-biogas.net/files/daten-redaktion/download/publi-task37/digestate_quality_web_new.pdf [Accessed: September 07, 2017]

[6] EU. Directive 91/676/EC of the European parlament and the council of 12 December 1991. Concerning the protection of waters against pollution caused by nitrates from agricultural sources. In: E. Comission (Ed.) Official Journal L. 1991;**375**:pp. 0001-0008

[7] Alburquerque JA, de la Fuente C, Campoy M, Carrasco L, Najera I, Baixauli C. Agricultural use of digestate for horticultural crop production and improvement of soil properties. European Journal of Agronomy. 2012;**43**:119-128. DOI: https://doi.org/10.1016/j.eja.2012.06.001

[8] Vaneeckhaute C, Janda J, Vanrolleghem P, Meers E. Phosphorus use efficiency of bio-based fertilizers: Bioavailability and fractionation. Pedosphere. 2016;**26**(3):310-325. DOI: 10.1016/S1002-0160(15)60045-5

[9] BioEnergy Farm. Digestate Treatment [Internet]. 2014. Available from: www.bioenergy-farm.eu/en/digestate-treatment/ [Accessed: 2017-09-07]

[10] Lebuf V, Snauwaert E, Michels E, Meers E, Sigurnjak I, De Clercq L, et al. Nutrient Recovery from Digestate: Case Study Report. Belgium: INTERREG IV.B NWE ARBOR; 2015. p. 33

[11] Wisniewski D, Gołaszewski J, Białowiec A. The pyrolysis and gasification of digestate from agricultural biogas plant. Archives of Environmental Protection. 2015;**41**(3):70-75

[12] Ritzkowski M, Heerenklage J, Stegmann R. An overview on techniques and regulations of mechanical-biological pre-treatment of municipal solid waste. Environmental Biotechnology. 2006;**2**(2):57-68

[13] Velis C, Longhurst P, Drew G, Smith R, Pollard S. Biodrying for mechanical-biological treatment of wastes: A review of process science and engineering. Bioresource Technology. 2009;**100**(11):2747-2761. DOI: https://doi.org/10.1016/j.biotech.2008.12.026

[14] Białobrzewski I, Miks-Krajni M, Dach J, Markowski M, Czekała W, Głuchowska K. Model of the sewage sludge-straw composting process integrating different heat generation capacities of mesophilic and thermophilic microorganisms. Waste Management. 2015;**43**:72-83. DOI: https://doi.org/10.1016/j.wasman.2015.05.036

[15] Mason I. Mathematical modelling of the composting process: A review. Waste Management. 2006;**26**(1):3-21. DOI: https://doi.org/10.1016/j.wasman.2005.01.021

[16] Yang B, Zhang L, Jahng D. Importance of initial moisture content and bulking agent for biodrying sewage sludge. Drying Technology 2014;**32**(2):135-144. DOI: http://dx.doi.org/10.1080/07373937.2013.795586

Section 3

Low-grade Coal Gasification

Chapter 11

Pyrolysis and Gasification Characteristics of High Ash Indian and Turkish Coals

Jayaraman Kandasamy and Iskender Gökalp

Additional information is available at the end of the chapter

http://dx.doi.org/10.5772/intechopen.73536

Abstract

Pyrolysis and gasification studies of Indian and Turkish high ash coal samples have been performed using coupled TGA-MS method. Coal samples were heated in the TGA apparatus in an argon, steam, CO_2 and blended mixtures of CO2 and steam in a temperature range from 25-1250°C with heating rates from 35 to 1000 K/min. Gas evolution measurements is performed using the mass spectrometry system. During the devolatilisation stage (350-700°C), the maximum mass loss has observed in which O_2, CO_2, CO, H_2 and small amount of hydrocarbon compounds are released. Char gasification is mainly influenced by operating conditions such as heating rate and reaction temperature and also the char production method, its physical structure and size and chemical composition of the char. The steam and CO_2 gasification rates of the chars are carried out at the temperatures of 850, 900, 950, and 1000°C. Three kinetic models are applied to describe the char conversion rates: volumetric model, grain model, and random pore model. The activation energy of Indian coal-char is varying from 122 to 177 kJ mol^{-1} under steam gasification and from 130 to 214 kJ mol^{-1} for CO_2 gasification. The activation energy for char-steam gasification is 156-173 kJ/mol, whereas in the steam blended with CO_2 gasification, it ranges between 162 and 196 kJ/mol for 3 mm particles. Similar trends are observed for the Arrhenius constant values for both sized particles.

Keywords: gasification, high ash coal, thermogravimetry, mass spectrometry, syngas production, kinetic models, clean coal technologies

1. Introduction

With the recent emphasis on clean coal technologies, numerous studies have been performed on coal gasification. Coal is a very complex heterogeneous material consisting of organic and

inorganic materials. Coal is mainly formed from partially decomposed and metamorphosed plant materials. Its formation has occurred over long time periods, and differences in plant materials and in their extent of decay influence the components present in coals Description of coal components is part of the science of petrography [1]. Several efforts have been made to categorize the coals, and to relate coal properties to their behaviour in coal conversion processes.

Lignite, the lowest rank coal, has high moisture content, relatively more ash and a low heating value when compared with the other types of high rank coals. In spite of their high ash content, these coals have been widely used for the generation of power and industrial steam in India and Turkey. The use of indigenous coals is encouraged in both countries for energy supply security and to insure fuel price stability. In addition, clean coal technologies are also encouraged, especially to reduce the carbon footprint of coal based electricity generation but also to reduce all harmful emissions.

At present, coal accounts for more than 50% of total primary commercial energy supply in India and shares for about 58.3% of total electricity generation. Coal is expected to continue a key energy source for India, for at least the next 30–40 years as India has a significant amount of domestic coal reserves (relative to other fossil fuels) and a large installed-capacity for coal-based electricity production. This situation is also very similar in Turkey, and also for example in Greece. Hence, strong R&D and demonstration efforts are developed to improve the global sustainability of using high-ash content coals for electricity generation in such countries. The present method of using high-ash coals is mostly through direct combustion processes. This method is not only inefficient, but also is associated with high levels of pollution. With the intention of solve these problems and increase the coal usage, many countries in the world are supporting research and development of clean coal technologies. It is crucial for new coal technologies to reach the market in an appropriate time, with less impact on environment, and also at a competitive cost.

1.1. Gasification

Greenhouse gas (GHG) emissions from thermal power plants based on fossil fuel combustion are considered as one of the main source for global climate change [2]. A number of developing technologies towards carbon capture and sequestration are currently under progress; including pre- and post-combustion capture and oxy-fuel combustion [3]. Coal gasification has much contemporary importance because of the fact that it is considered as the technology for the future in terms of efficiency and cleaner environment. Gasification converts heated solid fuels (coal or biomass or other organic materials) using only partial oxidant concentration (compared to that for full conversion or combustion) Therefore, the generated gas after this partial conversion or oxidation has a very low level of CO_2 and a large proportion of H_2 and CO, with smaller concentrations of hydrocarbons. This gas is called synthetic gas (or syngas) and can be combusted in a gas turbine or gas engine or in a burner. It can also be used as a feedstock for the production of various chemicals including liquid fuels through catalytic chemical processes.

An Integrated Gasification Combined Cycle (IGCC) has higher overall efficiency than a direct combustion process and the volume flow of the gas that needs to be cleaned is also reduced. In fluidized bed gasifiers, the coal enters the top of the gasifier, whereas the fluidizing gases (oxidant, steam, recycled gas) enter at the bottom for complete mixing with the coal particles and to ensure an isothermal operation. During coal gasification, particles become smaller and lighter and could be entrained in the product gas. Hence, the fluidizing gas flow rate must be sufficient enough to fluidize and gasify the coal particles for minimizing the particle entrainment. In entrained flow gasifiers, finely ground coal particles are injected together with the oxidant (steam and oxygen) and can either flow upward or downward through the gasifier. The residence time of the coal in these gasifiers is in the order of seconds and they should be operated at high temperatures to achieve high carbon conversion rates. The selection of a gasification process to produce syngas for energy generation or chemical production depends on numerous factors governed by the feedstock nature, plant requirements and environmental regulations. The main factors include coal and ash properties. Steam and air, or pure oxygen and even CO_2 can be used for feedstock gasification. Syngas composition also strongly depends on the gasifier, oxidant, coal types and operating conditions. Commercial gasifiers are typically optimized to enhance the gasification of a particular coal; however, most gasifiers have considerable flexibility towards different coal types. The man reactions occurring during coal gasification process are summarized in **Table 1**.

1.2. Thermogravimetry and mass spectrometry

In general, coal conversion technologies and virtually all end uses of coal are mainly based on the application of heat. The structural changes of coal particles upon heating influences all features of coal based technologies. During thermal decomposition of coal when heated towards higher temperature, it undergoes a variety of physical and chemical changes at which occurs. Hence, thermal decomposition of coal has been investigated under many aspects [4–7].

Reaction	Equation	Enthalpy
Combustion	$C + O_2 \rightarrow CO_2$	$\Delta H = -405.9$ kJ/mol
	$C + 0.5\ O_2 \rightarrow CO + H_2$	$\Delta H = -123$ kJ/mol
Steam gasification	$C + H_2O \rightarrow CO + H_2$	$\Delta H = 118.9$ kJ/mol
Hydrogasification	$C + 2H_2 \rightarrow CH_4$	$\Delta H = -87.4$ kJ/mol
Boudouard reaction	$C + CO_2 \rightarrow 2CO$	$\Delta H = 159.7$ kJ/mol
Water-gas-shift	$CO + H_2O \rightarrow CO_2 + H_2$	$\Delta H = -40.9$ kJ/mol
Methanation	$CO + 3H_2 \rightarrow CH_4 + H_2O$	$\Delta H = -206.3$ kJ/mol

Table 1. Main reactions occurring during coal gasification process [4].

Thermal analysis is mainly applied to evaluate the thermodynamic properties which are required to establish the behavior of materials which has undergone various heating and cooling rates, in inert, reduction or oxidation atmospheres or under different gas temperatures and pressures. Thermal analysis encompasses a cluster of techniques wherein a physical property of a substance is estimated under controlled temperature program. The thermogravimetric analysis (TGA) of coal is a well-known technique to understand the change in the structural features of coal during combustions [8–12].

Thermogravimetry coupled with mass spectrometry (TG-MS) is a well-recognized technique in the pyrolysis research of solid fuels. It can deliver real-time and elaborate information on the weight loss and gas release features as a function of temperature [9–15]. MS method is used to identify the gaseous species released from the sample, according to their molecular mass. All coals release volatile matters when heated. The quantities evolved depend upon coal rank, the heating rate, the temperature to which the coal is heated and the operating pressure. The chemical composition of coal has a strong influence on its combustibility.

The application of non-isothermal pyrolysis associated with released gas analysis delivers a qualitative data of the pyrolysis characteristics of coal [16]. Pyrolysis is a substantial intermediate stage over the major coal conversion process stages, such as combustion, gasification, carbonization and liquefaction. This method is considered as simple and effective method for removing sulfur from coal [17–23] as well. Mahajan et al. [24] reported the DSC results for 12 coals using various ranks in the helium ambience at 5.6 MPa and temperature up to 580°C with a heating rate of 10°C min^{-1}. The major conclusion is that the thermal effects during pyrolysis of coals ranks from anthracite to bituminous were endothermic. Exothermic heats were detected only in the case of sub-bituminous coals or lignites. Whereas, the net thermal effect was found to be strongly rank dependent. Morris [25] performed the pyrolysis experiments in the temperature range from ambient to 900°C for various particle sizes, and established an empirical correlation's for the evolution rates of carbon monoxide, hydrogen, and methane as a function of particle size and process temperature. Nali et al. [26] have conducted the pyrolysis coupled with gas chromatography and mass spectrometry investigation on lignite which is originated from Poland and USA. Seo et al. [27] have reported the coal pyrolysis features using thermo-gravimetric analysis and gas release measurements of the evolved species for Chinese coals in non-isothermal conditions at different heating rates.

Jayaraman et al. have produced char particles from Indian [28] and Turkish high ash coal [29] using a high speed thermogravimetry system (NETZSCH STA 429 thermal analyzer with platinum furnace) at the heating rates of 40, 100, 500, 800 and 1000 K/min in argon ambience. After pyrolysis, chars were cooled to ambient temperature in argon ambience and used for further gasification studies. A separate water vapor (steam) generator is attached with the TGA system. Steam generator and its transfer lines are preserved at 180 and 150°C respectively. The produced char particles are heated with a heating rate of 40 K/min under argon ambience up to 850°C and further gasified in steam, CO_2 and blended (steam+ CO_2) ambience under various partial pressure conditions. The gasification experiments have been repeated

for 900, 950 and 1000°C. Argon is used as carrier gas for steam. In the gasification tests, the mass of the char samples are maintained around 15 mg. The TGA system records the weight loss from a highly sensitive analytical balance and it has the resolution of 10^{-3} mg. The sample temperatures are measured using thermocouples which were connected at the bottom section of the crucible, which holds accurately underneath the sample layer. The experimental setup used for the gasification studies was presented in detail elsewhere [13–16, 28–31]. The ultimate and proximate analyses results of the investigated high ash Indian and Turkish coals are given in **Table 2**.

1.3. Coal pyrolysis and gasification under low heating rates

The experiments are performed in argon and steam (WV – water vapor) ambience to estimate the thermal decomposition of the coals. It can be seen from the TG-DTG curves that the Turkish and Indian coals are pyrolysed in the temperature range from 300 to 750°C, presented in **Figures 1** and **2**. The gaseous species evolution as a result of decomposition of the coal sample was concurrently monitored by mass spectrometry during the TG tests. The mass spectra of the evolved gases during pyrolysis and gasification are depicted in **Figures 3** and **4** for the Turkish and Indian coals respectively. A comparison of the evolution of the main species produced during thermal decomposition shows a relationship between volatile matter content and the species emissions. Wilson [32] has reported that the steam decomposition and coal gasification commence from 800°C. At temperatures below 350–400°C, different processes take place prior to primary pyrolysis, i.e. disruption of hydrogen bonds, vaporization and transport of the non-covalently bonded molecular phase [33].

Figures 1 and **3** show a first mass loss peak around 300°C corresponding to the elimination of moisture. The second peak, in which the major weight loss observed in the range of 350 to 700°C which is mainly due to the primary devolatilisation, during which carbon, hydrogen and oxygen compounds are evolved (**Figures 3** and **4**). The primary carbonization initially starts at 350°C in which the release of carbon dioxide and hydrogen has noticed. When the temperature is increased, methane and other lower aliphatics are also released together with carbon monoxide, hydrogen and alkyl aromatics. From the DTG curves of Turkish and Indian coal decomposition, it is concluded that the rate of devolatilization varies with coal type. The major devolatilization process is completed at around 550°C. Whereas, the secondary devolatilization of the coal is occurred over the

Coal type	Proximate analysis				Ultimate analysis				Heating value, MJ/kg
	Moisture	Ash	Volatile matter	Fixed carbon	C	H	N	S	
Indian coal	2.95	45.85	25.62	25.52	39.43	2.52	0.97	0.45	15.23
Turkish coal	11.15	32.33	36.4	21.7	54.34	3.74	1.57	3.74	10.81

Table 2. Proximate and ultimate analyses of Indian and Turkish high ash coal (as received).

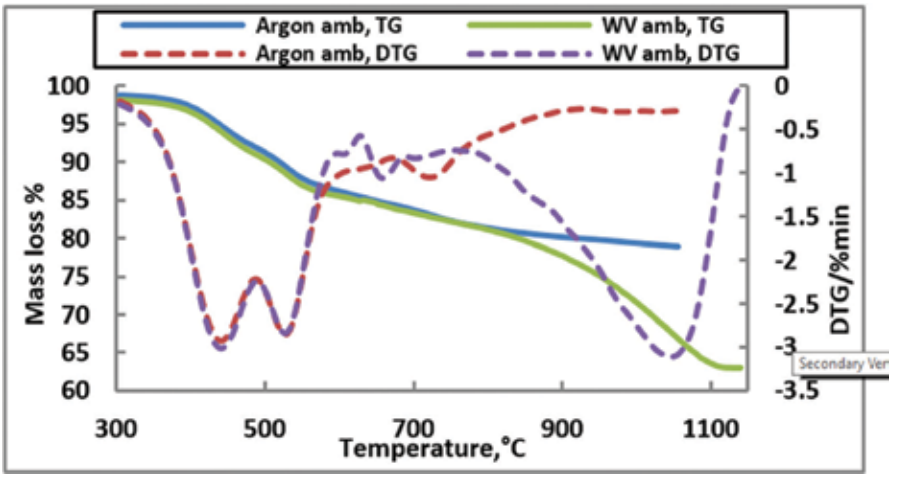

Figure 1. TGA curves of Turkish coal [14].

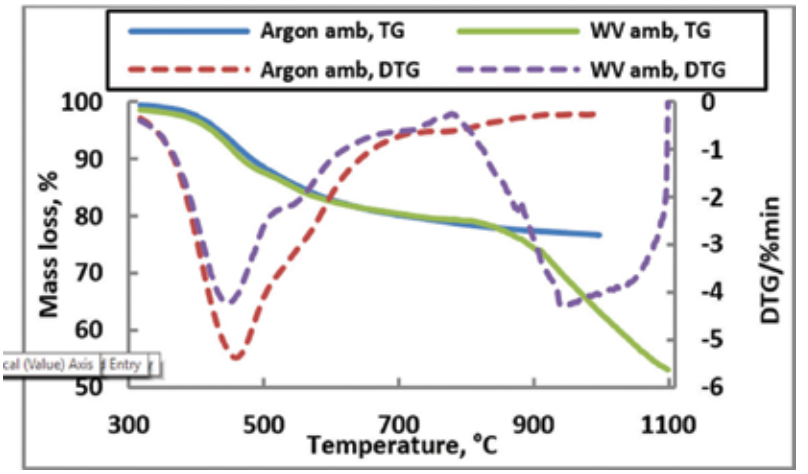

Figure 2. TGA curves of Indian coal [14].

temperature range from 600 to 800°C, produces CO, CO_2, H_2O, H_2 and CH_4 as the major products. The maxima in the DTG curve corresponds to maximum gas release rates. H_2 peaks were detected at the temperature range from 500 to 750°C. The H_2 evolved is, in fact, only a part of the hydrogen present due to the higher volatile matter content in the coal. It can be seen in **Figures 2** and **4** that the formation of CH_4 starts at temperatures higher than 450°C. In general, CO_2 is formed from aliphatic and aromatic carboxyl and carboxylate groups at low temperatures from these high ash coals. Thus thermal decomposition is a compound process which involves coal devolatilization and pyrolysis. The gasification process is also a major complex and several competing processes impact to the thermal decomposition curves (**Figure 5**).

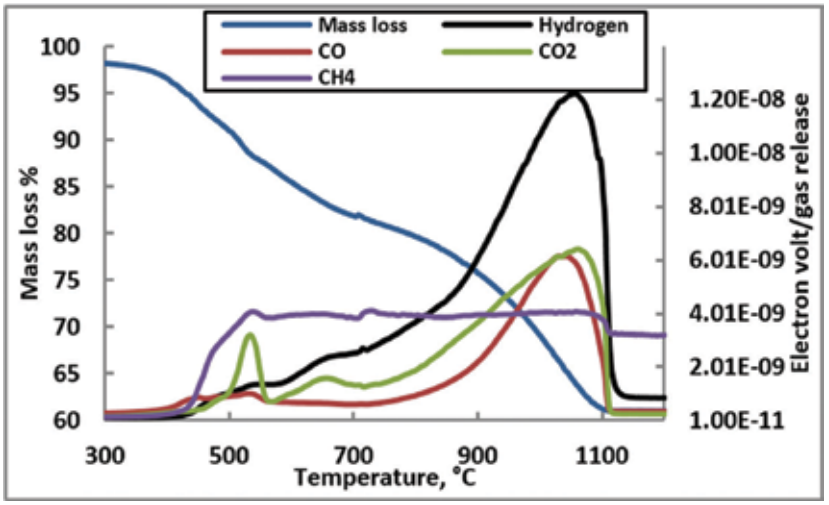

Figure 3. Mass spectrum analysis (gas detection).

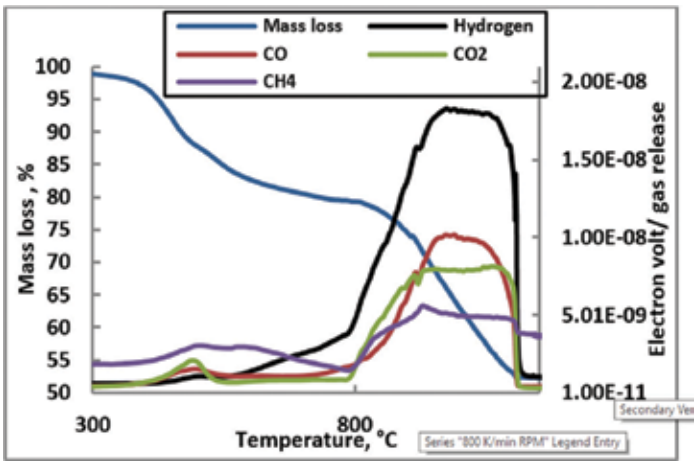

Figure 4. Mass spectrum analysis (gas Turkish coal samples at water vapor detection) of Indian coal samples at water vapor ambience [14] ambience [14].

1.4. Coal-char production under high heating rates

The TG experimental results, obtained as mass loss versus time data, are converted according to conversion level (X) versus time profiles (on ash-free basis).

$$X = \frac{m_o - m}{m_o - m_{ash}} \tag{1}$$

$$R = -\frac{dW}{dt}\frac{1}{m_o - m_{ash}}$$

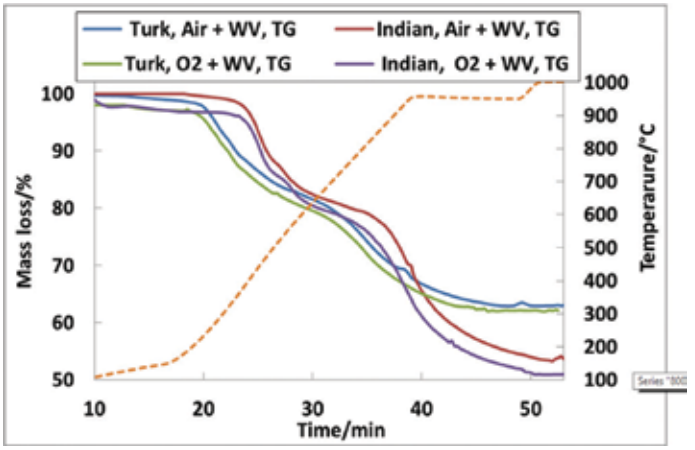

Figure 5. Comparison of TGA curves at blended gases of Turkish and Indian coal samples [14].

where m is the instantaneous mass of the sample, m_0 is the initial mass, and m_{ash} is the residual mass, and R is the reaction rate at time t. The apparent reaction rate is computed as a differential of the conversion degree versus time, denoted as $\frac{dX}{dt}$. The calculations from Eq. (1) are obtained and its validity is based on the assumption that reactions of mineral matter with steam and CO_2 is not occurred during gasification.

The half-life $t_{0.5}$ [34] was used as a reactivity index in order to decribe the gasification reactivity of coal chars for quantitative comparison. $t_{0.5}$ denotes the time required for 50% conversion of the carbon in chars.

Pyrolysis tests of Indian and Turkish coal samples are carried out using the high heating rate thermogravimetric system at the heating rates of 40, 100, 500, 800, and 1000 K/min in an argon ambience for different particle sizes. **Figure 6a** illustrates the curves of Indian coal mass conversion level and temperature versus time during pyrolysis. The particle temperature is preserved constant for 5 minutes once it attains the value of 1000°C to make assure the completeness of the pyrolysis process. As anticipated, the mass loss curves reveals that the devolatilisation (or char generation) essentially depends on the heating rate. For example @ 1000 K/min, the total devolatilisation occurs in 1 minute compared to more than 10 min at 100 K/min. Pyrolysis studies of Turkish coal samples are performed using high heating rate thermogravimetric analysis with the heating rates of 100 K/min, 500 K/min and 800 K/min in argon ambience, as shown in **Figure 6b**.

As the heating rate increases, the pyrolysis process is observed independent of particle sizes and the rate of volatilization is almost constant in the initial stage, illustrated in **Figure 6c** and **d**. It can be observed that 800 μm particles exhibit the maximum DTG value of 80%, compared to the 50% value for 3 mm particles. It is noticed that the effect of particle size is not influential at low heating rates. Whereas, the DTG_{max} variation is significant at 1000 K/min, in which it is raised by 20% when the particle sizes are reduced from 900 to 60 μm. Owing to the variation in the ash and volatile content of the Turkish coals, larger particles have comparatively

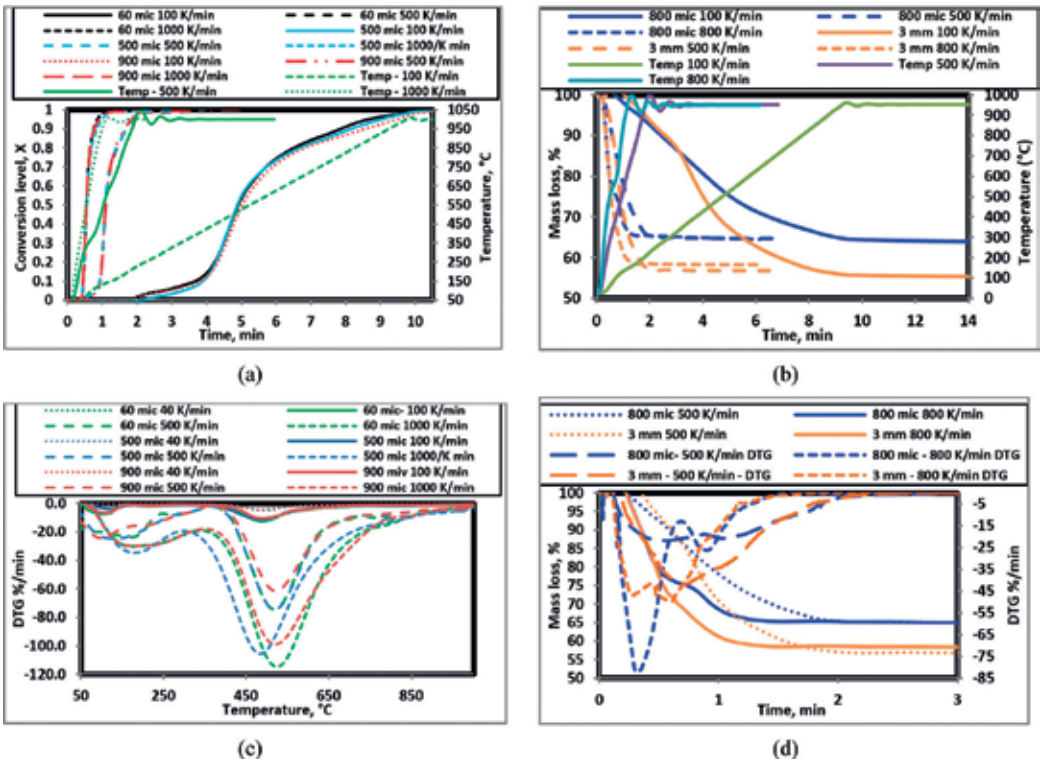

Figure 6. Char generation from Indian and Turkish coal in argon ambience. (a) Indian coal [34] (b) Turkish coal [36], (c) DTG – Indian coal [34], (d) DTG – Turkish coal [55].

higher content of residual char-mass, therefore, the DTG is quite low for 900 μm particles. This aspect can be elucidates by the fact that large particles exhibit more resistance to volatiles escape, in that way the secondary reactions rate increased and as a result of carbon deposition [37]. It can be seen that 800 μm particles shows the maximum DTG value of 80% when compared to the 50% value for 3 mm particles. Owing to the variations in the ash and volatile content of the different particle sizes, smaller particles exhibits relatively higher char mass. The effects of particle size can be directly related to heat and mass transfer effects and limitations.

The DTG results show that the maximum thermal degradation (DTG_{max}) of coal particles are shifted towards higher temperature as the heating rate increased. This is caused by differences in heat transfer and kinetic rates, thereby delaying sample decomposition [35, 37–39]. Hence, the heating rate mainly influences the primary pyrolysis stage of the coal, while the maximum weight loss rate and the corresponding temperature increases with heating rate. In addition to that, the primary pyrolysis is occurred over the temperature range from 300 to 600°C, whereas the secondary pyrolysis started at the temperature from 600 to 800°C at 40 K/min, represents almost agreed well with the results reported by Zhang et al. [30]. With increase in the heating rate, the primary pyrolysis stage of coal is prolonged up to 700°C and subsequently the secondary pyrolysis stage exhibited up to 900°C for 1000 K/min. These

features emphasize that the occurances of thermal lag increases along with the pyrolysis of heating rate of the coal, similar to the results reported in the literatures [28, 35, 37–39].

1.5. Coal-char characterization studies

The char particles produced from Indian coal are characterized using ultimate and proximate analyses; their surface surface features were determined by Scanning Electron Microscopy. The ultimate and proximate analyses of the 60 μm (mic- micron) and 900 μm chars produced at 40 K/min are given in **Table 3**. It is noted that 900 μm char particles displayed rather additional ash and have lower heating value as compared to 60 μm char. The char structural properties resulting from different heating rates are investigated using BET analyses. The surface area analysis (BET) depicted that the char particles generated from higher heating rates show higher surface area as illustrated in **Table 4**. The surface area of the char particles is almost doubled when the heating/production rate is raised from 40 k/min to 800 K/min. The BET surface analysis results is well agreed to other studies in which the char particles are produced at low heating rates [40, 41]. Lua et al. [42] also investigated that the growth of pores during initial pyrolysis is mainly due to the higher volatile matter release rate. Chars produced from high heating rate have already their pores open and exhibits high surface area [43, 44], while the chars prepared from low heating rate possess a less-developed reactive surface and a narrower porous network, as presented in the SEM images (**Figure 7**) and confirmed by BET surface area analysis [35, 37]. Hence, the heating rate affects the coal devolatilisation rate, thereby it also influences the pore structure of the generated char particles and the probability of participation of active sites located in micropores.

1.6. Coal – char steam and CO_2 gasification

1.6.1. Effect of char heating rate

The pyrolysis heating rate of char has a marked influence on the gasification reactivity of the char. This study is to investigate the pathways for char-CO_2 (Boudouard reaction: $C + CO_2 \leftrightarrow 2CO$) and its gasification rate [35]. **Figures 8–10** present the char conversion level of 900 μm char particles in steam and CO_2 gasification which are produced with different pyrolysis rates. The gasification process is conducted under isothermal regimes over the temperature of 900, 950 and 1000°C which are almost identical to the operating conditions of fluidized bed gasifiers. These outcome affirms that the chars produced at high heating rates exhibit better gasification rates

Proximate analysis				**Ultimate analysis (dry basis)**				**Heating value**
Particle size	Moisture	Ash (dry basis)	V.M (dry basis)	C	H	N	S	HCV
	%	%	%	%	%	%	%	MJ/kg
60 μm	2.44	64.4	2.33	36.6	0.39	0.75	0.59	12.01
900 μm	2.25	72.2	2.62	28.3	0.34	0.44	0.5	9.71

Table 3. Proximate and ultimate analysis of the Indian char produced at 40 K/min.

S.no	Heating rate of the char production, K/min	Surface area (BET), m^2/g
1	40	24
2	100	28
3	500	35
4	800	66

Table 4. Surface area of the 60 μm char particles produced at different heating rates.

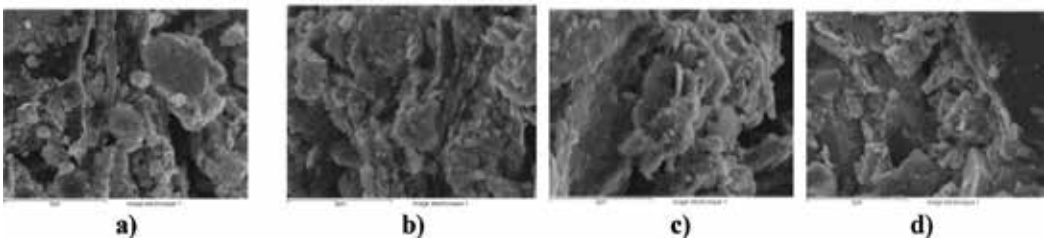

Figure 7. SEM images of Indian coal-char particles produced at various heating rates [35] (a) 40, (b) 100, (c) 500, (d) 800°C/min.

in all the cases over the three tested temperatures, also reported by other studies [34, 35, 45]. Wu et al. [46] and Chen et al. [47] have reported that the coal-char produced from fast pyrolysis show high gasification reactivity mainly because of the variation in the external surface area. Some authors [44, 46] also reported a identical behaviour from the coal-char and biomass-char gasification [10, 48, 49]. Wu et al. [46] also highlighted that surface area is among one of the main factors which majorly influence the gasification reactivity of carbonaceous materials. In general, the coal structure comprises randomly oriented large number of pores which is ranging from

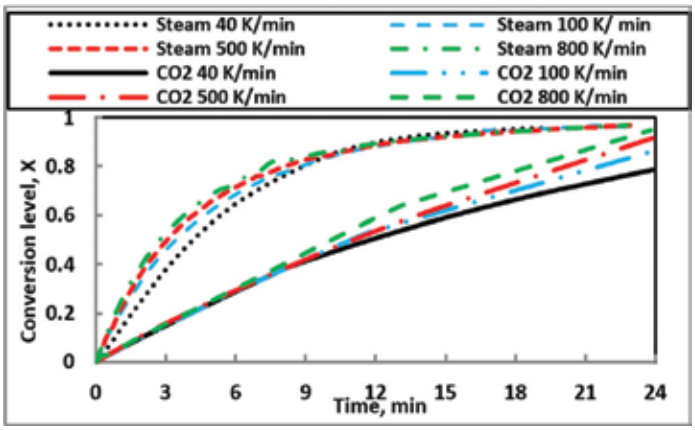

Figure 8. Comparison of Indian coal-char.

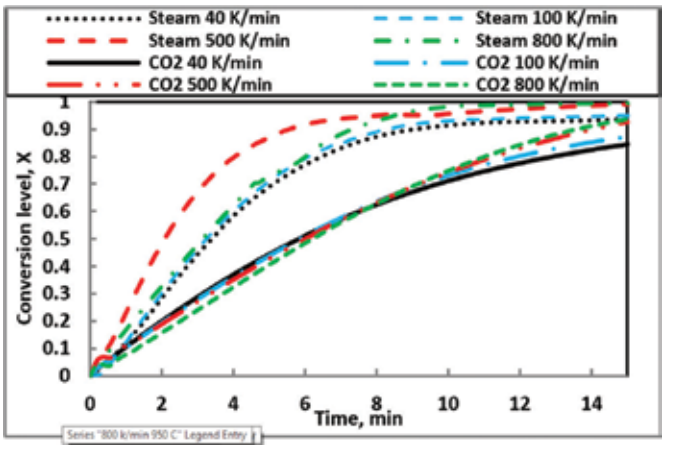

Figure 9. Comparison of Indian coal-char gasification rate produced at various heating conversion rate produced at various heating at rate at steam and CO_2 ambience with the coal rate at steam and CO_2 ambience with the size of 900 micron at 950°C coal size of 900 micron at 1000°C.

micropores (pore diameter < 2 nm) to macropores (pore diameter > 50 nm). The coal is subjected to structural modifications during the pyrolysis process owing due to the phenomena for instance pore enlargement, coalescence or blocking [50]. Heating rate of the coal have an effect on devolatilisation rate, hence these also impact the pore structure of the produced char particles. The participation probability of active sites towards gasification positioned in micropores is relatively higher from high heating rate chars. Both large (macro-and mesopores) and micropores pores are important in coal gasification [51]. These features have to be ascribed between the two contending effects which are regarded with char structure evolution throughout the reaction course: Initial pore growth in the early stages which are subsequently followed by gradual collapse of the pore structure that is mainly because of the coalescence of neighboring pores as gasification further advanced. The reacting gas enters into the macro-and mesopores

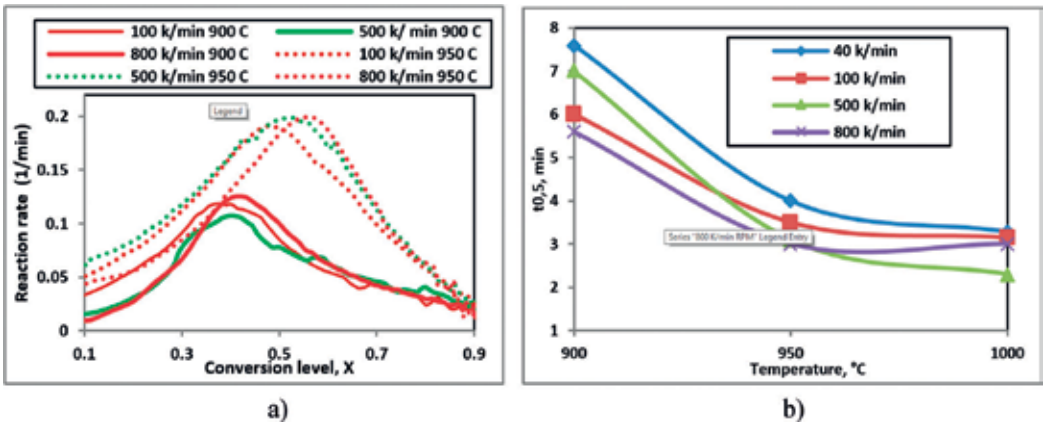

Figure 10. Gasification reactivity of 900 μm Indian coal-char in steam ambience. (a) Reaction rate vs. carbon conversion, (b) time required for 50% conversion level.

which are act as channels to the active sites in the micropores in which the char gasification reaction occurred. The diffusion of product gas occurred through the porous structure of the solid which pave the way to variations arises in the number of carbon-active sites accessible for the gasifying agents. These effects are significant at later stages with CO_2 gasification at high temperstures which is mainly observed beyond the conversion level of 0.4. Initially, the reaction rate is increased with different heating rate of char and passes through a maximum in the conversion range of about 30–70% as illustrated in **Figure 10a**. The half-life of each char have lessen effect as gasification temperature increases and this effect of gasification temperature on $t_{0.5}$ is relatively small above the gasification temperature of 950°C as represented in **Figure 10b**, whereas the heating rate effect exists. These type of trends are also noticed to the particle size of 60 and 500 μm in CO_2 gasification [35].

1.6.2. Effect of gas temperature and gasification agent

It can be noticed that the rate of a reaction influenced by the reaction temperature which emphasize the reaction rate will be higher at high temperature. Besides, the gasification time also reduces and also the influence of the gasification reactions towards higher particle temperature subsequently it increases the char conversion rate, mainly based on the higher activation energies from these reaction temperature, as expected. **Figures 8** and **9** illustrated the steam ambience outcome which depict that the conversion degree steeply rises from starting of the reaction until it reaches the conversion degree of approximately 0.65, 0.85, and 0.95 for the temperatures of 900, 950, 1000°C respectively [35]. Afterwards, very slow reaction is observed and approach towards plateau until complete conversion. The initial steep increment in the conversion degree can be directly related with the rapid evolution of the surface area, which is continued upto collapsing of all the pores. As the reaction surface is reduced, accordingly the gasification rate is also decreasing. These results are in accordance with the findings of other studies [52, 53]. For the same oxidant to coal ratio of the corresponding gasification agents, the gasification rate of steam is about two to three times faster than CO_2 at lower temperature ranges up to conversion level of 0.5. Wheras, gasification rate also increases along with the gasification temperature which is well agreed with the reported studies [44, 46, 47, 54].

1.6.3. Effect of particle size on CO_2 gasification

The particle size effect on Indian coal-char conversion is illustrated in **Figure 11**. During the starting stage of gasification, similar conversion rates are observed, as the time continues, the gasification rate variation diversified among the sizes of the particles. The complete gasification of the 60 μm particles are ocurred within 20 min, against with larger particles. As expected, higher gasification rates are noticed with smaller particles, the main features like diffusion restrictions and heat transfer limitations cannot be ignored while considering the high ash coal, over the temperature and sizes of coals tested [35]. As noted earlier [48, 54–57], the reduction in coal particle size, the TG and the DTG curves move into lower temperature regions, and burning rate increment of coal is seen so time for burnout is reduced. Owing to the fact that the more specific area available with the smaller pulverized coal particles influences the

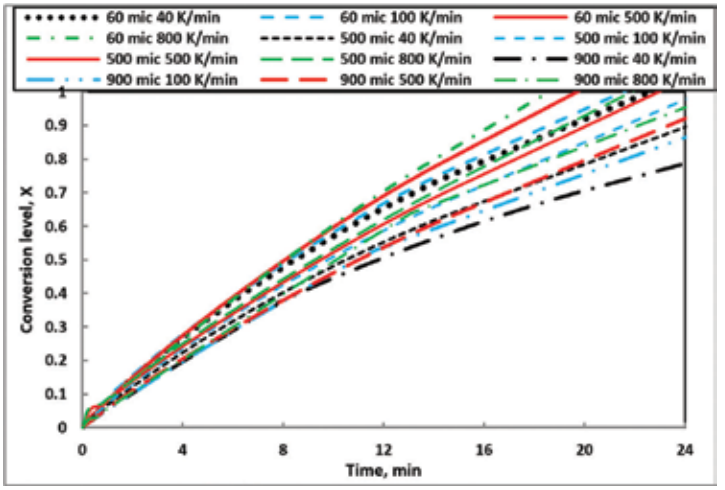

Figure 11. Comparison of Indian coal-char conversion produced at various heating rate at CO_2 ambience of different coal sizes at 950°C.

gasification rate over the larger ones, also smaller particles are favorable to the development and ignition of the coal particles. This again affirms that the finer pulverized coal particles are enabling towards gasification performance improvement.

1.6.4. Effect of partial pressure of steam and CO_2 on gasification

The gasification experiments of 800 μm Turkish coal-char are performed under isothermal conditions at the temperatures of 850, 900 and 950°C at (i) steam partial pressure of 0.9; (ii) steam partial pressure of 0.75; (iii) CO_2 partial pressure of 0.7 and (iv) blended ambience with steam partial pressure of 0.6 and CO_2 partial pressure of 0.2, as illustrated in **Figures 12** and **13**. The char gasification in steam with the partial pressure of 0.75 proceeded slowest whereas gasification of char proceeded fastest with higher concentration of H_2O when the char is produced under low heating rates. On the other hand, the partial pressure and temperature effects on 800 μm char conversion during the gasification in H_2O are weaker when the char particles were produced at higher heating rates [36]. **Figure 13a** shows that an increase in the pyrolysis heating rate and also of the gasification temperature increases the gasification reaction rate under CO_2 ambience. **Figure 13b** illustrates the effect of the blended ambience on gasification rate. Investigations concerning the reactions of H_2O and CO_2 with high ash chars during gasification are quite limited. According to reported results [29, 43, 47, 58–64], possiblility of two surface reaction mechanisms to be emerged. First approach claims that C—H_2O and C—CO_2 reactions takes place in common active sites, whereas the another approach asserts that the reaction of CO_2 and steam happen in separate active sites. The researchers [59, 65] also indicated that the overall carbon-conversion rate in the presence of CO_2 and steam/H_2O might be relatively more when compared to the sum of single ambiance char reactivities, which is otherwise considered that during the mixed atmosphere gasification, there is a possibility of

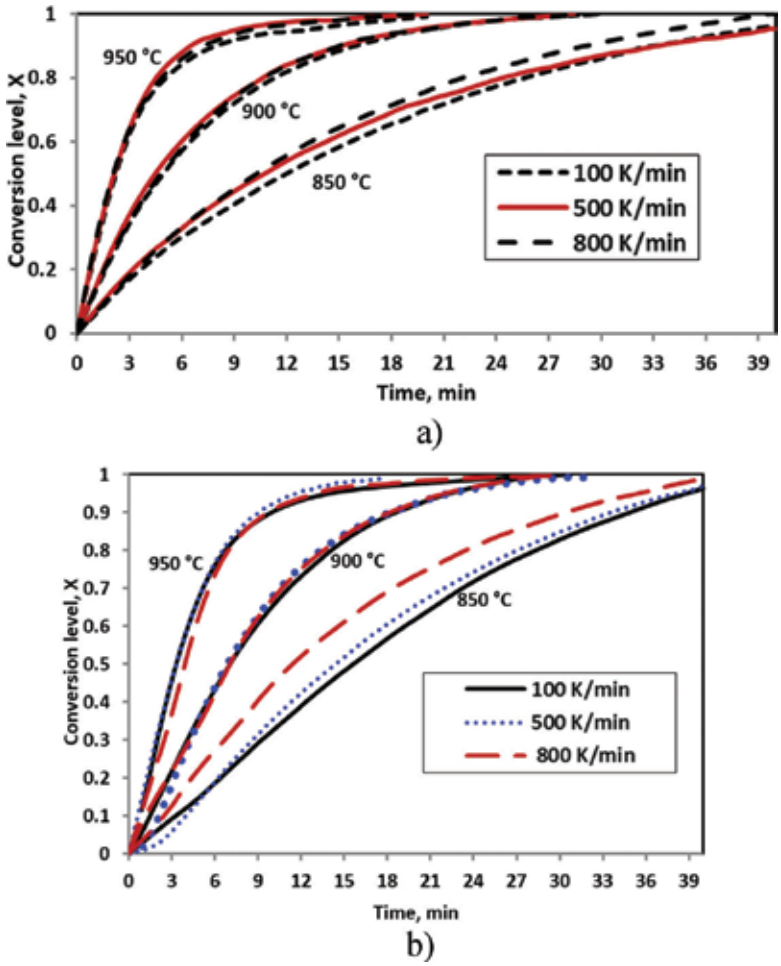

Figure 12. Comparison of Turkish coal-char gasification rate of 800 micron in steam at various partial pressure (a) steam partial pressure – 0.9 (b) steam partial pressure – 0.75.

synergetic phenomenon between the gases. In addition to that, even though the reactions are occurred on separate active sites [59, 65], an active cooperation between the gases is for seen for better accessibility to the reactive surfaces, which implies that one reactant may support to improve the char reactivity regarding to the second gas by the way of either creating additional porosity or by retenting the catalytic mineral species inside the char. **Figure 13** presents the conversion degrees versus time plots. The conversion degree graphs comparison has shown for steam-CO_2-char gasification at corresponding temperatures, the effect of the pyrolysis heating rate on mixed gasification is examined. While comparing the pyrolysis heating rate impact on the gasification time in single atmospheres, only slight differences are observed with blended ambience imparted. It can be seen that some decrement in the reaction rate for the blended ambience at the lowest gasification temperature (850°C). At higher gasification temperatures, this effect almost disappears. Thus also

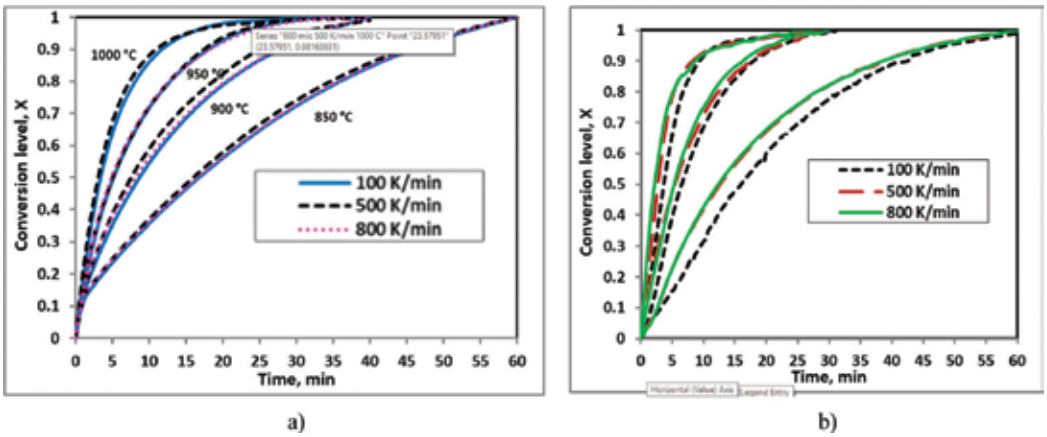

Figure 13. Comparison of Turkish coal-char gasification rate of 800 micron in CO_2 and steam + CO_2 blended ambience. (a) CO_2 ambience, (b) steam +CO_2 blended ambience.

reported from various studies [43, 44, 47, 59, 66] these results indicate that the introduction of CO_2 would not inhibit the steam-char gasification reactions, at least at high gasification temperatures, and do not compete for reactive sites.

1.7. Coal-char gasification kinetics

Various models have been reported in the literature to evaluate the gasification reactions of coal-char steam and CO_2 ambience. Three models are considered in the kinetic analysis, in which the assumption of one-step reaction mechanism are chosen. The variation in the apparent reaction rate can be termed as follows:

$$\frac{dX}{dt} = k(T)f(X)$$

where k is the rate constant, temperature dependent, T and f(X), explains the changes in the physical or chemical properties of the material as the gasification proceeds which corresponds to the selected n^{th}-order expressions. Based on the Arrhenius relationship, the kinetic constant as a function of temperature is derived,

$$k(T) = A\exp\left(-\frac{E}{RT}\right) \tag{2}$$

where E and A are the activation energy and the pre-exponential factor respectively, and T is the absolute temperature.

In the present study, three nth-order models were applied to faciliate the reactivity description of the studied chars: the volumetric model (VM), the grain model (GM) and the random pore model (RPM). All models provide various expressions for the term f(X) [35, 36].

The VM is considered as simplest model, in which the heterogeneous gas–solid reaction of coal gasification is converted into a homogeneous reaction using the assumption of uniform gas diffusion within the entire particle and char reaction over the all possible directions, together with outside and inside of the particle surface [67].

The reaction rate is represented based on the kinetic expression by equation.

$$\frac{dX}{dt} = k_{VM}(1 - X) \tag{3}$$

or in the integrated form by Eq. (2):

$$-\ln(1 - X) = k_{VM}\, t$$

The GM or shrinking core model, proposed by Szekely and Evans [68], in which the assumption of a porous particle that comprises of an assembly of uniform nonporous spherical grains and the occurrence of reaction as observed on the surface of these grains. The porous network is established using the space between the grains. The shrinking core bahiour is ascertained in each of these grains during the reaction stage. When the reaction proceeds gradually inside the particle, finally the ash layer retains. In chemical kinetics controlled regime, the expression for the overall reaction rate in these models is expressed as [67]:

$$\frac{dX}{dt} = k_{GM}(1 - X)^{2/3} \tag{4}$$

and in an integrated form by

$$3[1 - (1 - X)^{1/3})] = k_{GM}\, t \tag{5}$$

The RPM model considers the overlapping of pore surfaces, which reduces the area available for reaction [69]. The fundamental equation of this model follows:

$$\frac{dX}{dt} = k_{RPM}(1 - X)\sqrt{1 - \psi \ln(1 - X)} \tag{6}$$

The maximum reactivity can be able to predict from this model as the reaction proceeds, since it considers the competing effects of pore growth during the starting stages of gasification, and the pores collapse is observed owing to the coalescence of adjacent pores throughout the reaction. The main two parameters are considered in the RPM model, the reaction rate constant, k_{RPM}, and ψ, this parameter narrate the pore structure of the unreacted sample ($X = 0$). If, initial porosity, ε_0, surface area, S_0, and pore length, L_0, of the solid are identified this parameter is expressed as

$$\Psi = \frac{4\pi\pi_0(1 - \varepsilon_0)}{S_0^2}$$

Moreover, the structural parameter is computed using the value of maximal conversion degree of the solid fuel, X_{max}, for which the utmost reaction rate is noticed. The value of ψ can be evaluated based on the relation [53, 70]

$$\Psi = \frac{2}{2\ln(1 - X_{max}) + 1}$$

The rate constant is evaluated from the integrated form of relation (5) which provides

$$\frac{2}{\psi}\left(\sqrt{1 - \psi \ln(1 - X)} - 1\right) = k_{RPM}\, t$$

In order to evaluate the applicability of the choosen kinetic models and establish the kinetic behavior of the tested samples, experimental data is used to fit the models. At specific conversion level, the reactivity is calculated. To determine the kinetic parameters, reactivities at 10–50% of char conversion are frequently used; the latter is generally used in various similar investigations [35, 44]. In our investigation, the reaction rate is nearly stable until 50% conversion level as illustrated in **Figure 10a**, consequently, for calculating the kinetic parameters, this is considered as a reference. The reaction rate constants are determined using the slopes of the linearized relationships represented in the Eqs. (2), (3) and (5) depending on the test results of char conversion X, using the linear regression, for the VM, GM and RPM models respectively. Estimation of the rate constants are performed from the data for three temperatures. The kinetic parameters are evaluated using Arrhenius relationship, the reciprocal relationship between the logarithm of the rate constant and the absolute temperature (1/T) of the reaction arrived by each model at the studied temperature range is estimated.

1.8. Indian coals

The Arrhenius plots for the 900 μm chars are shown in **Figure 14**. Based on the slope and the intersection values, the activation energy E and the pre-exponential factor A were computed for the studied models. **Tables 5** and **6** show the summarized kinetic parameters (E and A) estimation from the test data for three models. A small inconsistency is noticed in model fitting for the char gasification rate at 100 K/min. Whereas, the other samples and models are found very satisfactory fits. As represented in **Figure 14**, observable changes in the slopes of the Arrhenius relations were noticed from 950 to 1000°C, affirms that temperature increment does shift the reactions from chemically controlled to diffusion controlled regimes. The slopes of the relationships calculated for the VM and the RPM models are an almost parallel line which indicates that almost similar activation energy values are calculated from these models. The activation energy of the steam gasification is varying from 129 to 177 $kJmol^{-1}$ using GM model, and around 110 $kJmol^{-1}$ using RPM model, and the reaction rate constants from 4×10^3 to 3×10^6 min^{-1} which are similar to values obtained in previous studies [33, 35, 36, 43, 44, 47, 64, 71] . It can be observed that the activation energy of VM model is always higher irrespective of the char generation method.

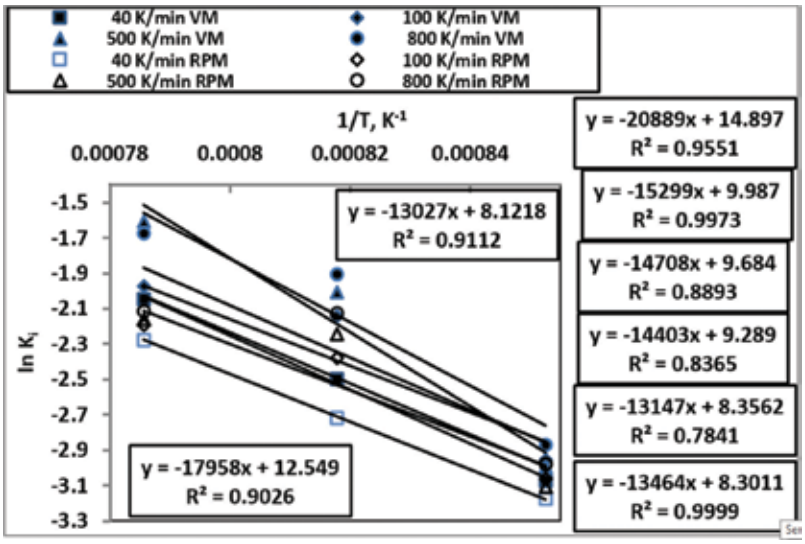

Figure 14. Arrhenius relationships of 900 μm char in steam ambience.

1.9. Turkish coal

Tables 7 and **8** summarize the kinetic parameters (the activation energy, E and pre-exponential factor, A) estimated from the TG data using the models for 800 μm and 3 mm Turkish coal samples. The activation energies estimated by the three models in CO_2 ambience are in the range of 115–138 kJ mol^{-1}. These values are in accordance with the reported literature values [43, 44, 47, 53, 72] even for similar rank of coals. The activation energy of 3 mm particles varies from 156 to 173 $kJmol^{-1}$ and 162 to 196 $kJmol^{-1}$ in steam and blended ambience respectively. These values are in the range of 111–169 $kJmol^{-1}$ for 800 μm particles. These values are in good agreement with the recently reported studies using different reactant concentration and origins of coal [35, 36, 43, 47, 73]. Also, the pre-exponential factors are in the range from 8.22×10^5 to 6.26×10^6 in steam ambience, 8.52×10^3 to 4.23×10^7 in blended ambience. These values are in accordance with those found in the literature [35, 43, 44, 47, 71]. Generally, the RPM model

Heating rate K/min	Activation energy values (kJ/mol)			A/min^{-1}		
	VM	GM	RPM	VM	GM	RPM
40	127.19	129.87	111.93	2.1E + 04	2.5E + 04	4E + 03
100	122.28	129.50	108.3	1.6E + 04	2.8E + 04	1E + 04
500	173.67	177.57	119.7	2.9E + 06	3.7E + 06	3.3E + 03
800	149.30	144.36	109.3	2.8E + 05	1.5E + 05	4.2E + 03

Table 5. Kinetic parameters of the 900 μm Indian coal-char gasification in steam using VM, GM and RPM models [35].

Heating rate K/min	900 μm			500 μm			60 μm		
	VM	GM	RPM	VM	GM	RPM	VM	GM	RPM
40	214.45	192.	179.88	151.83	138	129.24	161	143.54	134.24
100	202.69	179.41	167.94	189.28	168	157	197	181.27	175.58
500	195.52	175.77	171	210	190	184	194.8	181.31	175.5
800	212	189	184	171.75	156.8	153	207.8	193.27	187.3

Table 6. Comparison of the activation energy values (kJ/mol) of Indian coal-char gasified at 900, 950 and 1000°C in CO_2 ambience.

exhibits relatively lower values of activation energy as comparing with other two models. The changes in the activation energy over the char heating rate are almost consistent regardless of the particle sizes considered in the blended ambience. Moreover, a significant observation form this study is that the gasification activation energy of 3 mm char is higher when compared to 800 μm char particles. This is mainly caused due to the better reactivity potential of 800 μm char owing to its higher specific surface area.

(a) CO_2 ambience						
Heating rate K/min	**800 μm**			**3 mm**		
	VM	**GM**	**RPM**	**VM**	**GM**	**RPM**
CO_2 ambience						
100	132.5	132.51	131.63	132.9	132.93	132.33
500	115.71	115.63	115.26	130.85	130.66	130.32
800	128.21	128.47	128.19	138.34	138.35	137.37

(b) Steam and blended ambience [36]									
Heating rate	**100 ml argon (steam — 0.8)**			**75 ml argon +25 ml CO_2 (steam — 0.7 & CO_2 — 0.1)**			**75 ml argon +50 ml CO_2 (steam — 0.6 & CO_2 — 0.2)**		
K/min	VM	GM	RPM	VM	GM	RPM	VM	GM	RPM
3 mm									
100	161.2	158.8	156.4	179.0	179.1	179.6	173.9	164.2	162.3
500	172.9	172.9	173.6	172.7	172.6	172.8	169.1	169.1	167.6
800	170.6	170.9	171.2	190.7	190.6	190.9	196.7	196.7	194.7
800 micron									
100	155.3	154.6	154.5	156.7	156.7	156.6	133.4	133.5	131.3
500	132.3	131.8	131.6	111.5	111.8	112.1	127.4	127.6	126.2
800	152.1	152.1	152.2	169.4	169.1	169.0	149.9	150.1	147.1

Table 7. Comparison of the activation energy values (kJ/mol) of 800 μm and 3 mm chars gasified at 850, 900 and 950°C under argon, CO_2 and steam ambience.

(a) 3 mm coal-chars						
Heating rate	**100 ml argon (steam — 0.8)**			**75 ml argon +25 ml CO_2 (steam — 0.7 & CO_2 — 0.1)**		
K/min	VM	GM	RPM	VM	GM	RPM
100	1.6E + 06	1.2E + 06	8.2E + 05	1.0E + 07	9.6E + 06	8.8E + 06
500	6.2E + 06	5.7E + 06	5.1E + 06	6.3E + 06	5.7E + 06	5.2E + 06
800	4.9E + 06	4.6E + 06	4.2E + 06	4.2E + 07	3.7E + 07	3.3E + 07

Heating rate	**100 ml argon (steam — 0.8)**			**75 ml argon +25 ml CO_2 (steam — 0.7 & CO_2 — 0.1)**			**75 ml argon +50 ml CO_2 (steam — 0.6 & CO_2 — 0.2)**		
K/min	VM	GM	RPM	VM	GM	RPM	VM	GM	RPM
3 mm									
100	161.2	158.8	156.4	179.0	179.1	179.6	173.9	164.2	162.3
500	172.9	172.9	173.6	172.7	172.6	172.8	169.1	169.1	167.6
800	170.6	170.9	171.2	190.7	190.6	190.9	196.7	196.7	194.7
800 micron									
100	155.3	154.6	154.5	156.7	156.7	156.6	133.4	133.5	131.3
500	132.3	131.8	131.6	111.5	111.8	112.1	127.4	127.6	126.2
800	152.1	152.1	152.2	169.4	169.1	169.0	149.9	150.1	147.1

(b) 800 μm coal-chars						
Heating rate	**100 argon**			**75 ml argon +25 ml CO_2**		
K/min	VM	GM	RPM	VM	GM	RPM
100	6.9E + 05	5.4E + 05	4.8E + 05	8.1E + 05	7.6E + 05	6.5E + 05
500	8.9E + 04	7.3E + 04	6.6E + 04	9.9E + 03	9.3E + 03	8.5E + 03
800	5.6E + 05	4.8E + 05	4.4E + 05	3.2E + 06	2.9E + 06	2.5E + 06

Table 8. Comparison of the pre-exponential factor (min^{-1}) of 800 μm and 3 mm chars gasified at 850, 900 and 950 °C in argon, CO_2 and steam ambience.

2. Conclusions

Pyrolysis and gasification studies of Indian and Turkish high ash coal samples have been carried out using coupled TGA-MS method. Coal samples were heated in the TGA apparatus in various gaseous mixture combinations at a temperature range of 25–1250°C under various heating rates. The mass loss data show that the devolatilisation is essentially influenced by the heating rate. Even at higher heating rates, particle sizes do not influence the pyrolysis process and the rate of volatilization is essentially constant. During thermal decomposition and devolatilization of coal, CO, CO_2, H_2 and CH_4 are the major gaseous products. The reaction of coal with steam starts around 800 °C. The complete carbon conversion takes place in the temperature range of 900–950 °C. The syngas production rate is maximum in these temperature limits. In order to study

char gasification, char particles are generated in argon ambience with various heating rates. Char gasification rates investigation in steam and CO_2 blended ambience shows that the pyrolysis heating rate (for char generation) has a considerable impact on the gasification reactivity of the char. Also smaller particles exhibit higher char-CO_2 and char-steam gasification rates. Increasing the temperature from 850 to 950°C leads to the reduction of the time required for 50% conversion by a ratio of more than fourfold. The chars generated under high heating rates present enhanced gasification rates which are mainly due to the alteration of the char pore structure and the accessibility of more active sites to initiate reactions with the gasification agent. The gasification rate of char-H_2O is mainly dependent on H_2O partial pressure, temperature and particle sizes. The maximum reaction rate is shifted to the higher conversion stage for chars produced with high heating rates. The introduction of CO_2 did not inhibit the steam-char gasification reactions and also did not compete for reactive sites. Steam and CO_2 react simultaneously on different active sites on the char surface. Kinetic parameters of the char particles were estimated using different kinetic models. The activation energy for steam gasification is 156–173 kJ/mol, whereas in the steam blended with CO_2 ambience they are between 162 and 196 kJ/mol for 3 mm Turkish coal-char particles. For the Indian coal, the reaction rate is chemically controlled in steam ambience at lower temperatures. The activation energy for steam gasification varies from 122 to 177 kJ mol^{-1} for different sized char particles. The activation energies estimated by the GM model for the three particles are in the range of 138–193 kJ mol^{-1}. The RPM model predicted values in the range from 129 to 187 kJ mol^{-1} for CO_2 gasification. The activation energies for char gasification essentially depend on the char generation method (pyrolysis heating rate) and on the particle size.

Acknowledgements

Financial support for this work is provided by the European Commission under Project OPTIMASH FP7-ENERGY, 2011-1 Project No. 283050.

Author details

Jayaraman Kandasamy* and Iskender Gökalp

*Address all correspondence to: jayaraman_mit@yahoo.com

ICARE-CNRS, Orléans, France

References

[1] Henderson TA, editor. Synthetic Fuels Data Handbook. Denver, CO: Cameron Engineers, Inc.; 1975

[2] Wall T, Liu Y, Spero C, Elliott L, Khare S, Rathnam R, Zeenathal R, et al. An overview on oxyfuel coal combustion - state of the art research and technology development. Chemical Engineering Research and Design. 2007;**87**:1003-1016

[3] Scheffknecht G, Al-Makhadmeh L, Schnell U, Maier J. Oxy-fuel coal combustion - a review of the current state-of-the-art. International Journal of Greenhouse Gas Control. 2011;**5**:S16-S35

[4] Grabner M. Industrial Coal Gasification Technologies Covering Base Line and High Ash Coal. USA: Wiley; 2014

[5] Haykiri-Acma H, Yaman S, Kucukbayrak S, Okutan H. Investigation of the Combustion Characteristics of Zonguldak Bituminous Coal Using DTA and DTG. Energy Sources, Part A: Recovery, Utilization, and Environmental Effects. 2006;**28**:135-147

[6] Giroux L, Charland JP, MacPhee JA. Application of thermogravimetric Fourier transform infrared spectroscopy (TG-FTIR) to the analysis of oxygen functional groups in coal. Energy & Fuels. 2006;**20**:1988-1996

[7] Ozbas KE, Hicyilmaz C, Kök MV. Effect of heating rate on thermal properties and kinetics of raw and cleaned coal samples. Energy Sources. 2003;**25**:33-42

[8] Kok MV. Coal pyrolysis: Thermogravimetric study and kinetic analysis. Energy Sources. 2003;**25**:1007-1014

[9] Avid B, Purevsuren B, Born M, Dugarjav J, Davaajav Y, Tuvshinjargal A. Pyrolysis and TG analysis of shivee ovoo coal from mongolia. Journal of Thermal Analysis and Calorimetry. 2002;**68**:877-885

[10] Diaz-Faes E, Barriocanal C, Diez MA, Alvarez R. Applying TGA parameters in coke quality prediction models. Journal of Analytical and Applied Pyrolysis. 2007;**79**:154-160

[11] Arenillas A, Rubiera F, Arias B, Pis JJ, Faundez JM, Gordon AL, Garcia XA. A TG/DTA study on the effect of coal blending on ignition behaviour. Journal of Thermal Analysis and Calorimetry. 2004;**76**:603-614

[12] Saikia BK, Boruah RK, Gogoi PK, Baruah BP. XRD and FT-IR investigations of sub-bituminous Assam coals. Fuel Processing Technology. 2009;**90**:196-203

[13] Jayaraman K, Gokalp I. Gasification characteristics of petcoke and coal blended petcoke using thermogravimetry and mass spectrometry analysis. Applied Thermal Engineering. 2015;**80**:10-19

[14] Jayaraman K, Gokalp I. Thermogravimetric and evolved gas analyses of high ash indian and turkish coal pyrolysis and gasification. Journal of Thermal Analysis and Calorimetry. 2015;**121**:919-927

[15] Jayaraman K, Gokalp I. Thermal characterization, gasification and kinetic studies of different sized Indian coal and char particles. International Journal of Advances in Engineering Sciences and Applied Mathematics. 2014;**6**:31-40

[16] Jayaraman K, Kok MV, Gokalp I. Thermogravimetric and mass spectrometric (TG-MS) analysis and kinetics of coal-biomass blends. Renewable Energy. 2017;**101**:293-300

[17] Fangxian L, Shizong L, Youzhi C. Thermal analysis study of the effect of coal-burning additives on the combustion of coals. Journal of Thermal Analysis and Calorimetry. 2009;**95**:633-638

[18] Van Heek KH, Hodek W. Structure and pyrolysis behaviour of different coals and relevant model substances. Fuel. 1994;**73**:886

[19] Hu H, Zhou Q, Zhu S, Meyer B, Krzack S, Chen G. Product distribution and sulfur behavior in coal pyrolysis. Fuel Processing Technology. 2004;**85**:849-886

[20] Gryglewicz G. Effectiveness of high temperature pyrolysis in sulfur removal from coal. Fuel Processing Technology. 1996;**46**:217-226

[21] Zhou Q, Hu H, Liu Q, Zhu S, Zhao R. Effect of atmosphere on evolution of sulfur containing gases during coal pyrolysis. Energy & Fuels. 2005;**19**:892-897

[22] Karaca S. Desulfurization of a Turkish lignite at various gas atmospheres by pyrolysis: Effect of mineral matter. Fuel. 2003;**82**:1509-1516

[23] Czaplicki A, Smolka W. Sulfur distribution within coal pyrolysis products. Fuel Processing Technology. 1998;**55**:1-11

[24] Mahajan OP, Akira T, Nelson JR, Walker PL Jr. Differential scanning calorimetry studies on coal and hydrogenation of coals. Fuel. 1977;**56**:33-39

[25] Morris RM. Effect of particle size and temperature on volatiles produced from coal by slow pyrolysis. Fuel. 1990;**69**:776-779

[26] Nali M, Corana F, Montanari L, Pellegrini L. A pyrolysis-gas chromatography/mass spectrometry study on coals. Journal of Analytical and Applied Pyrolysis. 1994;**29**:15-23

[27] Seo DK, Parka SS, Kim YT, Hwang J, Yu TU. Study of coal pyrolysis by thermogravimetric analysis (TGA) and concentration measurements of the evolved species. Journal of Analytical and Applied Pyrolysis. 2011;**92**:209-216

[28] Di Nola G, De Jong W, Spliethoff H. TG-FTIR characterization of coal and biomass single fuels and blends under slow heating rate conditions: Partitioning of the fuel-bound nitrogen. Fuel Processing Technology. 2010;**91**:103-115

[29] Roberts DG, Harris DJ. Char gasification in mixtures of CO_2 and H_2O: Competition and inhibition. Fuel. 2007;**86**:2672-2678

[30] Zhang S, Zhu F, Bai C, Wen L, Zou C. Thermal behavior and kinetics of the pyrolysis of the coal used in the COREX process. Journal of Analytical and Applied Pyrolysis. 2013;**104**:660-666

[31] Butterman HC, Castaldi MJ. CO_2 as a carbon neutral fuel source via enhanced biomass gasification. Environmental Science & Technology. 2009;**43**(23):9030-9037

[32] Wilson. Method for increasing steam decomposition in a coal gasification process. US patent, No. 4,786,291; 1998

[33] Ladner WR. The products of coal pyrolysis: Properties, conversion and reactivity. Fuel Processing Technology. 1988;**20**:207-222

[34] Van Heek KH, Muhlen H-J. Effect of coal and char properties on gasification. Fuel Processing Technology. 1987;**15**:115-133

[35] Jayaraman K, Gökalp I, Bonifaci E, Merlo N. Kinetics of steam and CO_2 gasification of high ash coal-char produced under various heating rates. Fuel. 2015;**154**:370-379

[36] Jayaraman K, Gokalp I. Effect of char generation method on asteam, CO_2 and blended mixture gasification of high ash Turkish coals. Fuel. 2015;**153**:320-327

[37] Jayaraman K, Gokalp I, Bostyn S. High ash coal pyrolysis at different heating rates to analyze its char structure, kinetics and evolved species. Journal of Analytical and Applied Pyrolysis. 2015;**113**:426-433

[38] Seo DK, Park SS, Hwang J, Yu TU. Study of the pyrolysis of biomass using thermo-gravimetric analysis (TGA) and concentration measurements of the evolved species. Journal of Analytical and Applied Pyrolysis. 2010;**89**:66-73

[39] Arenillas A, Rubiera F, Pevida C, Pis JJ. A comparison of different methods for predicting coal devolatilization kinetics. Journal of Analytical and Applied Pyrolysis. 2001;**58-59**:685-701

[40] Ochoa J, Casanello MC, Bonelli PR, Cukerman AL. CO_2 gasification of Argentinean coal chars: A kinetic characterization. Fuel Processing Technology. 2001;**74**:161-176

[41] Sadhukhan AK, Gupta P, Saha RK. Characterization of porous structure of coal char from a single devolatilized coal particle: Coal combustion in a fluidized bed. Fuel Processing Technology. 2009;**90**:692-700

[42] Lua AC, Lau FY, Guo J. Journal of Analytical and Applied Pyrolysis. 2006;**76**:96-102

[43] Wu S, Gu J, Zhang X, Wu Y, Gao J. Variation of carbon crystalline structures and CO_2 gasification reactivity of Shenfu coal chars at elevated temperatures. Energy & Fuels. 2008;**22**:199-206

[44] Guizani C, Escudero Sanz FJ, Salvador S. The gasification reactivity of high heating-rate chars in single and mixed atmospheres of H_2O and CO_2. Fuel. 2013;**108**:812-823

[45] Li C, Zhao J, Fang Y, Wang Y. Pressurized fast-pyrolysis characteristics of typical Chinese coals with different ranks. Energy & Fuels. 2009;**23**:5099-5105

[46] Wu Y, Wu S, Gu J, Gao J. Differences in physical properties and CO_2 gasification reactivity between coal char and petroleum coke. Process Safety and Environmental Protection. 2009;**87**:323-330

[47] Chen C, Wang J, Liu W, Zhang S, Yin JS, Luo GQ, et al. Effect of pyrolysis conditions on the char gasification with mixtures of CO_2 and H_2O. Proceedings of the Combustion Institute. 2013;**34**:2453-2460

[48] Chin G, Kimura S, Tone S, Otake T. Gasification of coal char with steam. Part 2. Pore structure and reactivity. Industrial and Engineering Chemistry. 1983;**23**:113-120

[49] Kapteijn F, Meijer R, Moulijn JA. Transient kinetic techniques for detailed insight in gas-solid reactions. Energy & Fuels. 1992;**6**:494-497

[50] Gale TK, Bartholomew CH, Fletcher TH. Decreases in the Swelling and Porosity of Bituminous Coals during Devolatilization at High Heating Rates, Presented at the Twenty-Fifth Symposium (International) on Combustion, Irvine, California, 31 July-5 August 1994

[51] Feng B, Bathia SK. Variation of the pore structure of coal chars during gasification. Carbon. 2003;**41**:507-523

[52] Irfan MF, Usman MR, Kusakabe K. Coal gasification in CO_2 atmosphere and its kinetics since 1948: A brief review. Energy. 2011;**36**:12-40

[53] Fermoso J, Stevanov C, Moghtaderi B, Arias B, Pevida C, Plaza MG, et al. High pressure gasification reactivity of biomass chars produced at different temperatures. Journal of Analytical and Applied Pyrolysis. 2009;**85**:287-293

[54] Kajitani S, Suzuki N, Ashizawa M, Hara S. CO_2 gasification rate analysis of coal char in entrained flow coal gasifier. Fuel. 2006;**85**:163-169

[55] Kovacik G, Chambers A, Özüm B. CO_2 gasification kinetics of two alberta coal chars. Canadian Journal of Chemical Engineering. 1991;**69**:811-815

[56] Matsui I, Kunii D, Furusawa T. Study of char gasification by carbon dioxide. 1. Kinetic study by thermogravimetric analysis. Industrial and Engineering Chemistry Research. 1987;**26**:91-95

[57] Liu GS, Tate AG, Bryant GW, Wall TF. Mathematical modeling of coal char reactivity with CO_2 at high pressures and temperatures. Fuel. 2000;**79**:1145-1154

[58] Muhlen H-J, Heek KHV, Juntgen H. Kinetic studies of steam gasification of char in the presence of H2, CO_2 and CO. Fuel. 1985;**64**:944-949

[59] Tay HL, Kajitani S, Zhang S, Li C-Z. Effects of gasifying agent on the evolution of char structure during the gasification of Victorian brown coal. Fuel. 2013;**103**:22-28

[60] Nilsson S, Gomez-Barea A, Ollero P. Gasification of char from dried sewage sludge in fluidized bed: Reaction rate in mixtures of CO_2 and H_2O. Fuel. 2013;**105**:764-768

[61] Roberts DG, Harris DJ. Char gasification in mixtures of CO_2 and H_2O: Competition and inhibition. Fuel. 2007;**86**:2672-2678

[62] Umemoto S, Kajitani S, Hara S. Modeling of coal char gasification in coexistence of CO_2 and H_2O considering sharing of active sites. Fuel. 2013;**103**:14-21

[63] Bai Y, Wang Y, Zhu S, Yan L, Li F, Xie K. Synergistic effect between CO_2 and H_2O on reactivity during coal chars gasification. Fuel. 2014;**126**:1-7

[64] Jayaraman K, Gökalp I, Jeyakumar S. Estimation of synergetic effects of CO_2 in high ash coal-char steam gasification. Applied Thermal Engineering. 2017;**110**:991-998

[65] Bliek A, Lont JC, van Swaaij WPM. Gasification of coal-derived chars in synthesis gas mixtures under intraparticle mass-transfer-controlled conditions. Chemical Engineering Science. 1986;**41**:1895-1909

[66] Everson R, Neomagus H, Kasani H, Njapha D. Reaction kinetics of pulverized coal-chars derived from inertinite-rich coal discards: Gasification with carbon dioxide and steam. Fuel. 2006;**85**:1076-1082

[67] Molina A, Mondragon F. Reactivity of coal gasification with steam and CO_2. Fuel. 1998;**77**:1831-1839

[68] Szekely J, Evans JW. A structural model for gas—Solid reactions with a moving boundary. Chemical Engineering Science. 1970;**25**:1091-1107

[69] Alvarez T, Antonio BF, Jose J, Ehrburger PP. Influence of coal oxidation upon char gasification reactivity. Fuel. 1995;**74**:729-735

[70] Ochoa J, Casanello MC, Bonelli PR, Cukerman AL. CO_2 gasification of Argentinean coal chars: A kinetic characterization. Fuel Processing Technology. 2001;**74**:161-176

[71] Lee JM, Kim YJ, Lee WJ, Kim SD. Coal-gasification kinetics derived from pyrolysis in a fluidized-bed reactor. Energy. 1998;**23**:475-488

[72] Dhupe AP, Gorkarn AN, Doraiswamy LK. Investigations into the compensation effect at catalytic gasification of active charcoal by carbon dioxide. Fuel. 1991;**70**:839-844

[73] Aranda G, Grootjes AJ, van der Meijden CM, van der Drift A, Gupta DF, Sonde RR, Poojari S, Mitra CB. Conversion of high-ash coal under steam and CO_2 gasification conditions. Fuel Processing Technology. 2016;**141**:16-30

Chapter 12

Innovative Microreactors for Low-grade Feedstock Gasification

Said Samih, Sherif Farag and Jamal Chaouki

Additional information is available at the end of the chapter

http://dx.doi.org/10.5772/intechopen.74602

Abstract

The first fluidized bed thermogravimetric analyzer (FBTGA) has been developed. The proof of concept of the FBTGA has been carried out on the thermal decomposition of calcium hydroxide. The kinetics and modeling of coal pyrolysis and gasification were investigated in the FBTGA. The obtained activation energies for the individual gases that are produced from coal pyrolysis are 19 to 21% lower than those found for similar coals in the literature. This decrease in the activation energies is explained by a temperature gradient of 185 to 209°C. For the CO shift reaction, the resulting activation energy is 46.6 kcal/mol, increasing by 20% from the one used in the literature. The second reactor presented in this work is a TGA powered by electromagnetic irradiation. As an application for this reactor, a novel kinetic model based on a dual attempt to predict not only the yield but also the composition of bio-oil is presented. The validation of the developed models demonstrated an excellent capability of predicting the yield and quality of the produced oil. The third reactor is a saddle reactor, which consists of two V-shaped pairs of arms and minimizes the impact of the heat and mass transfer limitation on chemical reactions.

Keywords: fluidized bed TGA, microwave TGA, saddle reactor, kinetics, gas-solid reactions

1. Introduction

Due to environmental constraints and a lack of access to natural resources, the feedstocks of several industrial sectors are changing, which is one reason why many industrial applications use new fuel sources and blends of feedstocks, including biomass, lignin, coal, and petcoke. The intrinsic variability in feedstock makes it challenging to design, operate, and optimize a chemical process, where detailed information regarding hydrodynamics, transport phenomena, and reaction kinetics among other subjects, is essential.

The gasification of coal technology also faces many issues, including low efficiency, the presence of tar, high capital, and operating costs. Furthermore, power efficiency of gasification decreases by the presence of ash in coal, which is also a major constituent of air pollutants.

One of the main problems in a low-grade coal gasification process is the formation of deposits, which can prevent gas flow and heat transfer, thereby obstructing the operation of the process. High-process efficiency could be theoretically and thermodynamically obtained with low-rank coal by using better solid-gas contacting systems and catalysts.

The common problem of all gasification technologies is building an appropriate apparatus to develop reliable kinetics. Since the gasifier is at the heart of a coal gasification plant, the overall performance of the plant can be successfully analyzed based on the reliability of the reactor modeling. The design of a gasifier is based on the reliability of the kinetics used for this purpose.

During the last few decades, a limited effort has been made to investigate these topics when a complex feedstock is being processed. In addition, a few microreactors have been invented to overcome the issues and limitations associated with the conventional instruments used to investigate the abovementioned topics. Microreactors are used in the field of chemical engineering for their advantages over reactors of traditional sizes. The microreactors are more powerful due to their small size so the gravitational force can be neglected. The surface forces will therefore be greater and the mass and energy transfer to the reactor will be higher.

Different experimental techniques can be applied to help define some reactions, for instance, solid fuel pyrolysis, combustion, gasification and thermal decomposition of polymers. Thermogravimetric analysis, differential thermal analysis, and differential scanning calorimetry are three experimental techniques used to determine the kinetics and the mechanism of gas-solid reactions that are thermally activated. There are some limitations with the thermogravimetric technique due to non-uniform temperatures, non-homogeneity of the distribution of gas-solid and solid-solid materials, low heating rates, not enough solid samples to represent the homogeneity of it, and the bulk, interparticle, and intraparticle diffusion control. This led to the invention of the first fluidized bed thermogravimetric analyzer that has the potential to decrease and eliminate these limitations [1, 4].

One of the advantages of the FBTGA due to fluidization is good mixing for a better distribution of solid and gas particles. It is therefore possible using the fluidized bed reaction chamber to achieve uniformity in the sample temperature, eliminate bulk and interparticle diffusion controls, have an acceptable quantity of solid sample, and obtain a higher heating rate. The main benefit is the new FBTGA that can be used to test and define catalytic gas-solid reactions on a smaller scale to gain a better overall view on an industrial scale.

The second novel system presented in this work is a TGA powered by microwave heating (MWH). The dominant mechanism of MWH, which relies on the direct volumetric energy conversion within the irradiated material, has established MWH in a significant number of industrial applications. Superseding the superficial heat transfer of conventional heating (CH) with that of MWH avoids most of the problems associated with CH, the most paramount being the temperature gradient inside and outside the heated materials that prompt

the undesirable secondary reactions. Based on the dielectric properties of the irradiated materials, MWH can dramatically diminish operating costs and the potential of a thermal hazard since it only interacts with particular types of materials. This aspect would lead to producing materials with a novel microstructure and/or initiate reactions that cannot be initiated when CH is applied. Also, it can perform the existing reactions under conditions that are entirely different from that of CH. The main reason behind these unique merits is the ability to concentrate the generated heat energy at a particular component among others, which might affect the reaction kinetics. The high precision and safety of the microwave heating technology offer a greater level of control that, consequently, presides over the target end in a delegated manner. As microwave irradiation is easily and rapidly initiated and terminated, such a mechanism would lead to reducing the undesirable intermediate thermal steps and, in turn, enhance the production rate. Indeed, these unique advantages and others help in the fundamental understanding of the energy conversion mechanism of MWH and how it impacts the chemical reaction engineering, especially when a non-conventional feedstock is processed.

The main objective of this chapter is to demonstrate two of the up-to-date systems developed for a better understanding of the chemical reactions behind the processing of complex feedstocks. To do so, the abundance and characteristics of low-grade feedstocks are debated. The common problems associated with the processing of such non-conventional materials are presented. The novel microreactors that have recently been developed in academia, including the fluidized bed thermogravimetric analyzer and the microwave thermogravimetric analyzer that was developed in the PEARL group, are elucidated. PEARL stands for process engineering advanced research lab [5].

2. Experiments

2.1. Material

2.1.1. Experiments in the fluidized bed TGA

The materials that were used for the fluidized bed TGA are the Western Canadian lignite coal (WLC) and ash free coal. The ash free coal was produced by the Department of Chemical and Materials Engineering, University of Alberta, Canada. It was produced by solvent extraction [2, 3, 6, 7]. The proximate and the ultimate analyses are presented in **Table 1**. Furthermore, K_2TiO_3 was the commercial catalyst that was used for the catalytic ash free coal gasification experiments.

2.1.2. Materials for the experiments in the microwave thermogravimetric analyzer

The virgin material processed in the developed MW-TGA was softwood kraft lignin that precipitated from a Canadian kraft mill using the LignoForce System™, a patent pending process. The CHNS of lignin are C=63.27%, H=5.79%, N=0.07%, and S=1.56%, and the approximate analyses are fixed: carbon=37%, volatiles=62%, and ash=1%. Further analysis of the processed material can be found in the references [8–12].

	Canadian lignite coal	Ash free coal
Proximate analysis (wt. % a.r.)		
Fixed carbon	34.3	46.7
Volatile matter	39.3	53.2
Ash	15.4	Trace
Moisture	11.1	Trace
Ultimate analysis (wt. %)		
C	57.2	88.9
H	4.3	5.1
N	1.20	1.5
O	21.1	24.9
S	0.1	0.0
a.r. as received		

Table 1. Analysis of the Western Canadian lignite coal [2].

2.2. Apparatus description

2.2.1. Fluidized bed TGA

A schematic of the first microreactor presented in this book chapter is shown in **Figure 1**. This apparatus represents the first fluidized bed thermogravimetric analyzer (FB-TGA) in the world. It comprises a quartz reactor that can operate at temperatures from 25 to 1200°C, furnace and measuring instruments, such as thermocouples, two mass flow controllers, pressure transducers and load cell. The FBTGA is connected to a data acquisition system. The fluidization is set to the minimum rate for any temperature using specific software. The quartz operates at atmospheric pressure with a wide range of solid samples, with a maximum amount of 50 g.

2.2.2. Microwave thermogravimetric analyzer

Two significant modifications were performed to make a traditional microwave oven work as a TGA. To accurately measure the weight loss of the payload during exposure to microwaves, the carrier reactor was directly connected to a scale fixed on the top of the oven through two opposing side-holes, as shown in **Figure 2**. To measure the transient mean temperature of the payload during the exposure to microwaves, an innovative thermometer called an "air-thermometer" was designed and made. That thermometer's theory is mainly based on the direct relationship between the pressure and temperature of a constant volume of gas. As soon as the temperature of the thermometer probe increases, the pressure of the gas that is inside the probe increases as well. The measured increase in the gas pressure is, then, translated to find the temperature of the payload. It is worth mentioning that the thermometer probe is made of

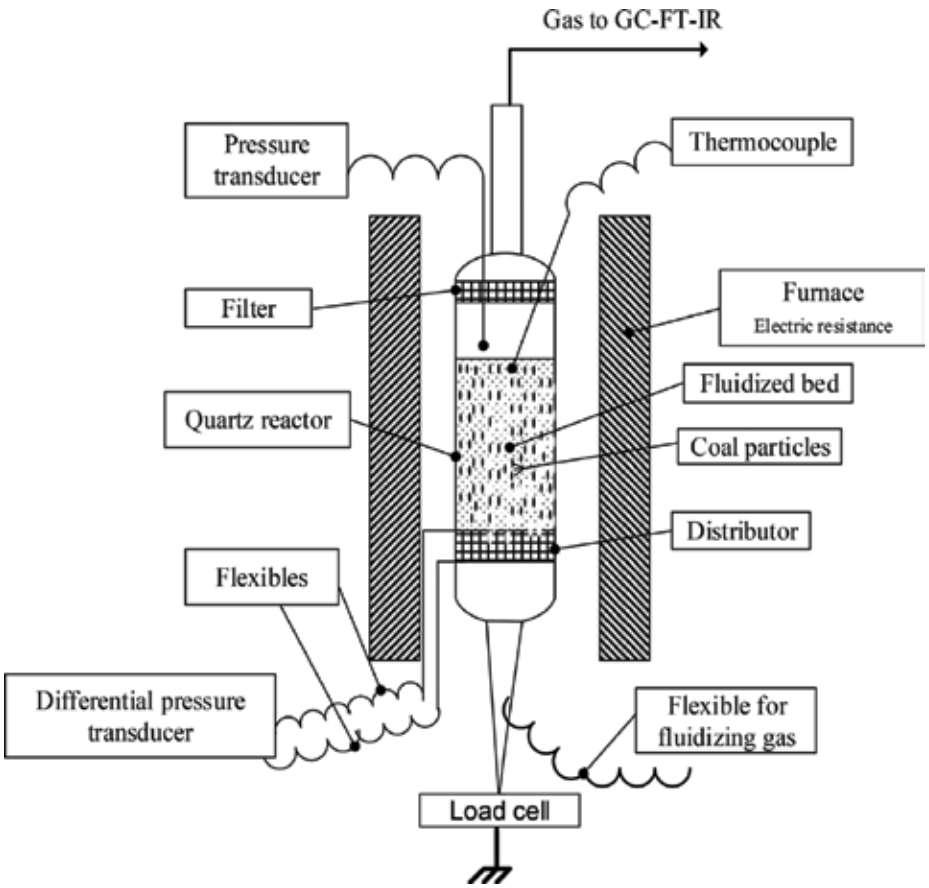

Figure 1. Fluidized bed TGA. Reproduced from reference [1].

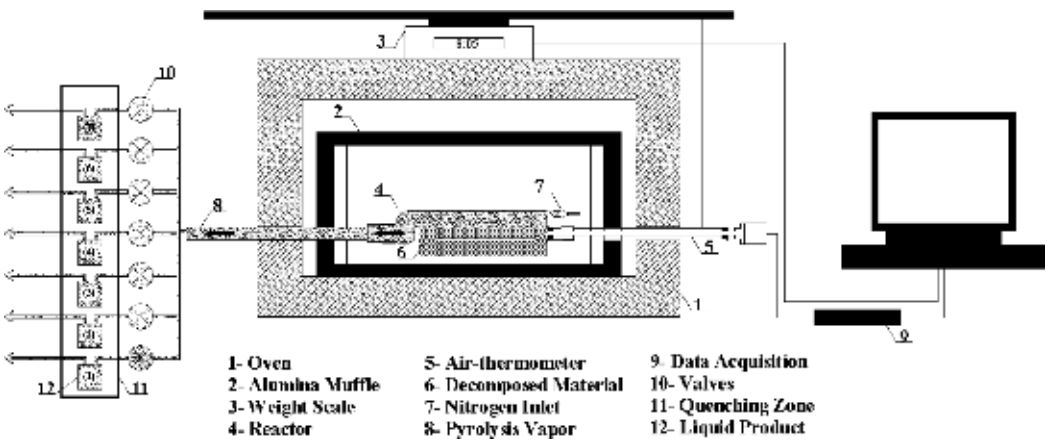

Figure 2. Microwave thermogravimetric analyzer.

quartz and the working gas is air. This means that almost no interactions between the applied electromagnetic waves and the materials mentioned above have taken place. This aspect ensures that the innovated thermometer does not suffer from the drawbacks of traditional thermometers. A manifold that consists of seven ports is connected at the outlet of the reactor to enable splitting the gas/vapor product at different times/temperatures for kinetics and other purposes. Farag and his co-authors have called the developed system the MW-TGA, which, at the time, was the first MW-TGA developed in the literature. For further details, kindly refer to [9, 10, 13, 14].

2.2.3. Saddle reactor

In the chemical reaction where a gas phase is one of the leading products, using a fluidized gas to overcome the heat and mass transfer limitations creates an issue. This issue is mainly related to the dilution of the produced gas. To overcome this problem, a novel reactor—called "saddle reactor"—has been designed and built in PEARL labs. As shown in **Figure 3**, the saddle reactor consists of two V-shaped pairs of arms connected at their bottoms by a small chamber. One of these two V-shaped is twisted by 90°; it is the optimum angle for the best mixing efficiency–which has been proofed in our previous publications. A set of heating elements is distributed in each arm to reach the needed temperature of performing the reaction. The power of those heaters was calculated and chosen to provide the heat energy required to achieve a particular end. Four built-in thermocouples are employed to control the input power to the heating elements and avoid reaching their melting points. A fifth thermocouple is fixed in the middle of the chamber that combines all the heating elements. This thermocouple controls the whole system based on the temperature of the payload. This means that the five measured temperatures are used to control the heating power of the system. The outlet of the saddle reactor is connected to two analytical techniques, GC and FTIR, to analyze the gas product.

2.3. Experimental procedures

2.3.1. Coal pyrolysis and gasification in the FB-TGA: the first application

The experiments for this first application of the FB-TGA were carried out in three steps: coal pyrolysis, partial oxidation of char, and coal gasification. The pyrolysis was performed in a nitrogen atmosphere. The heating rate was 40°C/min up to a maximum temperature of 700°C. The reactional system stabilized at 700°C for more than three hours. Novel kinetic parameters were developed for coal pyrolysis reactions from the collected data during the whole experiment time. During the second step, a specific gas mix of 5% oxygen-balance nitrogen was used to partially oxidize the produced char from the first step. The same heating rate and program were used. The experimental data were collected and used to derive kinetic parameters for the partial oxidation of the char. The third step in the FB-TGA was the coal gasification. During this third step, two different experiments were separately carried out under different conditions. The first one was at 650°C, while the second one was at 750°C. The two reactions were repeated three times. The method of collecting data was the same and the heating method was the same as the one that was used for the first two steps. The product gases, such as CO, CO_2, H_2, CH_4 and H_2O, were measured by a system of gas chromatography (GC)/Fourier-transform

infrared spectroscopy (FT-IR). For the three steps, the condensed tar at the exit of the reactor was burned off at 750°C.

2.3.2. Catalytic ash free coal gasification in FB-TGA: the second application

For this second application, about 5 g of lignite coal and ash free coals >500 μm and <600 μm in size were fluidized with 40 g of olivine sand, >180 μm and < 212 μm in size. The experiments of coal gasification were carried out in a gas mixture of 5% oxygen-balance nitrogen (N_2), whereas those for ash free coal gasification were established in a gas mixture of 3% oxygen-balance nitrogen. The heating rate was 40 °C/min and the particle density for the olivine sand was 3290 $kg \cdot m^{-3}$. The gas flow rate was changed, based on the strategy developed for the fluidized bed TGA, depending on the temperature to maintain the bed at the minimum fluidization regime [1].

To test the stability of the catalyst K_2TiO_3, 20 g of the commercial catalyst was fluidized and heated up to 800 °C under air atmosphere for 5 h. The results from the weight loss measurement and gas analysis demonstrated and confirmed that the commercial catalyst was stable. In all of the experiments, the K/C weight ratio was 10%, where K and C represent the amount of K and C that are contained in K_2TiO_3 and coal respectively.

2.3.3. Microwave thermogravimetric analyzer (MW-TGA)

Strategic procedures were performed to enable investigating the product yield and composition obtained from the microwave thermal cracking of lignin. The freezing zone that was used to collect the liquid product was kept at −18°C and the entire tubing barrier to the condensation system was kept at 200°C to prevent any condensation before the freezing zone. Then, the reactor was filled with the raw material and connected as shown in **Figure 2**. Subsequently, the signal cables and the air thermometer were installed, and an inert environment was created by purging the system with N_2.

When the reaction started, all the valves of the product manifold were closed, except one that was used for collecting the product. Afterward, at a certain temperature/time, the opened port was switched off, and the closed one was switched on to start receiving the product during another interval temperature/time. Once the reaction was eventually completed, the obtained liquids and the solid product were cold to the ambient temperature. The liquid product was separated into the oil phase, which has the most organic chemicals, and the aqueous phase, which is lower in density than the oil phase and mostly water and sent for analysis.

3. Results and discussion

3.1. Proof of the concept of the fluidized bed TGA

The proof of the concept of the fluidized bed TGA was carried out with the thermal decomposition of the calcium hydroxide. The results for the fluidized bed and conventional TGAs are shown in **Figure 3**. For the conventional TGA, three different amounts of calcium hydroxide (10, 25, and 140 mg) were tested, while 4 g of calcium hydroxide were used in the FB-TGA.

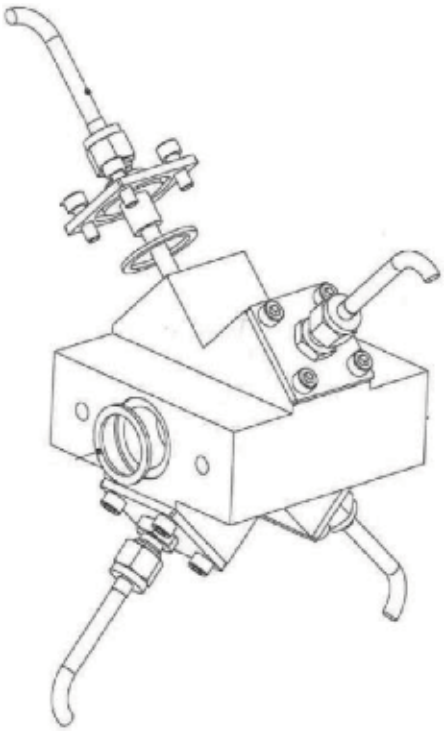

Figure 3. Saddle reactor.

For the first temperature interval, the results with 25 mg from the conventional TGA were similar to the ones for the FB-TGA with 4 g of calcium hydroxide. The conventional TGA results for 10 and 25 mg are similar, but they are different from those obtained for 140 mg. Two different parts can be distinguished in **Figure 4**. For 10 and 25 mg, the first part can be defined from 370°C to 470°C, whereas this first part is from 395°C to 565°C for 140 mg [1].

For the first part, the heat transfer limitation and/or the temperature gradient are responsible for the difference between the results obtained for 10, 25, and 140 mg. The intraparticle and the external diffusions of the produced water through a small layer of CaO that was formed around the $Ca(OH)_2$ became the rate-controlling step of the thermal decomposition during the second step [1].

Only for the first step, the results for 25 mg of $Ca(OH)_2$ in the conventional TGA agree with those for 4 g in the fluidized bed TGA. Indeed, the thermal decomposition of $Ca(OH)_2$ in the FB-TGA was carried out in one stage, from 360°C to 540°C. Thus, a better heat transfer and mass transfer of water vapor was obtained with the use of the FB-TGA and no diffusion control was observed.

3.2. Coal pyrolysis and gasification in the fluidized bed TGA

The experiments of coal pyrolysis and gasification were carried out in the fluidized bed TGA. These experiments were used to derive novel kinetic parameters from the fluidized bed TGA.

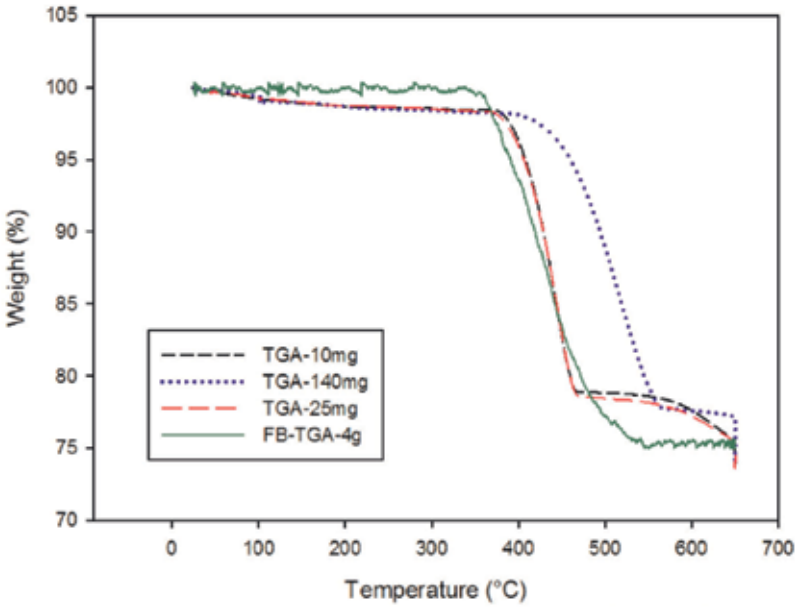

Figure 4. $Ca(OH)_2$ decomposition: comparison between conventional and fluidized bed TGAs. Reproduced from reference [1].

The weight loss measurement and the quantity of gas produced showed general agreement, for both coal pyrolysis and gasification results.

Due to a 170–209oC temperature gradient, the obtained values of some activation energies are lower or higher than what was found in the literature. The obtained activation energy for the CO shift reaction was 195.0 kJ/mol. This value is 20% higher than the one in the literature. The obtained activation energies for coal pyrolysis reactions were 19–21% lower than the ones obtained in the literature for similar coals [2]. These new results confirm that there was a measurement error of the temperature in certain past studies. Such measurement error means that for the past studies, the reaction chamber temperature was not the one that is used to find kinetic parameters. Thus, there is a temperature gradient between the measured temperature by the thermocouple of the conventional thermogravimetric analyzer and the real one of the reaction. Such increase of 19–21% of the activation energy is the equivalent of 185–209°C temperature gradient of similar relatively exothermic reactions [2, 4, 15]. Finally, the results obtained were as expected and confirmed that the FB-TGA provides reliable kinetic parameters. More discussion and results are shown in our previous work [3, 4].

3.3. Catalytic ash-free coal gasification in a fluidized bed TGA

The second experiment that was carried out on the FB-TGA is about the catalytic ash free coal gasification. In this work, the effect of the catalyst on ash free coal gasification is included. A comparison of the total product gas yield and the weight loss is represented in **Figure 5**.

The two experimental results are in global agreement, and the slight difference is due to the produced tar from ash coal experiments.

A comparison of the carbon conversion results of coal, ash free coal and catalyst with ash free coal is illustrated in **Figure 6**. CatAFC, AFC, and coal, stand for the catalyst with ash free coal, ash free coal and coal gasification, respectively. The lowest carbon conversion is obtained from ash free coal for temperatures lower than 730°C, after which the coal

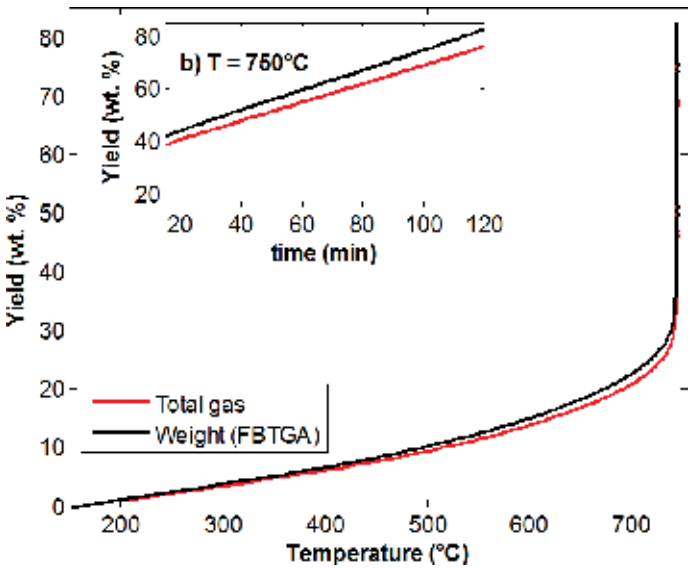

Figure 5. Catalytic ash free coal gasification in a fluidized bed TGA. Reproduced from reference [2].

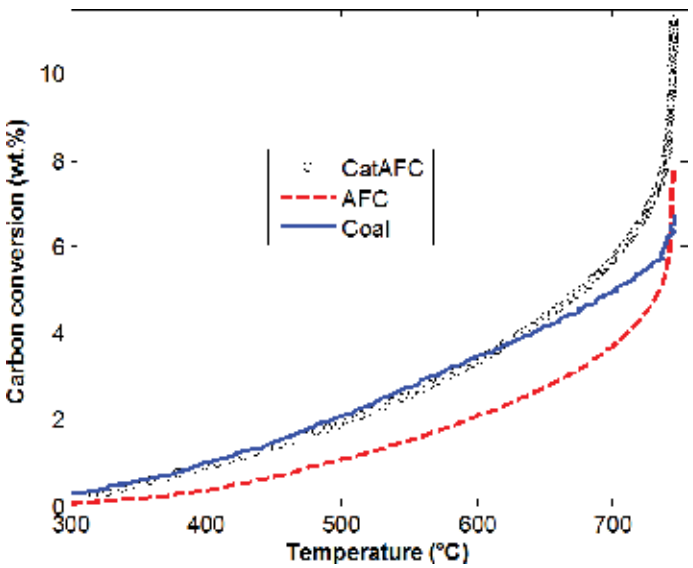

Figure 6. Temperature effect on carbon conversion. Reproduced from reference [2].

gasification had the lowest carbon conversion result. Thus, coal beneficiation has a negative affect on carbon conversion. Nevertheless, at 700°C, there is an increase of carbon conversion by 15.3 and 52.6%, for coal and ash free gasification. These values increased to 44.5 and 69.1% at 750°C [2].

Moreover, novel kinetic parameters are obtained form the FB-TGA experimental results for the reactions of partial oxidation, gas-water shift, and methane reforming. For char gasification, the results are similar to those found in literature [16]. For the gas-water shift and methane reforming reactions, the obtained activation energies were 56.5 and 77 kJ/mol, respectively. Compared to the values found in literature, these results are significantly lower. The lowest activation energy for the water-gas shift reaction was 70 kJ/mol [2, 17–19], which is 1.24 times higher than the one obtained in the fluidized bed TGA.

The lowest activation energy found in literature for the methane reforming reaction is 85 kJ/mol [2, 18], which is 10% higher than the one obtained with the fluidized bed TGA.

The values of the activation energies of the CO shift and the methane reforming reactions decreased by 56% and 33%, respectively, by using the catalyst. This catalyst was applied on other reactions in the literature and the activation energy was decreased by 43 to 75% [2, 20]. More results and discussions are given in our previous article [2].

3.4. Microwave thermogravimetric analyzer

Farag and his co-authors have employed the obtained experimental data from the developed MW-TGA, following the method presented in Section 2.3.3, to carry out a kinetic study based on the lumped approach. The established model in their work takes into consideration the chemical composition of the oil and aqueous products that are obtained from the microwave pyrolysis of lignin. As shown later, it considers that the virgin material converts into seven main products: remaining solid, phenolics, aromatic single ring and non-phenols (ASR-Non-Ph), aliphatics, heavy molecular weight compounds (HMWCs), water, and non-condensable gas, as shown later. The kinetic model demonstrated in Eq. (1) was used to estimate the kinetic parameters, activation energy, pre-exponential factor, and reaction order associated with every reaction toward producing these seven products.

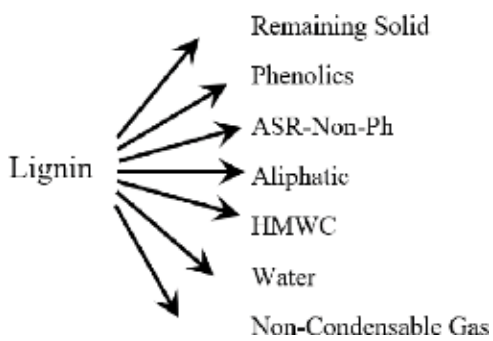

$$\frac{dS}{dt} = -k_{o_s}\left(e^{\frac{-E_s}{RT}}\right)(S-S_\infty)^{n_s} = -k_{o_{Ph}}\left(e^{\frac{-E_{s_{Ph}}}{RT}}\right)(S-S_\infty)^{n_{Ph}} - k_{o_{ASR-Non-Ph}}\left(e^{\frac{-E_{s_{ASR-Non-Ph}}}{RT}}\right)(S-S_\infty)^{n_{ASR-Non-Ph}}$$
$$-k_{o_a}\left(e^{\frac{-E_a}{RT}}\right)(S-S_\infty)^{n_a} - k_{o_{HMWC}}\left(e^{\frac{-E_{a_{HMWC}}}{RT}}\right)(S-S_\infty)^{n_{HMWC}} - k_{o_w}\left(e^{\frac{-E_w}{RT}}\right)(S-S_\infty)^{n_w} - k_{o_g}\left(e^{\frac{-E_g}{RT}}\right)(S-S_\infty)^{n_g} \quad (1)$$

In Eq. (1), k_o is the pre-exponential factor [time^{-1}], E_a is the apparent activation energy [J/mol K], T is the reaction temperature [K], and R is the universal gas constant [J/mol K]. The subscripts s, ph, ASR-Non-ph, a, HMWC, g, and w refer to solid, phenolic, aromatic single ring and non-phenolic, aliphatic, heavy molecular weight compound, gas and water products, respectively. **Figure 7**

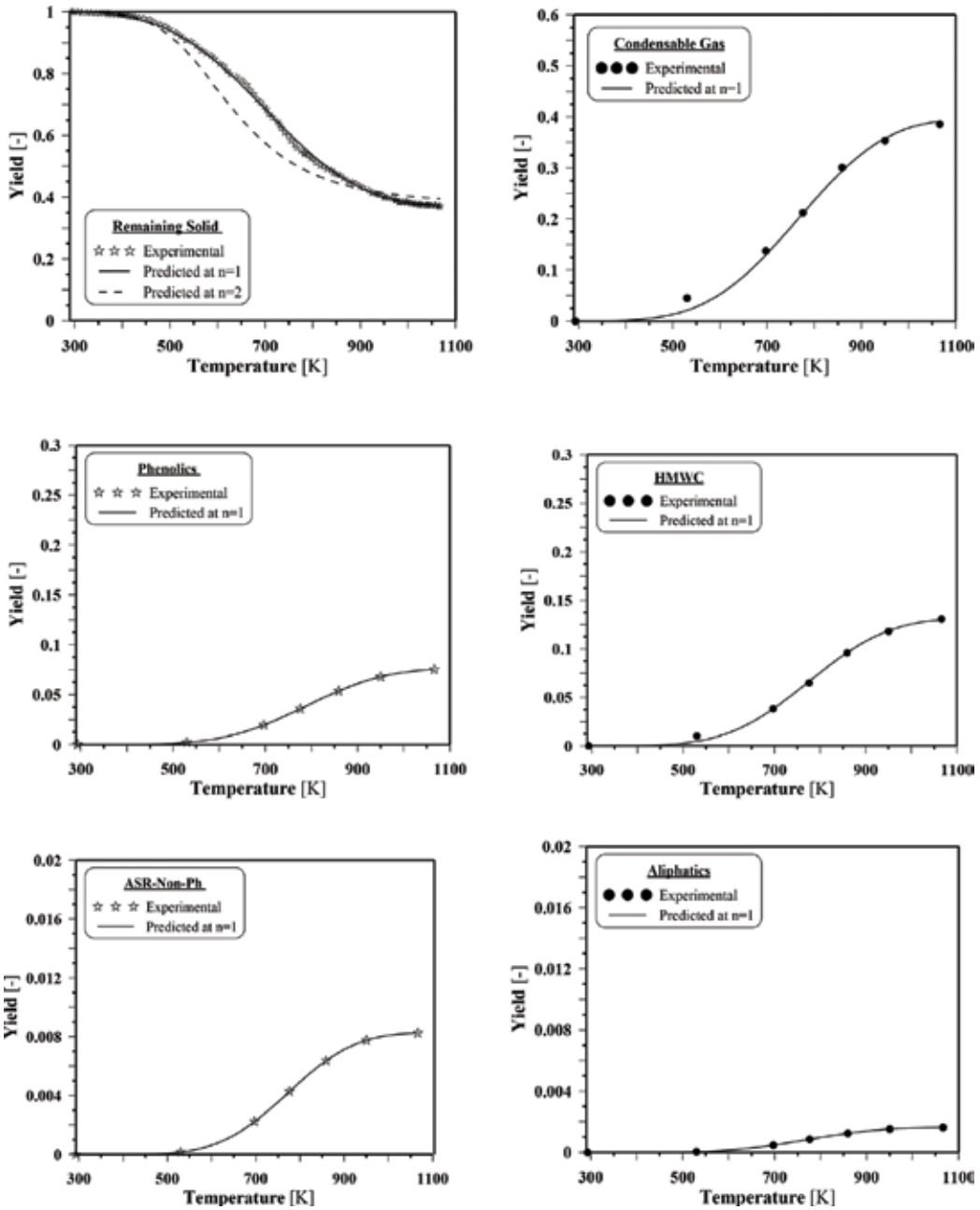

Figure 7. Experimental and predicted yields of lignin pyrolysis products. Reprinted with a permission form [5].

demonstrates the experimental and predicted yield of these products, except water, which can be calculated by subtracting the summation of these products from unity. **Table 2** shows that the estimated kinetic parameters of each single reaction lead to the production of each of these products. For the full details regarding how these parameters were determined, kindly refer to [10].

Farag et al. believe that up to 725 K the condensable gas yield is slightly lower than that of the non-condensable gas, which could be the result of the swift split in lignin-side aliphatic hydroxyl groups [10]. Beyond 725 K, the total liquid yield continues increasing because of the decomposition of strong chemical bonds in the lignin network. Based on the estimated kinetic parameters, the reaction rate of the liquid products is lower than that of the solid product. The authors have claimed that the low secondary reactions under these conditions might be the reason for this result. The non-condensable gas product is mostly produced from the cracking of lignin-side chains, and the liquid product is produced from the breakdown of bonds between lignin aromatic rings. Therefore, the estimated activation energy of the non-condensable gas is lower than that of all oil products. Since the structure of the decomposed material's network is totally poly-aromatics, the reaction rate to produce phenolics and HMWC groups is much higher than that of ASR-Non-Ph. Accordingly, the estimated activation energy of aliphatics is greater than that of the other groups. The authors also think about the impact of microwave heating to decrease the probability of a secondary reaction when producing aliphatics.

In the scientific literature, an apparent contradiction to the interpretation of the influence of electromagnetic irradiation on reaction kinetics has been documented. Wang et al. 2013, Li et al. [26], Fukushima et al. 2013, Adnadjevic and Jovanovic [25], Sun et al. [22], Jovanović 2012, and a few other research groups believe that the reaction activation energy decreases under microwave irradiation [21–28]. On the other hand, Mazo et al. [28] and Yadav and Borkar [27] have reported that E_a is the same in both cases, MWH and CH [13, 29–31]. It is well known that the wavelength of microwaves is significantly longer than the intermolecular distance of the target, which ideally doubles the impact of MWH on the activation energy. However, this does not reject the probability of producing some intermediates that could

Product	ko [min^{-1}]	Ea [kJ/mol]	n
Remaining solid	7	19	1
Water	9	27	1
Phenolics	21	38	1
HMWC	22	35	1
ASR-Non-Ph	1	40	1
Aliphatics	20	47	1
Condensable gas	22	29	1
Non-condensable gas	6	22	1

Table 2. The estimated kinetic parameters of the Farag et al. [5] model.

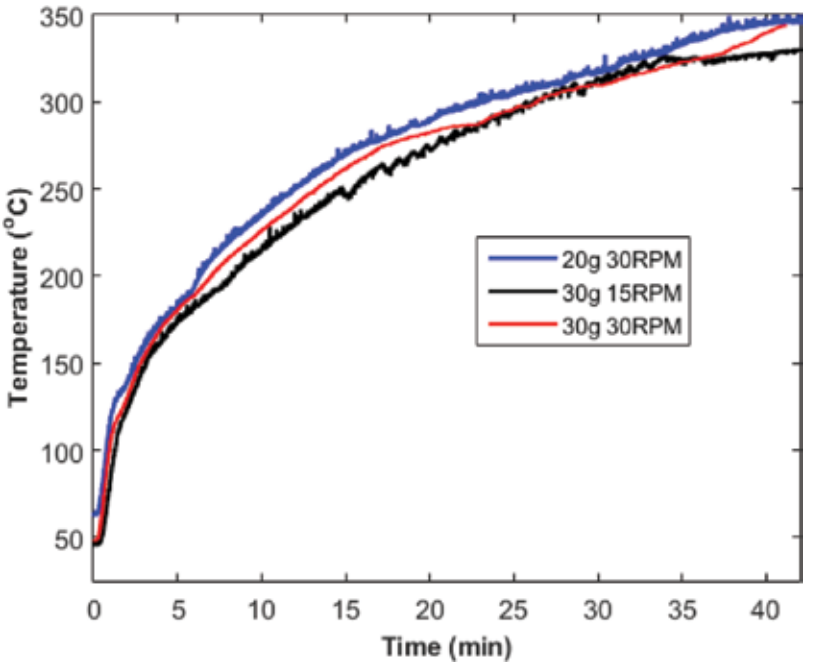

Figure 8. Effect of the speed mixing on the temperature profile in the saddle reactor.

have different behaviors than that of the starting material which would impact the activation energy. In such cases, the dielectric properties of the produced intermediates should be measured and investigated to understand the potential of having hot spots that affect the reaction kinetics locally [14, 32, 33]. Therefore, further investigations are required to discover the fact behind the reported effects on the activation energy and other reaction kinetic parameters.

3.5 Saddle reactor

As explained previously, the saddle reactor is mainly used to avoid the dilution of the product gas. Indeed, the solid sample can be very well mixed in the saddle reaction chamber without using a gas mixing agent. To prove this concept, different masses of silica sand—from 20 to 30 g—were mixed and heated up to 350°C in the reactor. The results shown in **Figure 8** are for different mixing speeds, ranging from 15 to 30 RPM. The similar temperature profiles confirm the good mixing in the developed reactor.

4. Conclusion

New microreactors for the gasification of low-grade feedstock have been developed. The fluidized bed TGA was applied to the coal and ash-free coal gasification. New values of activation energies are obtained. The values for coal pyrolysis are from 34.7 to 59.8 kcal/mol, whereas the one for the CO shift reaction is 46.6 kcal/mol. The use of the potassium catalyst is allowed to reduce the activation energies of the CO shift and the methane-reforming reactions

by 56 and 33%, respectively. A novel microwave-TGA equipped with an innovated air thermometer and a product manifold was built. The developed system was used to predict the product yield and the bio-oil composition from pyrolysis of kraft lignin using a lumping approach. The experimental data were employed to estimate the kinetic parameters of every reaction to produce the solid, water, alipahtics, phenols, aromatic with a single ring aromatic non-phenol, heavy molecular weight compounds, and gas product.

At a temperature below 725 K, the yield of the gas product was higher than that of the liquid products. This results from the swift split of the lignin chains that mainly produce water and/or gas products. The estimated kinetic parameters showed that the rate of thermal cracking of lignin is higher than that of the liquid product, which points out that the possibility of secondary reactions is low. The formation of the ASR-Non-pH and aliphatics families is lower than that of the HMWC, which could originate from the complex structure of the lining.

A saddle reactor is developed, and good mixing was observed for 20–30 g of silica sand and speed mixing of 15–30 RPM.

Author details

Said Samih[1,2], Sherif Farag[1,3,4] and Jamal Chaouki[1*]

*Address all correspondence to: jamal.chaouki@polymtl.ca

1 Department of Chemical Engineering, Process Engineering Advanced Research Lab (PEARL), Ecole Polytechnique de Montreal, Montréal, QC, Canada

2 AFMERICA TECHNOLOGY Inc., Corot, Verdun (QC), Canada

3 Faculty of Engineering at El-Mattaria, Helwan University, Cairo, Egypt

4 RMTech for Environmental Solutions Inc., Canada

References

[1] Samih S, Chaouki J. Development of a fluidized bed thermogravimetric analyzer (in English). Aiche Journal. Jan 2015;**61**:84-89

[2] Samih S, Chaouki J. Catalytic ash free coal gasification in a fluidized bed thermogravimetric analyzer. Powder Technology. Jul 1, 2017;**316**:551-559

[3] Samih S. Développement d'un analyseur thermogravimétrique à lit fluidisé : application à la gazéification catalytique du charbon. PhD Thesis, École Polytechnique de Montréal. 2016

[4] Samih S, Chaouki J. Coal Pyrolysis and Gasification in a Fluidized Bed TGA. The Canadian Journal of Chemical Engineering. 2018

[5] Process Engineering Advanced Research Lab (PEARL). Available: http://pearl.polymtl.ca/

[6] Kopyscinski J, Rahman M, Gupta R, Mims CA, Hill JM. K_2CO_3 catalyzed CO_2 gasification of ash-free coal. Interactions of the catalyst with carbon in N_2 and CO_2 atmosphere. Fuel, vol. 117, Part B, pp. 1181-1189, 1/30/ 2014

[7] Okuyama N, Komatsu N, Shigehisa T, Kaneko T, Tsuruya S. Hyper-coal process to produce the ash-free coal. Fuel Processing Technology. 2004;**85**:947-967

[8] Farag S, Chaouki J. Economics evaluation for on-site pyrolysis of kraft lignin to value-added chemicals. Bioresource Technology. 2015;**175**:254-261

[9] Farag S, Fu D, Jessop PG, Chaouki J. Detailed compositional analysis and structural investigation of a bio-oil from microwave pyrolysis of kraft lignin. Journal of Analytical and Applied Pyrolysis. 2014;**109**:249-257

[10] Farag S, Kouisni L, Chaouki J. Lumped Approach in Kinetic Modeling of Microwave Pyrolysis of Kraft Lignin. Energy & Fuels. Feb 2014;**28**:1406-1417

[11] Fu D, Farag S, Chaouki J, Jessop PG. Extraction of phenols from lignin microwave-pyrolysis oil using a switchable hydrophilicity solvent. Bioresource Technology. 2014; **154**:101-108

[12] Mudraboyina BP, Farag S, Banerjee A, Chaouki J, Jessop PG. Supercritical fluid rectification of lignin pyrolysis oil methyl ether (LOME) and its use as a bio-derived aprotic solvent. Green Chemistry. 2016;**18**:2089-2094

[13] Farag S, Chaouki J. A modified microwave thermo-gravimetric-analyzer for kinetic purposes. Applied Thermal Engineering. 2015;**75**:65-72

[14] Farag S, Mudrabovina BP, Jessop PG, Chaouki J. Impact of the Heating Mechanism on the Yield and Composition of Bio-oil from Pyrolysis of Kraft Lignin. Biomass and Bioenergy. 2016

[15] Ebrahimpour O, Chaouki J, Dubois C. Diffusional effects for the oxidation of SiC powders in thermogravimetric analysis experiments (in English). Journal of Materials Science. 2013;**48**:4396-4407

[16] Lee JM, Kim YJ, Lee WJ, Kim SD. Coal-gasification kinetics derived from pyrolysis in a fluidized-bed reactor. Energy. 1998;**23**:475-488

[17] Hakeem AA, Mu L, Berger RJ, Kapteijn F, Makkee M. Kinetics of the high temperature water-gas shift over Fe_2O_3/ZrO_2, Rh/ZrO_2 and $Rh/Fe_2O_3/ZrO_2$. Chemical Engineering Journal. 2015;**263**:427-34

[18] Wei J, Iglesia E. Structural requirements and reaction pathways in methane activation and chemical conversion catalyzed by rhodium. Journal of Catalysis. 2004;**225**:116-127

[19] Wang Y, Zhai Y, Pierre D, Flytzani-Stephanopoulos M. Silica-encapsulated platinum catalysts for the low-temperature water-gas shift reaction. Applied Catalysis B: Environmental. 2012;**127**:342-350

[20] Li S, Cheng Y. Catalytic gasification of gas-coal char in CO_2. Fuel. 1995;**74**:456-458,

[21] Adnadjevic BK. Jovanovic JD. A comparative kinetics study on the isothermal heterogeneous acid-catalyzed hydrolysis of sucrose under conventional and microwave heating. Journal of Molecular Catalysis A: Chemical. 2012;**356**:70-77

[22] Adnađević B, Gigov M, Sindjic M, Jovanović J. Comparative study on isothermal kinetics of fullerol formation under conventional and microwave heating. Chemical Engineering Journal. 2008;**140**:570-577

[23] Fukushima J, Kashimura K, Takayama S, Sato M, Sano S, Hayashi Y et al. In-situ kinetic study on non-thermal reduction reaction of CuO during microwave heating. Materials Letters. 2013;**91**:252-254

[24] Sun J, Wang W, Liu Z, Ma Q, Zhao C, Ma C. Kinetic Study of the Pyrolysis of Waste Printed Circuit Boards Subject to Conventional and Microwave Heating. Energies. 2012;**5**:3295-3306

[25] Chen F, Wang G, Shi C, Zhang Y, Zhang L, Li W et al. Kinetics of glycolysis of poly(ethylene terephthalate) under microwave irradiation. Journal of Applied Polymer Science. 2013;**127**: 2809-2815

[26] Yan W, Hu X, Zhang G, Deng M, Yi C, Xu Z. Microwave assisted preparation of monodisperse polymeric microspheres and its morphologies and kinetics. Journal of Wuhan University of Technology-Mater. Science Edition. vol. 27, pp. 1100-1104, 2012/12/01

[27] Adnadjević BK, Jovanović JD. Kinetics of Isothermal Ethanol Adsorption onto a Carbon Molecular Sieve under Conventional and Microwave Heating. Chemical Engineering & Technology. 2012;**35**:761-768

[28] Li Z, Han L, Xiao W. Influence of microwave heating on the liquefaction kinetics of corn stover in ethylene glycol. BioResources. 2013;**8**:3453-3460

[29] Yadav GD, Borkar IV. Kinetic modeling of microwave-assisted chemoenzymatic epoxidation of styrene. AIChE Journal. 2006;**52**:1235-1247

[30] Mazo P, Estenoz D, Sponton M, Rios L. Kinetics of the transesterification of castor oil with maleic anhydride using conventional and microwave heating. Journal of the American Oil Chemists Society. 2012;**89**(7):1355-1361

[31] Farag S. Production of chemicals by microwave thermal treatment of lignin [Philosophiae Doctor Ph.D. Thesis] Chemical Engineering. University of Montreal: École Polytechnique de Montréal, December 2013

[32] Farag S, Sobhy A, Akyel C, Doucet J, Chaouki J. Temperature profile prediction within selected materials heated by microwaves at 2.45GHz. Applied Thermal Engineering. 2012;**36**:360-369

[33] Doucet J, Laviolette J-P, Farag S, Chaouki J. Distributed microwave pyrolysis of domestic waste. Waste and Biomass Valorization. 2014;**5**(1):1-10

Section 4

Process Integration and Utilization

Chapter 13

Integrated Gasification System for Power and Hydrogen Production

Lukman Adi Prananto and Muhammad Aziz

Additional information is available at the end of the chapter

http://dx.doi.org/10.5772/intechopen.71841

Abstract

The growth of economic and living standard leads to more electricity demand. Unfortunately, due to more limitation of power station area and electricity grid development, energy delivery issue is rising up; hence, new method of delivering the power by different energy carrier is necessary to investigate. Hydrogen has the promising potential as an energy carrier due to its high gravimetric energy density and cleanliness to the environment. For comfortable storage and transportation, hydrogen is covalently bonded to methylcyclohexane (MCH) and liquid organic hydrogen carrier (LOHC). In this chapter, novel integrated gasification systems for coproduction of electricity and MCH from low-rank coal and microalgae have been proposed. The total energy efficiency is improved by applying enhanced process integration (EPI) technology to minimize exergy losses throughout the integrated system. The integrated system for microalgae is capable to provide more than 60% of total energy efficiency, while the integrated system for low-rank coal delivers the total energy efficiency of 84%.

Keywords: H_2 production, low-rank coal, microalgae, enhanced process integration, chemical looping, hydrogenation, energy efficiency

1. Introduction

Owing to the impact of economic growth and living standard improvement, the requirement for electricity is always climbing up, and therefore more power generators have to be developed to supply the demand [1]. Also, due to limitation of potential area for the plant and the high investment cost of both power station and electrical grid, further approach to deliver the energy by different energy carriers is favorable to meet the energy demand [2]. By far, fossil fuels act as both primary energy sources and energy carriers for electricity generation. However, despite the proven and relatively highly energy-efficient technologies, the adoption of the fossil energy promotes high environmental impacts and drawback of sustainability [3].

Therefore, together with the concern of energy scarcity and environmental issue, further investigation to discover alternative energy carrier is required not only to complement the fossil energy but also for primary utilization by achieving highly efficient energy systems.

Several parameters need to be accomplished for the future energy carrier, including the simple production method, high energy density, and environmentally benign performance. To this, the hydrogen (H_2) has the promising potential as an energy carrier [4]. Under the ambient condition, H_2 owns high gravimetric energy density (120 MJ kg^{-1}), much higher than gasoline or natural gas, which leads to the extensive heat capacity [5]. However, against the potentials as the future energy carrier, H_2 has severe characteristics in the extremely low volumetric energy density (10.8 MJ m^{-3}) and boiling temperature (−252.9°C), which leads to the difficult transportation and storage methods [6]. Thus, instead of dispatching H_2 individually, some pretreatment to bond the H_2 into the more convenient form of carrier is very beneficial.

Currently, transportation and storage of H_2 are carried out by the various schemes, including liquefaction, compression, chemical and physical storages. An alternative solution for H_2 storage with high storage capacity and low-risk level can be approached by employing the liquid organic hydrogen carriers (LOHCs) [7]. Covalently bonding the H_2 through the hydrogenation process, the LOHCs have the capability to carry out 5–8 wt% of the H_2 content [8]. Due to the characteristics of high reversibility (hydrogenation and dehydrogenation processes) in the moderate temperature, low GHG emissions, simple storage, and comfortable transportation method by using vessel or pipeline, LOHCs own the potential for the application of long-distance and large-scale H_2 transportation [9]. Moreover, the infrastructure of LOHCs is relatively compatible with current method of fuel transportation, due to the liquid phase of the LOHCs in the room temperature and standard pressure condition [10].

The LOHCs cycle involves hydrogenation and dehydrogenation processes. In this process, the generated H_2 is exothermically reacted with the particular compounds in the catalytic hydrogenation [11]. Recently available LOHCs include cyclohexane-benzene, decalin-naphthalene, and toluene-methylcyclohexane (MCH) cycles [8]. In this chapter, toluene (C_7H_8)–MCH (C_7H_{14}) cycle is investigated as the LOHC cycle for the transportation and storage of H_2. Both toluene and MCH are low cost, stable compound, and high flexibility of transportation as the liquid phase is very reliable in the wide temperature range, which is favorable for long-distance transport and long-term storage. In addition to this understanding, Chiyoda Corporation, a well-established process engineering company in Japan, has testified the applicability of the toluene-MCH cycle in a relatively large-scale facility [12].

The investigation is emphasized on the effort of integrating the corresponding processes, including the drying, gasification, chemical looping, power generation, and the hydrogenation process to achieve optimum energy circulation based on enhanced process integration (EPI) to obtain the excellent energy efficiency of the total system. EPI is a technology to minimize thoroughly the heat loss of the system by applying the combination of exergy recovery and process integration [13]. With EPI, instead of the optimization of each process individually, the entire energy management of the system is observed to develop a high-efficient integrated plant with minimum waste of energy [14].

In this chapter, integrated gasification systems which hold capabilities for coproduction of electricity and MCH from different feedstocks are discussed. The investigation of the systems is emphasized on the overall design of the process scheme and evaluation of some operating parameters for system optimization. Low-rank coal [15] and microalgae [8] are chosen as the feedstocks for the integrated system due to the opposite characteristics from each feedstock. However, since both feedstocks are far away from the standard quality of fuel due to high moisture content, a pretreatment stage, including the drying process is discussed also in this chapter. To obtain a high overall efficiency of the integrated system, EPI is applied to implement the optimum benefits of heat energy and reduce the exergy destruction.

2. Enhanced process integration technology

The theory of EPI has been introduced and applied to several raw materials, including algae [16], coal [17, 18], biomass wastes [19, 20], and black liquor [21]. EPI is established from two core technologies such as the process integration and the exergy recovery. The latter relates to the concept to circulate the heat throughout a single process. By applying the EPI, overall exergy loss throughout the integrated system can be reduced as the total energy efficiency of the system is improved.

Figure 1 illustrates the principle of heat circulation employed in the integrated system, including an example of the application of the term of exergy elevation of the process stream. Here, the dotted and solid lines represent the cold and hot streams, respectively.

In contrast to conventional process integration technology, the intensification of the process regarding energy efficiency is carried out in EPI through heat circulation to minimize the exergy losses in each process module before performing the overall process integration. Hence, the energy/heat associated with the process is recovered efficiently by employing heat circulation that promotes exergy recovery.

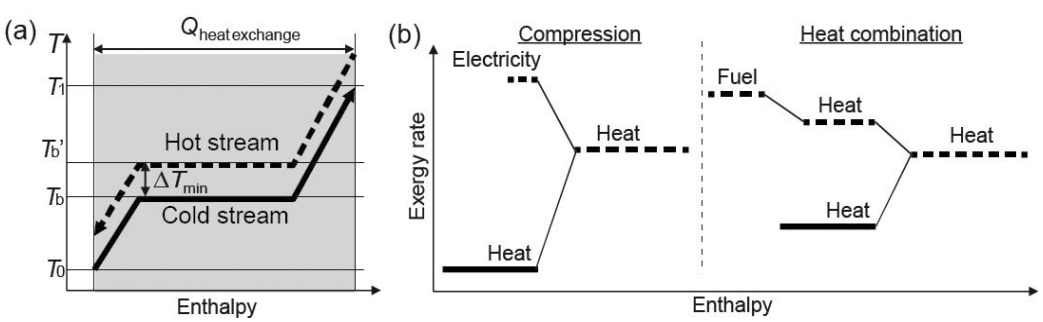

Figure 1. Basic heat circulation principle: (a) exergy elevation and heat coupling and (b) two examples of this method applied for stream exergy elevation: Compression and heat combination.

3. Power and H_2 production from various Feedstocks

3.1. Integrated systems from low-rank coal by syngas chemical looping

3.1.1. The characteristics of low-rank coal as energy source

Based on the current status of H_2 production, fossil fuel occupies dominant portion as the primary substance with more than 90% share [22]. In terms of sustainability, fossil fuel has a drawback in the issue of energy reserve. Hence, fossil fuel with abundant reserves is favorable for this system. One of the fossil fuel fit with this condition is low-rank coal (LRC). Besides the long-term reserves, LRC exhibits other advantages, including high concentration of volatiles, high reactivity, low sulfur content, and relatively low mining costs [23]. However, due to high inherent moisture content and readsorption behavior of the humidity, the drying of LRC is very challenging due to the energy intensive process [24]. Thus, an investigation based on EPI technology to effectively manage the heat circulation is carried out to develop an integrated system which can accommodate least expensive LRC for large-scale MCH production with optimum energy efficiency [25].

Another issue for the utilization of LRC is the large amounts of CO_2 emission, in which the plant has to be coupled with the CO_2 separation (capture) and sequestration facility. For the CO_2 capture, several technologies are available, including membrane, algae-based uptake, cryogenic, and chemical looping [26]. The latter is considered as the most potential method for the sequestration of CO_2 due to high capability of CO_2 capturing and high conversion efficiency.

Some investigations have been carried out to study the production of H_2 from coal. An integrated system consisting of hydrogasification, electrolysis, and electricity generation has been carried out by Minutillo and Perna [27] to produce synthetic natural gas. However, as the conventional process integration was adopted to develop the proposed system, the result of their study obtained relatively low energy efficiency due to significant losses of exergy. Another integrated system consisting of shell-type gasification, chemical looping, and electricity generation has been carried out by Xiang et al. In their proposed system [28], overall heat circulation was excluded, as the system adopted the pinch technology for heat recovery. Therefore, the system exhibits low energy efficiency. Moreover, Cleeton et al. carried out an integrated system with the combination of chemical looping and steam-coal gasification [29]. After the parameter evaluation, the delivered system showed energy efficiency up to 58%. However, if the effort of exergy optimization was applied, the energy efficiency of the system can be improved significantly.

3.1.2. Integrated system development

The schematic flow of energy and material of the integrated system is shown in **Figure 2**. Here, the dotted and solid lines represent electricity and material/heat flows, respectively. At the beginning of the process, the moisture content of raw LRC particles is extracted by the drying module. The product of this module is the high calorific value of LRC as the result of low moisture content. Next, the dried LRC particles are converted to syngas by the gasification module. The produced syngas is thus fed to the chemical looping module to generate H_2, CO_2,

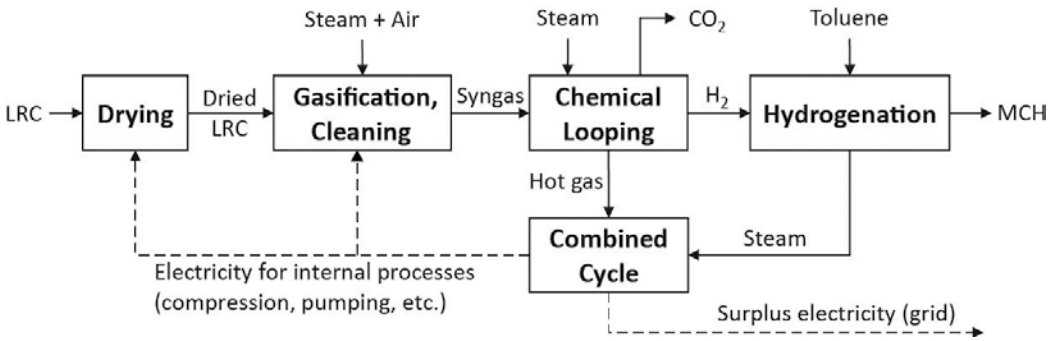

Figure 2. Schematic of material and energy flows in the integrated system.

and thermal energy for the power generation. The by-product of CO_2 generated in the chemical looping is sequestered to keep the clean energy of the integrated system, while the desired products of chemical looping are discharged to the combined cycle module and the hydrogenation module for the generation of electricity and MCH, respectively. The MCH is prepared in the liquid phase. Hence, the compound can be easily transported to the specified place. The generated electricity from the combined cycle is partially consumed for the house load operation for the internal processes, but the remainder can be sold to utilities via a connection to a power grid.

3.1.3. Analysis of integrated system

3.1.3.1. Drying and gasification

The drying process is carried out to meet the target of the moisture content of the LRC particle so that the calorific value is increasing and the high gasification temperature can be achieved. In the drying process, equilibrium moisture content significantly affects the immediate environment because the particle of LRC will reach a water concentration equal to the ambient environment. Hence, the temperature, pressure, and relative humidity of the environment, as well as the partial vapor pressure, determine the moisture content. Among any methods used for high moisture content drying process, the superheated steam exhibits numerous advantages, including the energy efficiency, high capacity, and has been widely investigated for drying scheme [30]. Thus, by employing the superheated steam as the drying method, the drying and gasification modules were developed, as shown in **Figure 3**. The relationship between the relative vapor pressure, p/p_o, and the equilibrium moisture content, M, can be approximated by Eq. (1) [31].

$$\frac{p}{p_o} = 1 - exp\left[-2.53(T_b - 273)^{0.47}\left(\frac{M}{(100 - M)}\right)^{1.58}\right] \tag{1}$$

Initially, the discharged heat produced in the chemical looping module and the high energy compressed steam is employed to preheat the high moisture content LRC particles (D1) in HX1 and HX2, respectively. Subsequently, the preheated LRC particles undergo drying process to omit the water content inside the particles. The type of dryer applied in this system is the

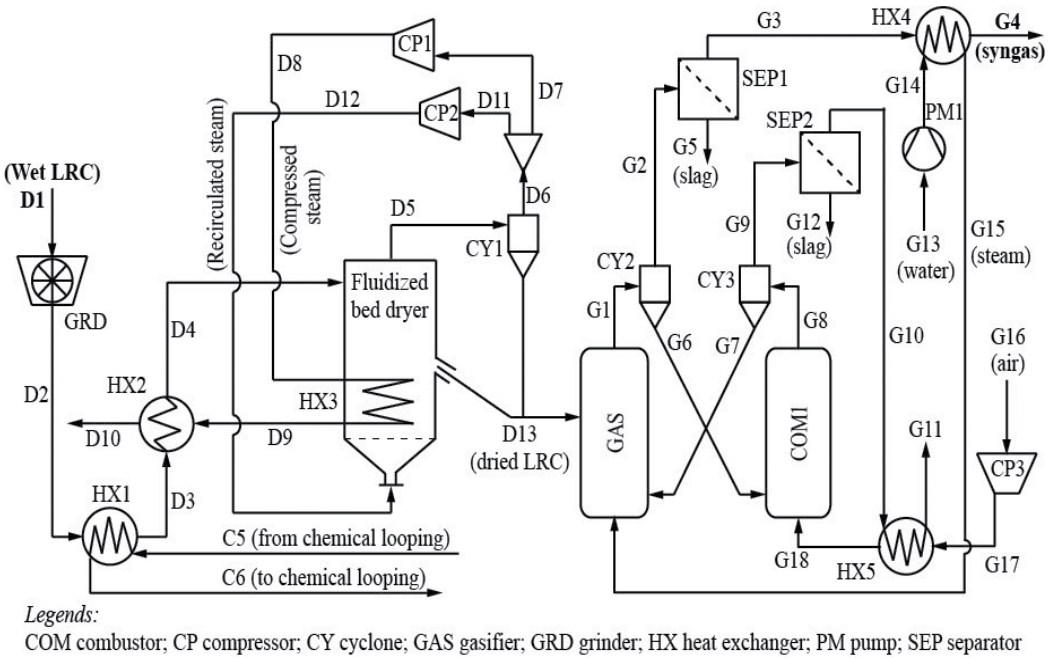

Figure 3. Schematic of drying and gasification modules.

fluidized bed owing to the benefit in the uniform temperature distribution and heat transfers, an extensive area of the contact surface, and proper particle mixing [32]. The immersed heat exchanger (HX3) is furnished inside the fluidized-bed dryer for the superheated steam process.

The next step is the gasification process, which produces combustible gases, including H_2, CO, and CH_4. Series of reactions are involved in this process, including the water-gas shift, Boudouard, and oxidation, as well as methanation. Due to the necessity of high gasification temperatures, dry-feeding gasification is employed in the system instead of slurry-feeding gasification [33]. Here, a dual-circulating fluidized bed (gasifier and combustor) is furnished to achieve higher carbon conversion efficiency and conversion rate [34].

After the gasification, both of the raw syngas and flue gas are fed into SEP1 and SEP2 for removal of ash and slag by the ceramic particulate removal which exhibits high efficiency under high-temperature conditions [35]. **Table 1** summarizes the conditions assumed for LRC drying and gasification study.

The effect of steam-to-fuel ratio during gasification is evaluated to define the optimum combination of steam and fuel. Two different steam-to-fuel ratios (0.9 and 1.4) are investigated to confirm the optimum ratio for the performance of the chemical looping system. **Table 2** shows the composition of the syngas resulting from different steam-to-fuel ratios.

3.1.3.2. Chemical looping and combined cycle

Among any methods, direct chemical looping and syngas chemical looping are the typical methods for the chemical looping. However, due to the utilization of the metal oxide for

Component	Value	Note
Drying conditions		
Coal flow rate (Mg h^{-1})	100	At moisture content of 18 wt% wb
Initial moisture content (wt% wb)	60	
Target moisture content (wt% wb)	18	
Fluidization velocity $U_{dry}/U_{mf,dry}$	1, 2, 3, 4	
Mean particle diameter (mm)	2.0	
Bulk density (kg m^{-3})	900	
Heating value (MJ kg^{-1} HHV)	19.33	
LRC ultimate analysis		
C (wt% db)	65.53	
H (wt% db)	3.75	
N (wt% db)	0.84	
O (wt% db)	25.22	
S (wt% db)	0.38	
Cl (wt% db)	0.05	
Ash (wt% db)	4.23	
Gasification conditions		
Combustion temperature (K)	1173	
Gasification temperature (K)	1123	
Steam-to-fuel ratio	0.9; 1.4	
LRC mean particle diameter (mm)	2.0	
Bed material	Olivine	
Mean bed material diameter (mm)	0.37	

Table 1. LRC drying and gasification conditions.

Produced syngas	Steam-to-fuel ratio	
	0.9	**1.4**
H_2 (Nm^3 kg-$fuel^{-1}$ daf)	0.820	0.762
CH_4 (Nm^3 kg-$fuel^{-1}$ daf)	0.063	0.066
CO (Nm^3 kg-$fuel^{-1}$ daf)	0.486	0.415
CO_2 (Nm^3 kg-$fuel^{-1}$ daf)	0.255	0.270
Steam content in produced gas (vol%)	19.1	28.7

Table 2. Composition of syngas generated using a dual-circulating fluidized bed with varying steam-to-fuel ratios.

oxygen carrier in the system, the syngas chemical looping is employed due to the beneficial in the solids handling and energy efficiency. The oxygen carrier exhibits no direct contact between atmospheric oxygen and the fuel during the combustion process; hence, the high-purity CO_2 can be immediately separated without any further handling, which thus promotes an efficient and clean energy conversion. Thus, due to the excellent mechanical properties, large capacity content of oxygen carrier, and the high conversion of syngas and steam, the iron-based materials are applied as the recirculated oxygen carriers [36].

Figure 4 represents a process flow diagram for the chemical looping and combined cycle modules. The chemical looping module is developed from three connected reactors: reducer (RED),

oxidizer (OXD), and combustor (COM2). In the reducer and oxidizer, a counter current moving bed reactor is employed, while an entrained fluidized bed is furnished for the combustor.

In the RED, the compressed syngas is fed as the fluidizing gas. After leaving the RED (C3), the high pressure fluidizing gas is thus recovered by the expander (GT1) for electricity generation. The reactions in the RED assumed to occur during reduction are as follows [37]:

$$Fe_2O_3 + CO \rightarrow 2FeO + CO_2 \qquad \Delta H = -2.8 \text{ kJ mol}^{-1} \tag{2}$$

$$FeO + CO \rightarrow Fe + CO_2 \qquad \Delta H = -11 \text{ kJ mol}^{-1} \tag{3}$$

$$Fe_2O_3 + H_2 \rightarrow 2FeO + H_2O \qquad \Delta H = 38.4 \text{ kJ mol}^{-1} \tag{4}$$

$$FeO + H_2 \rightarrow Fe + H_2O \qquad \Delta H = 30.2 \text{ kJ mol}^{-1} \tag{5}$$

$$4Fe_2O_3 + 3CH_4 \rightarrow 8Fe + 3CO_2 + 6H_2O \qquad \Delta H = 897.18 \text{ kJ mol}^{-1} \tag{6}$$

The formation of by-products, including Fe_3C and carbon soot due to Boudouard reaction has been noticed in the continuous operation in RED. However, efforts to diminish the formation of Fe_3C have been performed in previous studies, including the modification of iron-based oxygen carrier with CeO_2 and exhaustive selection of the used iron-based oxygen carriers [38].

CO_2 and steam are generated during the reduction step and then leave the reducer for the cooling process in preparation for separation (CD1). The separated CO_2 (C7) is then compressed and ready for the sequestration purposes. Other product from the reduction step, the

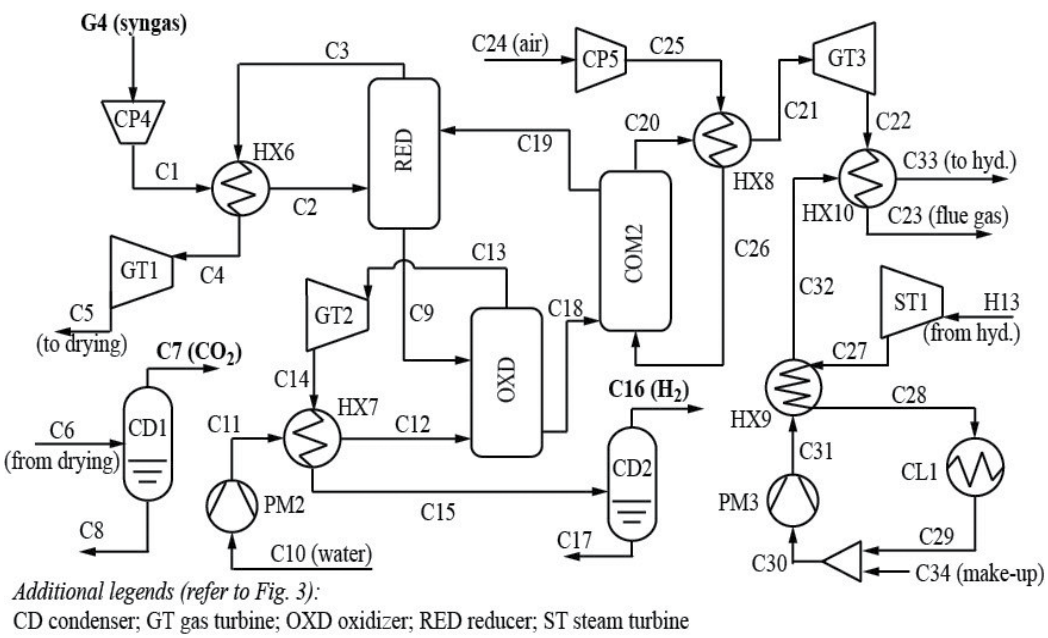

Figure 4. Process flow diagram of the chemical looping and combined cycle modules.

iron particles (C9), is fed to the OXD in which the oxidation takes place with the steam as reactant to produce highly pure H_2 (C16). The reactions inside the OXD in the presence of excess steam can be written as follows:

$$Fe + H_2O \rightarrow FeO + H_2 \qquad \Delta H = -30.2 \text{ kJ mol}^{-1} \tag{7}$$

$$3FeO + H_2O \rightarrow Fe_3O_4 + H_2 \qquad \Delta H = -60.6 \text{ kJ mol}^{-1} \tag{8}$$

The generated H_2 is discharged to the hydrogenation module for further process, while the metals move to the COM2 for recirculation. The reaction inside the COM2 is shown below.

$$4Fe_3O_4 + O_2 \rightarrow 6Fe_2O_3 \qquad \Delta H = -471.6 \text{ kJ mol}^{-1} \tag{9}$$

The reduction process is performed by the discharged heat from the combustion process implanted inside the metal oxide. The high energy from compressed flue gas is expanded for electricity generation in GT3 and ST1 by employing combined cycle. The conditions of chemical looping and combined cycle modules are explained in **Table 3**.

3.1.3.3. Hydrogenation

The conditions during toluene hydrogenation and the schematic flow diagram are shown in **Table 4** and **Figure 5**, respectively. The heat generated from the exothermic reaction of hydrogenation is applied as the heat source for electricity generation in the steam turbine (ST1). The theoretical gravimetric and volumetric hydrogen concentrations in MCH under ambient conditions are 6.2 and 47%, respectively [39]. The hydrogenation reaction is as follows:

$$C_7H_8 + 3H_2 \rightarrow C_7H_{14} \qquad \Delta H = -205.0 \text{ kJ mol}^{-1} \tag{10}$$

3.1.4. Performance of integrated system

Figure 6 indicates the effect of drying fluidization velocities to the compressor and blower duties, net generated power, and power efficiency. These values are carried out using a steam-to-fuel ratio during gasification and a basic chemical looping pressure of 0.9 and 3 MPa, respectively. A compressor (CP4) is prepared after the gasification module to pressurize the syngas into the pressure of chemical looping.

Based on the calculation results, there is barely significant shift in the compressor duty as the compression work is almost constant at 1.8 MW. On the other hand, the duty of blower is increasing as the fluidization velocities during drying are uprising. Here, the blower duty at the lowest fluidization velocity ($U_{mf,dry}$, 1.28 m s^{-1}) is 0.7 MW and rise to 2.7 MW when the fluidization velocity is increased to 4 $U_{mf,dry}$. As high amount of energy is required for the high duty of the blower, a rapid fluidization velocity during drying results in a lower total efficiency.

Figure 7(a) presents the effect of different steam-to-fuel ratios to the amount of H_2 generated, H_2 production efficiency, net generated power, and the total efficiency, while **Figure 7(b)** presents the effect of different steam-to-fuel ratios to the amounts of produced H_2 and MCH. These values are carried out using a specific fluidization velocity during drying and a basic

Component	Value	Note
Reducer		
Temperature (K)	1073	
Pressure (MPa)	2.0–4.0	
Syngas conversion (%)	100	
Iron particle diameter (mm)	2	
Produced CO_2 purity (%)	99.99	
Oxidizer		
Temperature (K)	1023	
Pressure (MPa)	2.0–4.0	
Produced H_2 purity (%)	99.99	
Excess steam at outlet (%)	10	
Combustor		
Temperature (K)	1473	
Pressure (MPa)	2.2–4.2	
Air excess at outlet (%)	10	
Gas turbine (F-class)		
Turbine polytrophic efficiency (%)	90	
Maximum turbine inlet temperature (K)	1473	
HRSG and steam turbine		
Turbine polytrophic efficiency (%)	90	
Inlet pressure (MPa)	15	
Maximum turbine inlet temperature (K)	973	
Minimum outlet vapor quality	0.9	

Table 3. Conditions and assumptions for chemical looping and the combined cycle.

Component	Value
Reaction temperature (K)	473
Operating pressure (kPa)	130
Catalyst	Ni-Mo/Al_2O_3
Catalyst particle size (mm)	0.3
Particle sphericity	0.5

Table 4. Conditions assumed for toluene hydrogenation.

chemical looping pressure of 2 $U_{mf,dry}$ and 3 MPa, respectively. Generally, the higher H_2 production efficiency and power generation are both achieved in the steam-to-fuel ratio of 0.9 instead of 1.4. The produced H_2 amount and net generated power at a steam-to-fuel ratio of 1.4 are 4.3 t h^{-1} (H_2 production efficiency of 66.5%) and 24.1 MW (power generation efficiency of 11.2%), respectively. These values rise up to 4.6 t h^{-1} (with a H_2 production efficiency of 71.9%) and 26.3 MW (with a power generation efficiency of 12.2%), when the steam-to-fuel ratio is set at 0.9.

Figure 8 Shows the effect of basic chemical looping pressure to the net generated power and power generation efficiency. These values are carried out by applying a fluidization velocity during drying and a steam-to-fuel ratio during gasification of 2 $U_{mf,dry}$ and 0.9, respectively.

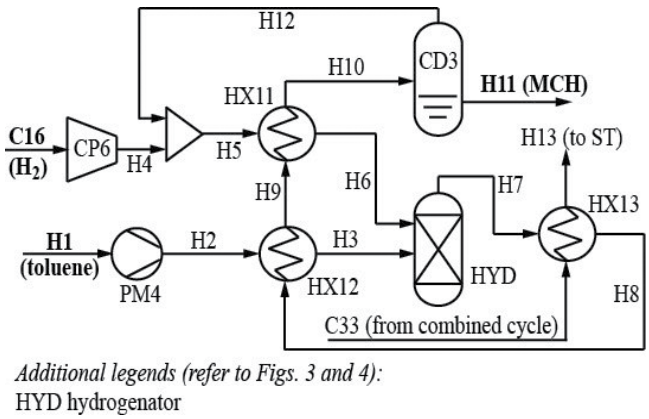

Figure 5. Process flow diagram of the hydrogenation module.

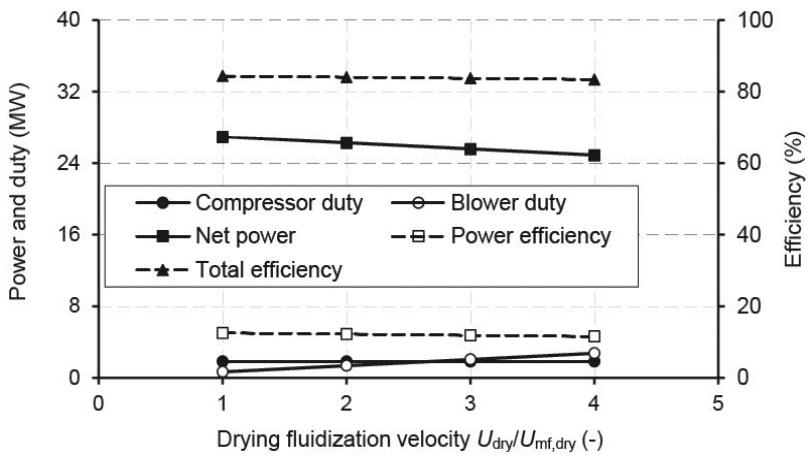

Figure 6. Effect of fluidization velocity during drying (at a steam-to-fuel ratio during gasification and basic chemical looping pressure of 0.9 and 3 MPa, respectively).

Generally, the increase of chemical looping process pressures leads to increase in both the net generated power and the power generation efficiency.

3.2. Integrated systems from microalgae by supercritical water gasification

3.2.1. The characteristics of microalgae as energy source

Besides the high potential in the pharmaceuticals, industrial materials, and food production, microalgae own a high potential for the energy source [40]. Among other biomasses, microalgae are very exceptional due to its excellent growth rate, ability to grow in a harsh environment, and highly efficient solar energy conversion [4]. Currently, many products of fuel are derived from the microalgae, including bio-oil, biohydrogen, and biodiesel [41]. However, as the microalgae grow in an aqueous environment far from the industrial or residential area, it has to be planted remotely and transported to the designated area for the utilization of microalgae

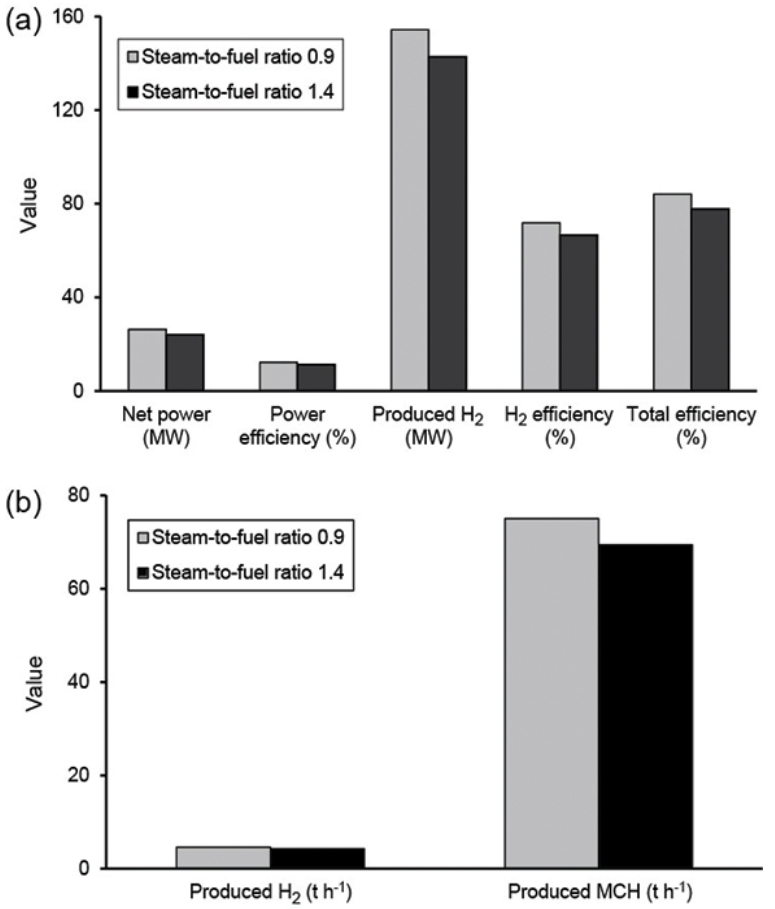

Figure 7. Effects of the steam-to-fuel ratio on (a) net generated power, power generation efficiency, produced H_2, H_2 production efficiency, and total efficiency and (b) produced H_2 and MCH amounts (U_{dry} = 2 $U_{mf,dry}$, basic chemical looping pressure = 3 MPa).

in the large scale. To this, a process chain from the microalgae cultivation to the H_2-based MCH for LOHC generation can solve the transportation and storage issues of the large-scale utilization of microalgae.

For the investigation, an alga species with ability to grow rapidly in normal condition and rich protein is necessary. To this, *Chlorella vulgaris* is selected as a sample for system evaluation. [42]. The properties of *Chlorella vulgaris,* including the results of proximate and ultimate analyses are listed in **Table 5**.

Among any candidates in the thermochemical process, gasification owns the highest rank due to its conversion efficiency [43]. There are two gasification methods widely used, the conventional thermal gasification and supercritical water gasification (SCWG). The former requires drying process to low moisture content before the gasification, while the latter is performed in the aqueous state, in which drying process is avoidable [44], and more favorable for the gasification of microalgae, owing to its high moisture content (70–90 wt% wb) [16]. However, SCWG is an energy

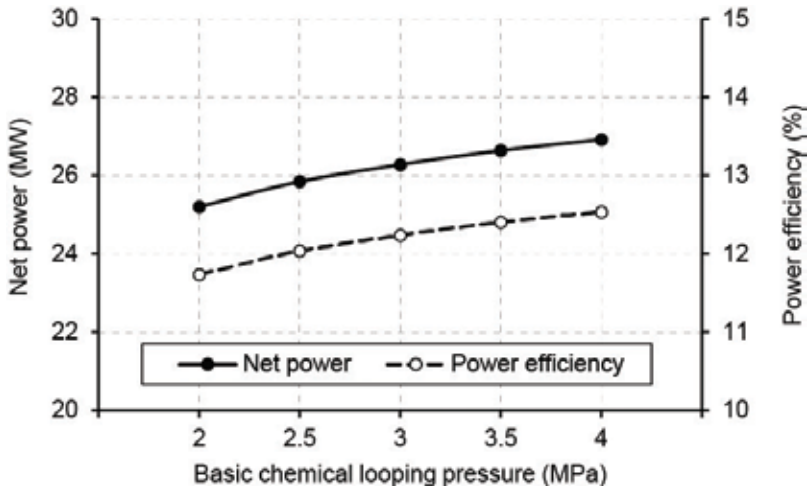

Figure 8. Correlations of net generated power and power generation efficiency with basic chemical looping pressure (U_{dry} = 2 $U_{mf,dry}$, steam-to-fuel ratio = 0.9).

Property	Value
Moisture content (wt% wb)	90
Dry solid content (wt% wb)	10
Chemical composition	
Protein (wt% db)	64.1
Fat (wt% db)	13
Fiber (wt% db)	21.1
Ash (wt% db)	7
Carbohydrates (wt% db)	15
Ultimate analysis	
Carbon (wt% db)	45.8
Hydrogen (wt% db)	7.9
Nitrogen (wt% db)	7.5
Oxygen (wt% db)	38.7
Calorific value (dried, MJ kg^{-1})	18.49

Table 5. Proximate and ultimate analyses of *Chlorella vulgaris*.

consuming process, which tends to absorb a huge portion of energy and create a lowly energy-efficient system [45]. To this, the EPI technology can tackle the challenge of the high energy issue of the SCWG, and leads to a novel process for the large-scale utilization of microalgae into LOHC.

3.2.2. Integrated system development

The basic schematic energy and material flows of the integrated system consists of SCWG, H_2 separation, hydrogenation, and the combined cycle. **Figure 9** explains the detailed schematic process flow diagram of the proposed integrated system.

3.2.3. Analysis of integrated system

3.2.3.1. Supercritical water gasification of microalgae

Due to the supercritical regime of the reaction, the decreasing water density causes a low static relative dielectric constant, hence, weaken the hydrogen bonds and improve the yield of the syngas [13]. Moreover, syngas cleaning can be disregarded due to no formation of NO_x or SO_x in the process. In the proposed process, a fluidized-bed reactor was selected due to its beneficial characteristics, including better particle mixing, ability to avoid plugging, uniform temperature distribution, and a high conversion rate [46].

For high performance of gasification, a catalyst set of Ru/TiO_2 which exhibits H_2-rich syngas and complete carbon conversion is injected inside the gasifier. Moreover, fluidizing particles (e.g., alumina) can be proposed to increase the particle dynamics inside the reactor and prevent the production of ash layer and char on the reactor wall [47]. In this study, the flow rate and initial moisture content of wet microalgae are fixed at 1000 t h^{-1} and 90 wt% wb, respectively. Two gasification pressures are evaluated: 25 and 30 MPa. **Table 6** gives the gasification conditions and produced syngas composition.

3.2.3.2. H_2 Separation and hydrogenation

Membrane-based separation is adopted for the H_2 extraction from the syngas. This method promotes low energy consumption, simple handling process, and mild conditionings. Among the membrane separation methods, polymeric membrane separation, consists of microporous film acting as a semipermeable barrier, owns the widest commercial application [48]. The assumed conditions during H_2 separation and hydrogenation are given in **Table 7**.

Property	**Value**
SCWG condition	
Temperature (°C)	600
Pressure (MPa)	25, 30
Fluidization velocity U/U_{mf} (−)	1, 2, 3, 4
Fluidizing material (−)	alumina
Density (kg m^{-3})	3400
Particle diameter (mm)	0.3
Sphericity (−)	0.67
Voidage at minimum fluidization (−)	0.45
Gasification catalyst (−)	Ru/TiO_2
Weight ratio of catalyst to wet algae (−)	2
Syngas composition	
Carbon conversion efficiency (%)	100
H_2 (dry mol%)	46.1
CO (dry mol%)	3.1
CH_4 (dry mol%)	18.1
C_2H_6 and C_3H_8 (dry mol%)	4.9
CO_2 (dry mol%)	27.8

Table 6. SCWG conditions and syngas composition used during calculation.

Property	Value
Separation	
Type (−)	Polymeric membrane
Hydrogen recovery (%)	70
Operating temperature (°C)	100
Feed inlet pressure (kPa)	800
Product outlet pressure (kPa)	110.0
Product H_2 concentration (mol%)	0.995
Product CO concentration (mol%)	0.000498
Product other gas concentration (mol%)	0.00448
Hydrogenation	
Pressure (kPa)	130
Temperature (°C)	200
Catalyst (−)	Ni-Mo/Al_2O_3
Catalyst particle size (mm)	0.3
Sphericity (−)	0.5

Table 7. Hydrogen separation and hydrogenation conditions.

3.2.3.3. Combined cycle and power generation

After the H_2 is separated from the syngas, the remaining syngas is employed as a fuel for combustion (COMB) in the combined cycle. Moreover, due to high temperature of the flue gas from the gas turbine (GT), it is thus used to superheat the mixture of syngas and steam from the SCWG reactor. At last, the remaining heat is recovered in HRSG for the steam turbine (ST). The conditions of the combined cycle modules, including combustor, gas and steam turbines are presented in **Table 8**.

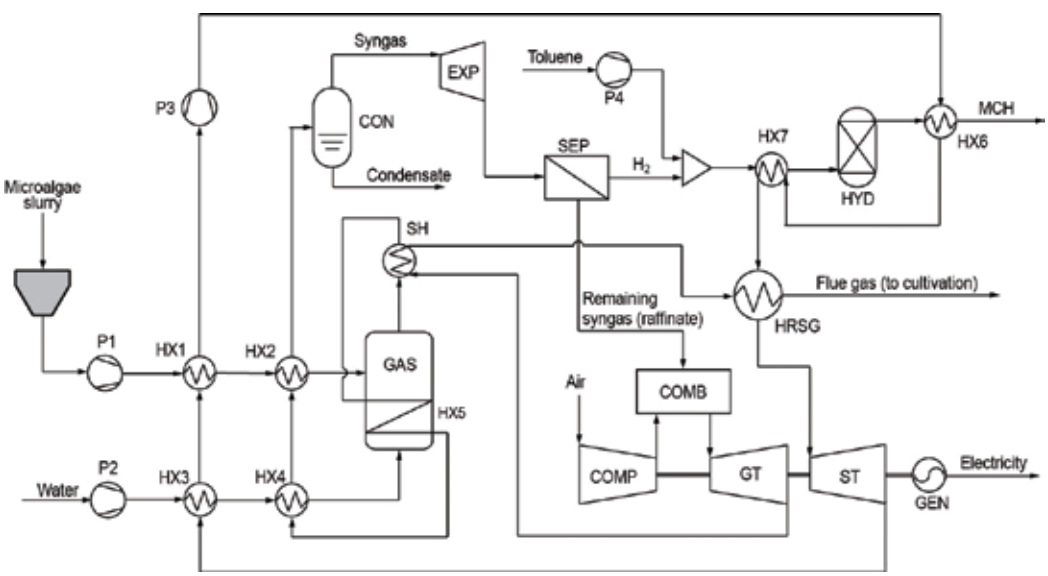

Figure 9. Schematic diagram of the process flow of the proposed integrated system.

3.2.4. Performance of integrated system

Figure 10 shows the relationship between total energy efficiency, η_{tot}, and fluidization velocity for different gasification pressures of 25 and 30 MPa. Subsequently, about 3.5 t-H_2 h^{-1} can be converted to MCH by hydrogenation process with toluene. The increase of fluidization velocity leads to lower total energy efficiency. Therefore, gasification carried out under a lower gasification pressure at 25 MPa has better total energy efficiency than that at 30 MPa.

The increasing in fluidization velocity leads to more water for the fluidizing steam which thus increases the flow rate of steam exhausted from the SCWG reactor. As a result, the heat available as hot stream in the HRSG decreases, leading to a decrease in actual work obtained from the steam turbine. On the other hand, the increasing of gasification pressure leads to more flow rate of the fluidizing steam under same fluidization velocity. Thus, the increase in gasification pressure finally leads to lower actual work by the steam turbine.

Property	Value
Combustor and gas turbine	
Compressor outlet pressure (MPa)	2
Compressor polytrophic efficiency (%)	87
Combustor pressure drop (%)	2
Gas turbine inlet temperature (°C)	1300
Gas turbine adiabatic efficiency (%)	90
Air to fuel ratio (−)	10
HRSG and steam turbine	
HRSG outlet pressure (MPa)	10
Heat exchanger temperature difference (°C)	10
HRSG pressure drop (%)	1
Steam turbine inlet temperature (°C)	600
Steam turbine polytrophic efficiency (%)	90
Minimum outlet vapor quality (%)	90

Table 8. Assumed conditions for the combined cycle, including combustion and gas and steam turbines.

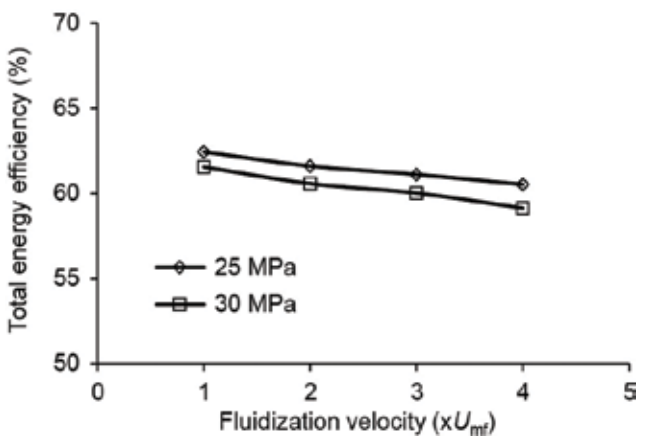

Figure 10. Relationship between total energy efficiency and fluidization velocity under different gasification pressures.

4. Conclusion

Novel integrated gasification systems for coproduction of electricity and MCH from low-rank coal and microalgae have been proposed. Enhanced process integration technology is applied for both systems to minimize exergy losses throughout the integrated system, thus improving the total energy efficiency. However, the models are carried out in the condition of ideal zero heat loss. Therefore, approximately 5–10% of heat losses are necessary to consider for the investigation in the actual case of the systems. For the case of microalgae, the effects of the fluidization velocity and gasification pressure on the total energy and electricity generation efficiencies were evaluated for optimum integrated system, while for the case of low-rank coal, the optimization is subjected to the investigation of fluidization velocity, steam-to-fuel ratio, and the chemical looping pressure. Finally, the integrated system for microalgae is capable to provide more than 60% of total energy efficiency, while the integrated system for low-rank coal delivers the total energy efficiency of 84%.

Author details

Lukman Adi Prananto and Muhammad Aziz*

*Address all correspondence to: maziz@ssr.titech.ac.jp

Institute of Innovative Research, Tokyo Institute of Technology, Japan

References

[1] Bilgen S. Structure and environmental impact of global energy consumption. Renewable & Sustainable Energy Reviews. 2014;**38**:890-902

[2] Aziz M, Zaini IN, Oda T, Morihara A, Kashiwagi T. Energy conservative brown coal conversion to hydrogen and power based on enhanced process integration: Integrated drying, coal direct chemical looping, combined cycle and hydrogenation. International Journal of Hydrogen Energy. 2017;**42**(5):2904-2913

[3] Aziz M. Power generation from algae employing enhanced process integration technology. Chemical Engineering Research and Design. 2016;**109**:297-306

[4] Aziz M, Oda T, Kashiwagi T. Advanced energy harvesting from macroalgae-innovative integration of drying, gasification and combined cycle. Energies. 2014;**7**(12):8217-8235

[5] Darmawan A, Budianto D, Aziz M, Tokimatsu K. Retrofitting existing coal power plants through cofiring with hydrothermally treated empty fruit bunch and a novel integrated system. Applied Energy. 2017;**204**:1138-1147

[6] Yavor Y, Goroshin S, Bergthorson JM, Frost DL. Comparative reactivity of industrial metal powders with water for hydrogen production. International Journal of Hydrogen Energy. 2015;**40**(2):1026-1036

[7] Miura D, Tezuka T. A comparative study of ammonia energy systems as a future energy carrier, with particular reference to vehicle use in Japan. Energy. 2014;**68**:428-436

[8] Aziz M. Integrated hydrogen production and power generation from microalgae. International Journal of Hydrogen Energy. 2016;**41**(1):104-112

[9] Teichmann D, Arlt W, Wasserscheid P. Liquid organic hydrogen carriers as an efficient vector for the transport and storage of renewable energy. International Journal of Hydrogen Energy. 2012;**37**(23):18118-18132

[10] Aziz M, Oda T, Kashiwagi T. Clean hydrogen production from low rank coal: Novel integration of drying, gasification, chemical looping, and hydrogenation. Chemical Engineering Transactions. 2015;**45**:613-618

[11] Müller K, Aslam R, Fischer A, Stark K, Wasserscheid P, Arlt W. Experimental assessment of the degree of hydrogen loading for the dibenzyl toluene based LOHC system. International Journal of Hydrogen Energy. 2016;**41**(47):22097-22103

[12] Okada Y, Shimura M. Development of large-scale H_2 storage and transportation technology with liquid organic hydrogen carrier (LOHC). In: The 21st joint GCC-Japan environment symposium; 5–6 February 2015; Doha, Qatar: 2013. pp. 5793-5803

[13] Aziz M. Integrated supercritical water gasification and a combined cycle for microalgal utilization. Energy Conversion and Management. 2015;**91**:140-148

[14] Zaini IN, Nurdiawati A, Aziz M. Cogeneration of power and H_2 by steam gasification and syngas chemical looping of macroalgae. Applied Energy. 2017;**207**:134-145

[15] Aziz M, Juangsa FB, Kurniawan W, Budiman BA. Clean co-production of H_2 and power from low rank coal. Energy. 2016;**116**:489-497

[16] Aziz M, Oda T, Kashiwagi T. Integration of energy-efficient drying in microalgae utilization based on enhanced process integration. Energy. 2014;**70**:307-316

[17] Aziz M, Kansha Y, Tsutsumi A. Self-heat recuperative fluidized bed drying of brown coal. Chemical Engineering and Processing: Process Intensification. 2011;**50**(9):944-951

[18] Aziz M, Kansha Y, Kishimoto A, Kotani Y, Liu Y, Tsutsumi A. Advanced energy saving in low rank coal drying based on self-heat recuperation technology. Fuel Processing Technology. 2012;**104**:16-22

[19] Prabowo B, Aziz M, Umeki K, Susanto H, Yan M, Yoshikawa K. CO_2-recycling biomass gasification system for highly efficient and carbon-negative power generation. Applied Energy. 2015;**158**:97-106

[20] Aziz M, Kurniawan T, Oda T, Kashiwagi T. Advanced power generation using biomass wastes from palm oil mills. Applied Thermal Engineering. 2017;**114**:1378-1386

[21] Darmawan A, Hardi F, Yoshikawa K, Aziz M, Tokimatsu K. Enhanced process integration of black liquor evaporation, gasification, and combined cycle. Applied Energy. DOI: 10.1016/j.apenergy.2017.05.058

[22] Dincer I, Acar C. Review and evaluation of hydrogen production methods for better sustainability. International Journal of Hydrogen Energy. 2014;**40**(34):11094-11111

[23] Aziz M, Budianto D, Oda T. Computational fluid dynamic analysis of co-firing of palm kernel shell and coal. Energies. 2016;**9**(3):137

[24] Yamaguchi D, Sanderson PJ, Lim S, Aye L. Supercritical water gasification of Victorian brown coal: Experimental characterisation. International Journal of Hydrogen Energy. 2009;**34**:3342-3350

[25] Zhang Y, Jin B, Zou X, Zhao H. A clean coal utilization technology based on coal pyrolysis and chemical looping with oxygen uncoupling: Principle and experimental validation. Energy. 2016;**98**:181-189

[26] Li P, Pan SY, Pei S, Lin YJ, Chiang PC. Challenges and perspectives on carbon fixation and utilization technologies: An overview. Aerosol and Air Quality Research. 2016;**16**(6):1327-1344

[27] Minutillo M, Perna A. Renewable energy storage system via coal hydrogasification with co-production of electricity and synthetic natural gas. International Journal of Hydrogen Energy. 2014;**39**(11):5793-5803

[28] Xiang W, Chen S, Xue Z, Sun X. Investigation of coal gasification hydrogen and electricity co-production plant with three-reactors chemical looping process. International Journal of Hydrogen Energy. 2010;**35**(16):8580-8591

[29] Cleeton JPE, Bohn CD, Müller CR, Dennis JS, Scott SA. Clean hydrogen production and electricity from coal via chemical looping: Identifying a suitable operating regime. International Journal of Hydrogen Energy. 2009;**34**(1):1-12

[30] Chen Z, Agarwal PK, Agnew JB. Steam drying of coal. Part 2. Modeling the operation of a fluidized bed drying unit. Fuel. 2001;**80**(2):209-223

[31] Xianchun L, Hui S, Qi W, Meesri C, Terry WALL, Jianglong Y. Experimental study on drying and moisture re-adsorption kinetics of an Indonesian low rank coal. Journal of Environmental Sciences. 2009;**21**:S127-S130

[32] Pawlak-Kruczek H, Plutecki Z, Michalski M. Brown coal drying in a fluidized bed applying a low-temperature gaseous medium. Drying Technology. 2014;**32**(11):1334-1342

[33] Cormos CC, Starr F, Tzimas E, Peteves S. Innovative concepts for hydrogen production processes based on coal gasification with CO_2 capture. International Journal of Hydrogen Energy. 2008;**33**(4):1286-1294

[34] Ruiz JA, Juárez MC, Morales MP, Muñoz P, Mendívil MA. Biomass gasification for electricity generation: Review of current technology barriers. Renewable and Sustainable Energy Reviews. 2013;**18**:174-183

[35] Gnanapragasam NV, Reddy BV, Rosen MA. Hydrogen production from coal using coal direct chemical looping and syngas chemical looping combustion systems: Assessment of system operation and resource requirements. International Journal of Hydrogen Energy. 2009;**34**(6):2606-2615

[36] Tong A, Sridhar D, Sun Z, Kim HR, Zeng L, Wang F, Wang D, Kathe MV, Luo S, Sun Y, Fan LS. Continuous high purity hydrogen generation from a syngas chemical looping 25 kWth sub-pilot unit with 100% carbon capture. Fuel. 2013;**103**:495-505

[37] Fan LS. Chemical Looping Systems for Fossil Energy Conversions. John Wiley & Sons; 2011

[38] Sun S, Zhao M, Cai L, Zhang S, Zeng D, Xiao R. Performance of CeO_2-modified iron-based oxygen carrier in the chemical looping hydrogen generation process. Energy and Fuels. 2015;**29**(11):7612-7621

[39] Biniwale RB, Rayalu S, Devotta S, Ichikawa M. Chemical hydrides: A solution to high capacity hydrogen storage and supply. International Journal of Hydrogen Energy. 2008; **33**(1):360-365

[40] Wang B, Li Y, Wu N, Lan CQ. CO_2 bio-mitigation using microalgae. Applied Microbiology and Biotechnology. 2008;**79**(5):707-718

[41] Aziz M, Oda T, Kashiwagi T. Enhanced high energy efficient steam drying of algae. Applied Energy. 2013;**109**:163-170

[42] Cersosimo M, Brunetti A, Drioli E, Fiorino F, Dong G, Woo KT, Lee J, Lee YM, Barbieri G. Separation of CO_2 from humidified ternary gas mixtures using thermally rearranged polymeric membranes. Journal of Membrane Science. 2015;**492**:257-262

[43] Aziz M, Prawisudha P, Prabowo B, Budiman BA. Integration of energy-efficient empty fruit bunch drying with gasification/combined cycle systems. Applied Energy. 2015;**139**: 188-195

[44] Lu Y, Jin H, Guo L, Zhang X, Cao C, Guo X. Hydrogen production by biomass gasification in supercritical water with a fluidized bed reactor. International Journal of Hydrogen Energy. 2008;**33**(21):6066-6075

[45] Fiori L, Valbusa M, Castello D. Supercritical water gasification of biomass for H_2 production: Process design. Bioresource Technology. 2012;**121**:139-147

[46] Matsumura Y, Minowa T. Fundamental design of a continuous biomass gasification process using a supercritical water fluidized bed. International Journal of Hydrogen Energy. 2004;**29**(7):701-707

[47] Chakinala AG, Brilman DWF, Van Swaaij WPM, Kersten SRA. Catalytic and non-catalytic supercritical water gasification of microalgae and glycerol. Industrial and Engineering Chemistry. 2010;**49**(3):1113-1122

[48] Liu K, Song C, Subramani V. Hydrogen and Syngas Production and Purification Technologies. John Wiley & Sons. 2009

Edited by Yongseung Yun

Most coveted energy forms nowadays are gas in nature and electricity due to their environmental cleanness and convenience. Recently, gasification market trend is starting to switch to low-grade feedstock such as biomass, wastes, and low-rank coal that are still not properly utilized. In this sense, the most promising area of development in gasification field lies in low-grade feedstock that should be converted to more user-friendly gas or electricity form in utilization. This book tried to shed light on the works on gasification from many parts of the world and thus can feel the technology status and the areas of interest regarding gasification for low-grade feedstock.

Published in London, UK

IntechOpen

ISBN 978-1-83881-421-2
9 781838 814212